

**Faculty of Science and Engineering
Department of Civil Engineering**

**Modelling of Ground Improvement by Vertical Drains in Highly Variable
Soils**

Md. Wasiul Bari

**This thesis is presented for the Degree of
Doctor of Philosophy
of
Curtin University**

April 2012

Declaration

To the best of my knowledge and belief this thesis contains no material previously published by any other person except where due acknowledgment has been made.

This thesis contains no material which has been accepted for the award of any other degree or diploma in any university.

Signature:

Date:

Abstract

The research presented in this thesis focuses on the probabilistic modelling of soil consolidation via prefabricated vertical drains (PVDs) considering soil spatial variability. Soils are highly variable from one point to another in the ground and yet this is often coupled with inadequate site data, probabilistic analysis is a more rational approach to assess the behaviour of soil consolidation by PVDs. Although the fact that spatial variation of soil properties can affect soil consolidation has long been realized, the design of soil consolidation via PVDs has been traditionally carried out deterministically and thus can be misleading due to the ignorance of the uncertainty associated with the inherent spatial variation of soil properties. One of the major advantages of probabilistic modelling over deterministic approach is that it can explicitly incorporate soil spatial variability in the analysis and design of a geotechnical problem and subsequently provides much physical insight into the impact of soil spatial variability on the behaviour of the problem under consideration. However, owing to the complexity of the stochastic problem, available research into consolidation of highly variable soils has been limited. The review of relevant literature has indicated that soil spatial variability in relation to ground improvement by PVDs has never been previously considered in a systematic, scientific manner in design and little research has been done in this area. Therefore, to obtain a more realistic measure of the degree of consolidation at any specified time, the effect of soil spatial variability needs to be taken into account by employing probabilistic modelling approach.

Among several available methods of stochastic modelling, the random finite element method (RFEM) using random variable soil input properties in a Monte Carlo framework has gained much popularity in recent years. The same approach is adopted in the present research for modelling soil spatial variability in soil consolidation by PVDs. The soil permeability, k , and volume compressibility, m_v , are considered as random variables and the variability of both k and m_v is characterised statistically in terms of the mean, standard deviation, lognormal probability distribution and scale of fluctuation (SOF). The random fields of k and m_v are generated using 2D local average subdivision (LAS) method developed by Fenton and Vanmarcke (1990). The generated random fields are then used as inputs in a

stochastic finite element modelling of soil consolidation by PVDs. In this research, all numerical analyses are carried out using the 2D finite element computer program AFENA (Carter and Balaam 1995), in which the consolidation process of soil is treated as a coupled transient problem governed by the Biot's consolidation theory (Biot 1941).

In order to investigate and quantify the effect of soil spatial variability on the stochastic behaviour (i.e. on the statistical moments of the degree of consolidation; and on the probability of achieving a target degree of consolidation) of soil consolidation by PVDs, extensive parametric studies are performed over a wide range of coefficient of variation (COV) and SOF of the spatially variable k and m_v , with various different assumed site conditions. It was found that spatial variation of soil permeability and volume compressibility within an affected soil mass significantly affects the degree of consolidation achieved via PVDs and thus the amount of soil improvement obtained.

One of the main objectives of the stochastic consolidation analyses is to estimate the probability that a deterministic degree of consolidation overestimates the true consolidation value. To determine such probability through a full scale random finite-element Monte-Carlo (FEMC) scheme, great volume of simulations that are necessarily very complex, computationally intensive and time consuming are required. Therefore, it is of great importance to develop a simplified reliability-based analytical model from which direct estimates of the probability of achieving a target degree of consolidation at a given consolidation time can be readily obtained, subsequently negates the need for the computationally intensive FEMC simulations. Accordingly, in this thesis, an approximate, easy to use reliability-based semi-analytical model (RBSA) is developed. In the proposed RBSA model, semi-analytical relationships for the distribution parameters (mean and standard deviation) of a monotonic function of the degree of consolidation that have a reasonable probability distribution are derived directly from the statistically defined input data relating to the spatially variable soil properties. The computed mean and standard deviation of the degree of consolidation function at any given consolidation time from the RBSA model are then used to estimate the probability of achieving a target degree of consolidation at that time using an appropriate probability expression. The

proposed model considers the spatial variability of soil permeability and volume compressibility including the impact of the smear zone. As the performance function of the proposed RBSA model is based on the well-known deterministic horizontal (radial) consolidation equation proposed by Hansbo (1981), the RBSA model considers soil consolidation due to horizontal drainage only. The RBSA model developed in this study is verified against the results of the FEMC analyses over the range of observed or suggested values of input statistical parameters of the random soil properties found in the literature. It was found that the predictions from the RBSA model are in good agreement with those obtained from the FEMC, implying that the developed RBSA is reliable and can be used with confidence for design of soil improvement by PVDs.

Publications

The following publications have been prepared as a result of this research:

Refereed Journal Papers

1. Bari, M. W., Shahin, M. A., and Nikraz, H. R. (2012). "Effects of soil spatial variability on axisymmetric versus plane strain analyses of ground improvement by prefabricated vertical drains." *International Journal of Geotechnical Engineering*, 6(2), 139-147.
2. Bari, M. W., and Shahin, M. A. "Reliability-based semi-analytical solution for soil consolidation by prefabricated vertical drains considering spatial variability of soil permeability." *Canadian Geotechnical Journal*, (under review).
3. Bari, M. W., Shahin, M. A., and Nikraz, H. R. "Probabilistic analysis of soil consolidation via prefabricated vertical drains." *International Journal of Geomechanics, ASCE*, (under review).

Refereed Conference Papers

1. Bari, M. W., Shahin, M. A., and Nikraz, H. R. (2012) "Probabilistic study into the impact of soil spatial variability on soil consolidation by prefabricated vertical drains." *Int'l Conference on Geomechanics and Engineering*, Seoul, Korea, (accepted).
2. Shahin, M. A., and Bari, M. W. (2012) "Modeling of Ground Improvement by Prefabricated Vertical Drains in Highly Variable Soils." *International Conference on Ground Improvement and Ground Control (ICGI 2012)*, University of Wollongong, Australia, (accepted).
3. Bari, M. W., Shahin, M. A., and Nikraz, H. R. (2011) "Probabilistic analysis of isotropic versus anisotropic spatial variability of soil in design of prefabricated vertical drains for ground improvement." *International Symposium on Advances in Ground Technology and Geo-Information (IS-AGTG)*, Singapore, 315-323.
4. Bari, M. W., Shahin, M. A., and Nikraz, H. R. (2011) "Axisymmetric versus plane strain analyses of ground improvement by prefabricated vertical drains

- considering soil spatial variability." *International Conference on Advances in Geotechnical Engineering (ICAGE)*, Perth, Western Australia, 437-444.
5. Bari, M. W., Shahin, M. A., and Nikraz, H. R. (2010) "Effects of spatial variability on consolidation of soft soil stabilized by prefabricated vertical drains." *Proceedings of the 17th Southeast Asian Geotechnical Conference*, Taipei, Taiwan, 43-46.

Acknowledgements

In the name of Allah, the most gracious, the most merciful. I would like to express my enormous gratitude to my supervisor, Associate Professor Mohamed Shahin, Department of Civil engineering, Curtin University, for his kindness, enthusiastic guidance, continual support in professional and personal matters and invaluable help in all aspects throughout this research. His patience and availability to answer my queries whenever needed with his heavy workload is deeply appreciated. In addition, his numerous comments, constructive criticisms, suggestions, encouragement and friendship have been of great value to me, and this work would not be possible without his contribution. My gratitude is also extended to my co-supervisor Professor Hamid Nikraz, Department of Civil engineering, Curtin University, for his kind support, precious suggestion and comments during my candidature.

I wish to thank the Department of Civil Engineering, Curtin University, for the provision of excellent research support and facilities. Heartfelt acknowledgments are expressed to all academic and non-academic members of the Department of Civil Engineering and in particular, Mrs. Diane Garth and Ms Liz Field for their tireless assistance and warm-hearted cooperation during my study at Curtin University. My special thanks are also extended to my fellow postgraduate students for their friendship and company.

The scholarship awarded to this research project by the Curtin University is sincerely acknowledged. I am also grateful to Ms Felicity Lewis for proof reading the thesis.

I wish to thank Dr. N. Balaam and Prof. J. P. Carter, Centre for Geotechnical Research, University of Sydney, for their kind permission to use the source code of program AFENA for this research. I would also like to articulate my thankfulness to Professor Gordon Fenton, of the Dalhousie University in Canada, for his valuable advice and insightful comments especially at the beginning of my research. Special thanks are also due for Asst. Professor Sumanta Halder, Indian Institute of Technology, India, for his generous support.

Finally, I am indebted to my family and in particular my parents, Abdul Bari and Dilara Bari. Without their encouragement, guidance and sacrifices, I may never have come this far in my studies. Very special and sincere gratitude is offered to my wife, Jannatul Ferdouse, for her constant love, patience, understanding and strength all throughout my PhD program. Her support, spoken or unspoken, has helped me to negotiate all the twists and turns of my PhD research.

Table of Contents

<i>Abstract</i>	i
<i>Publications</i>	iv
<i>Acknowledgements</i>	vi
<i>Table of Contents</i>	viii
<i>List of Figures</i>	xii
<i>List of Tables</i>	xxi
<i>List of Symbols</i>	xxiii
<i>Abbreviations</i>	xxx
Chapter 1 Introduction	1
1.1 Preface	1
1.2 Objectives and Scope of the Study	3
1.3 Organization of the Thesis	4
Chapter 2 Literature Review	6
2.1 Introduction	6
2.2 Purpose, History and Application of Prefabricated Vertical Drains	6
2.3 Characteristics of Vertical Drain Systems	8
2.3.1 Equivalent drain diameter for prefabricated vertical drains	8
2.3.2 Radius of influence zone	9
2.4 Factors Affecting Performance of PVDs	10
2.4.1 Smear effect	10
2.4.2 Discharge capacity and well resistance	12
2.5 Fundamentals of Soil Consolidation	12
2.5.1 Settlement of soil	12
2.5.2 Soil consolidation	13
2.6 Theory of Vertical Consolidation	14
2.6.1 Tarzaghi's theory of one-dimensional consolidation	14
2.6.2 Theory of consolidation due to radial drainage	15
2.6.3 Refinement of Hansbo's (1981) theory of radial consolidation by Walker (2006)	17
2.6.4 Consolidation due to combined vertical and radial drainage	21
2.6.5 Plane-strain consolidation model and matching procedure	21
2.7 Soil Variability	24
2.7.1 General terms for variability descriptors	25
2.7.1.1 Mean or expectation of a random variable	26
2.7.1.2 Variance/standard deviation of a random variable	26
2.7.1.3 Coefficient of variation of a random variable	27
2.7.1.4 Median and mode	27
2.7.1.5 Correlation between two random variables	27
2.7.2 Spatial variability of soil properties	28

2.7.2.1	Scale of fluctuation	30
2.7.2.2	Auto-correlation function	31
2.7.2.3	Local averaging and variance reduction function	32
2.7.2.4	Averages	33
2.7.3	Published data for soil variability	35
2.8	Probabilistic Methods of Soil Consolidation Analysis	38
2.8.1	First order second moment method	38
2.8.2	Point estimate method	40
2.8.3	Monte Carlo simulation	40
2.9	Application of Stochastic Analysis to Geotechnical Engineering Problems	41
2.10	Summary	44
Chapter 3	Stochastic Modelling of Soil Consolidation by Vertical Drains	46
3.1	Introduction	46
3.2	Stochastic Approach of Soil Consolidation by PVDs	46
3.2.1	Simulation of virtual soil profile	47
3.2.1.1	Identification and characterisation of spatially random soil properties	47
3.2.1.2	Generation of spatially random soil property field	50
3.2.1.3	Generation of two cross-correlated random soil property fields	56
3.2.2	Finite element modelling incorporating soil spatial variability	57
3.2.2.1	Average degree of consolidation of spatially variable soil	60
3.2.3	Repetition of process based on the Monte Carlo technique	61
3.3	Probabilistic Interpretation	64
3.4	General Considerations	66
3.5	Validation of Finite Element Computer Program AFENA	68
3.6	Preliminary Investigation on the Factor Affecting the Statistics of the Degree of Consolidation	69
3.6.1	Effect of mesh density	71
3.6.2	Effect of number of Monte Carlo simulations	72
3.7	Summary	73
Chapter 4	Soil Spatial Variability in Design of Ground Improvement by Vertical Drains	75
4.1	Introduction	75
4.2	Probabilistic Analysis of Soil Consolidation Without Considering Smear Effect	76
4.2.1	Description of consolidation problem under consideration	76
4.2.1.1	Deterministic solution	78
4.2.1.2	Probabilistic analysis of soil consolidation considering spatially random permeability	78
4.2.1.2.1	Results of sensitivity analyses	79
4.2.1.2.2	Effect of anisotropic correlation structure on the stochastic behaviour of soil consolidation	101
4.2.1.2.3	Matching comparison between axisymmetric and equivalent	107

	plane strain analyses	
4.2.1.3	Probabilistic analysis of soil consolidation considering both permeability and volume compressibility as random variables	119
4.2.1.3.1	Results of sensitivity analyses	120
4.2.1.3.1.1	Results of sensitivity analyses with $\nu_{m_v} = \nu_k$	121
4.2.1.3.1.2	Results of sensitivity analyses with $\nu_{m_v} = 0.25 \nu_k$	125
4.2.1.3.2	Results based on excess pore water pressure and settlement	129
4.2.1.3.3	Influence of cross correlation between spatially variable soil permeability and coefficient of volume compressibility	136
4.3	Probabilistic Analysis of Soil Consolidation Considering Smear Effect	140
4.3.1	Description of consolidation problem under consideration	141
4.3.1.1	Deterministic solution	142
4.3.1.2	Probabilistic analysis of soil consolidation considering spatially random permeability	143
4.3.1.2.1	Results of parametric study	145
4.3.1.2.1.1	Effect of variation of ν_k and θ_k on the mean and standard deviation of U and the probability of achieving 90% consolidation	145
4.3.1.2.1.2	Effects of variation of μ_{k_u} / μ_{k_s} and s on the mean and standard deviation of U and the probability of achieving 90% consolidation	152
4.3.1.3	Probabilistic analysis of soil consolidation considering both permeability and volume compressibility as random variables	156
4.3.1.3.1	Results of parametric study	157
4.3.1.3.1.1	Effect of variation of ν and θ on the mean and standard deviation of U and the probability of achieving 90% consolidation	157
4.3.1.3.1.2	Effects of variation of $\mu_{m_v s} / \mu_{m_v u}$ on the mean and standard deviation of U and the probability of achieving 90% consolidation	165
4.4	Summary and Conclusions	167
Chapter 5	Reliability-Based Semi-Analytical Model for Soil Consolidation by Vertical Drains	175
5.1	Introduction	175
5.2	Reliability-Based Semi-Analytical Model	175
5.2.1	Comparison between Finite-element Monte-Carlo approach and Reliability-based semi-analytical model	195
5.2.1.1	Comparison between FEMC and RBSA: G1C1	200
5.2.1.2	Comparison between FEMC and RBSA: G1C2	208
5.2.1.3	Comparison between FEMC and RBSA: G2C1	212
5.2.1.4	Comparison between FEMC and RBSA: G2C2	219
5.2.1.5	Comparison between RBSA: G1C1 and RBSA: G1C3	222
5.2.1.6	Comparison between RBSA: G2C1 and RBSA: G2C3	225

5.3	Summary and Discussions	227
Chapter 6	Summary, Conclusions and Recommendations	230
6.1	Summary	230
6.2	Recommendations for Future Work	237
6.3	Conclusions	238
	References	240
	Appendices	249
	Appendix A. Variance Reduction Function	249
	Appendix B. ForTRAN code for the developed RBSA model	251

List of Figures

Chapter 2 : Literature Review

Figure 2.1	: Typical schematic diagram of soil consolidation by PVDs	7
Figure 2.2	: Typical prefabricated vertical drain (courtesy: http://www.geosistem.com.id)	7
Figure 2.3	: Figure 2.3: Typical PVD installation rig (courtesy: http://www.soilwicks.com)	8
Figure 2.4	: Equivalent diameter of a PVD	9
Figure 2.5	: PVD installation layout and influence zone of individual drain	10
Figure 2.6	: Schematic diagram of soil cylinder with prefabricated vertical drain	17
Figure 2.7	: Radial piecewise constant permeability discretisation (after Walker 2006)	19
Figure 2.8	: Transformation of axisymmetric unit cell into a plane-strain condition (after Indraratna and Redana 1997)	24
Figure 2.9	: Uncertainty in estimation of soil properties (after Kulhawy 1992)	25
Figure 2.10	: Inherent soil variability (Phoon and Kulhawy 1999)	29
Figure 2.11	: Rough estimate of vertical scale of fluctuation (Vanmarcke 1977)	31

Chapter 3 Stochastic Modelling of Soil Consolidation by Vertical Drains

Figure 3.1	: Lognormal distribution plots with (a) constant standard deviation ($\sigma_X = 0.5$) and varying mean (b) constant mean ($\mu_X = 1.0$) and varying standard deviation	49
Figure 3.2	: Local average subdivision in two dimension (after Fenton and Griffiths 2008)	53
Figure 3.3	: Comparison of estimated and exact covariance structure of the LAS generated 2-D process, with (a) $\theta = 4$ and (b) $\theta = 0.5$ averaged over 10 realizations (after Fenton 1990)	54

Figure 3.4	: Typical realization of a random soil property field	62
Figure 3.5	: Geometric parameters and boundary conditions for unit cell analysis [Used by Hird et al. (1992)]	68
Figure 3.6	: Comparison of finite element and analytical results for consolidation of a unit cell (Modified after Hird et al. 1992)	69
Figure 3.7	: Geometric parameters and boundary conditions used for determining the minimum number of simulations and optimum mesh density	70
Figure 3.8	: Influence of mesh density on (a) μ_U and (b) σ_U	71
Figure 3.9	: Influence of number of simulations on (a) μ_U and (b) σ_U	73
Chapter 4	: Soil Spatial Variability in Design of Ground Improvement by Vertical Drains	
Figure 4.1	: Geometry of the consolidation problem for the analysis with no smear	77
Figure 4.2	: Finite element mesh of the selected consolidation problem (all elements being square in dimension: 0.05 m \times 0.05 m)	77
Figure 4.3	: Typical realization of a random permeability field for $v_k = 100\%$ and $\theta_k = 0.5$ ($\mu_k = 5 \times 10^{-10}$ m/sec)	80
Figure 4.4	: Comparison of the results defined by the excess pore water pressure and settlement for the effect of: (a) v_k on μ_U at $\theta_k = 0.5$; (b) θ_k on μ_U at $v_k = 100\%$	81
Figure 4.5	: Comparison of the results defined by the excess pore water pressure and settlement for the effect of: (a) v_k on σ_U at $\theta_k = 0.5$; (b) θ_k on σ_U at $v_k = 100\%$	82
Figure 4.6	: Effect of v_k on $\mu_{U(pp)}$ for (a) $\theta_k = 0.125$; (b) $\theta_k = 0.25$; (c) $\theta_k = 0.5$; (d) $\theta_k = 1.0$; (e) $\theta_k = 2.0$; and (f) $\theta_k = 4.0$	84
Figure 4.7	: Effect of v_k on $\sigma_{U(pp)}$ for (a) $\theta_k = 0.125$; (b) $\theta_k = 0.25$; (c) $\theta_k = 0.5$; (d) $\theta_k = 1.0$; (e) $\theta_k = 2.0$; and (f) $\theta_k = 4.0$	85
Figure 4.8	: Effect of θ_k on $\mu_{U(pp)}$ for (a) $v_k = 25\%$; (b) $v_k = 50\%$; (c)	86

	$v_k = 100\%$; (d) $v_k = 200\%$; and (e) $v_k = 400\%$	
Figure 4.9	: Effect of θ_k on $\sigma_{U(pp)}$ for (a) $v_k = 25\%$; (b) $v_k = 50\%$; (c) $v_k = 100\%$; (d) $v_k = 200\%$; and (e) $v_k = 400\%$	87
Figure 4.10	: Effect of v_k on (a) $\mu_{U(pp)}$ and (b) $\mu_{U^*(pp)}$ for $\theta_k = 0.25$	90
Figure 4.11	: Effect of v_k on (a) $\sigma_{U(pp)}$ and (b) $\sigma_{U^*(pp)}$ for $\theta_k = 2.0$	91
Figure 4.12	: Effect of θ_k on (a) $\mu_{U(pp)}$ and (b) $\mu_{U^*(pp)}$ for $v_k = 200\%$	92
Figure 4.13	: Effect of θ_k on (a) $\sigma_{U(pp)}$ and (b) $\sigma_{U^*(pp)}$ for $v_k = 400\%$	93
Figure 4.14	: Frequency density histograms and fitted distributions of: (a) U^*_{pp} and (b) U_{pp} , for $v_k = 200\%$, $\theta_k = 0.5$ at 67.9 days	95
Figure 4.15	: Frequency density histograms and fitted distributions of: (a) U^*_{pp} and (b) U_{pp} , for $v_k = 200\%$, $\theta_k = 2.0$ at 135.8 days	96
Figure 4.16	: Effect of v_k on $P[U \geq U_{90}]_{(pp)}$ for (a) $\theta_k = 0.125$; (b) $\theta_k = 0.25$; (c) $\theta_k = 0.5$; (d) $\theta_k = 1.0$; (e) $\theta_k = 2.0$; and (f) $\theta_k = 4.0$	98
Figure 4.17	: Effect of θ_k on $P[U \geq U_{90}]_{(pp)}$ for (a) $v_k = 25\%$; (b) $v_k = 50\%$; (c) $v_k = 100\%$; (d) $v_k = 200\%$; and (e) $v_k = 400\%$	99
Figure 4.18	: Effect of degree of anisotropy on $\mu_{U(pp)}$ for (a) $v_k = 50\%$; (b) $v_k = 100\%$; (c) $v_k = 200\%$; and (d) $v_k = 400\%$	103
Figure 4.19	: Effect of degree of anisotropy on $\sigma_{U(pp)}$ for (a) $v_k = 50\%$; (b) $v_k = 100\%$; (c) $v_k = 200\%$; and (d) $v_k = 400\%$	104
Figure 4.20	: Effect of degree of anisotropy on $P[U \geq U_{90}]_{(pp)}$ for (a) $v_k = 50\%$; (b) $v_k = 100\%$; (c) $v_k = 200\%$; and (d) $v_k = 400\%$	106
Figure 4.21	: Equivalent plane strain unit cell converted from axisymmetric unit cell shown in Fig. 4.1	109
Figure 4.22	: Typical realization of a random permeability field for a plane strain analysis with $v_k = 100\%$ and $\theta_k = 0.5$ ($\mu_k = 1.6 \times 10^{-10}$ m/sec)	109
Figure 4.23	: Comparison between the results from full and half unit cells (a) $\mu_{U(pp)}$ and (b) $\sigma_{U(pp)}$, for $v_k = 100\%$, $\theta_k = 0.125$	111
Figure 4.24	: Matching comparison for the effect of v_k on $\mu_{U(pp)}$ at (a) $\theta_k = 0.125$; (b) $\theta_k = 0.5$; (c) $\theta_k = 0.5$; (d) $\theta_k = 1.0$; (e) $\theta_k =$	112

	2.0; and (f) $\theta_k = 4.0$	
Figure 4.25	: Matching comparison for the effect of θ_k on $\mu_{U(pp)}$ at (a) $v_k = 25\%$; (b) $v_k = 50\%$; (c) $v_k = 100\%$; (d) $v_k = 200\%$; and (e) $v_k = 400\%$	113
Figure 4.26	: Matching comparison for the effect of v_k on $\sigma_{U(pp)}$ at (a) $\theta_k = 0.125$; (b) $\theta_k = 0.5$; (c) $\theta_k = 0.5$; (d) $\theta_k = 1.0$; (e) $\theta_k = 2.0$; and (f) $\theta_k = 4.0$	114
Figure 4.27	: Matching comparison for the effect of θ_k on $\sigma_{U(pp)}$ at (a) $v_k = 25\%$; (b) $v_k = 50\%$; (c) $v_k = 100\%$; (d) $v_k = 200\%$; and (e) $v_k = 400\%$	115
Figure 4.28	: Matching comparison for the effect of v_k on $P[U \geq U_{90}]_{(pp)}$ at (a) $\theta_k = 0.125$; (b) $\theta_k = 0.5$; (c) $\theta_k = 0.5$; (d) $\theta_k = 1.0$; (e) $\theta_k = 2.0$; and (f) $\theta_k = 4.0$	117
Figure 4.29	: Matching comparison for the effect of θ_k on $P[U \geq U_{90}]_{(pp)}$ at (a) $v_k = 25\%$; (b) $v_k = 50\%$; (c) $v_k = 100\%$; (d) $v_k = 200\%$; and (e) $v_k = 400\%$	118
Figure 4.30	: Effect of: (a) v on $\mu_{U(pp)}$ for $\theta = 2.0$; (b) θ on $\mu_{U(pp)}$ for $v = 100\%$	122
Figure 4.31	: Effect of: (a) v on $\sigma_{U(pp)}$ for $\theta = 2.0$; (b) θ on $\sigma_{U(pp)}$ for $v = 100\%$	123
Figure 4.32	: Effect of: (a) v on $P[U \geq U_{90}]_{(pp)}$ for $\theta = 2.0$; (b) θ on $P[U \geq U_{90}]$ for $v = 100\%$	124
Figure 4.33	: Typical example of frequency density histogram of simulated $U^*(t)$ with fitted lognormal distribution for $v_k = v_{m_v} = 200\%$, $\theta_k = \theta_{m_v} = 0.5$ at 271.6 days	125
Figure 4.34	: Effect of: (a) v on $\mu_{U(pp)}$ for $\theta = 2.0$; (b) θ on $\mu_{U(pp)}$ for $v_k = 100\%$, $v_{m_v} = 25\%$	126
Figure 4.35	: Effect of: (a) v on $P[U \geq U_{90}]_{(pp)}$ for $\theta = 2.0$; (b) θ on $P[U \geq U_{90}]$ for $v_k = 100\%$, $v_{m_v} = 25\%$	127
Figure 4.36	: Effect of: (a) v on $P[U \geq U_{90}]_{(pp)}$ for $\theta = 2.0$; (b) θ on $P[U \geq U_{90}]$ for $v_k = 100\%$, $v_{m_v} = 25\%$	128

Figure 4.37	:	Comparison of the results defined by the excess pore water pressure and settlement for the effect of v on (a) μ_U at $\theta = 1.0, \rho = 0.0$ and (b) μ_U at $\theta = 1.0, \rho = 1.0$	130
Figure 4.38	:	Comparison of the results defined by the excess pore water pressure and settlement for the effect of θ on (a) μ_U at $v = 100\%, \rho = 0.0$ and (b) μ_U at $v = 100\%, \rho = 1.0$	131
Figure 4.39	:	Comparison of the results defined by the excess pore water pressure and settlement for the effect of v on (a) σ_U at $\theta = 1.0, \rho = 0.0$ and (b) σ_U at $\theta = 1.0, \rho = 1.0$	132
Figure 4.40	:	Comparison of the results defined by the excess pore water pressure and settlement for the effect of θ on (a) σ_U at $v = 100\%, \rho = 0.0$ and (b) σ_U at $v = 100\%, \rho = 1.0$	133
Figure 4.41	:	Comparison of the results defined by the excess pore water pressure and settlement for the effect of v on (a) $P[U \geq U_{90}]$ at $\theta = 1.0, \rho = 0.0$ and (b) $P[U \geq U_{90}]$ at $\theta = 1.0, \rho = 1.0$	134
Figure 4.42	:	Comparison of the results defined by the excess pore water pressure and settlement for the effect of θ on (a) $P[U \geq U_{90}]$ at $v = 100\%, \rho = 0.0$ and (b) $P[U \geq U_{90}]$ at $v = 100\%, \rho = 1.0$	135
Figure 4.43	:	Comparison of the results obtained by $\rho = 0.0$ and $\rho = 1.0$ for the effect of: (a) v on μ_U at $\theta = 1.0$ and (b) θ on μ_U at $v = 100\%$	137
Figure 4.44	:	Comparison of the results obtained by $\rho = 0.0$ and $\rho = 1.0$ for the effect of: (a) v on σ_U at $\theta = 1.0$ and (b) θ on σ_U at $v = 100\%$	138
Figure 4.45	:	Comparison of the results obtained by $\rho = 0.0$ and $\rho = 1.0$ for the effect of: (a) v on $P[U \geq U_{90}]$ at $\theta = 1.0$ and (b) θ on $P[U \geq U_{90}]$ at $v = 100\%$	139
Figure 4.46	:	Geometry of the consolidation problem for the analysis considering smear	142
Figure 4.47	:	Typical realization of a random permeability field for $\nu_{k_u} = 100\%, \nu_{k_s} = 50\%, \theta_{k_u} = 1.0, \theta_{k_s} = 0.5$ ($\mu_{k_u} = 5 \times 10^{-10}$)	144

	m/sec and $\mu_{k_s} = 2.5 \times 10^{-10}$ m/sec)	
Figure 4.48	: Effect of ν_{k_u} and ν_{k_s} on μ_U for $\theta_{k_u} = \theta_{k_s} = 2.0$	146
Figure 4.49	: Effect of θ_{k_u} and θ_{k_s} on μ_U for $\nu_{k_u} = \nu_{k_s} = 100\%$	147
Figure 4.50	: Effect of ν_{k_u} and ν_{k_s} on σ_U for $\theta_{k_u} = \theta_{k_s} = 2.0$	148
Figure 4.51	: Effect of θ_{k_u} and θ_{k_s} on σ_U for $\nu_{k_u} = \nu_{k_s} = 100\%$	149
Figure 4.52	: Effect of ν_{k_u} and ν_{k_s} on $P[U \geq U_{90}]$ for $\theta_{k_u} = \theta_{k_s} = 2.0$	150
Figure 4.53	: Effect of θ_{k_u} and θ_{k_s} on $P[U \geq U_{90}]$ for $\nu_{k_u} = \nu_{k_s} = 100\%$	151
Figure 4.54	: Typical example of frequency density histogram of simulated $U^*(t)$ with fitted lognormal distribution for $\nu_{k_u} = 50\%$, $\nu_{k_s} = 100\%$, $\theta_{k_u} = \theta_{k_s} = 2.0$	152
Figure 4.55	: Effect of μ_{k_u} / μ_{k_s} on (a) μ_U (b) σ_U (c) $P[U \geq U_{90}]$ for $\nu_{k_u} = \nu_{k_s} = 100\%$, $\theta_{k_u} = \theta_{k_s} = 1.0$	154
Figure 4.56	: Effect of smear ratio, s , on (a) μ_U (b) σ_U (c) $P[U \geq U_{90}]$ for $\nu_{k_u} = \nu_{k_s} = 100\%$, $\theta_{k_u} = \theta_{k_s} = 1.0$	155
Figure 4.57	: Effect of ν_u and ν_s on μ_U for $\theta_u = \theta_s = 0.5$	158
Figure 4.58	: Effect of θ_u and θ_s on μ_U for $\nu_{k_u} = \nu_{k_s} = 100\%$, $\nu_{m_{v_u}} = \nu_{m_{v_s}} = 25\%$	159
Figure 4.59	: Effect of ν_u and ν_s on σ_U for $\theta_u = \theta_s = 0.5$	160
Figure 4.60	: Effect of θ_u and θ_s on σ_U for $\nu_{k_u} = \nu_{k_s} = 100\%$, $\nu_{m_{v_u}} = \nu_{m_{v_s}} = 25\%$	161
Figure 4.61	: Effect of ν_u and ν_s on $P[U \geq U_{90}]$ for $\theta_u = \theta_s = 0.5$	162
Figure 4.62	: Effect of θ_u and θ_s on $P[U \geq U_{90}]$ for $\nu_{k_u} = \nu_{k_s} = 100\%$, $\nu_{m_{v_u}} = \nu_{m_{v_s}} = 25\%$	163
Figure 4.63	: Typical example of frequency density histogram of simulated $U^*(t)$ with fitted lognormal distribution for $\nu_{k_u} = 50\%$, $\nu_{k_s} = 100\%$, $\nu_{m_{v_u}} = 12.5\%$, $\nu_{m_{v_s}} = 25\%$, $\theta_{k_u} = \theta_{k_s} =$	164

	$\theta_{m_{v_u}} = \theta_{m_{v_s}} = 0.5$ at 129.3 days	
Figure 4.64	: Effect of $\mu_{m_{v_s}} / \mu_{m_{v_u}}$ on (a) μ_U (b) σ_U (c) $P[U \geq U_{90}]$ for ν_u $= \nu_s = 100\%$, $\theta_u = \theta_s = 1.0$ ($\mu_{k_h} / \mu_{k_s} = 2.0$)	166
Chapter 5	: Reliability-Based Semi-Analytical Model for Soil Consolidation by Vertical Drains	
Figure 5.1	: Comparison between FEMC and RBSA: G1C1 for the effect of: (a) θ_u on $\mu_{\ln U^*}$ at fixed value of $\nu_k = 100\%$, $\nu_{m_v} = 25\%$, $\theta_s = 0.125$; (b) θ_s on $\mu_{\ln U^*}$ at fixed value of $\nu_k = 100\%$, $\nu_{m_v} = 25\%$, $\theta_u = 0.125$	201
Figure 5.2	: Comparison between FEMC and RBSA: G1C1 for the effect of: (a) ν_u on $\mu_{\ln U^*}$ at fixed value of $\nu_{k_s} = 50\%$, $\nu_{m_{v_s}} = 12.5\%$, $\theta = 0.5$; (b) ν_s on $\mu_{\ln U^*}$ at fixed value of $\nu_{k_u} = 50\%$, $\nu_{m_{v_u}} = 12.5\%$, $\theta = 0.5$	202
Figure 5.3	: Comparison between FEMC and RBSA: G1C1 for the effect of: (a) θ_u on $\sigma_{\ln U^*}$ at fixed value of $\nu_k = 100\%$, $\nu_{m_v} = 25\%$, $\theta_s = 0.125$; (b) θ_s on $\sigma_{\ln U^*}$ at fixed value of $\nu_k = 100\%$, $\nu_{m_v} = 25\%$, $\theta_u = 0.125$	203
Figure 5.4	: Comparison between FEMC and RBSA: G1C1 for the effect of: (a) ν_u on $\sigma_{\ln U^*}$ at fixed value of $\nu_{k_s} = 50\%$, $\nu_{m_{v_s}} = 12.5\%$, $\theta = 0.5$; (b) ν_s on $\sigma_{\ln U^*}$ at fixed value of $\nu_{k_u} = 50\%$, $\nu_{m_{v_u}} = 12.5\%$, $\theta = 0.5$	204
Figure 5.5	: Comparison between FEMC and RBSA: G1C1 for the effect of: (a) θ_u on $P[U \geq U_{90}]$ at fixed value of $\nu_k = 100\%$, $\nu_{m_v} = 25\%$, $\theta_s = 0.125$; (b) θ_s on $P[U \geq U_{90}]$ at fixed value of $\nu_k = 100\%$, $\nu_{m_v} = 25\%$, $\theta_u = 0.125$	206
Figure 5.6	: Comparison between FEMC and RBSA: G1C1 for the effect of: (a) ν_u on $P[U \geq U_{90}]$ at fixed value of $\nu_{k_s} =$	207

	50%, $\nu_{m_{v_s}} = 12.5\%$, $\theta = 0.5$; (b) ν_s on $P[U \geq U_{90}]$ at fixed value of $\nu_{k_u} = 50\%$, $\nu_{m_{v_u}} = 12.5\%$, $\theta = 0.5$	
Figure 5.7	: Comparison between FEMC and RBSA: G1C2 for the effect of: (a) θ on $\mu_{\ln U^*}$ for $\nu_k = 100\%$, $\nu_{m_v} = 25\%$; (b) ν on $\mu_{\ln U^*}$ for $\theta = 2.0$	209
Figure 5.8	: Comparison between FEMC and RBSA: G1C2 for the effect of: (a) θ on $\sigma_{\ln U^*}$ for $\nu_k = 100\%$, $\nu_{m_v} = 25\%$; (b) ν on $\sigma_{\ln U^*}$ for $\theta = 2.0$	210
Figure 5.9	: Comparison between FEMC and RBSA: G1C2 for the effect of: (a) θ on $P[U \geq U_{90}]$ for $\nu_k = 100\%$, $\nu_{m_v} = 25\%$; (b) ν on $P[U \geq U_{90}]$ for $\theta = 2.0$	211
Figure 5.10	: Comparison between FEMC and RBSA: G2C1 for the effect of: (a) θ_{k_u} on $\mu_{\ln U^*}$ at fixed value of $\nu_{k_u} = \nu_{k_s} = 100\%$, $\theta_{k_s} = 1.0$; (b) θ_{k_s} on $\mu_{\ln U^*}$ at fixed value of $\nu_{k_u} = \nu_{k_s} = 100\%$, $\theta_{k_u} = 1.0$	213
Figure 5.11	: Comparison between FEMC and RBSA: G2C1 for the effect of: (a) ν_{k_u} on $\mu_{\ln U^*}$ at fixed value of $\nu_{k_s} = 50\%$, $\theta_{k_u} = \theta_{k_s} = 2.0$; (b) ν_{k_s} on $\mu_{\ln U^*}$ at fixed value of $\nu_{k_u} = 50\%$, $\theta_{k_u} = \theta_{k_s} = 2.0$	214
Figure 5.12	: Comparison between FEMC and RBSA: G2C1 for the effect of: (a) θ_{k_u} on $\sigma_{\ln U^*}$ at fixed value of $\nu_{k_u} = \nu_{k_s} = 100\%$, $\theta_{k_s} = 1.0$; (b) θ_{k_s} on $\sigma_{\ln U^*}$ at fixed value of $\nu_{k_u} = \nu_{k_s} = 100\%$, $\theta_{k_u} = 1.0$	215
Figure 5.13	: Comparison between FEMC and RBSA: G2C1 for the effect of: (a) ν_{k_u} on $\sigma_{\ln U^*}$ at fixed value of $\nu_{k_s} = 50\%$, $\theta_{k_u} = \theta_{k_s} = 2.0$; (b) ν_{k_s} on $\sigma_{\ln U^*}$ at fixed value of $\nu_{k_u} = 50\%$, $\theta_{k_u} = \theta_{k_s} = 2.0$	216
Figure 5.14	: Comparison between FEMC and RBSA: G2C1 for the	217

	effect of: (a) θ_{k_u} on $P[U \geq U_{90}]$ at fixed value of $\nu_{k_u} = \nu_{k_s}$ $= 100\%$, $\theta_{k_s} = 1.0$; (b) θ_{k_s} on $P[U \geq U_{90}]$ at fixed value of $\nu_{k_u} = \nu_{k_s} = 100\%$, $\theta_{k_u} = 1.0$	
Figure 5.15	: Comparison between FEMC and RBSA: G2C1 for the effect of: (a) ν_{k_u} on $P[U \geq U_{90}]$ at fixed value of $\nu_{k_s} =$ 50% , $\theta_{k_u} = \theta_{k_s} = 2.0$; (b) ν_{k_s} on $P[U \geq U_{90}]$ at fixed value of $\nu_{k_u} = 50\%$, $\theta_{k_u} = \theta_{k_s} = 2.0$	218
Figure 5.16	: Comparison between FEMC and RBSA: G2C2 for the effect of: (a) θ on $\mu_{\ln U^*}$ for $\nu_k = 200\%$; (b) ν on $\mu_{\ln U^*}$ for θ $= 0.5$	220
Figure 5.17	: Comparison between FEMC and RBSA: G2C2 for the effect of: (a) θ on $\sigma_{\ln U^*}$ for $\nu_k = 200\%$; (b) ν on $\sigma_{\ln U^*}$ for θ $= 0.5$	221
Figure 5.18	: Comparison between FEMC and RBSA: G2C2 for the effect of: (a) θ on $P[U \geq U_{90}]$ for $\nu_k = 200\%$; (b) ν on $P[U$ $\geq U_{90}]$ for $\theta = 0.5$	222
Figure 5.19	: Comparison between (a) $\mu_{\ln U^*}$ (b) $\sigma_{\ln U^*}$ and (c) $P[U \geq U_{90}]$ obtained from FEMC, RBSA: G1C1 and RBSA: G1C3 for $\nu_{k_u} = \nu_{k_s} = 100\%$, $\nu_{m_u} = \nu_{m_s} = 25\%$, $\theta_{k_u} = \theta_{k_s} = \theta_{m_u}$ $= \theta_{m_s} = 1.0$	224
Figure 5.20	: Comparison between (a) $\mu_{\ln U^*}$ (b) $\sigma_{\ln U^*}$ and (c) $P[U \geq U_{90}]$ obtained from FEMC, RBSA: G2C1 and RBSA: G2C3 for $\nu_{k_u} = \nu_{k_s} = 100\%$, $\theta_{k_u} = \theta_{k_s} = 1.0$	226

List of Tables

Chapter 2	: Literature Review	
Table 2.1	: Auto-correlation functions (Vanmarcke 1977)	32
Table 2.2	: Coefficients of variation of different soil properties for summary data from (a) Lacasse and Nadim (1996) and (b) Lumb (1974) (after Beacher and Christian 2003)	36
Table 2.3	: Summary of scale of fluctuation of some geotechnical properties (after Phoon and Kulhawy 1999)	37
Chapter 3	Stochastic Modelling of Soil Consolidation by Vertical Drains	
Table 3.1	: Soil parameters of the problem used by Hird et al. (1992) and Equation (2.12)	69
Chapter 4	Soil Spatial Variability in Design of Ground Improvement by Vertical Drains	
Table 4.1	: Random field parameters for sensitivity analyses	79
Table 4.2	: Ranges of statistical parameters used in the analyses	120
Table 4.3	: Input parameters for parametric studies considering smear	142
Table 4.4	: Deterministic analyses under different smear zone parameters and the time required to achieve 90% consolidation	143
Table 4.5	: Random field parameters for parametric studies	144
Table 4.6	: Random field parameters for parametric studies	157
Chapter 5	Reliability-Based Semi-Analytical Model for Soil Consolidation by Vertical Drains	
Table 5.1	: Summary of the developed RBSA models	179
Table 5.2	: Random field parameters for the comparative study between FEMC and RBSA: G1C1	200

Table 5.3	: Random field parameters for the comparative study between FEMC and RBSA: G1C2	208
Table 5.4	: Random field parameters for the comparative study between FEMC and RBSA: G2C1	212
Table 5.5	: Random field parameters for the comparative study between FEMC and RBSA: G2C2	219

List of Symbols

ax	suffix used to represent parameters in axisymmetric condition
a_{vd}, b_{vd}	the width and thickness of the PVD, respectively
$[c]$	coupling matrix
c_h	horizontal coefficient of consolidation
c_v	vertical coefficient of consolidation
$\text{Cov}[\dots]$	covariance operator
d_m	diameter of the circle with an area equal to the cross-sectional area of the mandrel
d_s	diameter of the smear zone
$\delta_x, \delta_r, \delta_z$	displacements in the x , r and z directions, respectively
E	Young's modulus
E'	effective elastic Young's modulus
$E[\dots]$	expectation operator
F_n, F_s, F_r	drain spacing factor, smear factor and well resistance factor, respectively
F_{ns}	geometry/smear zone factor
F'_r	average well resistance factor over the entire drain length
$G(x)$	correlated standard normal random field with zero mean and unit variance
$G_k(x), G_{m_v}(x)$	independently generated standard normal random fields using the specified scale of fluctuation of permeability and compressibility, respectively
$G_{\ln k}(x)$	cross-correlated standard normal random field of k
$G_{\ln m_v}(x)$	cross-correlated standard normal random field of m_v
\bar{G}_k	arithmetic average of $G_k(i)$ over domain D
\bar{G}_{m_v}	arithmetic average of $G_{m_v}(i)$ over domain D
H_0	initial thickness of the compressible soil layer
i	element number, simulation number
k	coefficient of permeability of soil

k_h	coefficient of permeability in the horizontal direction
k_v	coefficient of permeability in the vertical direction
k_i	permeability of the i th element
k_x, k_r, k_z	soil permeability in the x , r and z directions, respectively
$[k_m]$	material stiffness matrix
$[\kappa]$	permeability matrix
\bar{k}	geometric average of compressibility over domain D
k_u, k_s	permeability coefficient of the undisturbed and smear zones, respectively
\bar{k}_u, \bar{k}_s	geometric average of k_u and k_s over domain D , respectively
L	maximum vertical drainage distance, length of the vertical drain
m	total number of elements in the mesh
m_v	coefficient of volume compressibility
\bar{m}_v	geometric average of permeability over domain D
m_{v_u}, m_{v_s}	coefficient of compressibility in the undisturbed and smear zones, respectively
$\bar{m}_{v_u}, \bar{m}_{v_s}$	geometric average of m_{v_u} and m_{v_s} over domain D , respectively
n	drain spacing ratio
n_{sim}	total number of simulations or realizations
pl	suffix used to represent parameters in plane strain condition
pp	suffix used to represent parameters based on excess pore water pressure
ρ_{XY}	cross-correlation coefficient between two random variables X and Y
ρ_{km_v}	cross-correlation coefficient between k and m_v
q_w	vertical discharge capacity of the drain
r_e	radius of the equivalent soil cylinder, radius of the influence zone
r_w	equivalent radius of the drain
r_s	radius of the smear zone
S	spacing of the vertical drain
s	smear zone ratio
S_c	consolidation or primary compression settlement

S_i	immediate (elastic) settlement
S_s	secondary compression settlement
S_t	total settlement
set	suffix used to represent parameters based on settlement
\bar{s}_u	average long-term settlement
$\bar{s}(t)$	average settlement at any time t
T_h	“time factor” for horizontal drainage
t	consolidation time
t_{D90}	time for deterministic 90% consolidation
$U(t)$	degree of consolidation at time t
$U_h(t)$	horizontal degree of consolidation at time t
U_{90}	90% target degree of consolidation
$U^*(t)$	natural logarithm of $[1 / (1-U(t))]$
u	excess pore water pressure
u_0	initial (uniform) excess pore water pressure
$u(t)$	excess pore pressure at any spatial location at time t
$\bar{u}(t)$	average excess pore water pressure at a given time t
W	ratio of \bar{k}_u to \bar{k}_s
V	ratio of $\bar{k}_{m_{v_s}}$ to $\bar{k}_{m_{v_u}}$
X_a	arithmetic average of a random soil parameter X
X_g	geometric average of a random soil parameter X
X_h	harmonic average of a random soil parameter X
z	depth from the top of the consolidating soil layer
γ_w	unit weight of water
$\Delta\sigma'$	increment in the effective stress
ν	Poisson’s ratio
ν'	effective Poisson’s ratio
v	coefficient of variation
v_X	coefficient of variation of variable X
v_k	coefficient of variation of permeability
v_{m_v}	coefficient of variation of volume compressibility

ν_{k_u}, ν_{k_s}	coefficient of variation permeability in the undisturbed and smear zone, respectively
$\nu_{\bar{k}_u}, \nu_{\bar{k}_s}$	coefficient of variation of \bar{k}_u and \bar{k}_s , respectively
$\nu_{m_{v_u}}, \nu_{m_{v_s}}$	coefficient of variation compressibility in the undisturbed and smear zone, respectively
$\nu_{\bar{m}_{v_u}}, \nu_{\bar{m}_{v_s}}$	coefficient of variation of \bar{m}_{v_u} and \bar{m}_{v_s} , respectively
γ_w	unit weight of water
α	a group parameter representing the smear effects and geometry of the PVD system
α^*	modified α parameter for the piecewise constant distribution of soil parameters across the unit cell
α_{ns}	modified geometry/smear zone factor for the piecewise constant distribution of soil parameters across the unit cell
α_r	modified well resistance factor for the piecewise constant distribution of soil parameters across the unit cell
α_{m_v}	smear zone compressibility parameter introduced by Walker (2006)
$\bar{\alpha}$	equivalent α parameter of the spatially variable soil
$\bar{\alpha}_{m_v}$	equivalent α_{m_v} parameter of the spatially variable soil
$\gamma(D)$	variance function giving variance reduction due to averaging over domain D
$\gamma(D)_{k_u}$	variance reduction factor for k_u due to averaging over domain D
$\gamma(D)_{k_s}$	variance reduction factor for k_s due to averaging over domain D
$\gamma(D)_{m_{v_u}}$	variance reduction factor for m_{v_u} due to averaging over domain D
$\gamma(D)_{m_{v_s}}$	variance reduction factor for m_{v_s} due to averaging over domain D
θ	correlation length or scale of fluctuation
θ_k	correlation length or scale of fluctuation of the random permeability field
$\theta_{k_u}, \theta_{k_s}$	scale of fluctuation for k_u and k_s , respectively
θ_{m_v}	scale of fluctuation of the random compressibility field
$\theta_{m_{v_u}}, \theta_{m_{v_s}}$	scale of fluctuation for m_{v_u} and m_{v_s} , respectively

μ	mean or expected value
μ_X	mean value of variable X
μ_k	mean of the lognormally distributed permeability
$\mu_{\ln k}$	mean of the underlying normally distributed permeability
$\mu_{\ln \bar{k}}$	mean of the logarithm of \bar{k}
μ_{k_u}, μ_{k_s}	mean of the lognormally distributed k_u and k_s , respectively
$\mu_{\ln k_u}, \mu_{\ln k_s}$	mean of the underlying normally distributed k_u and k_s , respectively
$\mu_{\bar{k}_u}, \mu_{\bar{k}_s}$	mean of \bar{k}_u and \bar{k}_s , respectively
$\mu_{\ln \bar{k}_u}, \mu_{\ln \bar{k}_s}$	mean of the logarithm of \bar{k}_u and \bar{k}_s , respectively
μ_{m_v}	mean of the lognormally distributed compressibility
$\mu_{\ln m_v}$	mean of the underlying normally distributed compressibility
$\mu_{\ln \bar{m}_v}$	mean of the logarithm of \bar{m}_v
$\mu_{m_{v_u}}, \mu_{m_{v_s}}$	mean of the lognormally distributed m_{v_u} and m_{v_s} , respectively
$\mu_{\ln m_{v_u}}, \mu_{\ln m_{v_s}}$	mean of the underlying normally distributed m_{v_u} and m_{v_s} , respectively
$\mu_{\bar{m}_{v_u}}, \mu_{\bar{m}_{v_s}}$	mean of \bar{m}_{v_u} and \bar{m}_{v_s} , respectively
$\mu_{\ln \bar{m}_{v_u}}, \mu_{\ln \bar{m}_{v_s}}$	mean of the logarithm of \bar{m}_{v_u} and \bar{m}_{v_s} , respectively
μ_U	mean of the degree of consolidation U
μ_{U^*}	mean of the degree of consolidation function U^*
$\mu_{\ln U^*}$	mean of the logarithm U^*
μ_W	mean of W
$\mu_{\ln W}$	mean of the logarithm of W
μ_V	mean of V
$\mu_{\ln V}$	mean of the logarithm of V
$\mu_{\bar{\alpha}}$	mean of $\bar{\alpha}$
$\mu_{\ln \bar{\alpha}}$	mean of the logarithm of $\bar{\alpha}$
$\mu_{\bar{\alpha}_{m_v}}$	mean of $\bar{\alpha}_{m_v}$
$\mu_{\ln \bar{\alpha}_{m_v}}$	mean of the logarithm of $\bar{\alpha}_{m_v}$

σ	standard deviation
σ^2	point variance
σ_X	standard deviation of variable X
σ_X^2	variance of variable X
σ_k	standard deviation of the lognormally distributed permeability
$\sigma_{\ln k}$	standard deviation of the underlying normally distributed permeability
$\sigma_{\ln \bar{k}}$	standard deviation of the logarithm of \bar{k}
$\sigma_{k_h}, \sigma_{k_s}$	standard deviation of the lognormally distributed k_u and k_s , respectively
$\sigma_{\ln k_h}, \sigma_{\ln k_s}$	standard deviation of the underlying normally distributed k_u and k_s , respectively
$\sigma_{\bar{k}_u}, \sigma_{\bar{k}_s}$	standard deviation of \bar{k}_u and \bar{k}_s , respectively
$\sigma_{\ln \bar{k}_u}, \sigma_{\ln \bar{k}_s}$	standard deviation of the logarithm of \bar{k}_u and \bar{k}_s , respectively
σ_{m_v}	standard deviation of the lognormally distributed compressibility
$\sigma_{\ln m_v}$	standard deviation of the underlying normally distributed compressibility
$\sigma_{\ln \bar{m}_v}$	standard deviation of the logarithm of \bar{m}_v
$\sigma_{m_{v_u}}, \sigma_{m_{v_s}}$	standard deviation of the lognormally distributed m_{v_u} and m_{v_s} , respectively
$\sigma_{\ln m_{v_u}}, \sigma_{\ln m_{v_s}}$	standard deviation of the underlying normally distributed m_{v_u} and m_{v_s} , respectively
$\sigma_{\bar{m}_{v_u}}, \sigma_{\bar{m}_{v_s}}$	standard deviation of \bar{m}_{v_u} and \bar{m}_{v_s} , respectively
$\sigma_{\ln \bar{m}_{v_u}}, \sigma_{\ln \bar{m}_{v_s}}$	standard deviation of the logarithm of \bar{m}_{v_u} and \bar{m}_{v_s} , respectively
σ_U	standard deviation of the degree of consolidation U
σ_{U^*}	standard deviation of the degree of consolidation function U^*
$\sigma_{\ln U^*}$	standard deviation of the logarithm U^*
σ_W	standard deviation of W
σ_V	standard deviation of V
$\sigma_{\ln W}$	standard deviation of the logarithm of W

$\sigma_{\ln V}$	standard deviation of the logarithm of V
$\sigma_{\bar{\alpha}}$	standard deviation of $\bar{\alpha}$
$\sigma_{\ln \bar{\alpha}}$	standard deviation of the logarithm of $\bar{\alpha}$
$\sigma_{\bar{\alpha}_{m_v}}$	standard deviation of $\bar{\alpha}_{m_v}$
$\sigma_{\ln \bar{\alpha}_{m_v}}$	standard deviation of the logarithm of $\bar{\alpha}_{m_v}$
$\rho(\tau)$	correlation function giving correlation between two points in the log-soil property field
τ	absolute distance between two points in the soil domain
$P(.)$	probability of its argument
$\Phi(.)$	standard normal cumulative distribution function

Abbreviations

AS	Axisymmetric solution
CMD	Covariance matrix decomposition
COV	Coefficient of variation
FEM	Finite element method
FEMC	Finite-element Monte-Carlo
FFT	Fast Fourier transform method
FOSM	First order second moment method
LAS	Local average subdivision
MCS	Monte Carlo simulation
PDF	Probability density function
PEM	Point estimate method
PS	Plane strain solution
PVD	Prefabricated vertical drain
RBSA	Reliability-based semi-analytical
SOF	Scale of fluctuation
TBM	Turning band method

Chapter 1

Introduction

Unfortunately, soils are made by nature and not by man, and the products of nature are always complex ... As soon as we pass from steel and concrete to earth, the omnipotence of theory ceases to exist. Natural soil is never uniform. Its properties change from point to point while our knowledge of its properties are limited to those few spots at which the samples have been collected ...

Karl Terzaghi (1936)

1.1 Preface

Over the past decade or so, the development activities in areas of soft soils have increased significantly in order to suit the demands of increased population in many countries and to ensure marginal use of limited land space. Construction over soft soils, which have low bearing capacity and excessive compressibility, often requires a pre-construction treatment of the existing soft subsoils in order to improve soil strength and stiffness, thus, eliminating the undue risks of excessive post construction deformations and associated instability.

Although a number of soft soil stabilization techniques are currently available, the use of prefabricated vertical drains (PVDs) with preloading has become the most popular as it is cost effective and environmentally friendly (Indraratna et al. 2003). Despite the fact that the theoretical design aspects of soil consolidation by PVDs are well established (e.g. Barron 1948; Hansbo 1981; Hird et al. 1992), satisfactory agreement between the theoretical predictions of soil consolidation and actual observed values is hardly achieved, especially for heterogeneous soils. This is mainly due to the deterministic nature of available design solutions in which the consolidating soil deposits are assumed to be homogeneous with constant values of soil properties across the soil mass. In reality, however, soils are seldom homogeneous and it is well documented that soil properties show significant variation in spatial directions and potentially induce uncertainty in their characterization (Vanmarcke 1984). The inherent variation of soil properties with

respect to spatial location is known as soil spatial variability, which is due to the uneven soil micro fabric, complex characteristics of geological deposition and stress history.

The degree of consolidation achieved by PVDs is greatly controlled by some soil properties (e.g. soil permeability and volume compressibility) that are highly variable from one point to another in the ground. The fact that spatial variation of soil properties can affect soil consolidation has long been recognised by several researchers. For example, Rowe (1972) indicated that reliable prediction of consolidation rates in soil deposits is difficult due to the variability of soil properties and fabric. Zhou et al. (1999) noted that the variability of coefficient of consolidation may result in untimely and unsatisfactory degrees of consolidation, which in turn leads to delays in the construction process and cost overruns. Rankine et al. (2005) reported a case study of a trial embankment that was built for the purpose of pre-consolidation of soft, organic clay by PVDs along the Sunshine Coast Motorway in South East Queensland, Australia. In this case study, it was found that the assumption of a single homogeneous soil layer used in the numerical modelling contributed to predicted settlements different from the field values. Consequently, unless soil spatial variability is considered in the treatment of soil consolidation via PVDs, the whole ground improvement process may be either unsuccessful or entirely uneconomic. The problem of ground heterogeneity (or soil spatial variability) in geotechnical engineering has been traditionally dealt with by assuming high safety factors, usually obtained from local experience and engineering judgement (Elkateb et al. 2002). However, the design based on the concept of safety factor does not provide much physical insight into the possibility of occurring undesirable events (Griffiths et al. 2002). Therefore, geotechnical analysis and design based on single “average” values of soil properties is insufficient, and information computing variability and uncertainty must also be incorporated into them.

In recent years, the significance of soil spatial variability in relation to risk and decision-making has received considerable attention in the geotechnical engineering community and efforts are being made to develop supplementary attempts to the factor of safety approach. In general, to acknowledge and quantify soil spatial variability in geotechnical engineering analysis and design, probabilistic modelling

by treating the soil properties as random variables is ideal. The primary objective of the probabilistic modelling is to relate the reliability of the geotechnical structures to the variability in the design soil parameters for the sake of making a rational decision.

Probabilistic methods to assess the influence of soil spatial variability on the estimated performance of geotechnical structures are becoming increasingly popular among engineers, and have been recently implemented in many geotechnical engineering problems. The review of relevant literature has indicated that although the significance of soil spatial variability in relation to ground improvement by PVDs has long been realized, it has never been previously considered in a systematic, scientific manner in design and little research has been done in this area. Given the complexity of the problem, available research into consolidation of highly variable soils has been limited to the following two categories: (i) one-dimensional consolidation of vertical drainage, i.e. no PVDs (e.g. Badaoui et al. 2007; Chang 1985; Freeze 1977; Hong 1992; Huang et al. 2010; Hwang and Witczak 1984); and (ii) soil consolidation by PVDs only considering the uncertainty associated with the testing errors in measuring the soil properties, and the inherent spatial variability of soil properties is not accounted for (e.g. Hong and Shang 1998; Zhou et al. 1999). Accordingly, there is an immense need to consider and include the effects of soil spatial variability in the treatment of ground improvement by PVDs and this study will essentially fill in this gap.

1.2 Objectives and Scope of the Study

This research has aimed to investigate and quantify the effects of soil spatial variability on soil consolidation by PVDs using a stochastic framework and to propose reliability based design methodologies for ground improvement by vertical drains. The results of this research will provide a better understanding and valuable insights into the impact of soil spatial variability on soil consolidation via PVDs. The overall aims of this research can be summarized as follows:

1. To quantify and evaluate the impact of spatial variability of soil properties on the amount of ground improvement by PVDs, including the variation and spatial correlation of soil permeability and volume compressibility, and cross-correlation between soil permeability and volume compressibility;

2. To develop advanced numerical models and computer algorithms based on stochastic finite element continuum mechanics, random field theory and Monte Carlo framework. The developed models underpin improved design of PVDs through explicit incorporation of the salient features of soil spatial variability and enhance our conceptual understanding of the mechanism of ground improvement by PVDs in highly variable soils;
3. To develop a simplified reliability-based semi-analytical (RBSA) model that allow the probability of achieving target consolidation rates within specified timeframe to be readily obtained from known or assumed statistical parameters of spatially variable soil properties, enabling the level of risk associated with the design to be quantified. The RBSA model can be considered as an alternative easy-to-use tool to replace the computationally intensive finite-element Monte-Carlo (FEMC) approach, for routine use by the practitioners. Computer codes will also be developed for the RBSA method to promote frequent use of the results and inferences gained through this research.

1.3 Organization of the Thesis

The dissertation is organized into five chapters apart from this first chapter. An overview of the work presented in each chapter is described as follows.

Following this introductory chapter, Chapter 2 presents a comprehensive survey of the literature associated with the present work. The history and development of vertical drains, factors that affect the efficacy of consolidation by vertical drains and present theories related to soil consolidation are reviewed in detail. In the same chapter, different elements of soil inherent spatial variability, such as mean, variance, characteristics of spatial correlation, local averaging and variance relationships and typical spatial variability parameters for various soil properties are thoroughly discussed together with their implications in relation to geotechnical analysis and design. Some of the most commonly used approaches adopted throughout the history of geotechnical engineering to perform stochastic soil consolidation analyses are thoroughly reviewed and criticized. Majority of previous works that dealt with

probabilistic soil consolidation are described in some detail with emphasis on their limitations to identify the scope of the present work.

Chapter 3 describes the stochastic approach used for the work presented in this dissertation to predict the probabilistic behaviour of soil consolidation by PVDs by taking into account soil spatial variability. This includes the procedures for simulation of spatially random soil profiles, the formulation and validation of the finite element consolidation analysis model, and some important aspects related to Monte Carlo simulation particularly the effect of mesh density and number of Monte Carlo simulation on the accuracy of the results of the finite element analysis.

Chapter 4 utilizes the stochastic approach described in Chapter 3 to perform parametric studies for investigating and quantifying the effects of soil variability on the reliability of the predicted consolidation rates under various different assumed site conditions such as, inclusion of the smear effect, unit cell geometries and isotropic versus anisotropic modelling. The obtained consolidation responses under those conditions are examined in terms of the statistics of the degree of consolidation and probability of achieving a target degree of consolidation at specified time frame, and comparisons among those conditions are elucidated, where applicable.

In Chapter 5, an approximate, easy-to-use reliability-based semi-analytical (RBSA) model for estimating the probability of achieving a target degree of consolidation is developed as an alternative tool to replace the computationally intensive stochastic finite element modelling. The performance function of the proposed RBSA model is based on the well-known deterministic equation proposed by Hansbo (1981), which only considers soil consolidation due to horizontal drainage. The proposed model is verified against the results obtained from the stochastic numerical simulations and is found to be in a good agreement with those obtained from the numerical simulations.

The summary of the research work, conclusions and recommendations for further studies are presented in Chapter 6. Finally, a list of references and appendices are given, following Chapter 6.

Chapter 2

Literature Review

2.1 Introduction

The formulation and solution of stochastic problems are often very complicated. Despite this complexity, stochastic models of geotechnical engineering problems are becoming increasingly common, simply because soil properties are spatially random. This trend is driven by expanded knowledge about the variability of natural soils and by recent innovations in tools which can capture this knowledge for use in reliability or risk analyses. In order to study the probabilistic nature of the behaviour of soil consolidation by prefabricated vertical drains (PVDs), a detailed cross-disciplinary knowledge is required. This includes an understanding of the fundamentals of soil consolidation, the characteristics of PVDs, the theory of probability and statistics, and the random field theory. Accordingly, the aim of this chapter is to provide an overview of the relevant literature and to present a background for this thesis. It is not intended to cover every piece of literature on soil consolidation; rather it is meant to broadly view the more important aspects of soil consolidation in relation to the present research.

2.2 Purpose, History and Application of Prefabricated Vertical Drains

Soft soils (e.g. estuarine and marine clays) are renowned for their low bearing capacity and excessive compressibility. Preloading is one of the oldest and most popular ways to pre-consolidate and strengthen such poor soils. This involves applying a surcharge load, usually in the form of an embankment or vacuum pressure, prior to construction until most of the primary consolidation is achieved. However, for thick soil deposits with low permeability, preloading alone can take considerably long time to achieve the required degree of consolidation. Under these circumstances, a system of PVDs is often introduced to accelerate the rate of consolidation, which is inversely proportional to the square of the length of drainage path. Installing PVDs into the ground means much shorter radial drainage paths and therefore less water flow resistance in the compressible soil mass. Thus the consolidation time is

significantly reduced. A typical scheme of soil consolidation by PVDs is illustrated in Fig. 2.1.

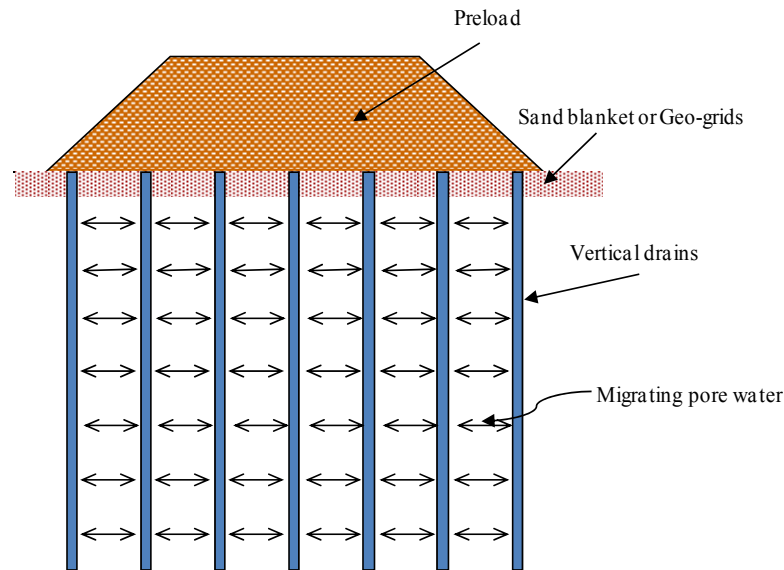


Figure 2.1: Typical schematic diagram of soil consolidation by PVDs

Prefabricated vertical drains were patented in Sweden in the late 1930s. Their use has increased since the mid-1980s. As shown in Fig. 2.2, a PVD comprises a solid plastic core (the band-shaped type is most commonly used) lined with a permeable geo-textile filter jacket. The PVD is generally 100 mm wide by 3-4 mm thick (Bo et al. 2003).



Figure 2.2: Typical prefabricated vertical drain
(courtesy: <http://www.geosistem.com.id>)

Depending on the site, prefabricated vertical drains can be installed using either a static or a dynamic method. In the static case, the steel mandrel is inserted into the soil using a static force, whereas in the dynamic case, the mandrel is driven into the ground by means of either a conventional drop hammer or a vibrating hammer. The static penetration method is more common than the dynamic one as the dynamic method creates greater disturbance to the closely-surrounding soil. A typical installation rig is shown in Fig. 2.3, where a vertical drain is driven into soft ground using a mandrel hoisted by a crane.



Figure 2.3: Typical PVD installation rig
(courtesy: <http://www.soilwicks.com>)

2.3 Characteristics of Vertical Drain Systems

2.3.1 Equivalent drain diameter for prefabricated vertical drains

The conventional theory used to predict the consolidation behaviour around vertical drains assumes that the drain cross-section is circular (Barron 1948). Since the drain is originally band-shaped, it needs to be converted to an equivalent circular diameter in order to retain the same theoretical radial drainage capacity. Kjellman (1948) stated that this capacity depends on the circumference of the cross-section rather than the cross-sectional area. Based on this, Hansbo (1981) established the equivalent diameter for a prefabricated band-shaped drain (d_w) by assuming that the equivalent

cylindrical drain has the same circumference as the band-shaped unit, as per the following equation:

$$d_w = 2 \frac{(a_{vd} + b_{vd})}{\pi} \quad (2.1)$$

Subsequent to this, Rixner et al. (1986) studied soil consolidation by PVDs, based on a finite element approach, and suggested the more appropriate d_w as given in Eq. 2.2.

$$d_w = \frac{(a_{vd} + b_{vd})}{2} \quad (2.2)$$

where: a_{vd} and b_{vd} , respectively, are the width and thickness of the PVD. The geometric parameters for the original band-shaped drain and a hypothetical cylindrical drain are shown in Fig. 2.4

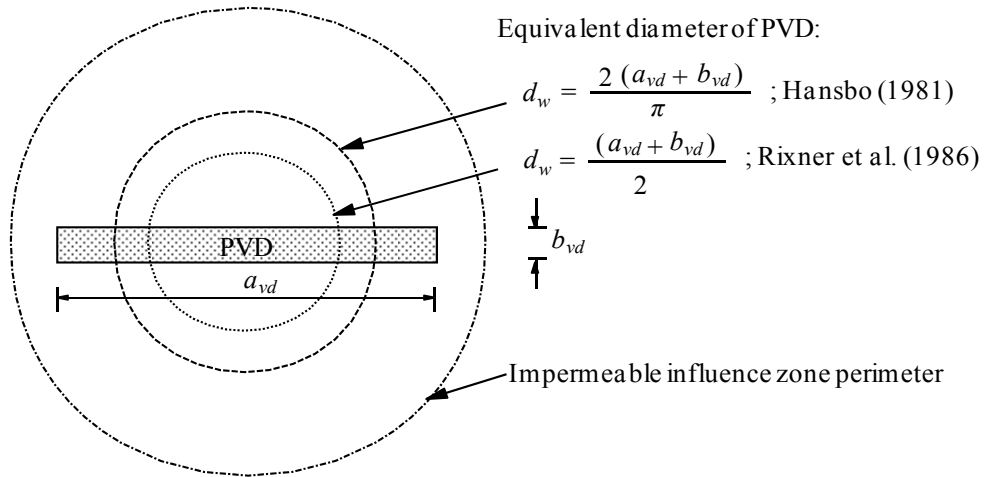


Figure 2.4: Equivalent diameter of a PVD

2.3.2 Radius of influence zone

In practice, PVDs can be installed in a square or triangular fashion (Fig. 2.5). However, a single-drain analysis is often sufficient to investigate the overall consolidation behaviour of soil (Indraratna and Redana 2000). To determine the influence zone of an individual PVD, an equivalent circular area equal to the area of

a square or hexagon is employed. The equivalent influence zone radius (r_e) of an individual PVD is therefore a function of the drain spacing (S) and can be given by:

$$r_e = 0.565 S \text{ for square pattern installation, and} \quad (2.3)$$

$$r_e = 0.525 S \text{ for triangular pattern installation} \quad (2.4)$$

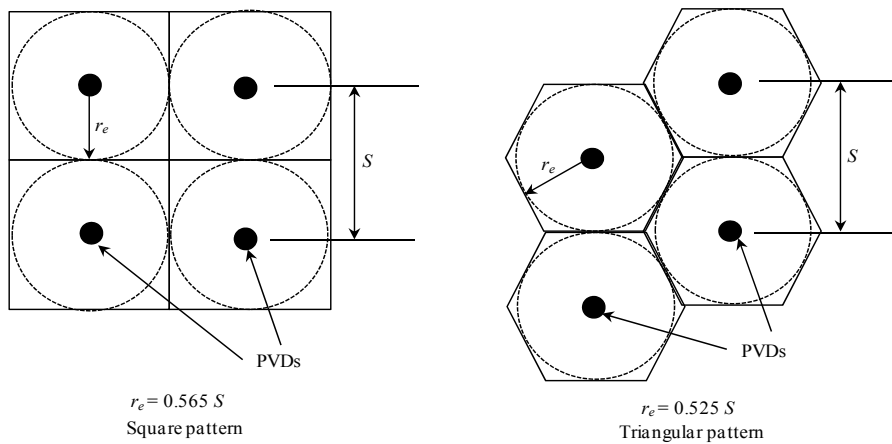


Figure 2.5: PVD installation layout and influence zone of individual drain

Although a square pattern installation of PVDs is easier to implement in the field, a triangular one is usually preferred as it gives a more uniform consolidation between the drains.

2.4 Factors Affecting Performance of PVDs

The PVD performance is affected by factors such as smear (soil disturbance) effect, discharge capacity and well resistance, drain spacing ratio and smear zone ratio. In general, the main factors affecting the performance of PVD are the soil smear and well resistance. Thus a basic understanding of soil smear and well-resistance is essential.

2.4.1 Smear effect

During the installation of PVDs, successive driving and pulling of the mandrel casing significantly distorts and remoulds the soil immediately adjacent to the drain. This is

called the smear effect, and it significantly affects the rate of radial consolidation. In the smear zone, permeability is reduced and compressibility increased. The extent of smearing depends on the mandrel size, installation procedure and soil type (Bo et al. 2003; Eriksson et al. 2000; Lo 1998). The shape of the smear zone around a rectangular PVD is roughly elliptical (Indraratna and Redana 1998; Welker et al. 2000) while it is circular around sand drains. In general, the extremity of the smear zone from the drain periphery depends on the total mandrel cross-sectional area and the shape of the anchor. Jamiolkowski and Lancellotta (1981) proposed that the diameter of the smear zone (d_s) and diameter of the circle (d_m) with an area equal to the cross-sectional area of the mandrel can be related as follows:

$$d_s = (2.5 \text{ to } 3) d_m \quad (2.5)$$

Based on large-scale laboratory testing carried out by Indraratna and Redana (1998), the relationship between the radius of the smear zone (r_s) and the equivalent radius of the drain (r_w) was proposed as follows:

$$r_s = (4 \text{ to } 5) r_w \quad (2.6)$$

The combined effect of reduced permeability and increased compressibility within the smear zone brings a different behaviour from that of the undisturbed soil. Hence there can be no accurate prediction of the behaviour of soil stabilised with PVDs if the smear effect is ignored. A number of researchers have indicated that this disturbance is spatially variable (Bergado et al. 1991; Bo et al. 2003; Chai and Miura 1999; Hird and Moseley 2000; Indraratna and Redana 1998; Sharma and Xiao 2000). Barron (1948), however, proposed the concept of reduced permeability, which is equivalent to lowering the overall value of the coefficient of consolidation. Hansbo (1979; 1981) also modelled the smear as a zone with spatially constant reduced-value of permeability. In that zone, the horizontal permeability close to the drain can be reduced by one order of magnitude (Bo et al. 2003) and is often assumed to be the same as the vertical permeability (Hansbo 1981; Indraratna and Redana 1998). The latter remains relatively unchanged. The ratio of the horizontal to vertical permeability (k_h / k_v) approaches unity at the drain soil interface (Indraratna and Redana 1998). For various undisturbed soils k_h / k_v varies between 1.36 and 2

(Bergado et al. 1991; Shogaki et al. 1995; Tavenas et al. 1983), whereas in the smear zone the ratio varies between 0.9 and 1.3 (Indraratna and Redana 1998). On the basis of laboratory experiments, Indraratna and Redana (1997) concluded that the ratio of horizontal permeability of soil in the undisturbed zone (k_h) to the horizontal permeability of soil in the smear zone (k_s) is approximately 1.5–2.0. However, depending on the type of drain, type of soil, and installation procedures, this ratio can vary from 1.5 to 5 (Saye 2003).

2.4.2 Discharge capacity and well resistance

PVDs are used to discharge water in soil. The term ‘discharge capacity of PVD’ is used to describe the rate of flow of water along the drain. Generally speaking, the higher the discharge capacity, the more effective the drain. The typical discharge capacity of most commercial PVDs is at least 150 m³/year and it can reach 500 m³/year (Bo et al. 2003). In practice, however, many factors can affect the value of PVDs discharge capacity. The drain might clog with fine soil grains, large soil settlement may cause bending and twisting of the drain, biological and chemical degradation and drain folding may also occur. If the discharge capacity of the PVD is less than the water volume to be discharged, well-resistance will result and this could retard the rate of consolidation. Based on laboratory experiments, Chai and Miura (1999) concluded that the discharge capacity of a PVD reduces significantly over time. Nevertheless, well-resistance does not seem to have an appreciable impact on soil consolidation unless the drains are very long and subjected to high lateral stresses (Bo et al. 2003). Holtz et al. (1989) concluded that if the working discharge capacity of PVDs exceeds 150 m³/year, the effect of well-resistance becomes insignificant and can be ignored.

2.5 Fundamentals of Soil Consolidation

2.5.1 Settlement of soil

When a compressive load is applied to a soil mass, there is a decrease in its volume. Conventionally, soil deformation can be divided into three components: immediate (elastic) settlement (S_i), consolidation or primary compression settlement (S_c), and

secondary compression settlement (S_s). The total settlement (S_t) of a loaded soil is the sum of these, that is:

$$S_t = S_i + S_e + S_s \quad (2.7)$$

The characteristics of the three settlement components are:

- (a) Immediate or elastic settlement (S_i): This occurs immediately after the load is applied. It is primarily due to a decrease in the volume of voids resulting from grain distortion, and changes in the relative position of the soil particles. In cohesive soils this settlement is assumed to occur without any change in volume.
- (b) Consolidation or primary compression (S_e): When a saturated soil mass is subjected to an incremental pressure, excess pore water pressure will develop, which dissipates over a long period of time as the water drains from the soil voids. It results in volume changes and is known as consolidation or primary compression. It is the largest component of soft soil settlement.
- (c) Secondary compression (S_s): This component of settlement is due to decomposition of soil particles, with no change in applied stresses and without a dissipation of excess pore pressure. In reality, both primary and secondary compression can occur simultaneously. However, for simplicity, it can be assumed that secondary compression occurs after primary consolidation (Mesri and Choi 1985). This settlement seems to be greater in organic soils and highly plastic clays. However, it is usually negligible in most soils, particularly sands and gravels.

2.5.2 Soil consolidation

Permeability plays a significant role in the consolidation behaviour of soils. For soil with low-permeability (fine grained soil), consolidation settlement is predominant. If the soil is laterally confined (negligible lateral deformations), then only the Terzaghi-type one-dimensional (1D) consolidation is expected. The assumptions of 1D consolidation (will be described later in the following section) are generally valid for embankments wider than the thickness of compressible soil layer. The consolidation

settlement is obtained from a soil property called the coefficient of volume compressibility, m_v , which can be measured from the pressure-void ratio ($e-\sigma'$) curve. The coefficient of volume compressibility is a measure of the compressibility of soft soil and is defined as the change in volume of soil per unit of initial volume due to a given unit increase in the pressure.

For one-dimensional consolidation, the consolidation settlement, S_c , can be calculated from the following expression:

$$S_c = m_v H_0 \Delta\sigma' \quad (2.8)$$

where: m_v , H_0 , and $\Delta\sigma'$ are, respectively, the coefficient of volume compressibility, initial thickness of the compressible layer and increment in the effective stress.

2.6 Theory of Vertical Consolidation

2.6.1 Terzaghi's theory of one-dimensional consolidation

The theory of one-dimensional (1D) consolidation presented by Terzaghi (1943), is often used to estimate the rate of consolidation settlement and excess pore pressure dissipation in low-permeability soils. In the development of the mathematical expression of the theory, the following simplifying assumptions are made: (a) the soil is homogeneous and fully saturated and obeys linear stress-strain relationships; (b) both soil and water are incompressible; (c) the small strain theory and Darcy's law for the velocity of flow of water through the soil is valid; (d) pore water drains out only in the vertical direction; (e) the coefficient of permeability is assumed to be constant during the consolidation process; (f) the deformation of the soil is due entirely to change in volume; and (g) there is no secondary consolidation during soil settlement.

Based on the above assumptions, Terzaghi (1943) established the following differential equation to estimate the rate of dissipation of excess pore water pressure, u , at a certain time t and depth z :

$$\frac{\partial u}{\partial t} = c_v \frac{\partial^2 u}{\partial z^2} \quad (2.9)$$

where: c_v is the coefficient of consolidation in the vertical direction and can be defined by:

$$c_v = \frac{k_v}{m_v \gamma_w} \quad (2.10)$$

where: k_v , m_v and γ_w are, respectively, the coefficient of permeability in the vertical direction, the coefficient of volume compressibility and the unit weight of water.

The solution of Eq. 2.9 in terms of the degree of consolidation due to vertical drainage, $U_v(t)$, at any time t for the entire thickness of the consolidating soil mass can be expressed as follows (Lambe and Whitman 1969):

$$U_v(t) = 1 - \sum_{i=0}^{\infty} \frac{2}{M^2} \exp\left(-M^2 \frac{c_v t}{L^2}\right) \quad (2.11)$$

where: $M = \pi/2(2i+1)$; t is the elapsed time; and L is the maximum length of the drainage path.

2.6.2 Theory of consolidation due to radial drainage

Based on Terzaghi's theory of 1D consolidation, Barron (1948) introduced a rigorous solution to the problem of soil consolidation due to radial drainage. Barron studied two extreme cases: (a) free strain; and (b) equal strain, and showed that the average consolidation in both cases is nearly the same. However, the solution obtained from the equal strain assumption is simpler than that of the free strain hypothesis. Although further refinement to the Barron solution has been reported by several researchers (e.g. Hansbo 1981; Hird et al. 1992; Indraratna and Redana 2000), Hansbo (1981) presented a simpler analytical solution by incorporating both the smear (with a spatially constant reduced-value of permeability) and well-resistance effects into Barron's (1948) equal strain formulation. The solution has gained a wide acceptance in practical applications and is used to estimate the degree of

consolidation due to radial drainage, $U_h(t)$, at depth z and time t as follows (see Fig. 2.6 for demonstration of parameters):

$$U_h(t) = 1 - \exp\left(-\frac{2c_h t}{r_e^2 \alpha}\right) \quad (2.12)$$

and

$$\alpha = F_n + F_s + F_r \quad (2.13)$$

where: F_n , F_s and F_r are the drain spacing factor, smear factor and well-resistance factor, respectively, and can be expressed as follows:

$$F_n = \frac{n^2}{(n^2 - 1)} \left[\ln(n) - \frac{3}{4} + \frac{1}{n^2} - \frac{1}{4n^2} \right] \approx \ln(n) - \frac{3}{4} \quad (2.14)$$

$$F_s = \left(\frac{k_h}{k_s} - 1 \right) \ln\left(\frac{r_s}{r_w} \right) = \left(\frac{k_h}{k_s} - 1 \right) \ln(s) \quad (2.15)$$

$$F_r = \pi z(2L - z) \frac{k_h}{q_w} \quad (2.16)$$

In the case of smear, the drain spacing and smear factor can be combined into a single geometrical/smear zone factor, F_{ns} , as follows:

$$F_{ns} = F_n + F_s = \ln\left(\frac{n}{s}\right) - \frac{3}{4} + \frac{k_h}{k_s} \ln(s) \quad (2.17)$$

where: $c_h = k_h/m_v\gamma_w$ is the coefficient of consolidation in the horizontal direction (k_h , m_v and γ_w are respectively the coefficient of permeability in the horizontal direction, coefficient of volume compressibility and unit weight of water); r_e is the radius of equivalent soil cylinder with impermeable perimeter or the radius of zone of influence; t is the consolidation time; α is a group parameter representing the smear

effects and geometry of the PVD system; $n = r_e/r_w$ is the drain spacing ratio (r_w is the equivalent radius of the drain); $s = r_s/r_w$ is the smear ratio (r_s is the radius of the smear zone); k_s is the horizontal permeability of the smear zone; L is the maximum vertical drainage distance; z is the depth from the top of the consolidating layer; and q_w is the vertical discharge capacity of the drains.

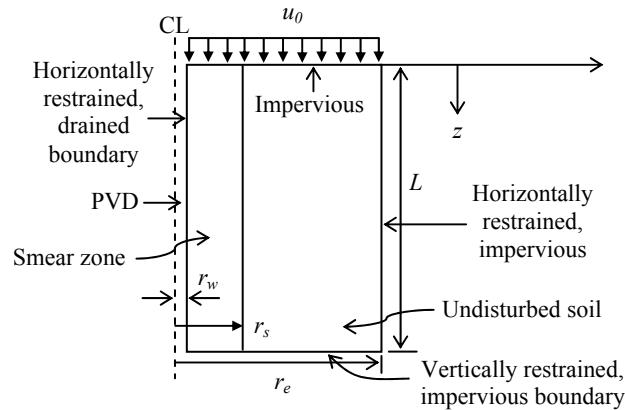


Figure 2.6: Schematic diagram of soil cylinder with prefabricated vertical drain

2.6.3 Refinement of Hansbo's (1981) theory of radial consolidation by Walker (2006)

As indicated earlier in Section 2.4.1, soil permeability in the smear zone is spatially variable. Despite this fact, the most common way to include the smear effects in the vertical drain analysis is to model the smear as a zone of constant reduced permeability (e.g. Hansbo 1981). This leads to a lack of precision in the analysis, as permeability close to the drain has a greater effect on radial consolidation than permeability further away from the drain. On the other hand, although a small zone of low-permeability close to the drain will significantly affect the radial consolidation rates (as all expelled water must pass through this zone), a small zone of increased compressibility (because of its small volume) will not largely affect consolidation. This is probably why smear zones are most often described with reference to permeability changes alone, and the effect of compressibility changes is neglected. However, field trials of vertical drains at different spacings indicate that for smaller drain spacings, the total settlement is higher and the values of the horizontal consolidation coefficients (back-calculated by ignoring the smear zone compressibility effects) are lower than those for widely spaced drains (Arulrajah et al.

2004; Bergado et al. 2002; Saye 2001). Both findings are consistent with increased compressibility in the smear zone. Walker (2006) indicates that the value of the smear zone compressibility may increase by about 20% from that of the undisturbed zone, implying a 20% increase in ultimate the settlement.

In an effort to rectify this situation, Walker (2006) presented a more general analytical soil consolidation model where soil properties within the smear zone vary with the radial distance from the drain. In this model, the modified α parameter (i.e. α^*) that is used in Hansbo's (1981) radial consolidation equation (see Eq. 2.12) is derived for linear, parabolic and piecewise constant distribution of soil parameters (permeability and compressibility) across the unit cell. Since the presentation of the piecewise constant distribution of soil parameters is analogous to the representation of soil spatial variability described in this dissertation (as will be seen later), only the expression of α^* based on the piecewise constant distribution is given here. Using α^* instead of α , Eq. 2.12 becomes:

$$U_h(t) = 1 - \exp\left(-\frac{2c_h t}{r_e^2 \alpha^*}\right) \quad (2.18)$$

and

$$\alpha^* = \alpha_m (\alpha_{ns} + \alpha_r) \quad (2.19)$$

where: α_{ns} and α_r , respectively, are the modified geometry/smear zone factor and well-resistance factor for piecewise constant distribution of permeability and α_m is a new parameter termed as 'smear zone compressibility parameter' which is introduced to take into account the compressibility variations.

By dividing the radial distribution of permeability into m zones, each with a constant horizontal permeability, k_{hi} , as shown in Fig. 2.7, Walker (2006) produced the following expression for α_{ns} based on the piecewise constant permeability:

$$\alpha_{ns} = \frac{n^2}{n^2 - 1} \sum_{i=1}^m \kappa_i \left[\frac{s_i^2}{n^2} \ln \left(\frac{s_i}{s_{i-1}} \right) - \frac{1}{2} \left(\frac{s_i^2 - s_{i-1}^2}{n^2} \right) - \frac{(s_i^2 - s_{i-1}^2)^2}{4n^4} \right] + \chi_i \left(\frac{s_i^2 - s_{i-1}^2}{n^2} \right) \quad (2.20)$$

and

$$\chi_i = \sum_{j=1}^{i-1} \kappa_j \left[\ln \left(\frac{s_j}{s_{j-1}} \right) - \frac{1}{2} \left(\frac{s_j^2 - s_{j-1}^2}{n^2} \right) \right] \quad (2.21)$$

where: n is the ratio of influence zone radius to drain radius, r_m/r_0 ; s_i is the ratio of the i th zone radius to drain radius, r_i/r_0 ; κ_i is the ratio of the m th permeability to the i th permeability, k_{hm}/k_{hi} . The r_0 , r_m and k_{hm} in index notations correspond respectively to the more conventional notation of drain radius r_w , influence zone radius r_e and undisturbed horizontal permeability k_h .

If the well-resistance is included in the derivation, then α_r can be expressed as follows:

$$\alpha_r = \pi z (2L - z) \frac{k_{hm}}{q_w} \left(1 - \frac{1}{n^2} \right) \quad (2.22)$$

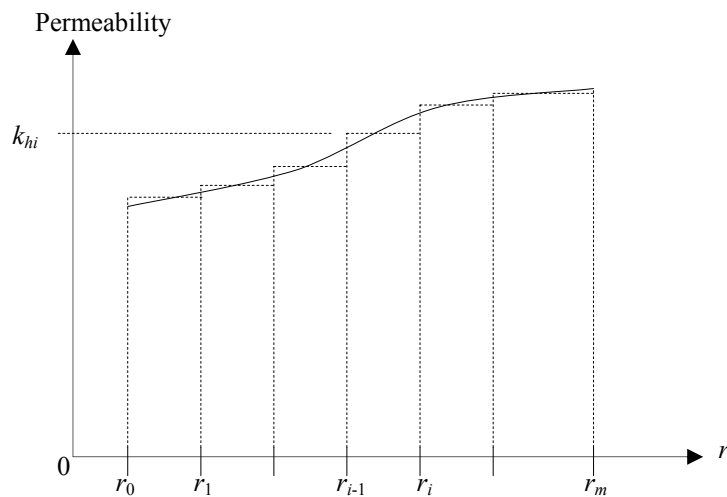


Figure 2.7: Radial piecewise constant permeability discretisation (after Walker 2006)

For the m zone discretisation of compressibility, the expression for α_{m_v} given by Walker (2006) is as follows:

$$\alpha_{m_v} = \frac{n^2}{n^2 - 1} \sum_{i=1}^m \frac{1}{\eta_i} \frac{s_i^2 - s_{i-1}^2}{n^2} \quad (2.23)$$

where: η_i is the ratio of the m th compressibility to the i th compressibility, m_{vm}/m_{vi} .

Hansbo's (1981) formulation for a smear zone with constant reduced permeability and an undisturbed zone is a special case of the multiple-segment solution described above. For a single smear zone, $m = 2$, $\kappa_1 = k_h/k_s = \kappa$, $\kappa_2 = 1$, $s_0 = 1$, $s_1 = r_s/r_w = s$, and $s_2 = r_e/r_w = n$, the α_{ns} parameter is given by:

$$\alpha_{ns} = \frac{n^2}{n^2 - 1} \left(\ln\left(\frac{n}{s}\right) + \kappa \ln(s) - \frac{3}{4} \right) + \frac{s^2}{n^2 - 1} \left(1 - \frac{s^2}{4n^2} \right) + \frac{\kappa}{n^2 - 1} \left(\frac{s^4 - 1}{4n^2} - s^2 + 1 \right) \quad (2.24)$$

Ignoring the insignificant higher order terms, Eq. 2.24 reduces to:

$$\alpha_{ns} = \ln\left(\frac{n}{s}\right) - \frac{3}{4} + \kappa \ln(s) \quad (2.25)$$

Similarly for a single smear zone with constant increased compressibility, Eq. 2.23 reduces to:

$$\alpha_{m_v} = 1 + \left(\frac{1 - \eta}{\eta} \right) \frac{(s^2 - 1)}{(n^2 - 1)} \quad (2.26)$$

where: η is the ratio of the undisturbed zone compressibility to the smear zone compressibility, m_{v_u}/m_{v_s} . Substituting the value of η in Eq. 2.26, α_{m_v} can be expressed as follows:

$$\alpha_{m_v} = \frac{n^2 - s^2}{n^2 - 1} + \frac{s^2 - 1}{n^2 - 1} \frac{m_{v_s}}{m_{v_u}} \quad (2.27)$$

Although this formulation is more realistic, the valid criticism of the above presentation of the piecewise constant permeability and compressibility is that it does not consider the possible variation of soil properties with depth - soil properties vary not only horizontally but also vertically.

2.6.4 Consolidation due to combined vertical and radial drainage

If the effects of both the horizontal and vertical drainage are considered, the analytical solution for the overall degree of consolidation, $U(t)$, at any time t can be obtained as follows (Carillo 1942):

$$U(t) = 1 - (1 - U_v(t))(1 - U_h(t)) \quad (2.28)$$

2.6.5 Plane-strain consolidation model and matching procedure

The consolidation of soil around an individual drain is more appropriately analysed as an axisymmetric problem. However, most previous numerical studies regarding soil consolidation via PVDs were conducted on the basis of plane-strain assumption so as to achieve computational efficiency. Analysing an axisymmetric problem using plane-strain conditions requires the equivalence between the axisymmetric and plane-strain analyses. The conversion techniques of an axisymmetric solution to an equivalent plane-strain model are demonstrated by several researchers (e.g. Hird et al. 1992; Indraratna and Redana 1997). This can be done by: (a) geometric matching in which the spacing of the drains is matched with permeability remains the same; (b) permeability matching in which the permeability coefficients are matched while the drain spacing remains the same; and (c) a combination of a permeability and geometric matching approach in which the plane-strain permeability is computed for convenient drain spacing (Indraratna et al. 2003).

Hird et al. (1992) presented a technique for matching the plane-strain and axisymmetric unit cells by adapting Hansbo's theory (Eq. 2.12) for plane-strain. In order to match the rate of consolidation in a plane-strain and an axisymmetric unit

cell, equality of the average degree of consolidation at every time and each level in the cell is necessary. Thus:

$$U_{h(pl)} = U_{h(ax)} \quad (2.29)$$

It should be noted that the suffixes *pl* and *ax* are used to differentiate between parameters in plane-strain and axisymmetric cases. Considering a plane-strain unit cell of half-width b_e (see Fig. 2.8) and using Eq. 2.12 in Eq. 2.29 gives:

$$\frac{c_{h(pl)}}{b_e^2 \alpha_{pl}} = \frac{c_{h(ax)}}{r_e^2 \alpha_{ax}} \quad (2.30)$$

For identical soil parameters in each case, Eq. 2.30 can be written as;

$$b_e^2 \alpha_{pl} = r_e^2 \alpha_{ax} \quad (2.31)$$

By substituting the expression for α_{pl} and α_{ax} in Eq. 2.31, the subsequent rearrangement yields

$$\frac{2}{3} b_e^2 - r_e^2 \left\{ \left(\ln \frac{n}{s} \right) + \left(\frac{k_h}{k_s} \right) \ln(s) - \frac{3}{4} \right\} = \left\{ \left(\frac{\pi r_e^2 k_h}{q_w} \right) - \left(\frac{2 b_e k_h}{q_{w(pl)}} \right) \right\} (2Lz - z^2) \quad (2.32)$$

(a) Geometric matching:

By ignoring the well-resistance in Eq. 2.32, the condition of geometric matching including the effect of the smear zone proposed by Hird et al. (1992) is as follows:

$$\frac{b_e}{r_e} = \left\{ \frac{3}{2} \left(\ln \left(\frac{n}{s} \right) + \left(\frac{k_h}{k_s} \right) \ln(s) - \frac{3}{4} \right) \right\}^{\frac{1}{2}} \quad (2.33)$$

The well-resistance effect is matched independently by accounting the RHS of Eq. 2.32 as equal to zero and yielding an equivalent plane-strain discharge capacity of drains as follows:

$$q_{w(pl)} = \left(\frac{2b_e}{\pi r_e^2} \right) q_{w(ax)} \quad (2.34)$$

(b) Permeability matching:

Instead of changing the drain spacing, an alternative procedure developed by Hird et al. (1992) can be used which involves changing the permeability by rewriting Eq. 2.30 as follows:

$$\frac{k_{h(pl)}}{b_e^2 \alpha_{pl}} = \frac{k_{h(ax)}}{r_e^2 \alpha_{ax}} \quad (2.35)$$

By assuming that the magnitudes of r_e and b_e are equal in Eq. 2.35, Hird et al. (1992) presented the following matching requirements relationships for the permeability and well-resistance, respectively.

$$k_{h(pl)} = \frac{2k_{h(ax)}}{3} \left\{ \ln\left(\frac{n}{s}\right) + \left(\frac{k_{h(ax)}}{k_s}\right) \ln(s) - \frac{3}{4} \right\} \quad (2.36)$$

and

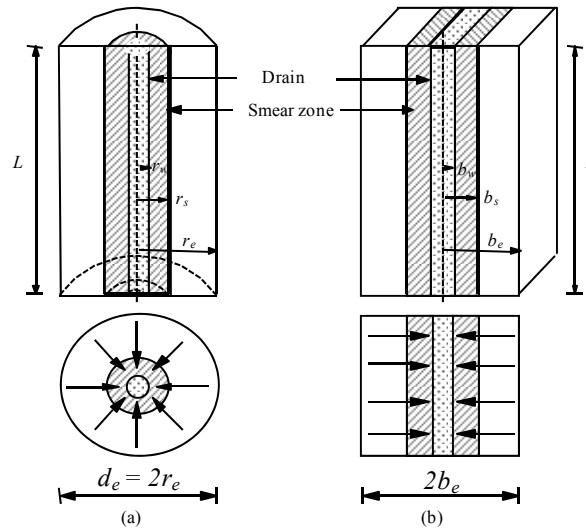
$$q_{w(pl)} = \left(\frac{2}{\pi r_e} \right) q_{w(ax)} \quad (2.37)$$

If both the smear and well-resistance effects are ignored in Eq. 2.35, the following simplified relationship between the plane-strain and axisymmetric permeabilities is proposed by Hird et al. (1992):

$$k_{h(pl)} = \frac{2}{3} \frac{k_{h(ax)}}{\left(\ln(n) - \frac{3}{4} \right)} \quad (2.38)$$

(c) Combination of permeability and geometric matching:

Both geometry and permeability matching procedures can be used simultaneously by setting b_e to a desired value in Eq. 2.35 and re-driving the matching requirements for $k_{h(pl)}$ and $q_{w(pl)}$.



a) Axisymmetric radial flow b) Equivalent plane-strain model

Figure 2.8: Transformation of axisymmetric unit cell into a plane-strain condition (after Indraratna and Redana 1997)

2.7 Soil Variability

Soils are the most variable of all engineering materials. As shown in Fig. 2.9, the variability of soil properties can be divided into three categories: inherent variability; measurement error; and transformation variability (Phoon and Kulhawy 1999). It has long been recognised that the properties of natural soils are inherently variable in spatial directions due to variations in the mineral composition and characteristics of soil strata during and after deposition (Vanmarcke 1977). The measurement errors occur mainly through inadequate equipment and poor procedures. The transformation variability is also called model variability and occurs during the translation of field or laboratory measurements into design soil properties using empirical or other correlation models (Phoon and Kulhawy 1999). To obtain a sophisticated reliable design of a geotechnical system, all of the above sources of uncertainty should be included. However, unlike inherent variability, the

measurement error and transformation variability can be reduced or even removed by collecting sufficient data and information, improving the measurement methods and/or enhancing the calculation models (Lacasse and Nadim 1996). Therefore, inherent variability is the most significant source of uncertainty in the reliability-based design of geotechnical systems and is the subject of the present research. In the following sections, the techniques used to quantify the inherent soil variability and published data associated with it are presented and discussed.

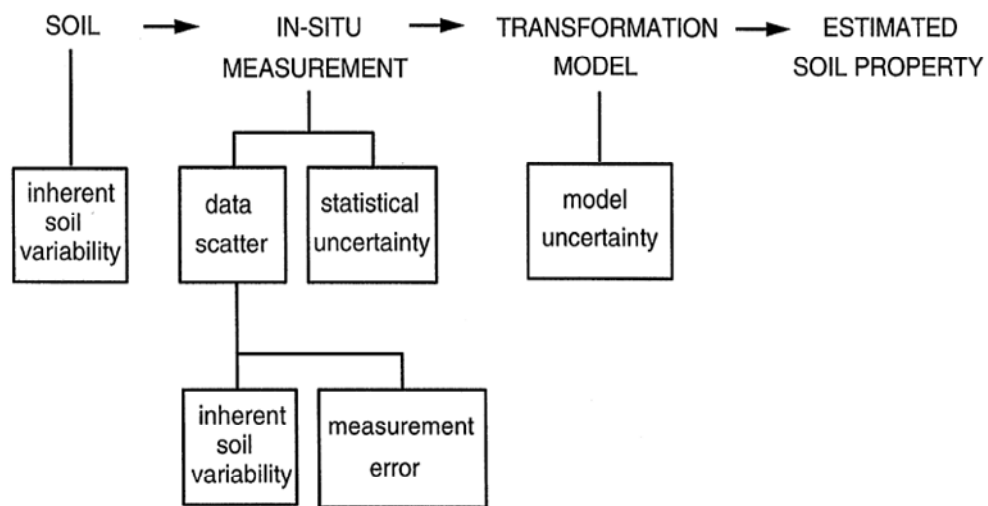


Figure 2.9: Uncertainty in estimation of soil properties (after Kulhawy 1992)

2.7.1 General terms for variability descriptors

Variability or uncertainty in soil properties can be mathematically characterised by treating the soil properties as random variables. In statistics, the random variable is defined by a numerical value, and the associated probability is determined from its probability distribution (usually referred to as the ‘PDF’ or probability density function). Several probability distributions, namely Gaussian/normal distribution, lognormal distribution, beta distribution and gamma distribution are commonly used to calculate the probability associated with a random variable. This can be represented by several classical statistical parameters, namely the mean or expected value, μ , variance, σ^2 , (variance can also be represented by standard deviation, σ) or coefficient of variation, v .

2.7.1.1 Mean or expectation of a random variable

The mean or expected value is the most significant property of a random variable and is a measure of the central tendency in the data. It is also known as the first central moment. If X is a continuous random variable with a probability density function (PDF) $f(x)$, the mean, μ_X , or expected value, $E[X]$, is given by:

$$E[X] = \mu_X = \int_{-\infty}^{\infty} xf(x)dx \quad (2.39)$$

if X is discrete, then:

$$E[X] = \mu_X = \frac{1}{n} \sum_{i=1}^n x_i \quad (2.40)$$

where n is the number of observations of X .

2.7.1.2 Variance/standard deviation of a random variable

Variance is another extremely important property of a random variable. It is also known as the second central moment. It is a measure of variability in the distribution, i.e. the deviation or spread (narrow or wide) of the sample data about their mean.

The variance of a continuous random variable X (i.e. σ_X^2) is defined as:

$$\text{Var}[X] = \sigma_X^2 = E[(X - \mu_X)^2] = \int_{-\infty}^{\infty} (x - \mu_x)^2 f(x)dx \quad (2.41)$$

if X is discrete, then:

$$\text{Var}[X] = \sigma_X^2 = E[(X - \mu_X)^2] = \frac{1}{n} \sum_{i=1}^n (x_i - \mu_x)^2 \quad (2.42)$$

where n is the size of the sample data.

The standard deviation of X , σ_X , is the square root of the variance. That is:

$$\sigma_X = \sqrt{\text{Var}[X]} \quad (2.43)$$

2.7.1.3 Coefficient of variation of a random variable

In engineering practice, the variability of a random variable is often expressed by a dimensionless parameter known as the coefficient of variation (COV), v . The COV of a random variable, X , is defined as the ratio of σ_X to μ_X as follows:

$$v_X = \frac{\sigma_X}{\mu_X} \quad (2.44)$$

The COV measures the degree of deviation of the data with respect to the mean, and is useful for comparing groups with different means.

2.7.1.4 Median and mode

The median is another central tendency descriptor of a random variable. It is the value of a random variable at which the PDF of the random variable divides into equal halves. The mode is defined as the most probable value of a random variable and is the value of a random variable at the peak of its PDF.

2.7.1.5 Correlation between two random variables

It is often necessary to deal with more than one random variable, where the uncertainties in one might be influenced by the uncertainties in the other. In such cases, the random variables are considered to be correlated, and the correlation is computed by the covariance. The covariance, $\text{Cov}[X, Y]$, between two correlated random variables X and Y , having the means μ_X and μ_Y , respectively, can be described as follows:

$$\text{Cov}[X, Y] = E[(X - \mu_X)(Y - \mu_Y)] \quad (2.45)$$

for continuous functions:

$$\text{Cov}[X, Y] = \int_{-\infty}^{\infty} \int_{-\infty}^{\infty} (x - \mu_X)(y - \mu_Y) f_{X,Y}(x, y) dx dy \quad (2.46)$$

for discrete functions:

$$\text{Cov}[X, Y] = \frac{1}{n} \sum_{i=1}^n (x_i - \mu_X)(y_i - \mu_Y) \quad (2.47)$$

where: n is the number of data points. Although the covariance describes the nature of the correlation between random variables, it does not reflect the strength of the relationship. The most common measure of the degree of linear dependence between random variables is the coefficient of correlation. The coefficient, ρ_{XY} , between two random variables X and Y , having standard deviations σ_X and σ_Y respectively, can be defined as follows:

$$\rho_{XY} = \frac{\text{Cov}[X, Y]}{\sigma_X \sigma_Y} \quad (2.48)$$

The correlation coefficient varies within ± 1 (i.e. $-1 \leq \rho_{XY} \leq +1$). When two variables are perfectly linearly correlated, ρ_{XY} will be either $+1$ (for positive correlation) or -1 (for negative correlation). On the other hand, $\rho_{XY} = 0$ indicates that the two random variables are linearly independent.

2.7.2 Spatial variability of soil properties

The formation of soil involves complex geological, physical and chemical processes. As a result, soil properties vary from one location to another, in all spatial directions. This variation can be divided into two components: trend component and fluctuation or residual component, (Beacher and Christian 2003; Cafaro and Cherubini 2002; DeGroot and Baecher 1993; Phoon 1995; Vanmarcke 1977). Therefore, the inherent variation in soil property can be represented as follows (Phoon and Kulhawy 1999):

$$\xi_s(z) = t(z) + w(z) \quad (2.49)$$

where: ξ_s is the in-situ soil property; z is the depth of soil and $t(z)$ and $w(z)$ are the trend component and fluctuation component, respectively. The characteristic of soil spatial variability with depth is also shown in Fig. 2.10.

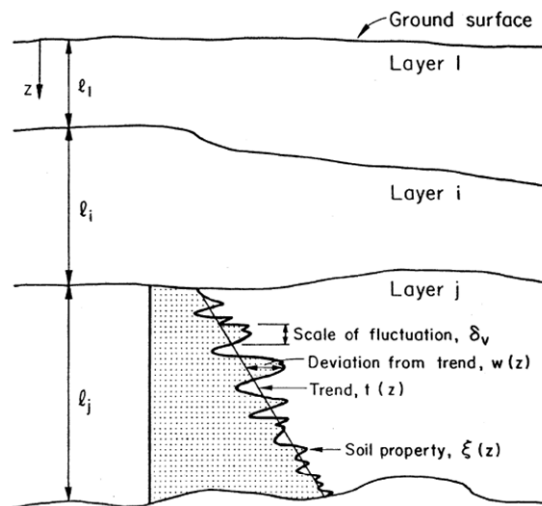


Figure 2.10: Inherent soil variability (Phoon and Kulhawy 1999)

The trend component represents the change in average soil properties with respect to spatial location, and is characterised deterministically by fitting the well-defined polynomial functions using regression analysis. The residual component corresponds to the random variation from the trend and is generally characterised as a stationary random field with a PDF of zero mean and non-zero variance (Beacher and Christian 2003; DeGroot and Baecher 1993; Vanmarcke 1977). Since the trend is considered to be deterministic, the fluctuating component, $w(z)$, is called the inherent variability. For real field, due to the existence of a particular trend in the data sets, non-stationary data sets are generally observed. To maintain the stationary status of the data, a trend is generally removed from the actual data (Brockwell and Davis 1987; Jaksa et al. 1999; Phoon et al. 2003). A quadratic polynomial trend is often sufficient to transform non-stationary data to stationary one (Jaksa et al. 1999).

The spatial variation of soil properties is not entirely random. Spatial dependencies also exist (e.g. Fenton and Vanmarcke 1990; Jaksa 1997; Vanmarcke 1977). That is,

a soil property at two separate spatial locations could be similar or not, depending on the distance they are located apart. This phenomenon is known as spatial correlation. Vanmarcke (1977) pointed out that adequate characterisation of random soil properties requires consideration (incorporation) of such spatial correlation. The mean and standard deviations are the point statistical measures with no consideration of the spatial correlation structure of soil properties. Therefore, a third parameter (i.e. the scale of fluctuation, SOF), is introduced as an additional statistic to consider correlation of soil properties in modelling spatial variability. The scale of fluctuation is also known as the correlation length and is usually denoted as θ . A number of mathematical techniques are currently available to model the spatial variability of soil parameters, namely, the random field theory (Vanmarcke 1984), geostatistics (Journel and Huijbregts 1978), regression analysis and fractal theory. Regression analysis and fractal theory have limited application to spatial variability models, and geostatistics suffer from an inability to test accuracy between competing model types (Jaksa et al. 1999). Consequently, the random field theory is the most commonly used mathematical technique to model the spatial variability of soil properties, in which the soil property is characterised stochastically by its mean, standard deviation and SOF.

2.7.2.1 Scale of fluctuation

As discussed, scale of fluctuation, or SOF, has been introduced to take into account the spatial correlation of soil properties in characterising soil spatial variability. Generally speaking, the SOF describes the limit of the spatial continuity of spatial correlation and can be defined simply as the distance over which the soil properties show significant correlation between two spatial points. The mathematical definition of SOF (or θ) is given by Vanmarcke (1984) as follows:

$$\theta = \lim_{L \rightarrow \infty} L\gamma(D) \quad (2.50)$$

where: $\gamma(D)$ is the variance function of a stationary random process, and L denotes the averaging length. Details of the variance function, $\gamma(D)$, will be described in the following section.

As illustrated in Fig. 2.11, the SOF can be approximately described as the average distance between intersecting points or crossings (Vanmarcke 1977). A large value of SOF indicates a higher degree of correlation, and thus a more uniform random field, whereas a small value of SOF implies a weak correlation between two points in the ground, hence, an erratic field. The SOF is dependent on the soil type and is a site-specific parameter. For example, the value of scale of fluctuation for sands is smaller than that for clays (Jaksa et al. 2004). In natural soil deposits, the horizontal scale of fluctuation is usually larger than that of the vertical one due to soil stratification.

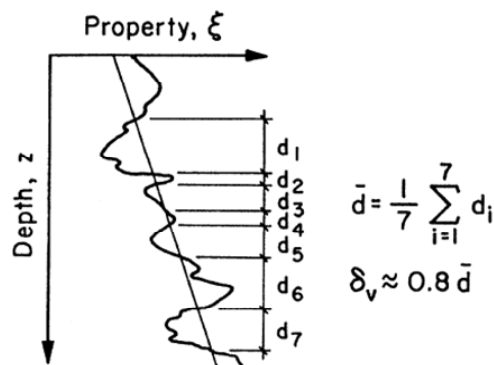


Figure 2.11: Rough estimate of vertical scale of fluctuation (Vanmarcke 1977)

2.7.2.2 Auto-correlation function

The concept of spatial correlation of soil properties can be captured mathematically using the theoretical auto-correlation function, which is generally fitted to the sample auto-correlation function to determine the scale of fluctuation. The sample auto-correlation function is the plots of sample auto-correlation against separation or lag distances, τ . To obtain this, the sample auto-covariance is generally normalised by the sample variance, $\text{Var}[X]$, as follows:

$$\rho(\tau) = \frac{\text{Cov}[X_i, X_{i+\tau}]}{\text{Var}[X]} \quad (2.51)$$

The computed sample auto-correlation is then fitted with an assumed theoretical auto-correlation function to determine the scale of fluctuation. Although

monotonically decaying exponential and Gaussian (squared exponential) auto-correlation functions are most commonly used, several auto-correlation functions are indicated in the literature (e.g. Vanmarcke 1977), and some are enumerated in Table 2.1.

Table 2.1: Auto-correlation functions (Vanmarcke 1977)

Function model	Auto-correlation function	Correlation distance	Scale of fluctuation
Single exponential	$\rho(\tau) = \exp[-\tau/a]$	a	$2a$
Squared exponential	$\rho(\tau) = \exp[-(\tau/b)^2]$	b	$\sqrt{\pi} \cdot b$
Second order Markov	$\rho(\tau) = \exp[-\tau/c] \cdot [1 + \tau/c]$	c	$4c$
Cosine exponential	$\rho(\tau) = \exp[-\tau/d] \cdot \cos(\tau/c)$	d	d

Vanmarcke (1984) suggested that any auto-correlation function can be fitted with the sample auto-correlation to estimate the scale of fluctuation. Sometimes the term ‘correlation distance’ is also used to refer to the ‘scale of fluctuation’.

2.7.2.3 Local averaging and variance reduction function

The statistics (mean, variance, etc.) relating to the random fields are assumed to be defined at the point level. However, soil properties are rarely measured at a point, and most engineering measurements concerned with soil properties are performed on samples of a finite volume. Therefore measured soil properties are actually a local average over the sample volume. In order to obtain the true point statistics, the locally averaged properties (measured), need to be corrected by taking into account the sample size. The process of spatial averaging results in a variance reduction by damping out the high frequency values in the observed values on a point scale. As a result, the locally averaged variance of a soil property is usually less than its point variance. The variance reduction factor, γ , due to local averaging is defined as:

$$\gamma = \frac{\sigma_D^2}{\sigma^2} \quad (2.52)$$

where: σ_D^2 is the variance of the soil property, spatially averaged over an averaging domain D ; and σ^2 is the point variance. The variance reduction factor is a function of the averaging domain and correlation function. For a stationary one-dimensional random field X , the variance function, $\gamma(D)$, is defined by Vanmarcke (1984) as follows:

$$\gamma(D) = \frac{2}{L^2} \int_0^L (L - \tau) \rho_X(\tau) d\tau \quad (2.53)$$

where: $\rho(\tau)$ is the correlation function and L is the averaging length. The extension of the variance functions in two and three-dimensions are also described in the literature (e.g. Vanmarcke 1984) and can be given in Eqs. 2.54 and 2.55, respectively, as follows:

$$\gamma(D) = \frac{4}{L_x^2 L_y^2} \int_0^{L_x} \int_0^{L_y} (L_x - \tau_1)(L_y - \tau_2) \rho_X(\tau_1, \tau_2) d\tau_1 d\tau_2 \quad (2.54)$$

$$\gamma(D) = \frac{8}{L_x^2 L_y^2 L_z^2} \int_0^{L_x} \int_0^{L_y} \int_0^{L_z} (L_x - \tau_1)(L_y - \tau_2)(L_z - \tau_3) \rho_X(\tau_1, \tau_2, \tau_3) d\tau_1 d\tau_2 d\tau_3 \quad (2.55)$$

where: x , y and z represent the horizontal, normal to the plane of paper and vertical directions respectively.

2.7.2.4 Averages

To derive the point statistics associated with local average measurements, in addition to the size of the sample over which the measurement represents an average and the correlation coefficient between all points in the idealized soil domain, it is also required to know the type of averaging that the observations represents. Moreover, it is often necessary to characterize a random variable (soil property) by averaging them over certain domains and the obtained averaged value can be used to represent the soil property in hand for geotechnical design purposes. The representative value has traditionally been based on the arithmetic average. However, two other types of

averages have geotechnical engineering importance, i.e. the geometric and harmonic averages. All three averages are discussed below:

- **Arithmetic average**

The arithmetic average, X_a , of a discrete random soil parameter X over some domain A is defined as:

$$X_a = \frac{1}{n} \sum_{i=1}^n X_i \quad (2.56)$$

where: A is assumed to be divided up into n samples.

If X is continuous, then:

$$X_a = \frac{1}{A} \int_A X(x) dx \quad (2.57)$$

Arithmetic average weights all of the values of X equally. Arithmetic averaging is appropriate if the quantity being measured is not dominated by low values. Porosity might be an example of a property which is simply an arithmetic average (sum of pore volumes divided by the total volume).

- **Geometric average**

The geometric average, X_g , of a random soil parameter X over some domain A is defined as:

$$X_g = \left[\prod_{i=1}^n X_i \right]^{1/n} = \exp \left[\frac{1}{A} \int_A \ln X(x) dx \right] \quad (2.58)$$

Geometric averaging is appropriate for soil properties which are dominated by low values, and for spatially varying soil properties, will always be less than the arithmetic average. Reasonable examples are the coefficient of permeability, elastic modulus, cohesion and friction angle. The geometric average is a “natural” average

of the lognormal distribution because an arithmetic average of the underlying normally distributed random variable leads to the geometric average when converted back to the lognormal distribution.

- **Harmonic average**

The harmonic average, X_h , of a random soil parameter X over some domain A is defined as

$$X_h = \left[\frac{1}{n} \sum_{i=1}^n \frac{1}{X_i} \right]^{-1} = \left[\frac{1}{A} \int_A \frac{dx}{X(x)} \right]^{-1} \quad (2.59)$$

Harmonic averaging is appropriate for soil properties which are strongly dominated by low values. In general, for a spatially varying random field, the harmonic average will be smaller than the geometric average, which in turn is smaller than the arithmetic average. Examples are the elastic modulus of horizontally layered soils and permeability in one dimensional flow (e.g. flow through a pipe). Unfortunately, the mean and variance of the harmonic average, for a spatially correlated random field are not easily found.

2.7.3 Published data for soil variability

The main obstacle in accounting for the variability of soil properties in geotechnical analysis and design is the limited in-situ soil data. Jaksa (2000) pointed out that in civil engineering projects, expenditure on the geotechnical features is usually limited and adequate site investigations seldom conducted. Accordingly, in the absence of precise field information, the statistical parameters associated with soil parameters of interest can be estimated from the values published in the relevant literature. In recent years, due to the advanced techniques of measuring the properties of natural soils, publications describing the extent of variation of various soil properties are more numerous. Beacher and Christian (2003) published a table of suggested COVs for a wide range of soil properties summarised from the literature, as shown in Table 2.2.

Table 2.2: Coefficients of variation of different soil properties for summary data from (a) Lacasse and Nadim (1996) and (b) Lumb (1974) (after Beacher and Christian 2003)

(a) Soil Property	Soil type	PDF	Mean	COV(%)
Cone resistance	Sand clay	LN	*	*
	Clay	N/LN	–	–
Undrained shear strength	Clay (triaxial)	LN	*	5–20
	Clay (index S_u)	LN	–	10–35
	Clayey silt	N	–	10–30
Ratio S_u/σ'_{v0}	Clay	N/LN	*	5–15
Plastic limit	Clay	N	0.13-0.23	3–20
Liquid limit	Clay	N	0.30-0.80	3–20
Submerged unit weight	All soils	N	5-11 (kN/m ³)	0–10
Friction angle	Sand	N	*	2–5
Void ratio, porosity, initial void ratio	All soils	N	*	7–30
Over consolidation ratio	Clay	N/LN	*	10–35
(b) Soil Property	Soil type	PDF	Mean	COV(%)
Density	All soils	–	–	5–10
Void ratio	All soils	–	–	15–30
Permeability	All soils	–	–	200–300
Compressibility	All soils	–	–	25–30
Undrained cohesion (clays)	All soils	–	–	20–50
Tangent of angle of shearing resistance (sands)	All soils	–	–	5–15
Coefficient of consolidation	All soils	–	–	25–50

Notes: N/LN = Normal and lognormal distribution; and

*Values are dependent on site and type of soil

The estimation of scale of fluctuation (SOF) is not straightforward, since it tends to be related to the distance over which it is measured. Popescu et al. (2002) reported that the SOF is dependent on sampling intervals, and that closely spaced data are rarely available in the horizontal direction. Consequently, the SOF is less well-

documented compared to the COV of soil properties, particularly in the horizontal direction. Despite that, Phoon and Kulhawy (1999) have reported values of SOF, as summarised in Table 2.3. It can be seen that the horizontal SOF is observed to be much higher than the vertical SOF (at least 10 times higher). Due to the lack of data regarding the horizontal direction, many researchers (e.g. Fenton and Griffiths 2003; Griffiths and Fenton 2004; Haldar and Sivakumar Babu 2008; Kuo et al. 2004) considered isotropic SOFs (i.e. identical values of vertical and horizontal scales of fluctuation) in their studies, for the sake of simplicity.

Table 2.3: Summary of scale of fluctuation of some geotechnical properties (after Phoon and Kulhawy 1999)

Property ^a	Soil type	No. of studies	Scale of fluctuation (m)	
			Range	Mean
Vertical fluctuation				
s_u	Clay	5	0.8–6.1	2.5
q_c	Sand, clay	7	0.1–2.2	0.9
q_T	Clay	10	0.2–0.5	0.3
S_u (VST)	Clay	6	2.0–6.2	3.8
N	Sand	1	–	2.4
w_n	Clay, loam	3	1.6–12.7	5.7
w_T	Clay, loam	2	1.6–8.7	5.2
γ'	Clay	1	–	1.6
γ	Clay, loam	2	2.4–7.9	5.2
Horizontal fluctuation				
q_c	Sand, clay	11	3.0–80.0	47.9
q_T	Clay	2	23.0–66.0	44.5
s_u (VST)	Clay	3	46.0–60.0	50.7
w_n	Clay	1	–	170

Notes: ^a s_u and s_u (VST) are the undrained shear strength from laboratory tests and vane shear tests, respectively; γ' is the effective unit weight

The variability in soil properties encountered on any project is inextricably related to the particular site and to a specific regional geology. It is neither easy nor wise to

apply typical values of soil property variability from other sites in conducting a reliability analysis. The discussion of soil variability in this chapter intends to suggest conditions that might be encountered in practice. The range of variability from one site to another is great and the data reported in the literature often compounds real variability with testing errors. In practice, soil variability measures should always be based on site-specific data.

2.8 Probabilistic Methods of Soil Consolidation Analysis

Soil consolidation analysis is usually performed in order to predict the consolidation rates in soil deposits. Over the years, consolidation analysis has evolved from approximate theoretical calculations to the more advanced numerical solutions using powerful computer and probabilistic analyses. Generally speaking, the improvement in the tools of soil consolidation analysis provides new insights, transparency and improved conceptual understanding about the soil consolidation problem. Traditionally, analysis of soil consolidation via prefabricated vertical drains (PVDs) by either theoretical or numerical methods has been carried out deterministically. This means that a single best estimate value of the input parameters (e.g., permeability, coefficient of volume compressibility, etc.) based on ‘average’ soil properties has been used to define an ‘equivalent’ homogeneous soil. As a result, there have been frequent discrepancies between the predicted and actually observed settlements, especially for heterogeneous soils. Hence, it is readily accepted that more reliable tools are needed to incorporate soil spatial variability and to quantify the resulting uncertainty for soil consolidation analysis. This issue has led to the development of probabilistic soil consolidation analysis in the late 1970s (e.g. Corotis et al. 1975; Freeze 1977). In the literature, several probabilistic approaches have been applied to soil consolidation analysis, including: (1) the first order second moment (FOSM) method; (2) the point estimate method (PEM), and (3) Monte Carlo simulation (MCS). These methods are described briefly below.

2.8.1 First order second moment method

The first order second moment (FOSM) method (Harr 1987) is a simple approximate method for the first order approximation to the mean and variance of a performance

function F (e.g. Eqs. 2.11, 2.12) from the mean and variance of the input random variables. This approach is based on the Taylor series expansion of the performance function around the mean values of the input random variables. Only the linear term of the expansion is retained (i.e. first order). The generalised performance function for n numbers of random variables can be written as:

$$F = g(X_1, X_2, \dots, X_n) \quad (2.60)$$

Considering the first order Taylor series expansion about the mean, the mean and variance of F are given as:

$$E[F] = \mu_F \approx g(\mu_{X_1}, \mu_{X_2}, \dots, \mu_{X_n}) \quad (2.61)$$

$$\text{Var}[F] = \sigma_F^2 \approx \sum_{i=1}^n \left[\left(\frac{\partial F}{\partial X_i} \right)^2 \text{Var}[X_i] \right] + 2 \sum_{i=1}^n \sum_{j=1}^n \left[\left(\frac{\partial F}{\partial X_i} \frac{\partial F}{\partial X_j} \right) \text{Cov}[X_i, X_j] \right] \quad (2.62)$$

where: $E[F]$ and $\text{Var}[F]$ are, respectively, the mean and variance of the performance function F ; $\text{Cov}[X_i, X_j]$ is the covariance between the random variables X_i, X_j ; and n is the number of random variables.

FOSM is simple to implement and can take into account different sources of uncertainty. It provides a direct approximation to the mean and variance of the performance function. Its biggest advantage is that it shows in an orderly way, the relative contribution of each random variable to the overall uncertainty, providing information about the most significant factors. However, it has limitations. Due to the truncation of the Taylor series after the first order term, its accuracy decreases for highly nonlinear performance functions and large soil variability. Moreover, calculation of the partial derivatives in Eq. 2.62, for highly non-linear relationships, can be cumbersome (Elkateb et al. 2002).

2.8.2 Point estimate method

Rosenblueth (1975) introduced a simple reliability analysis method known as the point estimate method (PEM). This is an approximate numerical method that can calculate the moments of a random variable that are a function of one or several random variables. The mathematical formulation of this method is discussed in detail by Harr (1987) and Wolff (1996). In the PEM, the continuous probability density function of each random variable is replaced by two probability concentrations (p^+ and p^-) at two discrete point masses (x^+ and x^-) of the input random variable. The two masses are multiplied by weighted factors to evaluate the first two moments of the performance function. The PEM is simple, direct and reasonably accurate. It does not require the calculation of derivatives, and is efficient for a small number of random variables. The main limitation of this technique is the complexity in calculations when multiple random variables are considered (Elkateb et al. 2002). Details of the accuracy, advantages and limitations of this method are summarised in Christian and Baecher (1999).

2.8.3 Monte Carlo simulation

Nowadays most geotechnical problems are analysed by numerical techniques such as finite element analysis and finite difference analysis. In these cases, the explicit performance functions are not available and the methods discussed in the earlier sections (i.e., FOSM and PEM) cannot be used for reliability analyses. To overcome this problem, the Monte Carlo simulation (MCS) based approaches have been introduced. This is essentially a repetitive simulation process in which numerous sets of values for the input random variables are generated based on their known or assumed PDF. The number of simulations can also be determined by examining the statistical fluctuations of the expected values and standard deviations of the output quantities. Using each generated set of values for the uncertain parameters, numerical simulations are performed using a deterministic numerical model. By analysing the outputs from each simulation, histograms of the response variables can be plotted to extract probabilistic information. The Monte Carlo simulation can also be used to obtain the statistical moments of an explicit performance function. In such case, no

assumption is required to the PDF shape of the performance function. In principle, this method is useful for the following reasons:

- (i) It can be applied to large and complex problems;
- (ii) It can capture non-linear behaviour; and
- (iii) Idealisations or simplifications required in the analytical methods can be relaxed.

Although MCS is conceptually simple compared to FOSM and PEM, it is computationally expensive as many repetitions (iterations) are required, depending on the number of variables in the simulation process in order to obtain adequate accuracy. In addition, MCS provides no information on the relative contribution of each random variable to the overall uncertainty associated with the output variables. Despite this, MCS is rapidly gaining in popularity due to the recent advances in computer technology. In this thesis, it will be used for the reliability analysis of soil consolidation by PVDs.

2.9 Application of Stochastic Analysis to Geotechnical Engineering Problems

In recent years, the stochastic analysis techniques discussed in the previous sections have been implemented for several applications to practical geotechnical problems, to quantify soil spatial variability and assess the resulting uncertainty. This is due to the advances in personal computer technology and enhanced understanding of the statistics of geotechnical data. Examples of these applications are the bearing capacity of shallow and deep foundations (Fenton and Griffiths 2003; Fenton et al. 2007; Haldar and Sivakumar Babu 2008), settlement of shallow foundations (e.g. Beacher and Ingra 1981; Fenton and Griffiths 2005; Griffiths and Fenton 2009; Paice et al. 1996; Zeitoun and Baker 1992), slope stability analysis (e.g. Griffiths and Fenton 2004; Griffiths et al. 2009), seepage flow (Griffiths and Fenton 1993; 1997) and liquefaction problems (e.g. Fenton and Vanmarcke 1998; Popescu et al. 1997; Yegian and Whitman 1978). Although the detailed methods of solution differ, the problems are modelled to provide probabilistic solutions using stochastic input parameters (mean, variance and probability density function) of soil properties. Elkateb et al. (2002) provide an excellent summary of some of the above mentioned

applications, together with their limitations, and this summary will not be repeated herein.

In the area of soil consolidation, several studies that consider stochastic approaches to investigate soil consolidation have been found in the literature. Freeze (1977) dealt with soil consolidation due to vertical drainage, in one-dimensional (1D) geometry, by taking into account the cross-correlation between the coefficient of volume compressibility and soil permeability. Both the coefficient of volume compressibility and soil permeability were chosen randomly from probability density functions. The study was fairly basic, as unrealistic spatial correlations and cross correlations was assumed. Furthermore, no information was provided to the probability distribution of output variables, and the effect of anisotropic correlation structure was not accounted for.

Hwang and Witczak (1984) investigated the dimensional effect on soil consolidation through an integrated finite difference method, combined with Monte Carlo simulations. Five soil properties including the initial void ratio, compression index, pre-consolidation pressure, log initial permeability and the void ratio versus permeability relationship were treated as the random variables with normal distributions. The major observation of this study is that the time rate of consolidation is faster with increasing dimensionality. The study was also basic, where the random soil property was characterised by total variability. The study's main limitations were that the sensitivity of the results to the number of realisations was not considered, and no information to the probability distribution of output variables was provided.

Chang (1985) investigated the influence of a gamma-distributed vertical coefficient of consolidation (c_v) on Terzaghi-type (uncoupled) 1D layered systems. Using the Monte Carlo simulations, the uncertainties in the degree of consolidation and excess pore water pressure were assessed in terms of their mean and standard deviations. The study also had limitations, e.g. the spatial correlations between c_v values at each layer were not considered, and the effect of the number of realisations on the output quantities was not assessed.

Badaoui et al. (2007) performed uncoupled soil consolidation analysis due to vertical drainage, using only the thin-layer method, combined with the Monte Carlo simulations, to assess the effect of spatially variable elastic modulus and soil permeability on the statistics of the degree of consolidation. The main limitations of the study lie in the assumption of an isotropic correlation structure for spatially variable soil properties, and the disregarding of cross-correlation between the elastic modulus and soil permeability. In addition, no information about the probability distribution of the output variables was provided, and the study was conducted over a limited range of parametric variations.

Most recently, Huang et al. (2010) performed a comprehensive study in 1D and 2D geometries on both coupled and uncoupled soil consolidation due to vertical drainage. Soil permeability and the coefficient of volume compressibility were assumed to be lognormally distributed random variables. The effects of spatial correlation and cross-correlation were taken into consideration. The results described the effect of COV, spatial correlation length, and cross-correlation on the output statistics relating to the overall 'equivalent' coefficient of consolidation, determined by the log-time method (Casagrande 1936) and root-time method (Taylor 1948). The study's major observations can be summarised as: (1) coupled theory must be adopted for heterogeneous soil consolidation; and (2) both the coefficient of volume compressibility and coefficient of soil permeability play crucial roles in the consolidation of heterogeneous soil, and cannot be embodied into a single coefficient of consolidation. A major limitation of the study is that the coefficient of variation of both soil permeability and volume compressibility were assumed to be equal, even though the permeability coefficient of variation is usually much higher than that of volume compressibility. Furthermore, an isotropic correlation structure was assumed for both soil parameters.

Although all of the above studies dealt with probabilistic soil consolidation over a wide range of circumstances, they are restricted to soil consolidation due to vertical drainage only (i.e., without PVDs) either in 1D or 2D geometries. In the area of ground improvement via PVDs, only two studies conducted by Hong and Shang (1998) and Zhou et al. (1999) have been found in the literature in which soil consolidation via PVDs was analysed using PEM, focusing only on the uncertainty

associated with the measurement errors of soil properties. However the inherent spatial variability of soil properties was not investigated. These studies concluded that the single most important uncertain soil parameter that affects the process of soil consolidation by PVDs is the coefficient of consolidation in the horizontal direction.

2.10 Summary

A thorough review of the theories and influencing factors in preloading consolidation by PVDs were presented in this chapter, particularly those aspects addressed in the present research. Different elements of inherent soil spatial variability, such as mean, variance, characteristics of spatial correlation, local averaging and variance relationships, and typical spatial variability parameters for various soil properties were thoroughly discussed, together with their implications in relation to geotechnical analysis and design. Different approaches adopted throughout the history of geotechnical engineering in efforts to perform stochastic soil consolidation analyses were thoroughly reviewed and criticized. Examples of these applications to various geotechnical field problems were acknowledged for reference purposes. Most of the earlier works that dealt with probabilistic soil consolidation were described in some detail, with emphasis on their limitations, in order to pave the way for the present research.

This review of a broad range of relevant literature shows that the significance of soil spatial variability in relation to the treatment of soft soils by preloading consolidation with PVDs has long been realised. However, very few studies for coupled soil consolidation by PVDs consider the effects of soil spatial variability and there are no systematic studies of the problem over a practical range of parametric variations. Therefore, comprehensive studies on the effect of soil variability, correlation structure and cross correlation between soil parameters on the stochastic behaviour of soil consolidation by PVDs are required. In addition, the past few years have seen growing worldwide interest in the development of a rational reliability-based geotechnical design code to properly deal with the uncertainty associated with soil spatial variability. This trend was heightened with the transformation of design codes around the world towards some sort of reliability-based design (e.g., Eurocode 7, 2004, Australian Standard AS 4678, 2002). Although Zhou et al. (1999) presented a

probabilistic design method of PVDs for soil stabilisation, by considering the uncertainty in the coefficient of horizontal (radial) consolidation due to measurement errors, no simple solution (either in the form of equations or charts) has considered soil spatial variability. Therefore there is a need to develop such probabilistic design method for soil consolidation via PVDs and this will be one focus of the present research. In the following chapter, a stochastic approach dealing with soil spatial variability in treatment of soft soils by PVDs is introduced and discussed.

Chapter 3

Stochastic Modelling of Soil Consolidation by Vertical Drains

3.1 Introduction

Since soils and rocks are the most variable of all engineering materials and yet this is often coupled with inadequate site data, probabilistic analysis is a more rational approach to assess the behaviour of soil consolidation by PVDs. This is because of the fact that the uncertainty and variability in soil properties can be explicitly taken into account through stochastic modelling. Unlike deterministic analysis, which is based on single best estimate (average or characteristic) values of soil properties, probabilistic analysis considers the variable nature of soil properties, based on their statistical characteristics. The latter approach leads to a more realistic measure of the degree of consolidation, which is usually characterised by the risk associated with the measure of the degree of consolidation. Among several methods to model stochastic problems discussed in the previous chapter, the use of deterministic finite element analysis with stochastic input soil parameters in a Monte Carlo framework has gained much popularity in recent years (e.g. Elachachi et al. 2004; Fenton and Griffiths 2002; Fenton and Vanmarcke 1998; Fenton et al. 2007; Griffiths and Fenton 1993; Griffiths et al. 2009; Hicks and Onisiphorou 2005; Huang et al. 2010; Popescu et al. 1997; 2005). The same approach is adopted in the present research to investigate the effects of soil spatial variability on the behaviour of soil consolidation by PVDs. The detailed formulation and implementation of the approach are discussed in the subsequent sections in this chapter.

3.2 Stochastic Approach of Soil Consolidation by PVDs

In order to consider soil spatial variability in the course of design of ground improvement by PVDs, true site conditions of soil properties that vary in a random fashion within the soil mass need to be modelled in the design process. This is achieved in this work by creating *virtual* or *simulated* soil profiles that are merged with a finite element modelling of soil consolidation by PVDs in a Monte Carlo

framework. For a certain problem of ground improvement by PVDs, the proposed approach can be applied using the following steps:

1. Create a virtual soil profile for the problem in hand which comprises a grid of elements that is assigned design values of soil properties different from one element to another across the grid. The virtual soil profile allows arbitrary distributions of soil properties to be realistically and economically modelled;
2. Incorporate the generated soil profile into a finite element modelling of soil consolidation by PVDs; and
3. Repeat Steps 1 and 2 many times using the Monte Carlo technique so that a series of consolidation responses can be obtained from which the statistical distribution parameters and probability of achieving a target degree of consolidation can be estimated and analysed.

Details of the above steps, as well as the numerical procedures, are described below.

3.2.1 Simulation of virtual soil profile

To incorporate soil spatial variability in consolidation analysis, it is essential to create a soil profile that can represent the variability and spatial correlation of the properties in real soil deposits. In this dissertation, two dimensional (2D) spatially random soil profile is simulated based on the random field theory (Vanmarcke 1984). The simulation process of random soil profile can be subdivided into two steps as follows:

- Identify and characterise the spatially random soil properties; and
- Generate spatially random field of each of the chosen soil properties based on their specified statistical parameters.

3.2.1.1 Identification and characterisation of spatially random soil properties

Prior to proceeding with the random field generation process, it is necessary to identify the soil properties that are required to be treated as random variables. As indicated earlier in Chapter 1, spatial variability of several soil properties can affect the consolidation behaviour of heterogeneous soils, such as coefficient of soil permeability, k , coefficient of volume compressibility, m_v (i.e. elastic modulus, E ,

and Poisson's ratio, ν), vertical discharge capacity of the drains, q_w , etc. However, the coefficient of soil permeability, k , and coefficient of volume compressibility, m_v , have the most significant impact on soil consolidation by PVDs, as indicated by several researchers (e.g. Huang and Griffiths 2010; Lee et al. 1992; Pyrah 1996). Accordingly, throughout this research, only the soil permeability and volume compressibility are modelled as random fields, while the other parameters are held constant and treated deterministically to reduce the superfluous complexity of the problem.

The randomness of the selected soil properties also needs to be characterized statistically in terms of their mean (μ), standard deviation (σ), probability distribution and SOF (θ) prior to their generation. In order to determine these characteristics for a certain site, a geotechnical investigation program of closely-spaced soil testing in the vertical and horizontal directions needs to be undertaken and the obtained field data analysed. However, such comprehensive site investigation is often beyond the scope of most projects. Consequently, in the absence of such site information, traditional site investigation together with information from geological maps and knowledge from previous site investigations of nearby locations can be used to assign a particular level of spatial variability to the site in question. In addition, there is an increasing number of publications that provide typical ranges of the statistical parameters of most familiar soil properties (e.g. Beacher and Christian 2003; Duncan 2000; Kulhawy et al. 1991) and can be used in the absence of improved information.

In this study, the variability of both k and m_v is characterised by following a lognormal distribution. The probability density function of a lognormally distributed random variable, X , with a mean, μ_X , and a standard deviation, σ_X , is given by:

$$f(x) = \frac{1}{x\sigma_{\ln X}\sqrt{2\pi}} \exp\left[-\frac{1}{2}\left(\frac{\ln x - \mu_{\ln X}}{\sigma_{\ln X}}\right)^2\right] \quad (3.1)$$

where: $\mu_{\ln X}$ and $\sigma_{\ln X}$ are, respectively, the mean and standard deviation of the underlying normally distributed $\ln(X)$ obtained from the specified μ_X and σ_X of lognormally distributed X using the following transformations (Fenton and Griffiths 2008):

$$\mu_{\ln X} = \ln \mu_X - \frac{1}{2} \sigma_{\ln X}^2 \quad (3.2)$$

and

$$\sigma_{\ln X} = \sqrt{\ln\left(1 + \frac{\sigma_X^2}{\mu_X^2}\right)} = \sqrt{\ln(1 + \nu_X^2)} \quad (3.3)$$

The lognormal distribution ranges between zero and infinity, thus, includes no negative values. Typical lognormal distribution plots with constant σ_X ($\sigma_X = 0.5$) and varying μ_X and constant μ_X ($\mu_X = 1.0$) and varying σ_X are shown respectively in Figs. 3.1(a) and (b). In Fig. 3.1(a) as the curves consistently move to the right with the increase of μ_X , the probability of getting any stationary target of X is increased. While in Fig. 3.1(b) the opposite effect on the probability of X is found as σ_X increases.

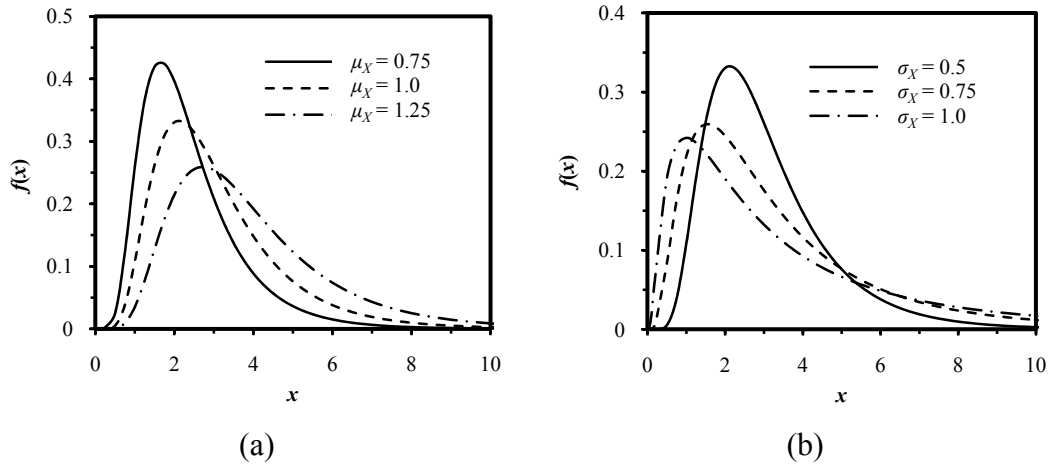


Figure 3.1: Lognormal distribution plots with (a) constant standard deviation ($\sigma_X = 0.5$) and varying mean (b) constant mean ($\mu_X = 1.0$) and varying standard deviation

Rearrangement of Eqs. (3.2) and (3.3) gives the following relationship for μ_X and σ_X of the lognormally distributed X in terms of $\mu_{\ln X}$ and $\sigma_{\ln X}$ of the underlying normally distributed $\ln(X)$:

$$\mu_X = \exp\left(\mu_{\ln X} + \frac{1}{2}\sigma_{\ln X}^2\right) \quad (3.4)$$

$$\sigma_X = \mu_X \sqrt{\left[\exp(\sigma_{\ln X}^2) - 1\right]} \quad (3.5)$$

The selection of lognormal distribution for k is based on the findings from field tests data of permeability reported by Hoeksema and Kitanidis (1985) and Sudicky (1986). There are also a number of previous studies in which soil permeability was characterized by lognormal distribution (e.g. Badaoui et al. 2007; Freeze 1977; Griffiths and Fenton 1993; Huang et al. 2010). Although little is currently known about the probability distribution of m_v , a thorough review of the literature (e.g. Freeze 1977; Huang et al. 2010) indicates that it is reasonable to assume lognormal probability density functions for m_v , as the lognormal distribution guarantees non-negative values of volume compressibility and offers advantage of simplicity because of having simple relationship with the normal distribution.

3.2.1.2 Generation of spatially random soil property field

A number of different algorithms are currently available to generate multi-dimensional random field of which the covariance matrix decomposition (CMD), the fast Fourier transform (FFT) method, turning band method (TBM) and local average subdivision (LAS) method are the most common. By considering the accuracy, effectiveness, simplicity of use, suitability of implementation and compatibility of the above mentioned techniques with the soil consolidation problem, LAS method developed by Fenton and Vanmarcke (1990) is used in this thesis to generate random fields of a soil property (i.e. k or m_v). Using LAS, random fields of soil property is generated in the form of a grid of cells that are assigned values of soil property different from one another across the grid. The generated random field is then mapped onto a finite element modelling of soil consolidation by PVDs, taking into account the number of finite elements and element size in the FE mesh. In other words, the random field is generated in such a way that the number of grid cells is equal to the number of finite elements, and the FE size is taken into full account in the local averaging process. The value of soil property assigned to each cell of the

grid is itself a random variable, thus the FE mesh contains a number of random variables that is equal to the number of the finite elements.

Details of LAS method in 1D, 2D and 3D are described by Fenton and Vanmarcke (1990). Since both k and m_v are generated as 2D random fields, a brief overview of the 2D implementation of LAS is repeated here. The 2D LAS method involves a several staged subdivision process in which a parent cell is divided into four equal sized cells at each stage. The values in the four new cells are selected in such a way that the upward averaging is preserved and they are properly correlated with each other. Following this process, the total number of cells, i.e. $N_1 \times N_2$, desired in the final field can be expressed as:

$$N_1 = k_1(2^m) \quad (3.6)$$

$$N_2 = k_2(2^m) \quad (3.7)$$

where: m is the number of performed subdivision which should be as minimum as possible and the two positive integers k_1 and k_2 should be such that $k_1 \times k_2 \leq 256$. At Stage 0, initial network of $k_1 \times k_2$ cells (parent cells for Stage 1) are generated directly using CMD. The details of CMD can be found in Fenton and Griffiths (2008). As shown in Fig. 3.2, the parent cells from Stage 0 denoted P_l^i , $l = 1, 2, 3, \dots$, is subdivided into four equal sized cells (child cells) at Stage 1 and are denoted P_j^{i+1} , $j = 1, 2, 3$. Although each parent cell is eventually subdivided in the LAS process, subdivision of only P_5^i is shown in Fig. 3.2 for simplicity. By adding a mean term to a random component and using vector notation, the values of the column vector are obtained as follows:

$$\mathbf{P}^{i+1} = \{P_1^{i+1}, P_2^{i+1}, P_3^{i+1}, P_3^{i+1}\} \quad (3.8)$$

As the mean term derives from a best linear unbiased estimate using a 3×3 neighbourhood of the parent values, in such case the column vector can be written as:

$$\mathbf{P}^i = \{P_1^i, \dots, P_9^i\} \quad (3.9)$$

Therefore, in specific:

$$\mathbf{P}^{i+1} = \mathbf{A}^T \mathbf{P}^i + \mathbf{L} \mathbf{O} \quad (3.10)$$

where: \mathbf{O} is a random vector with elements of independent standard normally distributed random variable, $N(0,1)$. By defining the covariance matrices as follows

$$\mathbf{R} = \text{E} \left[\mathbf{Z}^i \mathbf{Z}^{iT} \right] \quad (3.11)$$

$$\mathbf{S} = \text{E} \left[\mathbf{Z}^i \mathbf{Z}^{i+1T} \right] \quad (3.12)$$

$$\mathbf{B} = \text{E} \left[\mathbf{Z}^{i+1} \mathbf{Z}^{i+1T} \right] \quad (3.13)$$

The matrix \mathbf{A} is determined by:

$$\mathbf{A} = \mathbf{R}^{-1} \mathbf{S} \quad (3.14)$$

while the lower triangular matrix \mathbf{L} satisfies:

$$\mathbf{L} \mathbf{L}^T = \mathbf{B} - \mathbf{S}^T \mathbf{A} \quad (3.15)$$

The covariance matrices \mathbf{R} , \mathbf{S} and \mathbf{B} must be evaluated as the covariances between the local averages over the region of the parent and child cells using the variance function where the upward averaging is preserved, i.e.

$$P_5^i = \frac{1}{4} (P_1^{i+1} + P_2^{i+1} + P_3^{i+1} + P_3^{i+1}) .$$

This means that one of the elements of \mathbf{P}^{i+1} is explicitly determined once the other three are known.

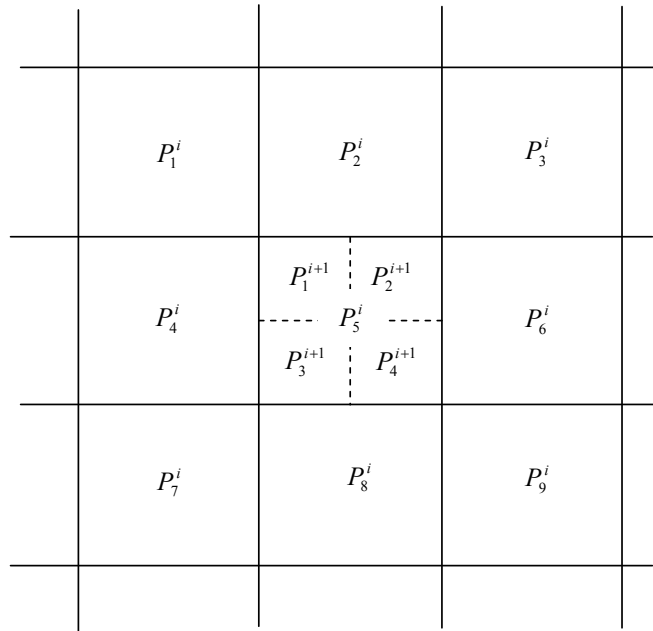
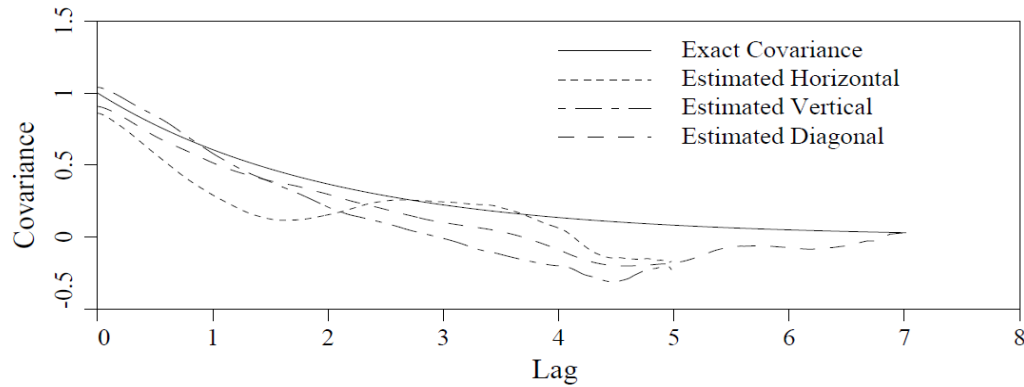


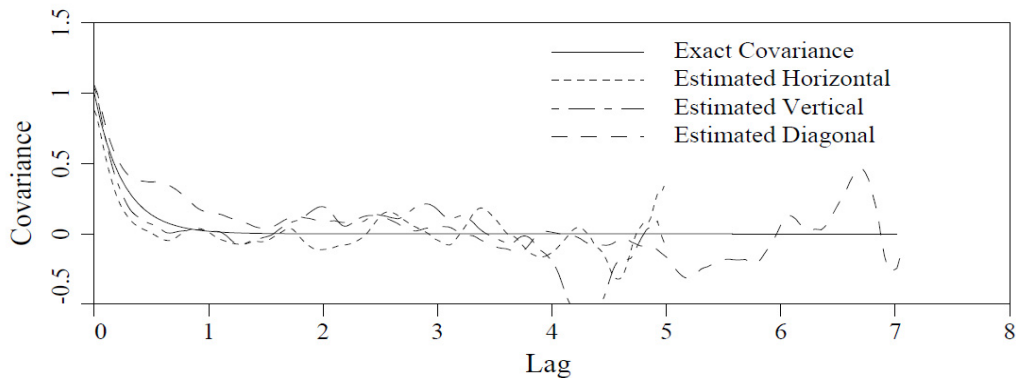
Figure 3.2: Local average subdivision in two dimension (after Fenton and Griffiths 2008)

As customary in any numerical methods, the LAS method has a systematic bias in the variance field, in two and higher dimensions. However, the major motivation of using LAS method arises out from the fact that it produces a field of local average cells whose statistics are consistent with the field resolution. As a result, it is well suited to problems where the system is represented by a set of elements and average properties over each element are desired. Paice et al. (1994) pointed out that, LAS simplifies the task of generating finite elements from the random field and has the ability to increase the resolution of certain regions in the finite element modelling of random fields. Since the degree of consolidation is estimated by averaging over spatial ground, the local average representation of the soil properties through LAS method is the most logical choice. In an investigation on the accuracy of the 2D LAS method, Fenton (1990) conducted the comparisons of the estimated and exact covariance structure of the LAS generated 2D process with SOF of $\theta = 4$ and $\theta = 0.5$ as shown in Figs. 3.3 (a) and (b), respectively. The results have been averaged over 10 realisations and indicate that the exponentially decaying correlation structure has been estimated by 2D LAS method with a reasonable accuracy. It should be noted that, there are now a significant number of research works available in the literature for various practical applications in geotechnical engineering in which LAS method

has been efficiently used to generate random field of the relevant soil properties (e.g. Fenton and Griffiths 1996; 2003; Fenton and Vanmarcke 1998; Griffiths and Fenton 1993; 2004; Griffiths et al. 2002; Paice et al. 1996).



(a)



(b)

Figure 3.3: Comparison of estimated and exact covariance structure of the LAS generated 2-D process, with (a) $\theta = 4$ and (b) $\theta = 0.5$ averaged over 10 realizations (after Fenton 1990)

In the process of simulating the random soil property field, correlated local averages standard normal random field $G(x)$ are first generated with zero mean, unit variance and a spatial correlation function using LAS technique. The correlation coefficient between a soil property measured at a point x_1 and a second point x_2 is specified by a correlation function, $\rho(\tau)$, where $\tau = |x_1 - x_2|$ is the absolute distance between the two points. An exponentially decaying (Markovian) spatial correlation function is assumed in this research as follows (Fenton and Griffiths 2008) :

$$\rho(\tau) = \exp\left(-\sqrt{\left(\frac{2|\tau_h|}{\theta_h}\right)^2 + \left(\frac{2|\tau_v|}{\theta_v}\right)^2}\right) \quad (3.16)$$

where: $|\tau_h|$ and $|\tau_v|$ are the absolute distances between two points in the horizontal and vertical directions, respectively; θ_h and θ_v are the spatial correlation lengths in the horizontal and vertical directions, respectively. For isotropic condition, $\theta_h = \theta_v = \theta$ and Eq. (3.16) reduces to:

$$\rho(\tau) = \exp\left(-\frac{2|\tau|}{\theta}\right) \quad (3.17)$$

The scale of fluctuation controls the decay rate of the correlation function given in Eqs. 3.16 and 3.17, i.e. it describes the limit of spatial continuity of spatial correlation. As previously discussed in Chapter 2, a small value of θ implies rapid fluctuation of the soil property in the ground about the mean, whereas a large value of θ implies a smoothly varying field.

If a soil property X is assumed to be characterised statistically by a lognormal distribution (note that both k and m_v are assumed to be lognormally distributed) defined by μ_X and σ_X , the underlying normally distributed correlated random field, $G(x)$, generated by the LAS method is then necessary to be transformed into a lognormal distribution using the following transformation (Fenton and Griffiths 2008):

$$X_i = \exp\{\mu_{\ln X} + \sigma_{\ln X} G(x_i)\} \quad (3.18)$$

where: x_i and X_i are, respectively, the vector containing the coordinates of the centre of the i th element and the soil property value assigned to that element; $\mu_{\ln X}$ and $\sigma_{\ln X}$ are, respectively, the mean and standard deviation of the underlying normally distributed $\ln(X)$. $\mu_{\ln X}$ and $\sigma_{\ln X}$ can be computed using Eqs. (3.2) and (3.3), respectively, as previously shown in Section 3.3.1. It is worthy to note that, the spatial correlation length (θ) is estimated with respect to the underlying normally

distributed random field ($\ln X$) and the correlation coefficient operates between the values of $\ln X$.

3.2.1.3 Generation of two cross-correlated random soil property fields

Although the generation procedure of an individual random soil property field using LAS method is described in the previous section, it is often necessary to deal with more than one random variable together, where the uncertainty in one may be influenced by the uncertainties in the other. That is, the uncertainty in two random variables may be cross-correlated instead of being independent. The effects of spatially variable m_v and its cross correlation with k will be investigated in Chapter 4 of this dissertation. Accordingly, a review of the generation procedure of cross-correlated k and m_v fields implemented in LAS algorithm is described later in this section. As mentioned in Chapter 2 (see Section 2.7.1.5), the cross-correlation between two random variables usually measured in terms of the correlation coefficient (see Eq. 2.37). It expresses the degree to which two soil properties vary together. Although little currently known about the level of correlation between k and m_v , it is often considered in soil mechanics that for the same soil, k and m_v are strongly correlated. Strong positive correlation between the compressibility and permeability for fine-grained dredged materials have also been shown by Morris (2003). In LAS technique, cross-correlation between k and m_v is implemented using the covariance matrix decomposition (CMD) approach. The algorithm is summarised as follows:

1. Specify the cross-correlation coefficient, ρ_{km_v} ($-1 \leq \rho_{km_v} \leq 1$). Values of ρ_{km_v} of 1, 0, and -1 correspond to completely positively correlated, uncorrelated, and completely negatively correlated, respectively; and
2. Form the stationary (i.e. the same at all points x in the field) correlation matrix between the underlying normally distributed correlated random field $G_{\ln k}(x)$ and $G_{\ln m_v}(x)$, of k and m_v as follows:

$$\rho = \begin{bmatrix} 1.0 & \rho_{km_v} \\ \rho_{km_v} & 1.0 \end{bmatrix} \quad (3.19)$$

3. Compute the Cholesky decomposition of ρ . That is, find the lower triangular matrix L such that $LL^T = \rho$;
4. Generate two independent standard normally distributed random fields, $G_1(x)$ and $G_2(x)$, each having a scale of fluctuation of θ ;
5. At each spatial point, x , form the underlying normally distributed point-wise correlated random fields, as follows:

$$\begin{Bmatrix} G_{\ln k}(x_i) \\ G_{\ln m_v}(x_i) \end{Bmatrix} = \begin{bmatrix} L_{11} & 0 \\ L_{21} & L_{22} \end{bmatrix} \begin{Bmatrix} G_1(x_i) \\ G_2(x_i) \end{Bmatrix} \quad (3.20)$$

6. Transform the cross-correlated standard normal random field of k and m_v (i.e. $G_{\ln k}(x_i)$ and $G_{\ln m_v}(x_i)$) to the final lognormal random field using Eq. 3.18.

In this research, the random fields of the associated soil property are generated using a free available computer code based on 2D LAS technique that is written by Prof. G. A. Fenton of Dalhousie University, Canada (<http://www.engmath.dal.ca/rfem/>). It has to be noted that, since the random soil property field is generated by employing a 2D model, the scale of fluctuation in the circumferential direction of the axisymmetric solution will be infinite and thus the soil properties in this direction remain constant. Likewise, the scale of fluctuation in the out-of-plane direction of the plane strain solution will also be infinite and thus the soil properties in this direction remain constant. Despite the above limitation, it is believed that the two-dimensional model will still yield valuable insights.

3.2.2 Finite element modelling incorporating soil spatial variability

With the complete subsurface profile having been simulated in the previous step, the spatial variability of the soil property of interest is now known and can be employed as input in a finite element consolidation modelling of soil improvement via PVDs by mapping the generated field onto the finite element mesh. In this research, all numerical analyses are carried out using the 2D finite element computer program AFENA (Carter and Balaam 1995), which can solve a range of geotechnical engineering problems and has been used successfully in a number of research and commercial projects around the world (e.g. Rowe and Hinchberger 1998; Rowe and

Li 2002). Although AFENA can take into account anisotropic properties and stratification, it is fundamentally deterministic. Consequently, in order to perform probabilistic simulation, the source code of AFENA is modified by invoking the LAS code into it and performing the subsequent arrangement for the repetitive analyses of the Monte Carlo process. Since a single-drain analysis is often enough to investigate the soil consolidation behaviour, all the numerical analyses in this research are performed at the unit cell level. In AFENA, the soil skeleton is treated as linear elastic solid and the consolidation process of soil is treated as a coupled transient problem governed by the Biot's consolidation theory (Biot 1941). In the Biot's theory, the isotropic consolidation of saturated media is represented through coupled solid-fluid interaction equations, formulated by the condition of equilibrium and continuity. Assuming axisymmetric condition and small strain, the governing equilibrium equation of Biot's consolidation in terms of displacement is given by Eq. 3.21.

$$\frac{E'(1-\nu')}{(1+\nu')(1-2\nu')} \left[\frac{\partial^2 \delta_z}{\partial z^2} + \frac{1-2\nu'}{2(1-\nu')} \left(\frac{\partial^2 \delta_z}{\partial r^2} + \frac{1}{r} \frac{\partial \delta_z}{\partial z} \right) \right] + \frac{\partial u}{\partial z} = 0 \quad (3.21a)$$

$$\frac{E'(1-\nu')}{(1+\nu')(1-2\nu')} \left[\frac{\partial^2 \delta_r}{\partial r^2} + \frac{1}{r} \frac{\partial \delta_r}{\partial r} + \frac{1-2\nu'}{2(1-\nu')} \left(\frac{\partial^2 \delta_r}{\partial z^2} - \frac{1}{r^2} \delta_r \right) \right] + \frac{\partial u}{\partial r} = 0 \quad (3.21b)$$

where: E' and ν' are the effective elastic parameters; δ_z and δ_r are the displacements in the vertical (z) and radial (r) directions, respectively, and u is the excess pore water pressure.

From continuity, and assuming fluid incompressibility, the net flow rate equals the rate of the soil element volume change, such that:

$$\frac{\partial}{\partial t} \left(\frac{\partial \delta_r}{\partial r} + \frac{1}{r} \delta_r + \frac{\partial \delta_z}{\partial z} \right) + \frac{k_r}{\gamma_w} \left(\frac{\partial^2 u}{\partial r^2} + \frac{1}{r} \frac{\partial u}{\partial r} \right) + \frac{k_z}{\gamma_w} \frac{\partial^2 u}{\partial z^2} = 0 \quad (3.22)$$

where: γ_w is the unit weight of water and k_z and k_r are the soil permeabilities in the z - and r -directions, respectively.

For plane strain condition, Eqs. 3.21 and 3.22 become:

$$\frac{E'(1-\nu')}{(1+\nu')(1-2\nu')} \left[\frac{\partial^2 \delta_z}{\partial z^2} + \frac{1-2\nu'}{2(1-\nu')} \frac{\partial^2 \delta_z}{\partial x^2} + \frac{1}{2(1-\nu')} \frac{\partial^2 \delta_x}{\partial x \partial z} \right] + \frac{\partial u}{\partial z} = 0 \quad (3.23a)$$

$$\frac{E'(1-\nu')}{(1+\nu')(1-2\nu')} \left[\frac{\partial^2 \delta_x}{\partial x^2} + \frac{1-2\nu'}{2(1-\nu')} \frac{\partial^2 \delta_x}{\partial z^2} + \frac{1}{2(1-\nu')} \frac{\partial^2 \delta_z}{\partial x \partial z} \right] + \frac{\partial u}{\partial x} = 0 \quad (3.23b)$$

and

$$\frac{\partial}{\partial t} \left(\frac{\partial \delta_x}{\partial x} + \frac{\partial \delta_z}{\partial z} \right) + \frac{k_x}{\gamma_w} \frac{\partial^2 u}{\partial x^2} + \frac{k_z}{\gamma_w} \frac{\partial^2 u}{\partial z^2} = 0 \quad (3.24)$$

where: δ_x and k_x are, respectively, the displacement and permeability in the horizontal (x) direction, respectively.

The finite element discretization and the Galerkin process can transform the equilibrium and continuity equations into a set of element matrix equations, which can be resolved by applying the implicit integration technique, and these matrix equations can be expressed as follows:

$$[k_m]\{\delta\} + [c]\{u\} = \{f\} \quad (3.25)$$

$$[c]^T \left\{ \frac{d\delta}{dt} \right\} - [k]\{u\} = \{0\} \quad (3.26)$$

where: $[k_m]$ and $[\kappa]$ are the material stiffness and permeability matrices, respectively; $[c]$ is the coupling matrix; and $\{u\}$, $\{f\}$ and $\{\delta\}$ are, respectively, the excess pore pressure, total applied load and displacement. A solution of Eqs. 3.25 and 3.26 will enable the displacements and excess pore water pressure to be obtained at spatial location at a given time t from which the average degree of consolidation can be estimated.

3.2.2.1 Average degree of consolidation of spatially variable soil

For a coupled system, the average degree of consolidation can be estimated by either the excess pore water pressure or settlement. In this dissertation, the average degree of consolidation at any particular stage of analysis is defined in terms of the excess pore water pressure, as follows:

$$U_{pp}(t) = 1 - \frac{\bar{u}(t)}{u_0} \quad (3.27)$$

where: $U_{pp}(t)$ and $\bar{u}(t)$ are, respectively, the average degree of consolidation and average excess pore water pressure at a given time t , and u_0 is the initial (uniform) excess pore water pressure. It has to be emphasized that, $\bar{u}(t)$ is obtained by performing numerical integration over the depth and width of the discretized mesh, as follows:

$$\bar{u}(t) = \frac{1}{(r_e - r_w)L} \int_{r_w}^{r_e} \int_0^L \frac{u(t)}{u_0} dx dy \quad (3.28)$$

where: $u(t)$ is the excess pore pressure at any spatial location at time t .

If the average long-term settlement and the average settlement at any time t are given by \bar{s}_u and $\bar{s}(t)$, respectively, the average degree of consolidation at any time defined by settlement can be calculated as:

$$U_{set}(t) = \frac{\bar{s}(t)}{\bar{s}_u} \quad (3.29)$$

In case of spatially variable soil, the settlement will be different in different places, therefore, the average values of $s(t)$ and s_u are used to estimate the average degree of consolidation $U_{set}(t)$. It has to be noted that, the average degree of consolidation defined by the excess pore water pressure (U_{pp}) will be different from that defined by settlement (U_{set}) for heterogeneous soils, and U_{pp} and U_{set} will be equal only when m_v is constant across the soil mass (see e.g. Huang and Griffiths 2010; Lee et al. 1992). It should also be noted that, $U(t)$ described in Eqs. 3.27 and 3.29 is the average degree of consolidation over the soil domain but hereafter will be simplified by denoting it as the degree of consolidation. This is to avoid the conflict that may occur with the mean (over a suite of Monte Carlo simulations) degree of consolidation, μ_U , that will be described later in Eqs. 3.30 and 3.32.

3.2.3 Repetition of process based on the Monte Carlo technique

Following the procedures of the Monte Carlo technique, the process of generating a random field of soil properties of interest (Section 3.2.1) and the subsequent finite element analysis (Section 3.2.2) are repeated many times to produce reasonably stable statistics of the degree of consolidation. A single generation of such random field over the finite element mesh and the subsequent finite element analysis is termed “realization”. In the present research, 1000 realizations are conducted in such a way that each realization (out of 1000 realizations) of the random soil property field is generated with the same mean, standard deviation and spatial correlation length; however, the spatial distribution of soil property varies from one realization to the next. The number of realizations required for the case studies considered in this research to estimate the degree of consolidation statistics with reasonable accuracy is investigated and discussed further in Section 3.3.1. The nature of the generated random soil property fields (whether uniform or erratic) is regulated by the magnitudes of $\frac{\sigma}{\mu}$ (i.e. v) and θ . It should be noted that, although the variability in the distribution is measured in terms of σ , it cannot impart the degree of deviation with respect to μ . In probabilistic study it is often necessary to encounter a soil parameter with different μ and/or more than one soil parameter each with different μ . Under

such circumstances, the variability of a random variable is often expressed by the dimensionless parameter v for the purpose of comparison. Under this reasoning, in the subsequent part of this thesis, σ of a random soil property is expressed by the normalized form v . Fig. 3.4 shows a typical random soil property realization field in which the magnitude of soil property remains constant within each element but differs from one element to another.

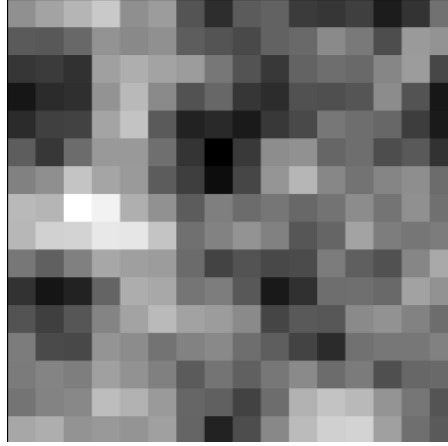


Figure 3.4: Typical realization of a random soil property field

The obtained outputs from the suite of 1000 realizations of the Monte Carlo simulation are collated and statistically analysed to produce estimates of the mean and standard deviation of the degree of consolidation. To determine the mean (over the 1000 realizations of the Monte Carlo simulations) of the degree of consolidation, it is first necessary to determine the representative mean (over the suite of 1000 Monte Carlo simulations) of $\bar{u}(t)$ (remember that, in order to determine the degree of consolidation, U , the average excess pore water pressure throughout the soil mass, \bar{u} , needs to be calculated first). In this thesis, at any given time t , the mean of the degree of consolidation based on the pore water pressure, $\mu_{U(pp)}$, is estimated by utilizing the geometric average (considered as the representative mean) of $\bar{u}(t)$, as follows:

$$\mu_{U(pp)} = 1 - \exp \left[\frac{1}{n_{sim}} \sum_{i=1}^{n_{sim}} \ln \left(\frac{\bar{u}(t)}{u_0} \right)_i \right] \quad (3.30)$$

The standard deviation of the average degree of consolidation at any time t defined by the pore water pressure, $\sigma_{U(pp)}$, is estimated as follows:

$$\sigma_{U(pp)} = \sqrt{\frac{1}{n_{sim} - 1} \sum_{i=1}^{n_{sim}} \left[(U_{pp}(t))_i - \mu_{U(pp)} \right]^2} \quad (3.31)$$

where: n_{sim} is the number of Monte Carlo simulations; $(\bar{u}(t)/u_0)_i$ and $(U_{pp}(t))_i$ are, respectively, the ratio of the average excess pore water pressure to the initial (uniform) excess pore pressure and the degree of consolidation at any time t for the i th simulation (see Eq. 3.27). The use of the geometric average of \bar{u} in computing $\mu_{U(pp)}$ is due to the fact that, in a 2D space, compared to the 1D space, the flow of water has more freedom for escaping from the consolidated soil mass and therefore, the geometric average may be a better estimator (e.g. Dagan 1989) for computing the representative mean of the average excess pore water pressures. Furthermore, Hwang and Witczak (1984) stated that at any certain consolidation time, the degree of consolidation in a 2D space is higher than that of in a 1D space. As mentioned in Section 2.7.2.4, geometric average is smaller than the arithmetic average. Therefore, the use of geometric average instead of arithmetic average of \bar{u} will lead to a higher μ_U , which is reasonable for 2D and higher dimensions. Use of the arithmetic average of \bar{u} will lead to a lower μ_U and is therefore more appropriate for 1D consolidation problem. Since the degree of consolidation defined by the excess pore water pressure, U_{pp} , will be different from that defined by settlement (i.e. U_{set}) for heterogeneous soil, it is necessary to ensure that this differences arise only from the constitutive behaviour of soil and not from other sources. Therefore, to remain consistent with the calculation of $\mu_{U(pp)}$ and $\sigma_{U(pp)}$, the mean, $\mu_{U(set)}$, and standard deviation, $\sigma_{U(set)}$, of the average degree of consolidation in terms of settlement at any time t are estimated as follows:

$$\mu_{U(set)} = 1 - \exp \left[\frac{1}{n_{sim}} \sum_{i=1}^{n_{sim}} \ln \left(\frac{\bar{s}_u - \bar{s}(t)}{\bar{s}_u} \right) \right] \quad (3.32)$$

$$\sigma_{U(set)} = \sqrt{\frac{1}{n_{sim} - 1} \sum_{i=1}^{n_{sim}} \left[(U_{set}(t))_i - \mu_{U(set)} \right]^2} \quad (3.33)$$

3.3 Probabilistic Interpretation

One of the main objectives of the stochastic consolidation analyses is to estimate the probability that a deterministic degree of consolidation overestimates the true consolidation value. To determine such probability for a specific stochastic simulation test, it is necessary to establish the probability distribution nature of the degree of consolidation data obtained from the suite of 1000 realizations. In order to obtain a reasonable probability distribution, the degree of consolidation data obtained at any time t from the suite of 1000 realizations are transformed to $U^*(t)$, which is used as an alternative representing form to the degree of consolidation $U(t)$. The reason for using $U^*(t)$ instead of $U(t)$ is that the obtained fit using the raw data of $U(t)$ was typically poor while a reasonable probability distribution for the obtained degree of consolidation data is better facilitated using $U^*(t)$, which gives sufficiently reasonable approximation to the degree of consolidation behaviour of natural soils. $U^*(t)$ is assumed to be lognormally distributed and can be determined as follows:

$$U^*(t) = \ln \left[\frac{1}{1 - U(t)} \right] \quad (3.34)$$

The legitimacy of the lognormal distribution hypothesis for $U^*(t)$ is examined by the well-known Chi-square test through the frequency density plot of $U^*(t)$ data obtained from the 1000 realizations and a fitted lognormal distribution superimposed for many cases at several different consolidation time. For each of the cases considered, the goodness-of-fit p -value is found to be high enough to approve the reasonableness of the lognormal distribution hypothesis for the simulated $U^*(t)$ data. The rationality of the lognormal distribution assumption for $U^*(t)$ is assessed and discussed in detail in the relevant sections in Chapter 4.

By accepting the lognormal distribution for $U^*(t)$ and for estimating the probability of achieving a target degree of consolidation, the statistical moments μ_{U^*} and σ_{U^*} that represent the mean and standard deviation of the lognormally distributed $U^*(t)$ are calculated from the suite of 1000 realizations using the following transformations:

$$\mu_{U^*} = \frac{1}{n_{sim}} \sum_{i=1}^{n_{sim}} U^*_i(t) \quad (3.35)$$

$$\sigma_{U^*} = \sqrt{\frac{1}{n_{sim} - 1} \sum_{i=1}^{n_{sim}} [U^*_i(t) - \mu_{U^*}]^2} \quad (3.36)$$

where: $U^*_i(t)$ is the $U^*(t)$ from the i 'th realization ($i = 1, 2, 3, \dots, n_{sim}$) at time t and n_{sim} is the total no. of realizations (i.e. 1000). The probability of achieving a target degree of consolidation can then be obtained from the following lognormal probability distribution transformation:

$$P[U^*(t) \geq U_s^*(t)] = 1 - \Phi\left(\frac{\ln U_s^*(t) - \mu_{\ln U^*}}{\sigma_{\ln U^*}}\right) \quad (3.37)$$

where: $P[.]$ is the probability of its argument; $\Phi(.)$ is the standard normal cumulative distribution function; $U_s^*(t)$ is the target $U^*(t)$ that needs to be achieved; $\mu_{\ln U^*}$ and $\sigma_{\ln U^*}$ are, respectively, the mean and standard deviation of the underlying normally distributed $\ln U^*(t)$ and can be estimated from μ_{U^*} and σ_{U^*} with reference to Eqs. 3.2 and 3.3, as follows:

$$\mu_{\ln U^*} = \ln \mu_{U^*} - \frac{1}{2} \sigma_{\ln U^*}^2 \quad (3.38)$$

$$\sigma_{\ln U^*} = \sqrt{\ln\left(1 + \frac{\sigma_{U^*}^2}{\mu_{U^*}^2}\right)} \quad (3.39)$$

Since $U^*(t)$ is a monotonically increasing function of $U(t)$, the following equation holds (Benjamin and Cornell 1970):

$$P[U^*(t) \geq U_s^*(t)] = P[U(t) \geq U_s(t)] \quad (3.40)$$

In this research, it is assumed that the target degree of consolidation is 90% (i.e. $U_s(t) = 0.9$) and for convenience, it is simply denoted as U_{90} , therefore, the probability of

getting 90% target degree of consolidation at any given time, t , can be estimated as follows:

$$P[U(t) \geq U_{90}] = P[U^*(t) \geq 2.3026] = 1 - \Phi\left(\frac{\ln 2.3026 - \mu_{\ln U^*}}{\sigma_{\ln U^*}}\right) \quad (3.41)$$

Note that when $U_s(t) = U_{90} = 0.9$, $U_s^*(t) = \ln[1/(1-0.9)] = 2.3026$. It should also be noted that, when U^* is calculated by transforming U_{pp} (i.e. based on the pore water pressure), it is denoted as U_{pp}^* and the corresponding μ , σ , of U^* and $P[U \geq U_{90}]$ are denoted as $\mu_{U^*(pp)}$, $\sigma_{U^*(pp)}$ and of $P[U \geq U_{90}]_{(pp)}$ respectively, while for the case of settlement they are denoted as U_{set}^* , $\mu_{U^*(set)}$, $\sigma_{U^*(set)}$ and $P[U \geq U_{90}]_{(set)}$.

3.4 General Considerations

One of the main advantages of using numerical techniques is that it offers the ability to model problems with various different conditions to make the problem more realistic. However, the formulation of the problem often becomes very difficult if too many different conditions are incorporated into the same problem. Therefore, it is reasonable to consider only the salient aspects that govern the behaviour of the problem. Given the complexity of the stochastic problem of soil consolidation by PVDs, and since this study is devoted solely to investigate the effect of soil spatial variability on soil consolidation, some conditions are restricted to some limits throughout this research, and this restrictions are described below.

- **Drainage condition**

In soil improvement by PVDs, consolidation of soil can take place by simultaneous vertical and horizontal (radial) drainage of water. However, as the drainage length in the vertical direction is significantly higher than that of the horizontal direction and permeability in the vertical direction is often much lower than that of the horizontal direction (Hansbo 1981), soil consolidation due to vertical drainage is much less than that of the horizontal drainage and may be neglected without considerable reduction in the accuracy of predicted consolidation. Under this reasoning, only soil

consolidation due to horizontal drainage is analysed in the current study (i.e. no drainage is permitted in the vertical direction).

- **Loading condition**

All the consolidation problems considered in this dissertation are subjected to a uniform initial excess pore pressure distribution at $t = 0$.

- **Well resistance effect**

As mentioned earlier in Chapter 2 (see Section 2.1.2), the well resistance factor may affect the rate of consolidation. Based on laboratory experiments carried out by Chai and Miura (1999), it has been concluded that the discharge capacity of PVD reduces significantly with the elapsed consolidation time; however, Bo et al. (2003) stated that the effect of well resistance does not seem to have an appreciable impact unless the drains are very long and are subjected to high lateral stresses. In addition, typical discharge capacity of most commercial PVDs exceeds $150 \text{ m}^3/\text{year}$ and can reach up to $500 \text{ m}^3/\text{year}$ (Bo et al. 2003), and Holtz et al. (1989) suggested that if the working discharge capacity of PVDs exceeds $150 \text{ m}^3/\text{year}$, the effect of well resistance becomes insignificant and can be ignored. Consequently, to avoid superfluous complexity, the effect of well resistance is not considered in this thesis.

- **Problem boundary**

Since a single-drain analysis is often enough to investigate the soil consolidation behaviour, the effect of spatial variability of soil permeability is examined using a unit cell of soil around a single drain.

- **Probability of achieving 90% consolidation**

Every soil improvement project is executed to eliminate future settlement by specifying a certain degree of consolidation equivalent to the surcharge load. As 90% consolidation is usually acceptable for the purpose of design of any soil improvement

project (Bo et al. 2003), only probability of achieving 90% consolidation is analysed in this dissertation.

3.5 Validation of Finite Element Computer Program AFENA

Prior to using the finite element code AFENA in the stochastic analyses, its predictive ability in the deterministic consolidation modelling by PVDs is verified for an example solved by Hird et al. (1992) using the finite element software CRISP. In addition, AFENA is further verified for the same example against the analytical solution of Hansbo (1981) using Eq. 2.12. The geometry of the problem along with the boundary conditions is shown in Fig. 3.5, in that no drainage is permitted at the top, bottom and right side boundaries. To reproduce the result obtained by Hird et al. (1992), axisymmetric finite element consolidation analysis using linear stress-stress behaviour is carried out using his provided test data shown in Table 3.1, without considering smear or well resistance effects. A unit load u_0 is applied to the top surface at time $t = 0$ and is maintained at that value.

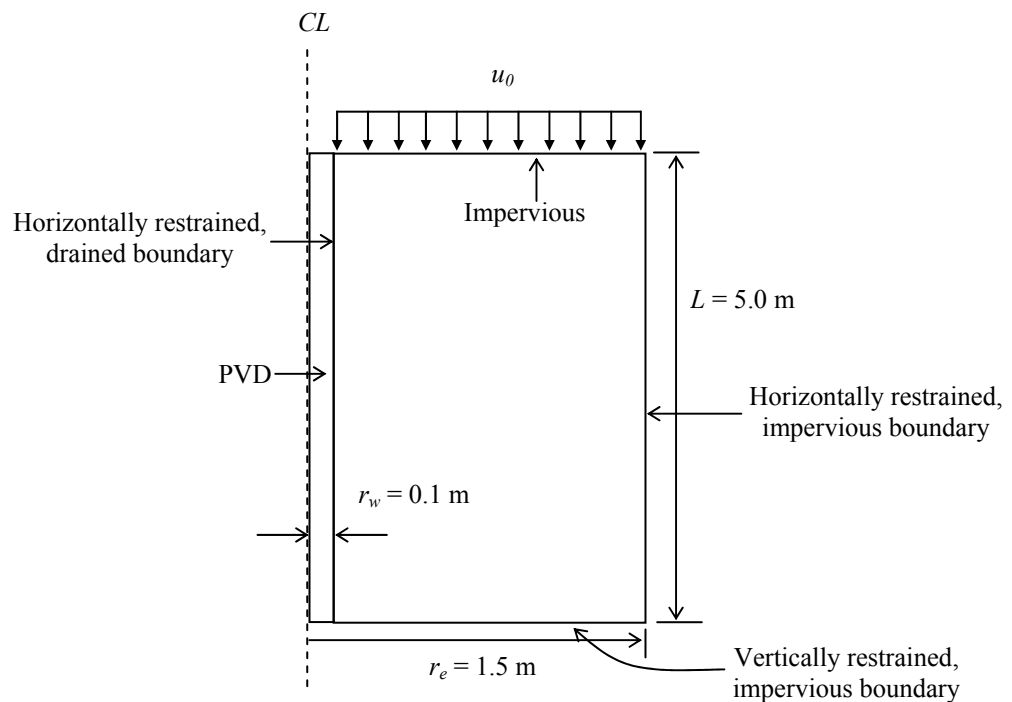


Figure 3.5: Geometric parameters and boundary conditions for unit cell analysis [Used by Hird et al. (1992)]

Table 3.1: Soil parameters of the problem used by Hird et al. (1992) and Equation (2.12)

Solution	Parameter	Value	Solution	Parameter	Value
Hird FE solution	E' (MPa)	10	Equation (2.12)	c_h (m ² /sec)	1.02×10^{-5}
	k (m/sec)	10^{-8}		α	1.958
	ν'	0.0		m_v (m ² /kN)	10^{-4}

To remain consistent with Hird's solution, the average degree of consolidation at any particular stage of the analysis is calculated in terms of nodal excess pore pressures using Eq. 3.27. The comparison results are shown in Fig. 3.6 where T_h in the horizontal axis is known as the time factor for radial (horizontal) drainage and is equal to $c_h t / 4r_e^2$. It can be seen that the result from the present AFENA finite element analysis illustrates an excellent agreement as that presented by Hird et al. (1992), and also with the analytical method proposed by Hansbo (1981). Thus, the author is satisfied that the finite element analysis using AFENA would provide reasonably accurate predictions of the degree of consolidation over the entire study.

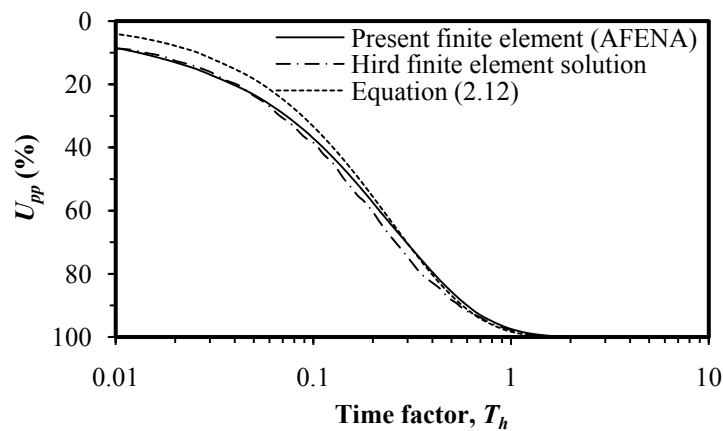


Figure 3.6: Comparison of finite element and analytical results for consolidation of a unit cell (Modified after Hird et al. 1992)

3.6 Preliminary Investigation on the Factor Affecting the Statistics of the Degree of Consolidation

As indicated in Section 3.2.3, the accuracy of the statistics of the degree of consolidation is dependent on both the number of Monte Carlo simulations and mesh density. Generally speaking, the accuracy of the finite element solutions increases as

the number of realisations and mesh density increase. However, as the repetitive finite element analysis is time consuming and the estimated statistics of the degree of consolidation usually converges within a certain number of realisations, it is important to determine the minimum number of realisations and optimum mesh density required to produce a reliable and reproducible results. The consolidation problem under consideration that was used to investigate the sensitivity of the degree of consolidation statistics to the mesh density and number of Monte Carlo simulations implies an axisymmetric finite element simulation (Fig. 3.7) of geometry $L = 1.0$ m, $r_e = 1.025$ m and $r_w = 0.025$ m, without considering the smear effect. As the minimum number of realisations required to produce accurate result is dependent on the number of component random variables (Hahn and Shapiro 1967), in this investigation, both k and m_v are considered as random variable. The mean value of the spatially variable permeability, μ_k , and volume compressibility, μ_{m_v} , are selected to be equal to 1×10^{-9} m/sec and 7.43×10^{-5} m²/kN, respectively. One of the “worst” case (as can be seen later in Chapter 4) with the permeability coefficient of variation $\nu_k = 400\%$, compressibility coefficient of variation $\nu_{m_v} = 100\%$ and scales of fluctuation $\theta_k = \theta_{m_v} = 2.0$ is chosen to investigate the effects of mesh density and the number of Monte Carlo simulations on the degree of consolidation statistics. The detailed treatment of these two aspects, namely, the mesh density and number of simulation are described below.

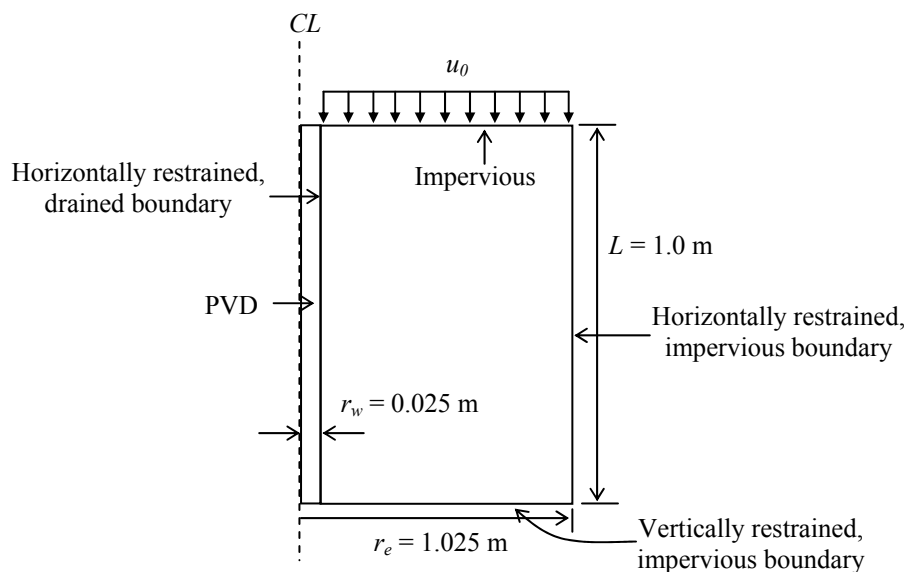
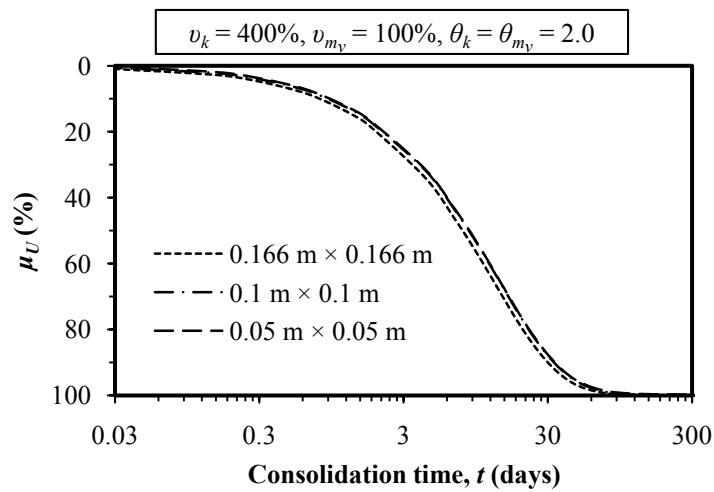


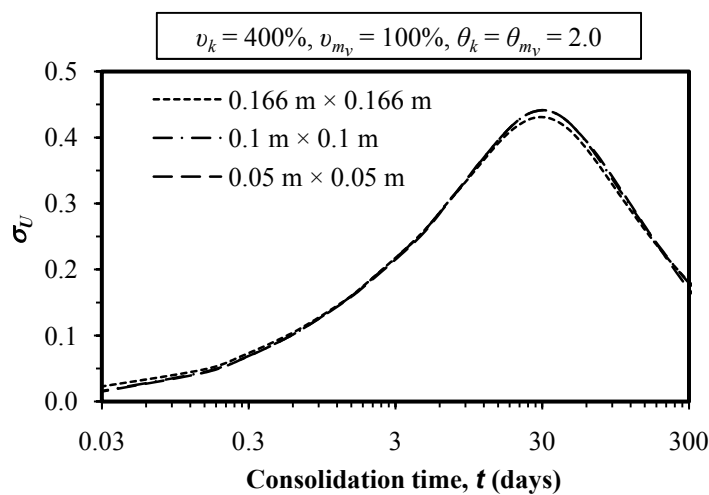
Figure 3.7: Geometric parameters and boundary conditions used for determining the minimum number of simulations and optimum mesh density

3.6.1 Effect of mesh density

To investigate the effect of element size of the finite element mesh on the estimated statistics of the degree of consolidation, three different mesh densities are considered: (a) $0.166 \text{ m} \times 0.166 \text{ m}$; (b) $0.1 \text{ m} \times 0.1 \text{ m}$; and (c) $0.05 \text{ m} \times 0.05 \text{ m}$. Using each mesh, 1000 Monte Carlo simulations are performed. The mean, μ_U , and standard deviation, σ_U , of the degree of consolidation for each mesh densities are estimated based on the excess pore water pressure from Eqs. 3.30 and 3.31 and are presented as a function of time in Fig 3.8.



(a)



(b)

Figure 3.8: Influence of mesh density on (a) μ_U and (b) σ_U

The comparison of the estimated μ_U obtained from the finite element Monte Carlo simulation using different mesh densities is shown in Fig. 3.8(a). It can be seen that μ_U obtained from the mesh sizes $0.1 \text{ m} \times 0.1 \text{ m}$ and $0.05 \text{ m} \times 0.05 \text{ m}$ are identical and is slightly different from that obtained from the mesh size $0.166 \text{ m} \times 0.166 \text{ m}$. Fig 3.8(b) plots the estimated σ_U obtained from different mesh densities as a function of time. It can be seen that σ_U also identical for the mesh sizes $0.1 \text{ m} \times 0.1 \text{ m}$ and $0.05 \text{ m} \times 0.05 \text{ m}$, and is marginally different from that obtained from the mesh size $0.166 \text{ m} \times 0.166 \text{ m}$. Since there is little or no change in μ_U and σ_U from the mesh sizes $0.1 \text{ m} \times 0.1 \text{ m}$ to $0.05 \text{ m} \times 0.05 \text{ m}$, the $0.1 \text{ m} \times 0.1 \text{ m}$ mesh size is deemed to give reasonable precision for the stochastic consolidation analysis. Therefore, a mesh with element size less than 0.1 m will be used for the consolidation problems considered in the subsequent parts of this thesis.

3.6.2 Effect of number of Monte Carlo simulations

In order to maintain reasonable accuracy in the estimated μ_U and σ_U , the sensitivity of μ_U and σ_U on the number of Monte Carlo simulations is examined in this section. As it was shown in the previous section that a mesh with element size of $0.1 \text{ m} \times 0.1 \text{ m}$ gives reasonable precision, the mesh with element size of $0.1 \text{ m} \times 0.1 \text{ m}$ is employed in this investigation. A total of 5 stochastic finite element consolidation analyses are performed with number of Monte Carlo simulations, $n_{sim} = 10, 100, 500, 1000$ and 2000 . The effect of n_{sim} on the estimated μ_U and σ_U is demonstrated in Fig. 3.9. The convergence of μ_U with the increase of n_{sim} is shown in Fig. 3.9(a). It can be seen that μ_U values are quite close for $n_{sim} \geq 100$; however, identical responses of μ_U are found only when $n_{sim} \geq 1000$. The effect of n_{sim} on the estimated σ_U is demonstrated in Fig. 3.9(b). It can be seen that σ_U is less sensitive for $n_{sim} \geq 100$ and behaviour similar to that of μ_U with respect to n_{sim} , identical σ_U are found only for $n_{sim} \geq 1000$. Based on this observation, it is concluded that 1000 simulations are enough to give reliable and reproducible estimates of μ_U and σ_U of the degree of consolidation.

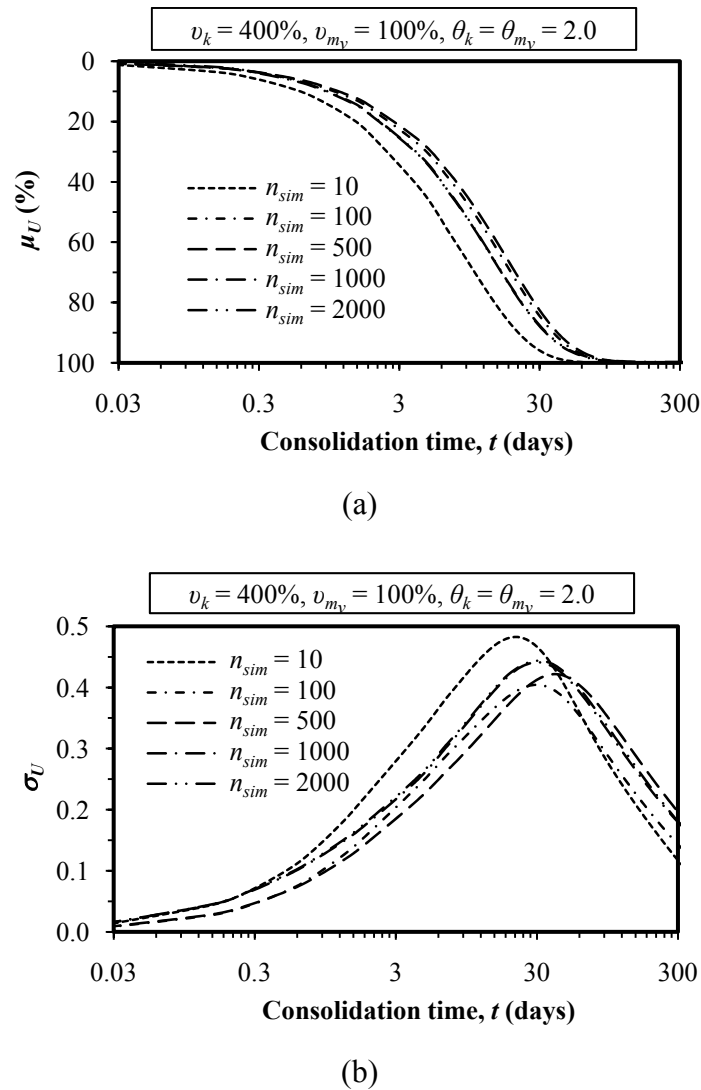


Figure 3.9: Influence of number of simulations on (a) μ_U and (b) σ_U

3.7 Summary

In this chapter, details on the stochastic approach to predict probabilistic behaviour of soil consolidation by PVDs were presented. The approach merges the LAS method of random field theory (to simulate random soil property field) and the finite element modelling (to calculate soil consolidation by PVDs) into a Monte Carlo framework. It was found that the LAS method (Fenton and Vanmarcke 1990) is the most viable choice for the simulation of spatially random soil profiles. It was also found that the spatial variabilities of soil permeability and volume compressibility are the most influencing factors affecting soil consolidation by PVDs and both

factors can be stochastically modelled by assuming lognormal distribution. The formulation and validation of the finite element consolidation analysis model was discussed in some detail in this chapter. The calculation procedure for the mean and standard deviation of the degree consolidation using the consolidation responses obtained from a suite of Monte-Carlo simulations was also described. In the same chapter, an approximate method to obtain the probability of achieving a desired degree of consolidation was presented and discussed. Preliminary studies were undertaken to determine the minimum number of realisations and optimum mesh density required to produce reliable result from the finite element analysis. It was shown that 1000 Monte Carlo simulations and a mesh with element size of $0.1 \text{ m} \times 0.1 \text{ m}$ can give reasonable precision in the stochastic consolidation analysis. In the following chapter, parametric studies will be performed to investigate and quantify the effects ν and θ on the output quantities of interest in relation to the degree of consolidation.

Chapter 4

Soil Spatial Variability in Design of Ground Improvement by Vertical Drains

4.1 Introduction

Although soil is highly variable in the ground, the computed spatial variability of any soil property is not the same for all sites or soils. Accordingly, the statistical parameters of a certain soil property, namely the coefficient of variation (COV), v , and the scale of fluctuation (SOF), θ , can vary by several orders of magnitude and the varying range of the statistical parameters of one soil property differs from that of the other soil properties (see e.g. Tables 2.2 and 2.3). As the spatial distribution of a soil property within a domain of interest depends on the magnitude of v and θ , it is reasonable to expect that the consolidation behaviour of soil will be different according to the magnitude of v and θ . In addition, even with the same magnitude of spatial variation, the effect of one soil property on the estimated behaviour of soil consolidation may be relatively more significant than that of another soil property. The aim of this chapter is therefore to investigate and quantify the effects of v and θ on the stochastic behaviour of soil consolidation by PVDs. In order to achieve this goal, parametric studies are performed using the stochastic approach described in Chapter 3 over a wide range of v and θ of soil permeability, k , and volume compressibility, m_v ; and under various different assumed site conditions. The complete study presented in this chapter is divided into two parts. In the first part, the smear effect is excluded, it is however, investigated in the second and final part. These parts of the study are then further subdivided into two ‘groups’. In the first group, only soil permeability, k , is considered as the random variable, while in the second group both k and m_v are selected as random variables. Details of each part and each group in the study are described below.

4.2 Probabilistic Analysis of Soil Consolidation Without Considering Smear Effect

As mentioned in Section 2.4.1, during installation of PVDs, successive driving and pulling of the mandrel casing significantly distorts and remoulds the adjacent soil. This is called the smear effect, and it affects the rate of soil consolidation to a major degree. However, in this first section, the smear effect is excluded in order to focus on and isolate the fundamental characteristics of the stochastic soil consolidation behaviour. This ‘separation’ allows simplification and clarification of the case prior to commencing the second part of the study, which then investigates the more complex smear effect.

4.2.1 Description of consolidation problem under consideration

In order to carry out the stochastic analysis using the steps described in Chapter 3, a certain consolidation problem must first be selected. In this study, the problem under consideration is represented by an illustrative example that implies an axisymmetric unit cell of geometry (see Fig. 4.1): $L = 1.0$ m, $r_e = 0.85$ m and $r_w = 0.05$ m, where L is the maximum vertical drainage distance; r_e is the radius of the equivalent soil cylinder with an impermeable perimeter or radius of the zone of influence; and r_w is the equivalent radius of the drain. Although the sensitivity analysis presented in Section 3.6.1 to ensure reasonable mesh discretization indicated that a $0.1 \text{ m} \times 0.1 \text{ m}$ mesh is enough to give reasonable precision for the analysis, the problem is discretized into a more refined $0.05 \times 0.05 \text{ m}$ square element mesh of 16×20 elements (see Fig. 4.2) to comply with the minimum correlation length used. It should be noted that the size of the finite element grid is dependent on the scale of fluctuation. For a small scale of fluctuation values, fine grids are required. Harada and Shinozuka (1986) pointed out that the minimum grid dimension should be less than or equal to half of the scale of fluctuation. Each finite element consists of eight bi-quadratic displacement nodes and four bilinear pore pressure nodes. The vertical displacements at the left and right boundaries of the mesh are free to move, while the movement at the bottom boundary of the mesh is completely fixed. No drainage is permitted at the top, bottom and right hand side boundaries. The soil skeleton is modelled as a linear elastic solid and the mean value of the spatially variable

permeability, μ_k , and volume compressibility, μ_{m_v} , are selected to be equal to 5×10^{-10} m/sec and 1.67×10^{-4} m²/kN, respectively. It is to be noted that when permeability is considered as the only random variable, a constant m_v equal to μ_{m_v} (i.e. 1.67×10^{-4} m²/kN) is used across the soil mass.

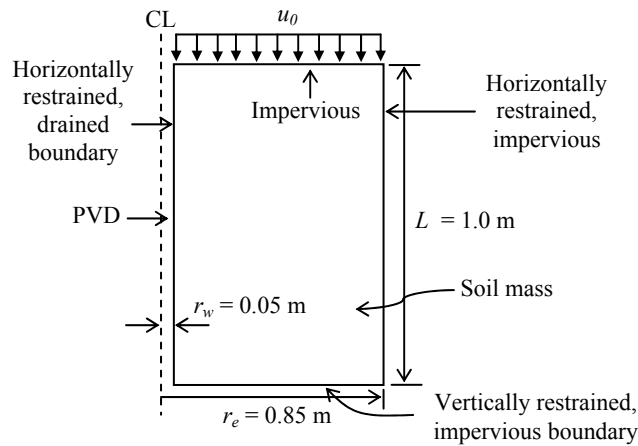


Figure 4.1: Geometry of the consolidation problem for the analysis with no smear

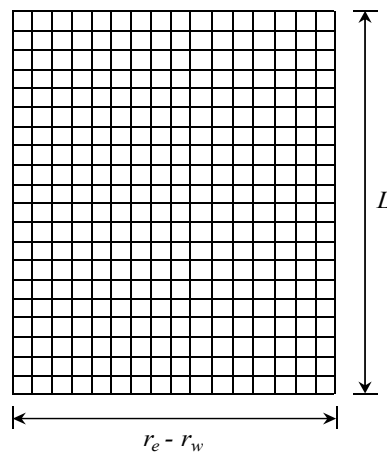


Figure 4.2: Finite element mesh of the selected consolidation problem (all elements being square in dimension: 0.05 m × 0.05 m)

It should also be noted that, the equivalence between axisymmetric and plane strain analyses is also investigated in this study in a probabilistic context. The details of the transformation of the axisymmetric unit cell (described above) to an equivalent plane strain case and the results obtained from the matching comparison are described later in Section 4.2.1.2.3.

4.2.1.1 Deterministic solution

To make comparison with the stochastic analyses results, an initial deterministic analysis relating to the consolidation problem shown in Fig. 4.1 is performed prior to the probabilistic analyses, by assuming a homogeneous soil medium. The permeability and volume compressibility of all elements are assumed to be constant and equal to 5×10^{-10} m/sec and 1.67×10^{-4} m²/kN, respectively. These values are chosen as they would then be taken as the mean value of the subsequent stochastic analyses. It should be noted that the deterministic solution in this case yielded 90% consolidation, U_{90} , at $t = 67.9$ days. The deterministic 90% consolidation time is denoted as t_{D90} (i.e. $t_{D90} = 67.9$ days).

4.2.1.2 Probabilistic analysis of soil consolidation considering spatially random permeability

As discussed in Chapter 3, among all soil properties, k and m_v were found by many researchers (e.g. Huang and Griffiths 2010; Lee et al. 1992; Pyrah 1996) to have the most significant impact on soil consolidation by PVDs. However in this section, only k is treated as a random variable and m_v is assumed to be constant across the unit cell. This is because k can possess a spatial variability of up to 300%, which is much higher than that of m_v that usually ranges from 25% to 30% (Beacher and Christian 2003; Kulhawy et al. 1991; Lee et al. 1983). This can be seen from Table 2.2 in Section 2.7.3. Therefore, it is anticipated that the spatial variability of k will constitute the most significant impact on soil consolidation. The effects of the spatial variability of m_v and its cross-correlation with the spatially variable k are investigated in a later section of this chapter. In this section, the following work is conducted:

- (a) Axisymmetric analyses are performed to investigate the sensitivity of the statistics of the degree of consolidation and probability of achieving 90% consolidation over a range of statistically defined input parameters (i.e. v and θ) of k .
- (b) Following the sensitivity analysis, the effect of anisotropic θ over isotropic θ on the probabilistic behaviour of soil consolidation is investigated and discussed.

- (c) At the end of this section, equivalent plane strain analyses versus axisymmetric analyses are carried out to make a matching comparison between the stochastic solutions obtained from these two conditions.

4.2.1.2.1 Results of sensitivity analyses

In this section, the sensitivity of the degree of consolidation, U , over a range of values of the permeability coefficient of variation, v_k , and scales of fluctuation, θ_k , is investigated. The values of v_k and θ_k used in the parametric studies are given in Table 4.1. The scale of fluctuation, θ_k , is assumed to be isotropic, i.e. $\theta_h = \theta_v = \theta$. The effect of anisotropy in θ_k is investigated and discussed later. It should be noted that since the spatial variation of soil permeability is known to be very large and possibly as high as 300% (Kulhawy et al. 1991; Lee et al. 1983), the upper limit of v_k is set to be equal to 400%. However, in practice the scale of fluctuation tends to be related to the size of the domain over which its estimate is taken. Typical approaches involve estimating the scale of fluctuation indicate that it is significantly smaller than the sampling domain (Dagan 1989; Gelhar 1993). For this reason, it is believed that the values of the spatial variability parameters used represent sufficiently practical ranges that establish general trends for the stochastic soil consolidation behaviour.

Table 4.1: Random field parameters for sensitivity analyses

Parameter	Value
v_k (%)	25, 50, 100, 200, 400
θ_k (m)	0.125, 0.25, 0.5, 1.0, 2.0, 4.0

Following the procedure described in Chapter 3, the lognormally distributed permeability field is generated first by incorporating a certain combination of v_k and θ_k into the LAS method. The coupled consolidation analysis is then performed by mapping the generated field onto the finite element mesh. With the same v_k and θ_k the analysis is repeated 1000 times, using Monte Carlo simulations. A single generation of a random field and the subsequent finite-element analysis of that field are termed “realisation”. Fig. 4.3 shows a typical example of a discretized mesh and the corresponding soil domain represented by a grey scale of a typical permeability

field realisation in which the magnitude of permeability remains constant within each element but differs from one element to another. The lighter elements represent “higher” soil permeability regions, whereas the darker elements refer to “lower” soil permeability regions. Each realisation of the Monte Carlo process differs in the locations at which low and high permeability zones are situated. For example, in one realisation, more low permeability regions may be situated in locations near to the PVD, causing a lower drainage rate, whereas in another realisation, high permeability regions in those locations means a faster drainage rate.

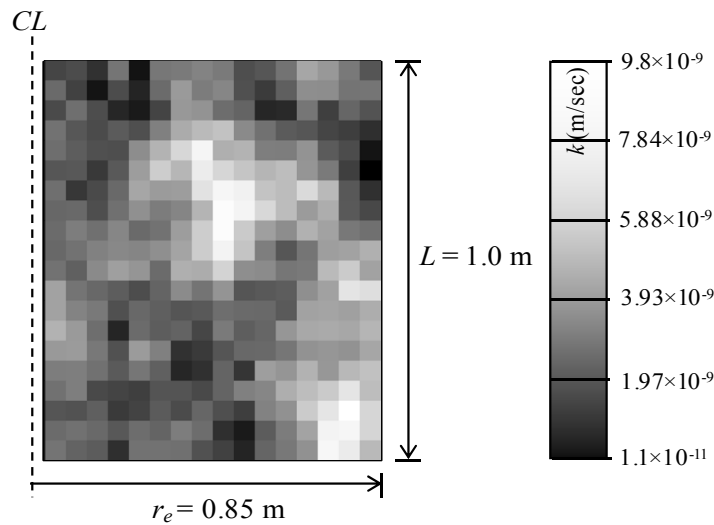


Figure 4.3: Typical realization of a random permeability field for $v_k = 100\%$ and $\theta_k = 0.5$ ($\mu_k = 5 \times 10^{-10}$ m/sec)

Using each combination of the statistical parameters v_k and θ_k shown in Table 4.1, a series of 35 stochastic finite element simulations (i.e. a total 35000 Monte Carlo simulations) are carried out. The obtained outputs from each random consolidation analysis are assimilated and statistically analysed to produce estimates of the mean, standard deviation and probability density functions of the output quantities of interest (i.e. U and U^*) using both the excess pore water pressure and settlement. Note that these quantities (i.e. mean, standard deviation and probability) are quantified with appropriate subscripts “ pp ” and “ set ” depending on whether they are defined by the excess pore water pressure or settlement, where pp and set refer to the solutions based on the excess pore water pressure and settlement, respectively. As mentioned in Section 3.2.2.1, U_{pp} and U_{set} are equal when m_v is constant across the soil mass. Therefore, prior to presenting the results of the sensitivity analyses, it is

necessary to ensure that U_{pp} and U_{set} are equal (i.e. at any consolidation time, $\mu_{U(pp)} = \mu_{U(set)}$ and $\sigma_{U(pp)} = \sigma_{U(set)}$).

- **Comparison between the statistics of U obtained from excess pore water pressure and settlement**

The comparison between the mean, μ_U , and standard deviation, σ_U , of the degree of consolidation, U , defined by the excess pore water pressure and settlement are shown in Figs. 4.4 and 4.5, in which μ_U and σ_U are expressed as functions of the consolidation time, t . Since the general trend of the distribution parameters remains unaltered over the range of the statistical parameters v_k and θ_k , only a small number of test results are presented.

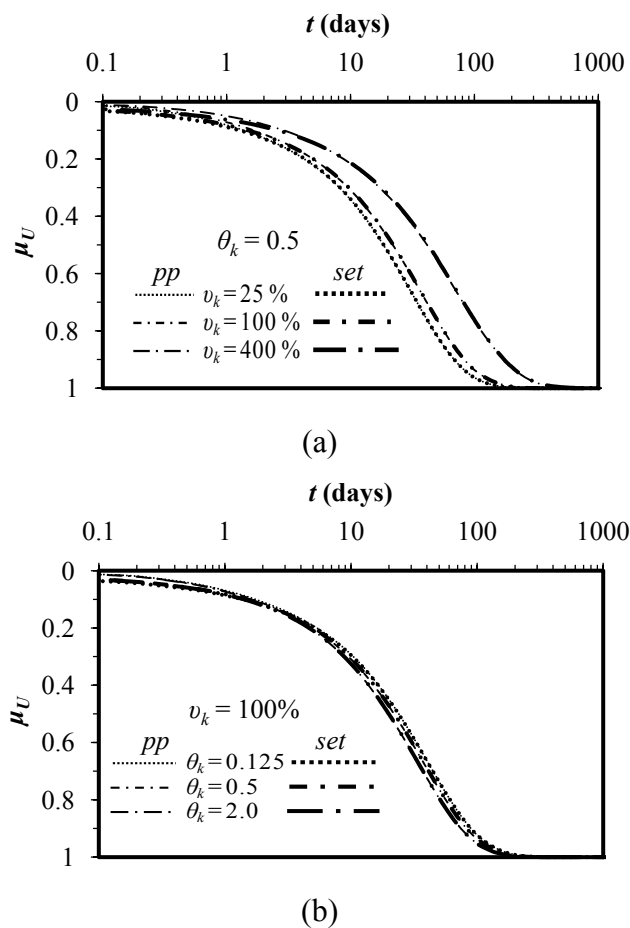
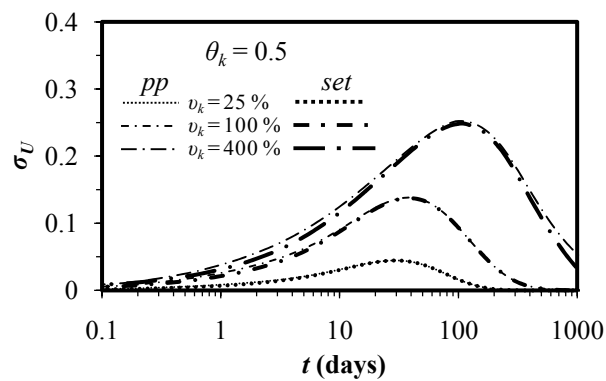


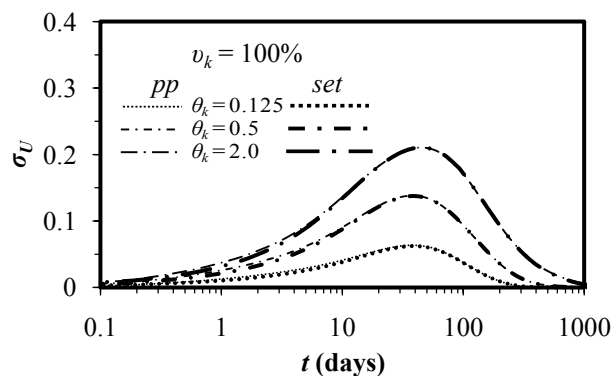
Figure 4.4: Comparison of the results defined by the excess pore water pressure and settlement for the effect of: (a) v_k on μ_U at $\theta_k = 0.5$; (b) θ_k on μ_U at $v_k = 100\%$

The relationship between μ_U and the consolidation time, t , for various v_k with a constant $\theta_k = 0.5$, for various θ_k with a constant $v_k = 100\%$ is illustrated in Figs. 4.4. It can be seen from Fig. 4.4 that, for any certain v_k and θ_k , the estimated $\mu_{U(pp)}$ and $\mu_{U(set)}$ are identical.

Fig. 4.5 shows the agreement between $\sigma_{U(pp)}$ and $\sigma_{U(set)}$ for various v_k with a constant $\theta_k = 0.5$, for various θ_k with a constant $v_k = 100\%$. Visual inspection of Figs. 4.5(a) and (b) suggest that the difference between $\sigma_{U(pp)}$ and $\sigma_{U(set)}$ is negligible for any particular combination of v_k and θ_k . The overall conclusion that can be derived from Figs. 4.4 and 4.5 is that the results obtained on the basis of the excess pore water pressure are identical with those obtained on the basis of settlement, as long as k is spatially variable and m_v is spatially constant. Therefore, only the results computed on the basis of excess pore water pressure are presented below to investigate the effects of spatial variability of k on soil stabilization by PVDs.



(a)



(b)

Figure 4.5: Comparison of the results defined by the excess pore water pressure and settlement for the effect of: (a) v_k on σ_U at $\theta_k = 0.5$; (b) θ_k on σ_U at $v_k = 100\%$

- **Effect of v_k and θ_k on the mean and standard deviation of U**

Although the probability of achieving 90% consolidation is estimated on the basis of the statistics of U^* , the effects of v_k and θ_k on the statistics of U are presented herein. This is due to the fact that in practice, the influence of the soil spatial variability itself on U must be known, rather than U^* per se. Since U^* is a monotonically increasing function of U (noting that $U^* = \ln[1/(1-U)]$), the effects of v_k and θ_k on μ_{U^*} and σ_{U^*} will be qualitatively similar to the effects of v_k and θ_k on μ_U and σ_U . However, the actual implications of v_k and θ_k on U may be somewhat different from that of U^* . It should be noted that as the actual probability distribution of U is unknown, the parameter U^* is introduced only to obtain a reasonable probability distribution of the degree of consolidation data, and in turn the probability of achieving a target degree of consolidation. A qualitative comparison between the mean and standard deviation of U and U^* however will be made later in this section. The results of the sensitivity analyses are presented in Figs. 4.6–4.9, in which $\mu_{U(pp)}$ and $\sigma_{U(pp)}$ are expressed as a function of consolidation time, t .

Fig. 4.6 shows the effects of v_k on $\mu_{U(pp)}$ for each prescribed values of θ_k , which also includes the deterministic solution of no soil variability. It can be seen that at any particular consolidation time, there is a reduction in $\mu_{U(pp)}$ for spatially varied soils compared to the deterministic case. The reduction rate of $\mu_{U(pp)}$ gradually increases as v_k increases. Fig. 4.6 also indicates that the $\mu_{U(pp)}$ curve of a less heterogeneous soil of $v_k = 25\%$ is closer to the deterministic U curve, but gradually shifts to the right for more heterogeneous soils with a higher v_k , implying a delay in consolidation. At any one time, a reduction in $\mu_{U(pp)}$ with the increase of v_k is ‘intuitive’ due to the fact that the volume of low permeability material (in comparison to high permeability material) in the soil mass increases with the gain in permeability variance (i.e. for a fixed value of μ_k an increase of v_k implies an increase in σ_k). Consequently, there is a reduction in the average coefficient of consolidation and in turn in the $\mu_{U(pp)}$. It is worthwhile noting that the spatial variability of soil permeability has no effect on the final amount of consolidation settlement but rather affects the rate of consolidation (the degree of consolidation with time).

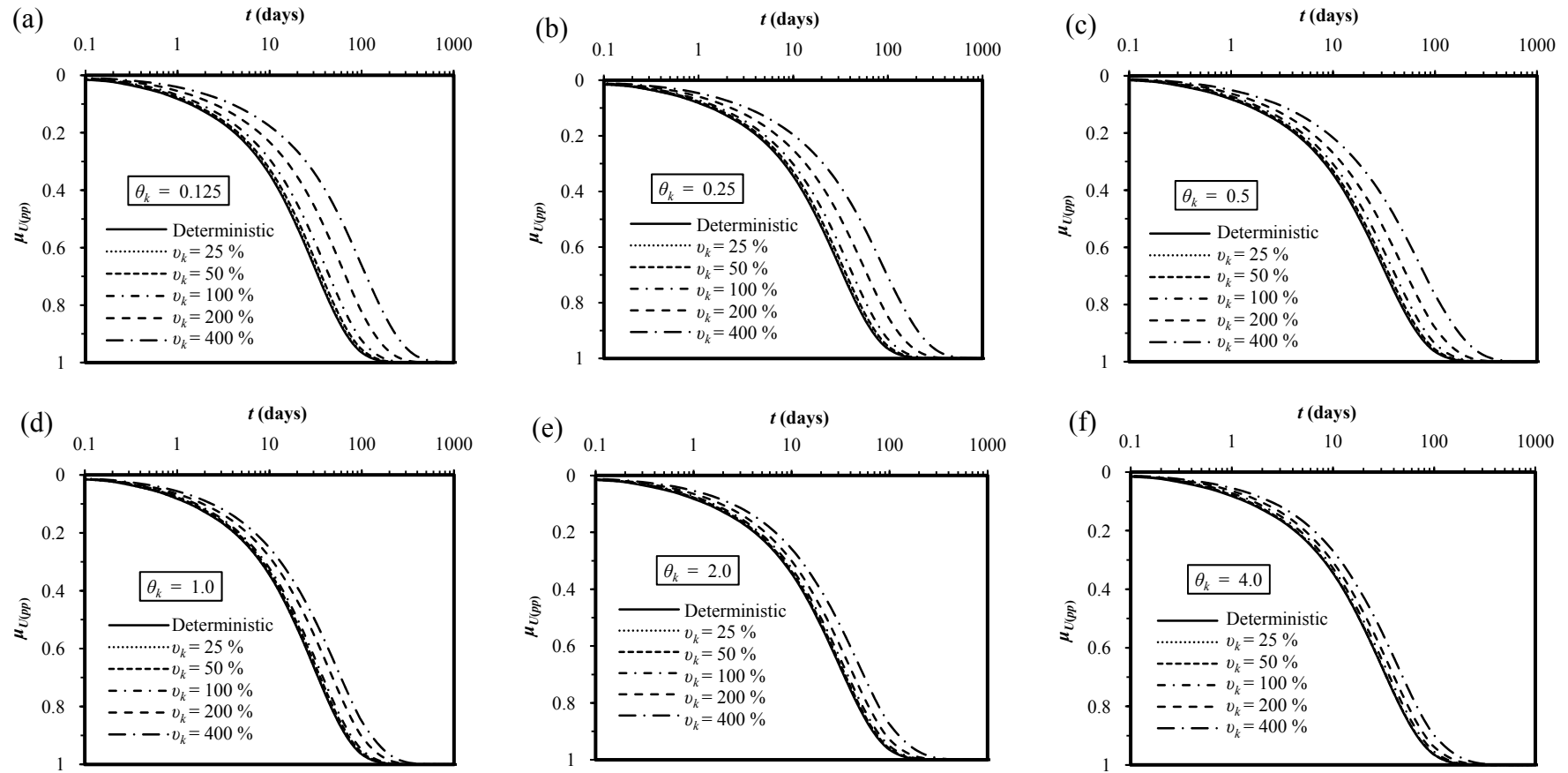


Figure 4.6: Effect of v_k on $\mu_{U(pp)}$ for (a) $\theta_k = 0.125$; (b) $\theta_k = 0.25$; (c) $\theta_k = 0.5$; (d) $\theta_k = 1.0$; (e) $\theta_k = 2.0$; and (f) $\theta_k = 4.0$

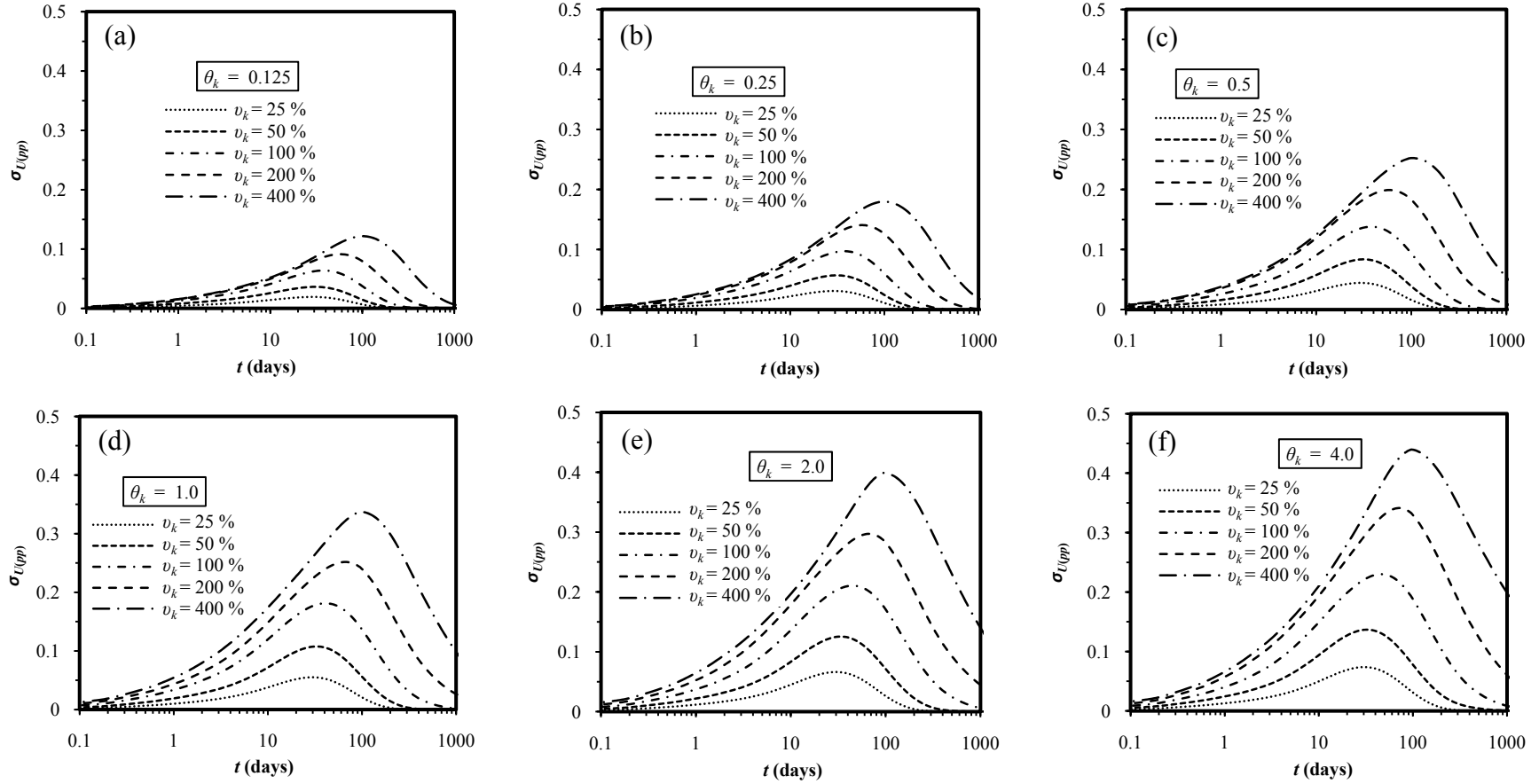


Figure 4.7: Effect of v_k on $\sigma_{U(pp)}$ for (a) $\theta_k = 0.125$; (b) $\theta_k = 0.25$; (c) $\theta_k = 0.5$; (d) $\theta_k = 1.0$; (e) $\theta_k = 2.0$; and (f) $\theta_k = 4.0$

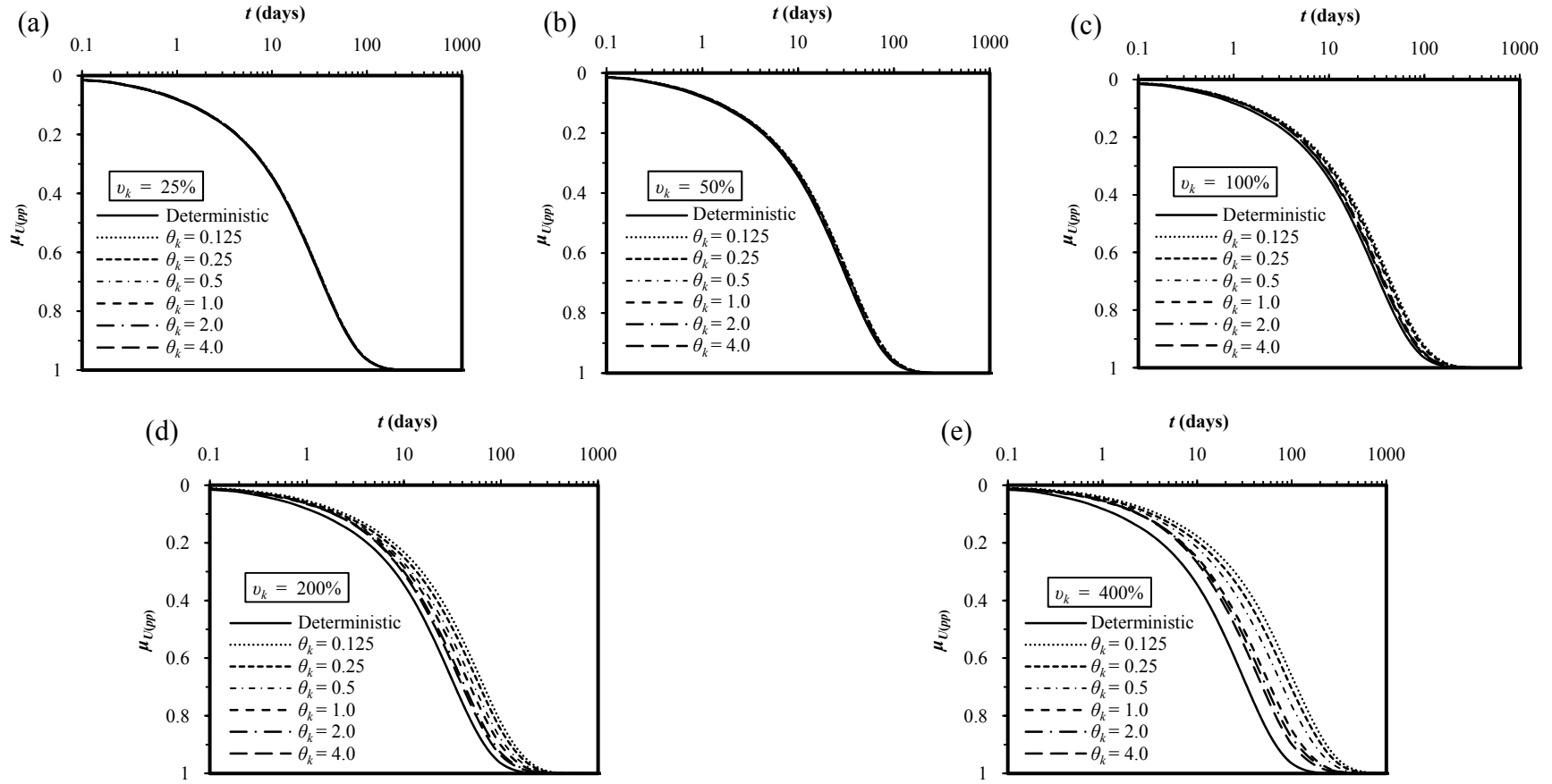


Figure 4.8: Effect of θ_k on $\mu_{U(pp)}$ for (a) $v_k = 25\%$; (b) $v_k = 50\%$; (c) $v_k = 100\%$; (d) $v_k = 200\%$; and (e) $v_k = 400\%$

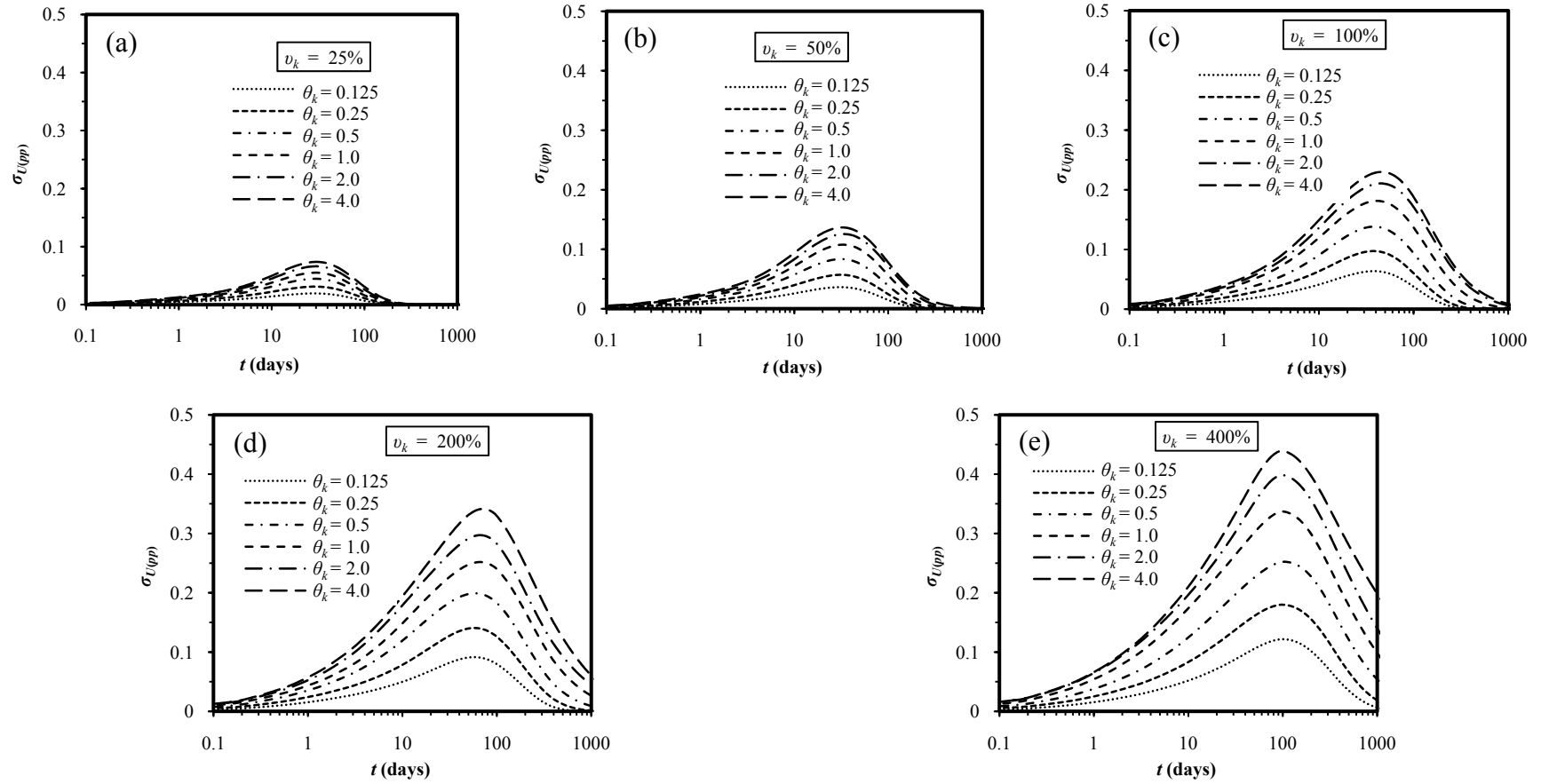


Figure 4.9: Effect of θ_k on $\sigma_{U(pp)}$ for (a) $v_k = 25\%$; (b) $v_k = 50\%$; (c) $v_k = 100\%$; (d) $v_k = 200\%$; and (e) $v_k = 400\%$

The effect of v_k on $\sigma_{U(pp)}$ is shown in Fig. 4.7 for each considered θ_k . The general trend which can be found by observing each individual graph plotted for different θ_k , is that the distribution patterns of $\sigma_{U(pp)}$ with respect to the consolidation time, t , in all cases of v_k is bell-shaped. Initially, $\sigma_{U(pp)}$ is zero at the beginning of consolidation (i.e. at $t = 0.0$), and gradually increases with the gain in consolidation time until it reaches a maximum value at a certain t , then it decreases with further increase of consolidation time until it approaches zero again after the full consolidation has occurred. This behaviour can be explained by noting that $\mu_{U(pp)}$ approaches 0 and 1 as t approaches 0 and ∞ regardless of the variability of k . It can also be observed that, as expected, at any particular t between 0 to ∞ , $\sigma_{U(pp)}$ rises commensurately with the increase of v_k and the point at which the maximum $\sigma_{U(pp)}$ occurs moves to the right as v_k increases.

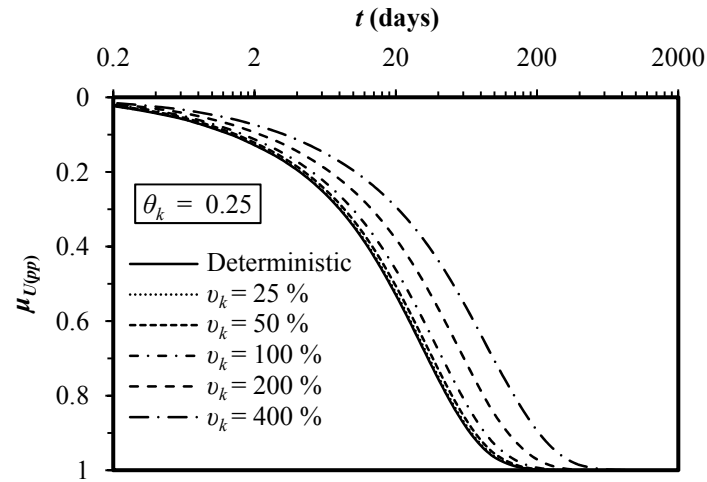
The effect of θ_k on $\mu_{U(pp)}$ is illustrated in Fig. 4.8 for all of considered v_k in ascending an order. It can be seen that for a certain v_k and at any particular consolidation time, t , there is a gradual increase of $\mu_{U(pp)}$ as θ_k increases. However, this behaviour is not distinguishable in Figs. 4.8 (a) and (b) as all curves of $\mu_{U(pp)}$ lie very close together, implying that the influence of the scale of fluctuation on $\mu_{U(pp)}$ is marginal, when $v_k \leq 50\%$. It is also worthy noting that as θ_k increases, the $\mu_{U(pp)}$ curve approaches the deterministic curve which is to be expected, as a strongly correlated permeability field ($\theta_k \rightarrow \infty$) implies more homogeneous soil, hence a deterministic solution. In other words, as the correlation length increases to infinity, the random field becomes relatively uniform (although individual realizations show considerable variability in $\mu_{U(pp)}$ as can be seen later in Fig. 4.9) and $\mu_{U(pp)}$ approaches the value predicted by the constant $k = \mu_k$. The reduction in $\mu_{U(pp)}$ for a small correlation length can also be explained by noting that as the correlation length becomes negligible compared to the size of the problem, the effective permeability approaches the geometric mean, i.e. the effective permeability gradually decreases with decreasing θ_k . By comparing Figs. 4.6 and 4.8, it can be seen that μ_U is relatively less sensitive to θ_k than v_k .

Fig. 4.9 illustrates the effect of θ_k on $\sigma_{U(pp)}$ over the range of v_k considered. It can be seen that for a particular value of v_k , at any certain consolidation time t , $\sigma_{U(pp)}$ increases as θ_k increases. Looking at each graphs presented in Fig. 4.9, very little variation in $\sigma_{U(pp)}$ is observed for small θ_k , even for high v_k . It is well known in statistics that the variance of an average decreases linearly with the number of independent samples used in the average. In the random field context, the effective number of independent samples increases as the correlation length decreases, and thus the decrease in variance in $U_{(pp)}$ is to be expected. Conversely, when the correlation length is large, the variance in $U_{(pp)}$ is also expected to be larger as there is less averaging variance reduction within each realization. The closely grouped curves corresponding to $\theta_k = 2.0$ and 4.0 clearly demonstrate that the increasing rate of $\sigma_{U(pp)}$ gradually decreases with the increase of $\theta_k \geq 2.0$. By comparing Figs. 4.8 and 4.9, it can also be seen from that for low variability soil ($v_k \leq 25\%$), the value of θ_k has little effect.

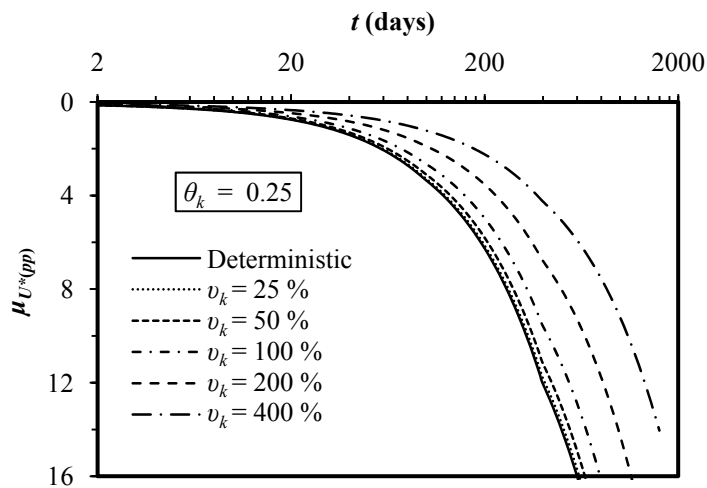
- ***Qualitative comparison between the statistics of U and U^****

Since the probability of achieving 90% consolidation is estimated on the basis of the statistics of U^* , it is of interest to investigate the effects of v_k and θ_k on the statistic of U^* . It is also necessary to confirm that the effects of v_k and θ_k on the statistics of both U and U^* is qualitatively similar. Prior to presenting the results of the analyses, it should be noted that at $t = 0$, both U and U^* are equal to 0, while when t approaches ∞ , U and U^* approach 1 and ∞ , respectively.

Fig. 4.10 shows the effects of v_k on $\mu_{U(pp)}$ and $\mu_{U^*(pp)}$ for a fixed value of $\theta_k = 0.25$. It can be seen that at any certain t between 0 to ∞ , both $\mu_{U(pp)}$ (see Fig. 4.10(a)) and $\mu_{U^*(pp)}$ (see Fig. 4.10(b)) decrease as the v_k increases.



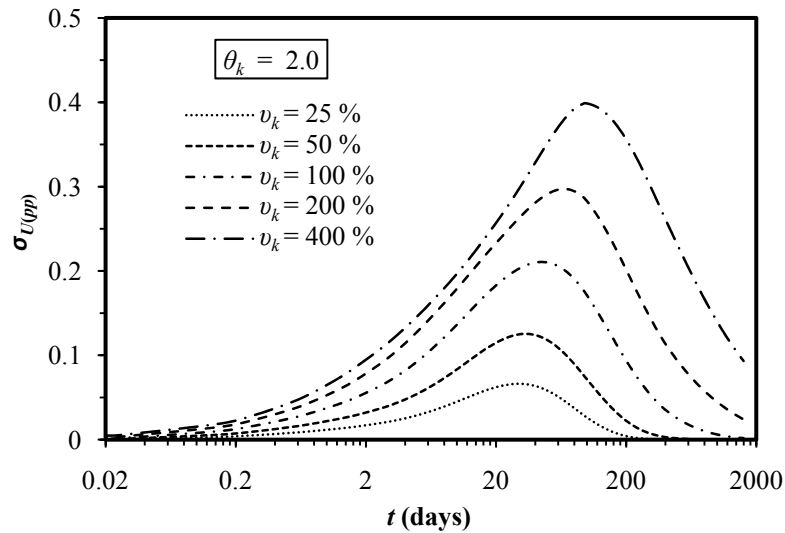
(a)



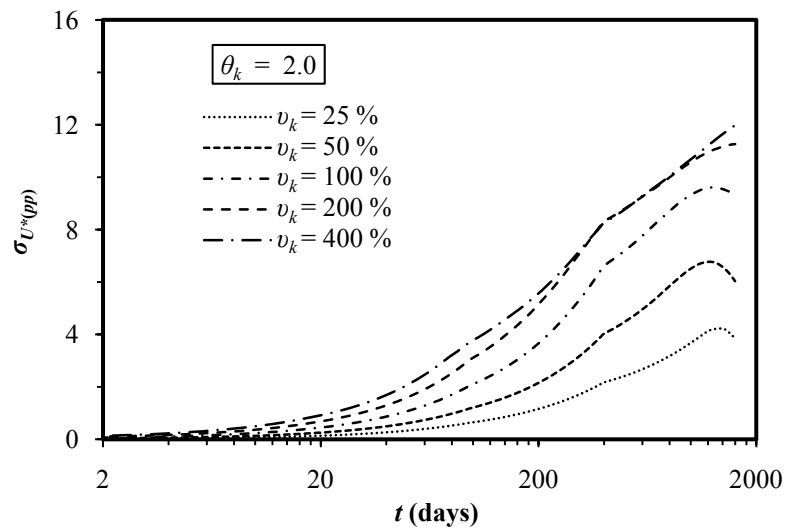
(b)

Figure 4.10: Effect of v_k on (a) $\mu_{U(pp)}$ and (b) $\mu_{U^*(pp)}$ for $\theta_k = 0.25$

The effects of v_k on $\sigma_{U(pp)}$ and $\sigma_{U^*(pp)}$ for a fixed value of $\theta_k = 2.0$ is demonstrated in Fig 4.11. The distribution patterns of both $\sigma_{U(pp)}$ and $\sigma_{U^*(pp)}$ with respect to the consolidation time, t , as shown in Figs. 4.11(a) and (b) respectively are similar. Similar to the behaviour of $\sigma_{U(pp)}$ shown in Fig. 4.11(a), it can be seen from Fig. 4.11(b) that $\sigma_{U^*(pp)}$ approaches 0 at two limiting values of t (i.e. 0 and ∞). This is due to the fact that $\mu_{U^*(pp)}$ approaches 0 and ∞ as t approaches 0 and ∞ regardless the values of the variability parameters of k . At any certain t between 0 and ∞ , both $\sigma_{U(pp)}$ and $\sigma_{U^*(pp)}$ increase with the increase of v_k .



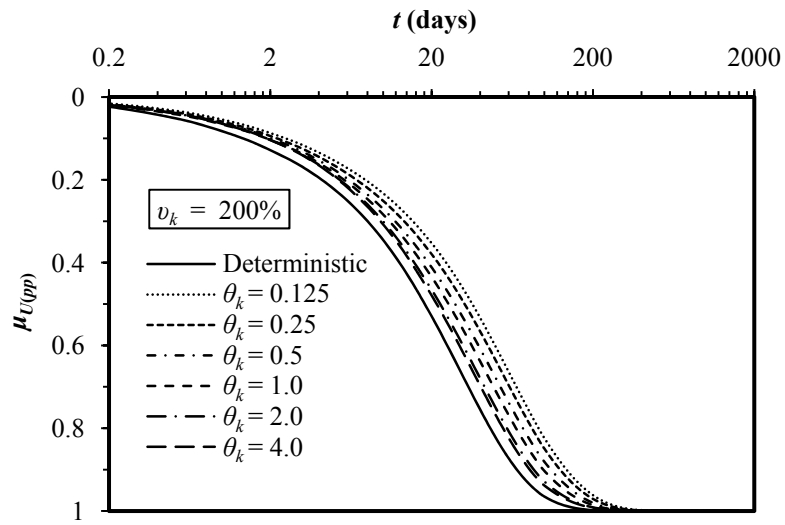
(a)



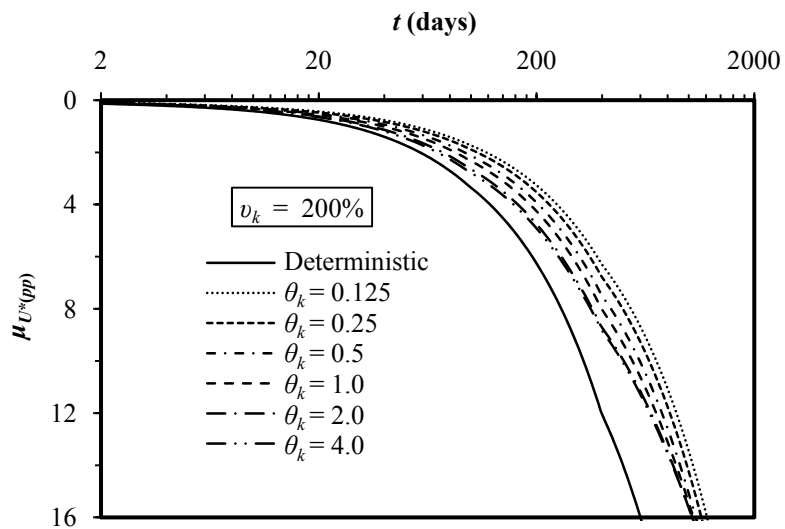
(b)

Figure 4.11: Effect of v_k on (a) $\sigma_{U(pp)}$ and (b) $\sigma_{U^*(pp)}$ for $\theta_k = 2.0$

The effects of θ_k on $\mu_{U(pp)}$ and $\mu_{U^*(pp)}$ are illustrated in Figs. 4.12 for a constant $v_k = 200\%$. It can be seen that the effects θ_k on $\mu_{U^*(pp)}$ are qualitatively similar to the effects of θ_k on $\mu_{U(pp)}$. This conclusion is also valid for the effects of θ_k on $\sigma_{U(pp)}$ and $\sigma_{U^*(pp)}$ shown in Fig. 4.13.



(a)



(b)

Figure 4.12: Effect of θ_k on (a) $\mu_{U(pp)}$ and (b) $\mu_{U^*(pp)}$ for $v_k = 200\%$

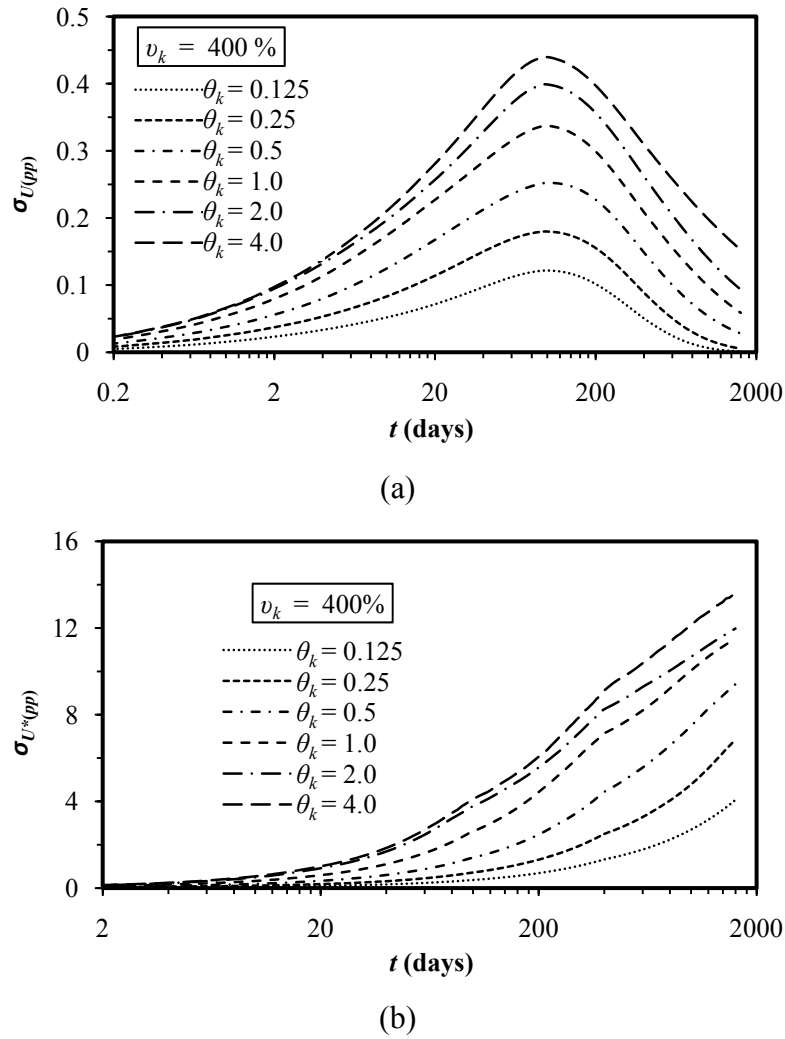


Figure 4.13: Effect of θ_k on (a) $\sigma_{U(pp)}$ and (b) $\sigma_{U^*(pp)}$ for $v_k = 400\%$

- ***Effects of v_k and θ_k on the probability of achieving 90% consolidation***

At any given time, the estimation of the probability of achieving a target degree of consolidation requires the determination of a reasonable probability distribution for the degree of consolidation data obtained from the suite of 1000 Monte-Carlo realizations. In order to obtain a reasonable probability distribution, the degree of consolidation data obtained at any time t , from the suite of 1000 realizations, is transformed to $U^*(t)$, which is used as an alternative form to represent the degree of consolidation $U(t)$. The reason for using $U^*(t)$ instead of $U(t)$ is that the obtained fit (assuming a Beta distribution, as $U(t)$ is bound between 0 and 1) using the raw data of $U(t)$ was typically poor while a reasonable probability distribution for the obtained

degree of consolidation data is better facilitated using $U^*(t)$, which gives a sufficiently reasonable approximation of the degree of consolidation behaviour of natural soils. In this study, $U^*(t)$ is assumed to be lognormally distributed and the hypothesis of lognormal distribution for $U^*(t)$ is derived analytically using Hansbo's (1981) theory by assuming that both the Finite Element Method and Hansbo theory represent the actual soil behaviour reasonably well. A detailed description of the analytical formulations used to derive the rationality of the lognormal distribution hypothesis for $U^*(t)$ will be described in Chapter 5. The legitimacy of the lognormal distribution hypothesis for $U^*(t)$ is further examined by the well-known Chi-square test through the frequency density plot of $U^*(t)$ data obtained from the 1000 realizations and a fitted lognormal distribution is superimposed. This process is performed on multiple combinations of v_k and θ_k at several different consolidation times. For each considered case, the goodness-of-fit p -value is found to be high enough to approve the rationality of the lognormal distribution hypothesis of simulated $U^*(t)$ data. It should be noted that, the rationality of the lognormal distribution assumption for $U^*(t)$ is assessed for both $U^*_{pp}(t)$ and $U^*_{set}(t)$. However, the histograms plotted using $U^*_{pp}(t)$ are almost identical to those plotted using $U^*_{set}(t)$ (note that μ_U and σ_U obtained based on pore water pressure are identical to those obtained based on settlement). Therefore, only the histograms plotted using $U^*_{pp}(t)$ are presented. Fig. 4.14(a) illustrates the typical histograms of $U^*_{pp}(t)$ for the case of $v_k = 200\%$, $\theta_k = 0.5$ at 67.9 days, along with their fitted lognormal distributions. For the purpose of comparison with the $U^*_{pp}(t)$ histogram, the frequency histogram of $U_{pp}(t)$ for the same case as that presented for $U^*_{pp}(t)$ is plotted in Figure 4.14(b), with the fitted Beta distribution superimposed. The goodness-of-fit test using the well-known Chi-square test yielded p -values of 0.99 for Fig. 4.14(a) (i.e. for U^*_{pp}) and 0.1 for Fig. 4.14(b) (i.e. for U_{pp}). Another example of histograms along with the fitted distributions superimposed is presented in Fig 4.15 for the case of $v_k = 200\%$, $\theta_k = 2.0$ at 135.8 days. The goodness-of-fit test for this case yielded p -values of 0.67 for $U^*_{pp}(t)$ (Fig. 4.15(a)) and 0.00016 for $U_{pp}(t)$ (Fig. 4.15(b)). For both cases presented in Figs. 4.14 and 4.15, it can be seen that p -values for $U^*_{pp}(t)$ with lognormal distribution assumption are much higher than those of the p -values for $U_{pp}(t)$ with the Beta distribution assumption. Since a high p -value strongly supports the lognormal hypothesis for $U^*(t)$, the probability of achieving 90% consolidation is estimated based on the statistics of $U^*(t)$ data using Eq. 3.41. It should be noted that

although there are significant differences in p -values between lognormal distribution assumption for $U^*(t)$ and Beta distribution assumption for $U(t)$, the estimated probability of achieving 90% consolidation from both of these probability distributions is similar. The probabilities of achieving 90% consolidation for lognormal distribution are 16% and 48%, respectively (see Fig. 4.14(a) and 4.15(a)), while for Beta distribution the probabilities are 20% and 51%, respectively (see Fig. 4.14(b) and 4.15(b)), implying that the Chi-square test is quite sensitive. It should also be noted that there is no particular trend in the degree of fitness as far as the two parameters v_k and θ_k are concerned.

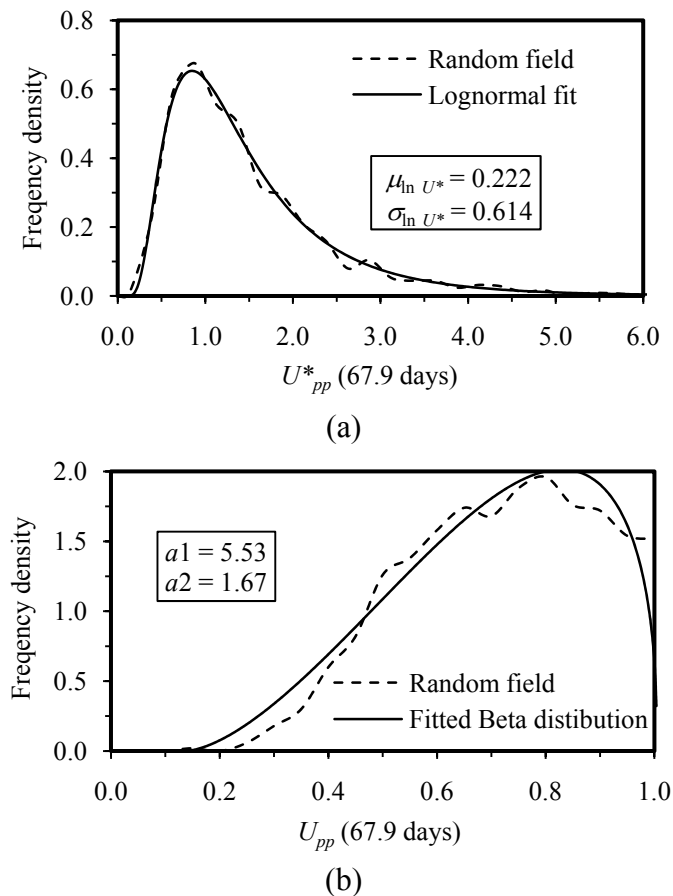


Figure 4.14: Frequency density histograms and fitted distributions of: (a) U^*_{pp} and (b) U_{pp} , for $v_k = 200\%$, $\theta_k = 0.5$ at 67.9 days

Once the distribution of $U^*(t)$ is determined, the statistical moments μ_{U^*} and σ_{U^*} that represent the mean and standard deviation of the lognormally distributed $U^*(t)$ are estimated from the suite of 1000 realizations. The calculated μ_{U^*} and σ_{U^*} are then

transformed into the mean, $\mu_{\ln U^*}$, and standard deviation, $\sigma_{\ln U^*(t)}$, of the underlying normally distributed $\ln U^*(t)$ using Eqs. 3.38 and 3.39, respectively. By making use of the estimated $\mu_{\ln U^*}$ and $\sigma_{\ln U^*}$ in Eq. 3.41, the variation of $P[U \geq U_{90}]$ over a range of v_k and θ_k at any consolidation times, t , is obtained. Although the probabilities of achieving 90% consolidation are estimated using both the excess pore water pressure and settlement data, only $P[U \geq U_{90}]_{(pp)}$ is presented below, as $P[U \geq U_{90}]_{(pp)}$ and $P[U \geq U_{90}]_{(set)}$ are almost identical.

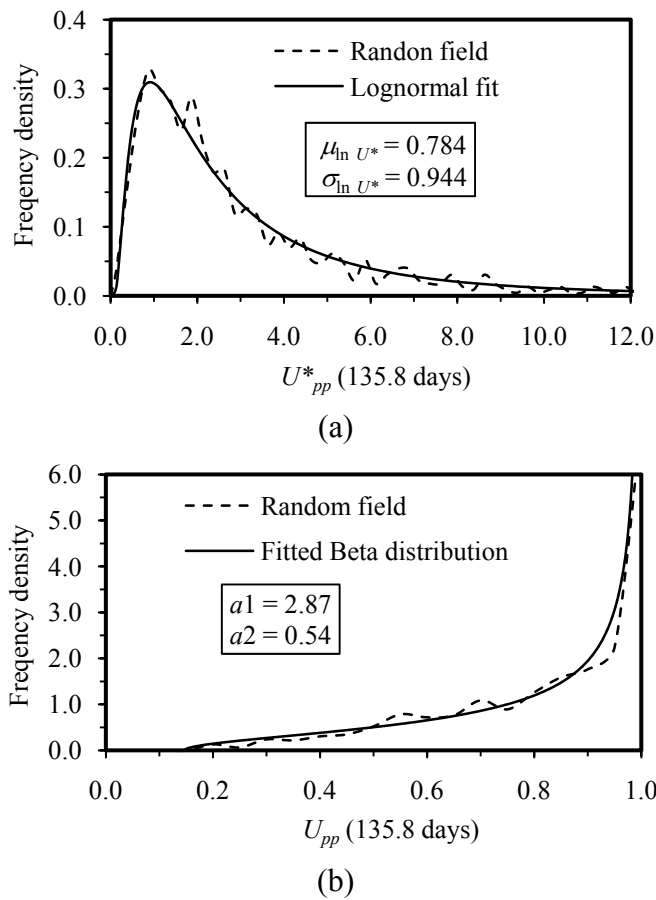


Figure 4.15: Frequency density histograms and fitted distributions of: (a) U^*_{pp} and (b) U_{pp} , for $v_k = 200\%$, $\theta_k = 2.0$ at 135.8 days

The effects of the spatial variability of k on the probability of achieving 90% consolidation are shown in Figs. 4.16 and 4.17. The deterministic time of achieving 90% consolidation, t_{D90} , is also shown in Figs. 4.16 and 4.17 by the vertical solid lines to give $P[U \geq U_{90}]_{(pp)}$ at that time for any combination of v_k and θ_k . The influence of v_k on $P[U \geq U_{90}]_{(pp)}$ is illustrated in Fig. 4.16 for all six prescribed values of θ_k . It can be seen that, for all curves, $P[U \geq U_{90}]_{(pp)}$ increases with the

increase of consolidation time, as expected. For a certain θ_k , it can be also seen that at any certain consolidation time, $P[U \geq U_{90}]_{(pp)}$ decreases with the increase of v_k , implying that the probability of achieving 90% target degree of consolidation decreases with the increase of permeability variance. The exception to this trend occurs before the deterministic 90% consolidation time (i.e. t_{D90}). As shown in the Fig. 4.16, $P[U \geq U_{90}]_{(pp)}$ in such cases is understandably low, however, the role of v_k has the opposite effect with lower values of v_k tending to give the lowest values of $P[U \geq U_{90}]_{(pp)}$. This is expected because the range of values of U^* (or U) over which the frequency density curve is distributed increases as v_k increases. In other words, U^* distribution “bunching up” at low v_k rapidly excludes the area to the right of the stationary target value of $U^* = 2.3026$.

Figure 4.17 shows the effect of θ_k on $P[U \geq U_{90}]_{(pp)}$ for all considered values of v_k , one by one. Looking at the results for a certain v_k it can be seen that, as expected, $P[U \geq U_{90}]_{(pp)}$ increases with the increase of t for all θ_k ; however, all curves crossover at a critical value of $P[U \geq U_{90}]_{(pp)} \approx 50\%$ at which $P[U \geq U_{90}]_{(pp)}$ becomes independent of θ_k . At any certain time prior to the crossover point, $P[U \geq U_{90}]_{(pp)}$ increases with increasing θ_k , whereas after the crossover point, $P[U \geq U_{90}]_{(pp)}$ decreases as θ_k increases. It can also be seen that, for all curves, there is a decrease in the increasing rate of $P[U \geq U_{90}]_{(pp)}$ with respect to t as θ_k increases. The explanation behind this behaviour lies in the fact that the excess pore water pressure always “seeks out” the easiest escape path from the regime. For vanishingly small θ_k , soil becomes infinitely rough, i.e. any point at which soil has low permeability, it will be surrounded by points where the soil has high permeability. What this means is that the flow path initially becomes infinitely tortuous with infinitely long drainage length, hence, the flow is forced to find a shorter passage by cutting through the low permeability regions. In contrast, for larger θ_k , regions of low permeability are bunched together and as a result, the draining pore water takes a detour from the bunched up low permeability regions instead of cutting through them; this leads to a longer drainage length and consequently a slower increasing rate of $P[U \geq U_{90}]_{(pp)}$ with respect to t . The closely grouped curves corresponding to $\theta_k = 2.0$ and 4.0 clearly demonstrate that $P[U \geq U_{90}]_{(pp)}$ becomes ‘insensitive’ to $\theta_k \geq 2.0$ (i.e. for θ_k of the order of the influence zone diameter).

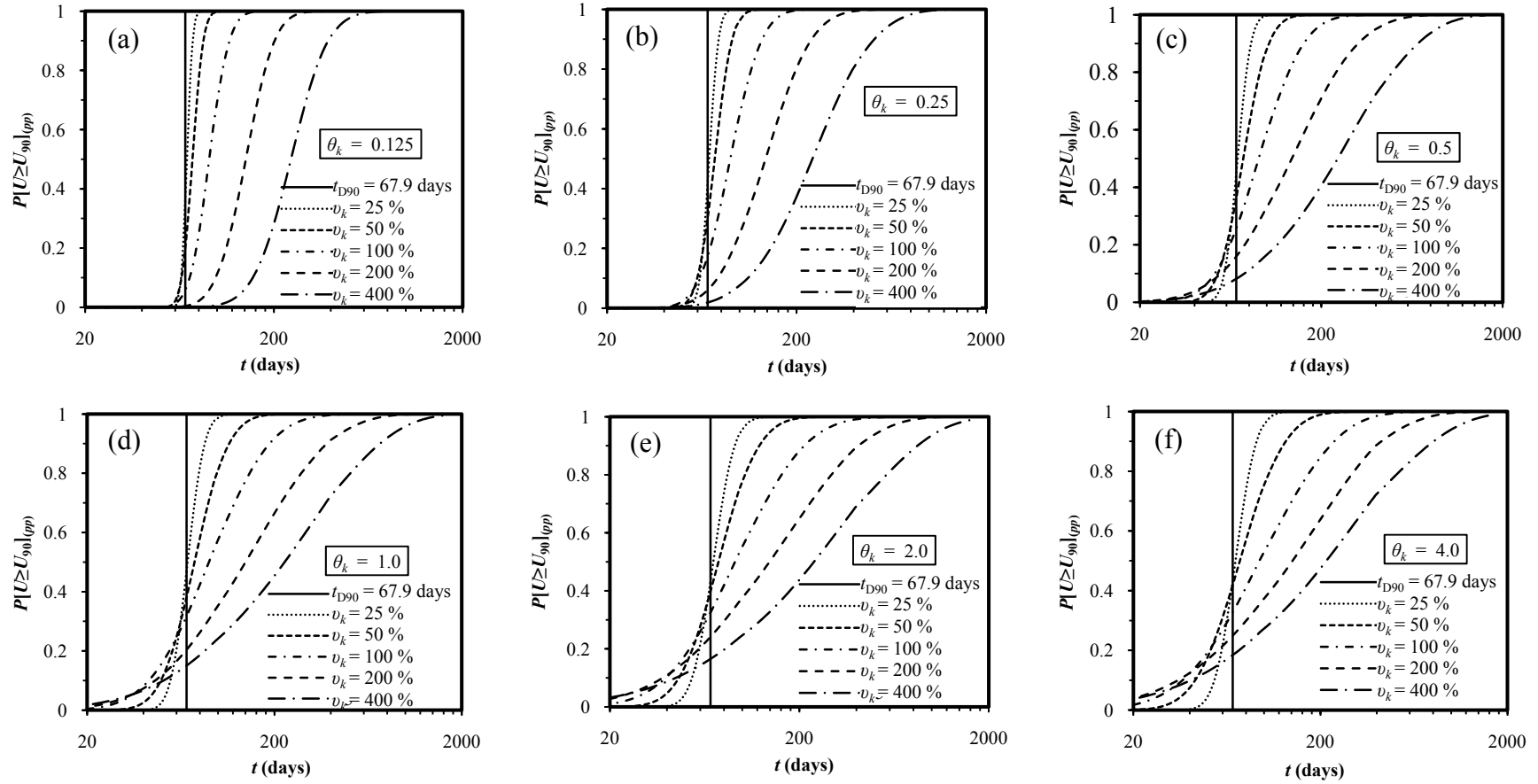


Figure 4.16: Effect of v_k on $P[U \geq U_{90}]_{pp}$ for (a) $\theta_k = 0.125$; (b) $\theta_k = 0.25$; (c) $\theta_k = 0.5$; (d) $\theta_k = 1.0$; (e) $\theta_k = 2.0$; and (f) $\theta_k = 4.0$

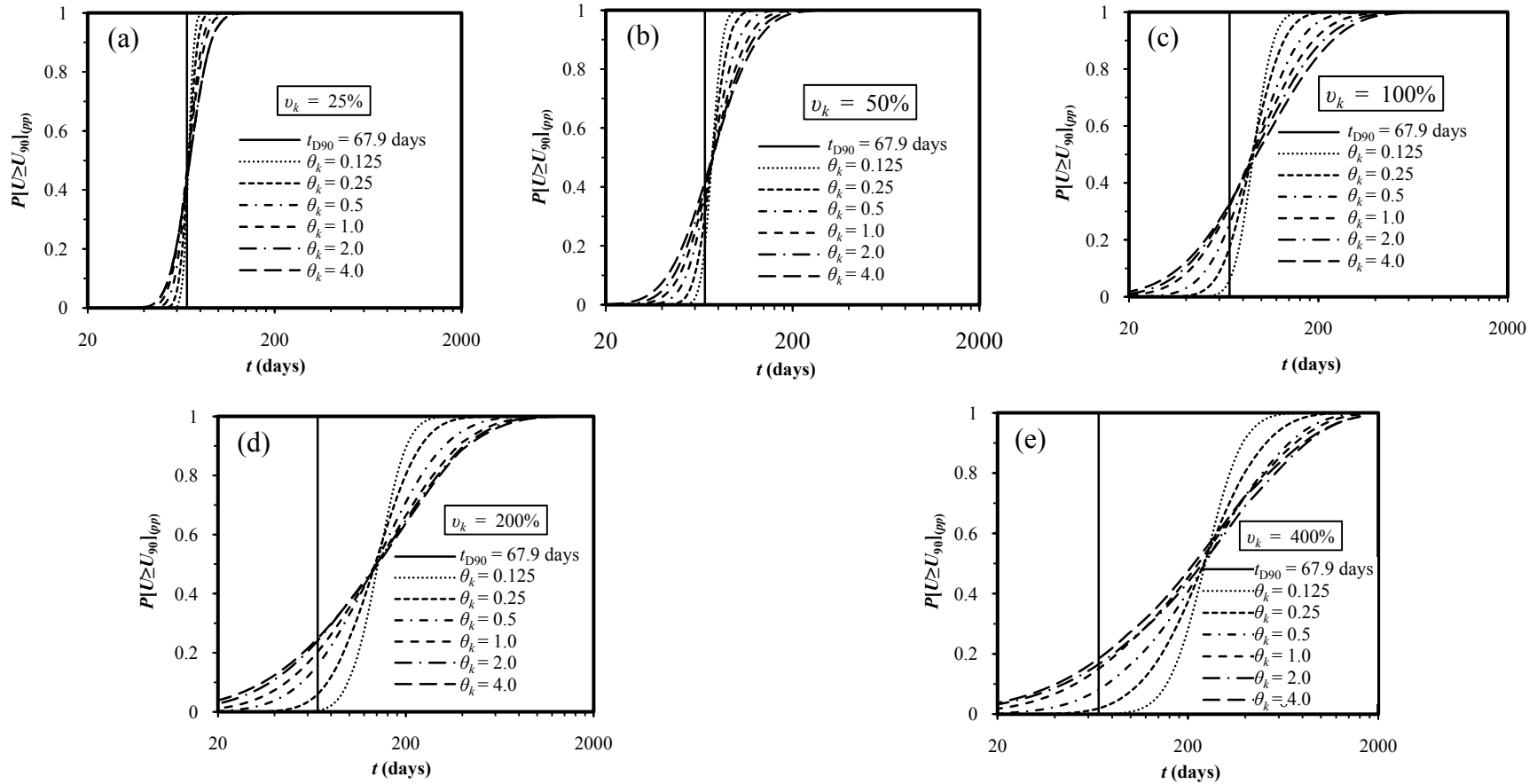


Figure 4.17: Effect of θ_k on $P[U \geq U_{90}]_{(pp)}$ for (a) $v_k = 25\%$; (b) $v_k = 50\%$; (c) $v_k = 100\%$; (d) $v_k = 200\%$; and (e) $v_k = 400\%$

When closely viewing the insensitivity of $P[U \geq U_{90}]_{(pp)}$ for $\theta_k \geq 2.0$, it can also be seen that, the time rate of $P[U \geq U_{90}]_{(pp)}$ tends to increase when $\theta_k > 2.0$ (see Figs. 4.17(c) and (d)). These results indicate that there is a maximum value of θ_k up to which the time rate of $P[U \geq U_{90}]_{(pp)}$ will decrease and for any θ_k greater than that maximum θ_k , it will start to increase. This behaviour can be explained by noting that, when $\theta_k = 0$, the simulated soil profile will consist of an infinite number of independent ‘observations’ of which the average permeability is equal to the true mean permeability (or true median, if the average is a geometric average). Since the rate of consolidation depends also on the average soil permeability, it ‘sees’ the same true mean (or true median) value predicted by the soil profile. Consequently, the predicted mean of the degree of consolidation becomes ‘perfect’ when the correlation length is zero and therefore the probability of achieving a desired degree of consolidation approaches 100%. At the other extreme of θ_k , when $\theta_k = \infty$, the soil becomes uniform, having the same value everywhere. In this case, any soil profile also perfectly predicts conditions in the unit cell. At intermediate θ_k the soil profile becomes imperfect estimator of the conditions surrounding the PVD, and the time rate of $P[U \geq U_{90}]_{(pp)}$ decreases. Therefore, the maximum decrease in the time rate of $P[U \geq U_{90}]_{(pp)}$ will occur at some correlation length between 0 and ∞ . The precise value depends on the geometric characteristics of the problem under consideration and the COV of soil permeability.

By comparing Figs. 4.16 and 4.17, it can be seen that $P[U \geq U_{90}]_{(pp)}$ is relatively less sensitive to θ_k than v_k . It should be noted that the deterministic solution based on the mean permeability will always lead to unconservative estimate of the degree of consolidation (i.e. $P[U \geq U_{90}]_{(pp)} < 50\%$) for all combinations of values of v_k and θ_k , as can be seen in Figs. 4.16 and 4.17. This means that the deterministic predicted consolidation time will have at least 50% risk of not being able to achieve 90% consolidation at the designed time. For the range of v_k values considered (see Fig. 4.17), the estimated $P[U \geq U_{90}]_{(pp)}$ at t_{D90} varied from less than 6% for $v_k = 400\%$ (with $\theta_k = 0.125$) to a probability of 47% for $v_k = 25\%$ (with $\theta_k = 4.0$). In the latter case (i.e. when $v_k = 25\%$), as the computed standard deviation of U^* is also small (even for $\theta_k = 4.0$), so the range of U^* values resemble more a normal distribution than a lognormal one. In the limit as $v_k \rightarrow 0$, the representative mean of the random permeability field tends to its target (deterministic) mean, but in probabilistic terms

this implies an equal likelihood of the true degree of consolidation falling on either side of the predicted deterministic 90% consolidation, U_{D90} , value. Hence the curves in Fig. 4.17(a) tend towards $P[U \geq U_{90}]_{(pp)} \approx 50\%$ for small values of v_k . These results are reassured from the design viewpoint because they indicate that the traditional approach of design of soil consolidation by PVDs leads to unconservative estimate of the true degree of consolidation and the more variable the soil, the more unconservative the solution.

4.2.1.2.2 Effect of anisotropic correlation structure on the stochastic behaviour of soil consolidation

The results of the parametric studies presented in the previous section are based on the assumption that the scale of fluctuation is isotropic (i.e. $\theta_h = \theta_v$). However, as discussed in Chapter 2, in natural soil deposits, the horizontal scale of fluctuation, θ_h , is generally larger than the vertical scale of fluctuation, θ_v , due to the nature of soil stratification and deposition. In other words, the correlation coefficient of a measured soil property at two spatial locations is different in different spatial directions. Therefore, it is of interest to investigate the effects of isotropic versus anisotropic soil spatial variability on the consolidation of soft clay stabilized by PVDs.

In this study, only the anisotropic correlation length of soil permeability, k , is considered for comparison with the results based on the isotropic correlation length. The horizontal and vertical scales of fluctuation of k are denoted as $\theta_{k(h)}$ and $\theta_{k(v)}$, respectively. By using different combinations of unequal values of $\theta_{k(h)}$ and $\theta_{k(v)}$ (of course $\theta_{k(h)} > \theta_{k(v)}$) in Eq. 3.16, it is possible to generate random permeability fields with different degrees of anisotropy. It should be noted that the degree of anisotropy of the generated permeability field is expressed as the ratio of $\theta_{k(h)}$ to $\theta_{k(v)}$, and is denoted by ζ (i.e. $\zeta = \theta_{k(h)} / \theta_{k(v)}$). In the previous section, it was shown that for the consolidation problem under consideration, μ_U , σ_U and $P[U \geq U_{90}]$ become insensitive when θ_k (isotropic) ≥ 2.0 . Therefore, to obtain different degrees of anisotropy, $\theta_{k(v)}$ is varied systematically by keeping $\theta_{k(h)}$ fixed at 4.0m. The following values of v_k and θ_k are considered:

- v_k (%) = 50, 100, 200 and 400

- $\theta_{k(h)}(\text{m}) = 4.0$; $\theta_{k(v)}(\text{m}) = 0.125, 0.25, 0.5$ and 1.0

For each set of v_k and θ_k mentioned above, a series of 16 stochastic simulation tests are carried out for the anisotropic condition. Based on the 1000 realizations of Monte Carlo simulations, μ_U , σ_U and $P[U \geq U_{90}]$ are computed for each simulation test. A detailed comparison between μ_U , σ_U and $P[U \geq U_{90}]$ obtained from the isotropic and anisotropic conditions is presented and discussed in Figs. 4.18–4.20 by expressing them as a function of time. It should be noted that as the results computed based on the excess pore water pressure are presented for isotropic θ_k in the previous section, only the results obtained based on the excess pore water pressure for both isotropic and anisotropic conditions are compared herein. It should also be noted that for the sake of readability of the figures, the results of a few tests are only presented in Figs. 4.18–4.20, which are believed to be sufficient to demonstrate the main features of the influence of anisotropic spatial variability of k on soil consolidation by PVDs.

- ***Effect of degree of anisotropy on the mean and standard deviation of U***

The comparison between the isotropic versus anisotropic spatially variable soil permeability in terms of the estimated $\mu_{U(pp)}$ for various v_k is illustrated in Fig. 4.18. The general observation that can be found by looking at each individual graph plotted for different values of v_k is that, at any particular t , the isotropic solution underestimates $\mu_{U(pp)}$, and this underestimation is marginal when the degree of anisotropy is as low as 4.0. The amount by which the isotropic assumption underestimates $\mu_{U(pp)}$ decreases with the decrease in both ζ and v_k . This is expected as the anisotropic soil is more uniform in the horizontal direction and this uniformity increases as $\theta_{k(v)}$ approaches $\theta_{k(h)}$, and v_k decreases. It can be seen that the difference in $\mu_{U(pp)}$ from the anisotropic solution (with different degrees of anisotropy), is nominal. In other words, the anisotropic solutions give almost identical results of $\mu_{U(pp)}$ irrespective of the degree of anisotropy. However, slight discrepancies in $\mu_{U(pp)}$ for high ζ (e.g. $\zeta = 32$) and low ζ (e.g. $\zeta = 4$) are found only when v_k is as high as 200%. It can also be seen from Figs. 4.18(a) and (b) that the effect of the degree of anisotropy on $\mu_{U(pp)}$ is insignificant even for a high degree of anisotropy (e.g. $\zeta = 32$) when the coefficient of variation of soil permeability is as low as 50%.

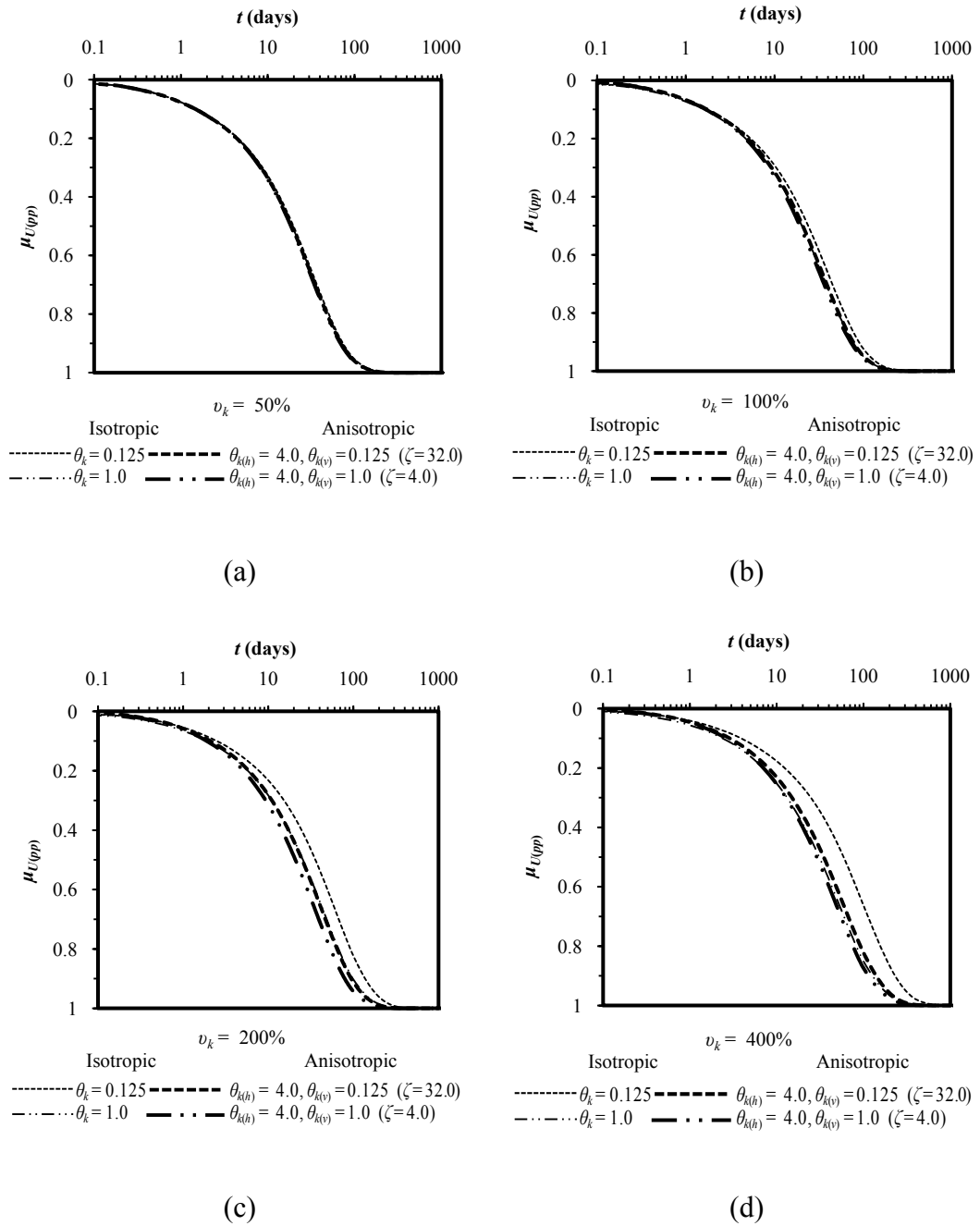


Figure 4.18: Effect of degree of anisotropy on $\mu_{U(pp)}$ for (a) $v_k = 50\%$; (b) $v_k = 100\%$; (c) $v_k = 200\%$; and (d) $v_k = 400\%$

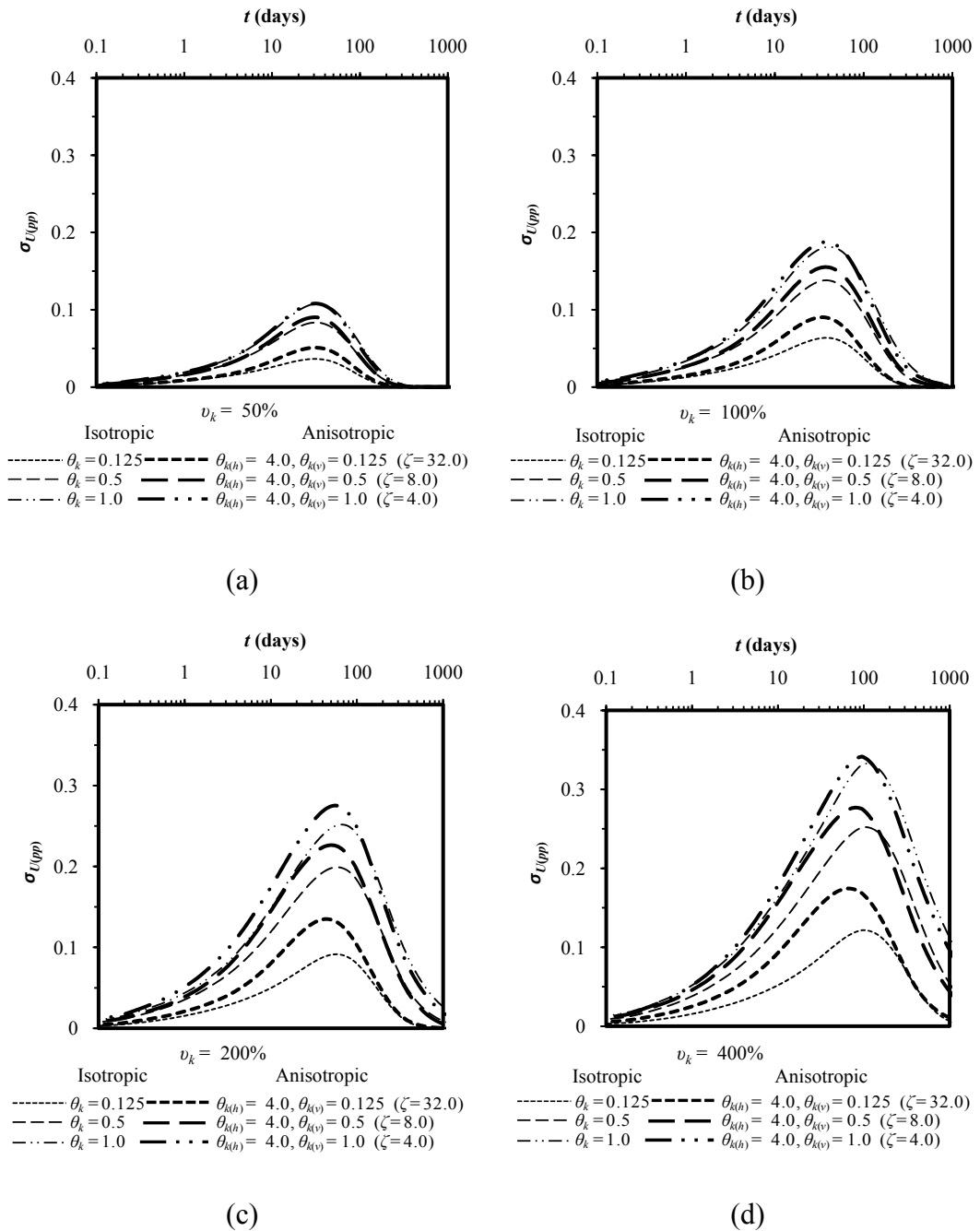


Figure 4.19: Effect of degree of anisotropy on $\sigma_{U(pp)}$ for (a) $v_k = 50\%$; (b) $v_k = 100\%$; (c) $v_k = 200\%$; and (d) $v_k = 400\%$

The effect of the anisotropic θ_k over the isotropic θ_k on $\sigma_{U(pp)}$ within the range of v_k under consideration is illustrated in Fig. 4.19. The overall observation that is true for

any v_k is that, at any certain t between 0 to ∞ , the anisotropic solutions give higher values of $\sigma_{U(pp)}$ than the isotropic solutions. The difference in obtained $\sigma_{U(pp)}$ decreases with the decrease of both ζ and v_k . Since $\theta_{k(h)}$ is higher than $\theta_{k(v)}$ for the anisotropic conditions, the effective number of independent samples used in the average of the anisotropic cases decreases from that of the isotropic cases. This lower number of independent samples used in the average of the anisotropic cases is responsible for higher $\sigma_{U(pp)}$. Looking at each graph presented in Fig. 4.19, it can be observed that for a certain ζ , the discrepancy between the anisotropic and isotropic $\sigma_{U(pp)}$ solutions increases with the increase of v_k .

- ***Effect of degree of anisotropy on the probability of achieving 90% consolidation***

Fig. 4.20 shows the comparison between the isotropic versus anisotropic spatially variable soil permeability in terms of the estimated probability of achieving 90% consolidation for different values of v_k in which $P[U \geq U_{90}]_{(pp)}$ is expressed as a function of the consolidation time, t . Generally speaking, the curves shown in Fig. 4.20 provide the confidence levels (y -axis) of achieving 90% consolidation corresponding to the consolidation time (x -axis).

It can be seen from Fig. 4.20(a) that, in general, the difference between the isotropic and anisotropic solutions is insignificant for $v_k = 50\%$. However, at any certain consolidation time, t , the isotropic condition provides slightly lower values of $P[U \geq U_{90}]_{(pp)}$ than the anisotropic condition, and this behaviour is more pronounced when the degree of anisotropy, ζ , is as high as 32. Similar view is taken regarding $v_k = 100\%$ in Fig. 4.20(b), however, the difference in $P[U \geq U_{90}]_{(pp)}$ between the isotropic and anisotropic cases becomes more recognisable when ζ becomes as high as 16. In Fig. 4.20(c) and (d), it can be seen that when $v_k \geq 200\%$ the difference in $P[U \geq U_{90}]_{(pp)}$ at any consolidation time between the isotropic and anisotropic solutions becomes distinguishable, even when ζ is as low as 4.0.

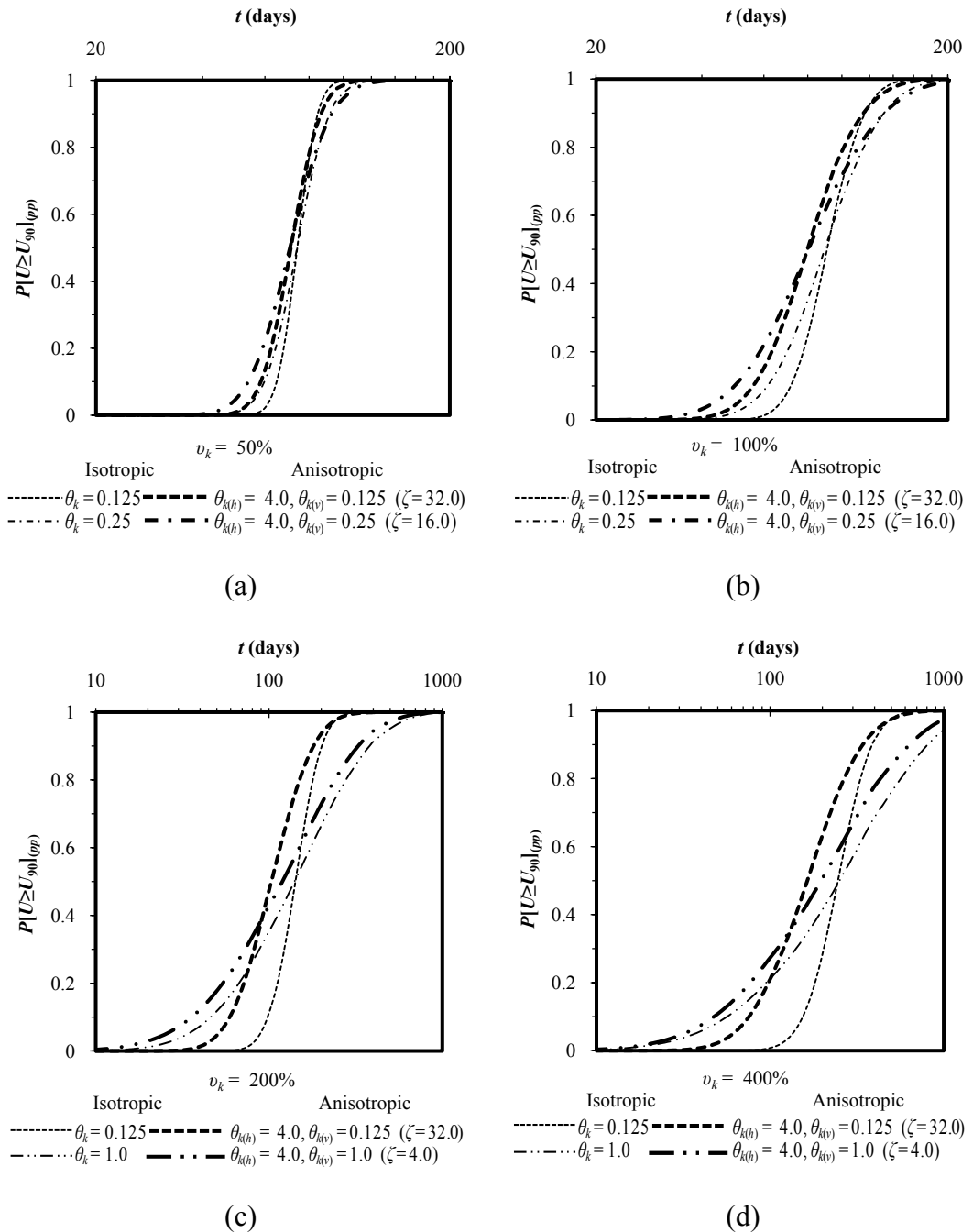


Figure 4.20: Effect of degree of anisotropy on $P[U \geq U_{90}]_{(pp)}$ for (a) $v_k = 50\%$; (b) $v_k = 100\%$; (c) $v_k = 200\%$; and (d) $v_k = 400\%$

The overall observation that can be derived from the comparison made above is that, for any coefficient of variation of soil permeability, v_k , the isotropic assumption always provides lower (conservative) values of $P[U \geq U_{90}]_{(pp)}$ than the anisotropic condition. This conservative estimate of $P[U \geq U_{90}]_{(pp)}$ becomes more pronounced with the increase of ζ . This result has potential practical implication in the sense that

the more realistic anisotropic condition will ensure improved economy in the reliability-based design of soil consolidation via PVDs. This is particularly true when the coefficient of variation of soil permeability is as high as 200% and the degree of anisotropy is as high as 32. However, it should be noted that this conclusion is true for almost all probability (confidence) levels but the difference between the isotropic and anisotropic solutions becomes less pronounced for higher probability levels close to unity (i.e. at $P[U \geq U_{90}]_{(pp)} \approx 95\sim 100\%$).

4.2.1.2.3 Matching comparison between axisymmetric and equivalent plane strain analyses

As mentioned earlier in Chapter 2, analysing an axisymmetric problem using plane strain conditions requires establishment of equivalence between axisymmetric and plane strain analyses. By employing the established matching theories (e.g. Hird et al. 1992; Indraratna and Redana 1997) described in Section 2.6.5, it was found in the literature that under deterministic conditions, satisfactory equivalence between plane strain and axisymmetric analyses is achievable. However, to the author's best knowledge, the matching procedures have not yet been tested with regard to the more realistic stochastic soil consolidation approaches. Accordingly, in this section, stochastic analyses are performed for both axisymmetric and equivalent plane strain cases, considering soil permeability as the only random variable, and the equivalence between the axisymmetric and plane strain analyses is assessed in terms of μ_U , σ_U and $P[U \geq U_{90}]$.

To achieve equality in the degree of consolidation obtained from the axisymmetric and plane strain conditions at any consolidation time, it is necessary to transform the axisymmetric solution to an equivalent plane strain model. This can be done by: (i) geometric matching in which the spacing of the drains is matched while the permeability is kept the same; (ii) permeability matching in which the permeability coefficients are matched while the drain spacing is kept the same; and (iii) a combination of a permeability and geometric matching approach in which the plane strain permeability is computed for convenient drain spacing (Indraratna et al. 2003). Of the above three matching theories, the permeability matching technique is

considered to be the most appropriate for the stochastic analyses carried out in the current study. As no smear and well resistance effects are considered herein, the equivalent permeability for the plane strain solution, k_{pl} , can be estimated from the permeability of the axisymmetric solution, k_{ax} , using the transformation function shown in Eq. 2.38. To perform plane strain analyses equivalent to those of the axisymmetric analyses presented earlier in Section 4.2.1.2.1, the axisymmetric unit cell described in Section 4.2.1 and shown in Fig. 4.1 is transformed into an equivalent plane strain unit cell, as shown in Fig. 4.21. Since the permeability matching theory is used, the geometry of the plane strain unit cell (i.e. the half width of the unit cell, b_e , and the half width of the drain, b_w) will remain equal to their corresponding axisymmetric radii, r_e and r_w , respectively, to give $r_e = b_e = 0.85$ m and $r_w = b_w = 0.05$ m. The length of the drain for the plane strain unit cell will also be the same as that of the axisymmetric unit cell (i.e. $L = 1.0$ m). It should be noted that the 0.05 m \times 0.05 m mesh as previously shown in Fig. 4.2 is used to discretize the problem. The applied boundary conditions for the equivalent plane strain unit cell are shown in Fig. 4.21. In order to establish the necessary matching between the axisymmetric and plane strain analyses, the mean permeability of the plane strain is computed by making use of the mean axisymmetric permeability of 5×10^{-10} m/sec into Eq. 2.38. Thus, the resulting mean permeability of plane strain, $\mu_{k_{pl}}$, would be equal to 1.6×10^{-10} m/sec. The deterministic soil property m_v for the plane strain condition will also remain the same as that used for the axisymmetric condition (i.e. $m_v = \mu_{m_v} = 1.67 \times 10^{-4}$ m²/kN).

The equivalent plane strain analyses using the permeability matching theory are performed over the same range of v_k and θ_k given in Table 4.1 used for the axisymmetric analyses. Fig. 4.22 shows a typical example of a discretized mesh and the corresponding soil domain represented by a grey scale of a typical permeability field used for the plane strain analysis. It can be noticed that although in the plane strain analysis there is no axis of symmetry for heterogeneous soil, only one half of the unit cell is modelled. This is to allow for computational efficiency. However, a comparison carried out considering full and half unit cells showed no significant difference. This is due to the fact that the number of elements in the mesh and the number of Monte Carlo simulations considered are sufficient to produce reasonably

reproducible results. An initial deterministic analysis under the plane strain condition is also performed prior to the stochastic analyses considering equal permeability of all elements (i.e. $\mu_{k_{pl}} = 1.6 \times 10^{-10}$ m/s). It should be remembered that the deterministic solution in this case yields $t_{D90} = 69.4$ days.

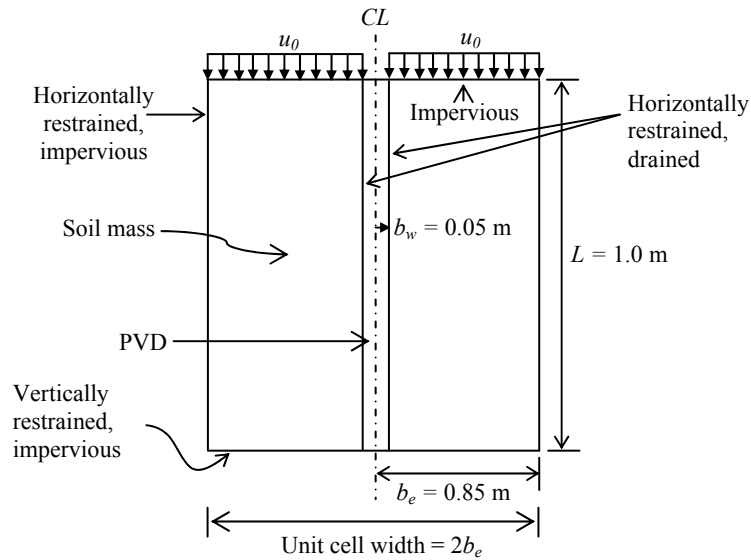


Fig. 4.21: Equivalent plane strain unit cell converted from axisymmetric unit cell shown in Fig. 4.1

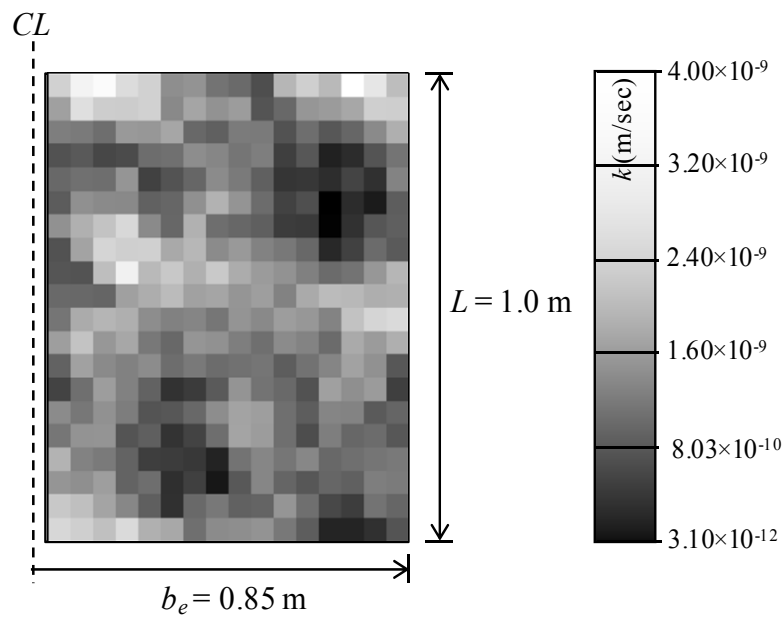


Fig. 4.22: Typical realization of a random permeability field for a plane strain analysis with $v_k = 100\%$ and $\theta_k = 0.5$ ($\mu_k = 1.6 \times 10^{-10}$ m/sec)

- **Matching comparison for the effect of v_k and θ_k on the mean and standard deviation of U**

For each set of v_k and θ_k given in Table 4.1, a series of 30 stochastic simulation tests are carried out for the equivalent plane strain conditions. On the basis of the 1000 realizations, μ_U , σ_U and $P[U \geq U_{90}]$ are estimated for each simulation test. A detailed comparison between μ_U , σ_U and $P[U \geq U_{90}]$ obtained from the axisymmetric and plane strain conditions is presented and discussed in Figs. 4.24–4.29, by expressing them as a function of the consolidation time, t . Since the results computed based on the excess pore water pressure and settlement do not show a considerable difference, only the results obtained based on the excess pore water pressure are presented herein. In Figs. 4.24–4.29, “AS” and “PS” refer to the solutions under axisymmetric and plane strain conditions, respectively. It should be noted that as the general trend of the distribution parameters remain unaltered over the range of the statistical parameters v_k and θ_k , only the results of a few tests are presented to keep the figures manageable. It is felt that the presented tests are sufficient to demonstrate the main features of the matching comparison.

Prior to presenting the results of the matching comparison, the legitimacy of using a half unit cell instead of a full unit cell is examined in Fig. 4.23, for the case where $v_k = 100\%$ and $\theta_k = 0.125$. It should be noted that to carry out a plane strain analysis using a full unit cell, two separate random fields for each half of the unit cell are generated with the same v_k and θ_k . It can be seen that both the solutions of the half and full unit cells are identical (i.e. $\mu_{U(pp)}$ and $\sigma_{U(pp)}$ demonstrated in Figs. 4.23(a) and (b)).

The effect of v_k on the matching between $\mu_{U(pp)}$ obtained from the axisymmetric and equivalent plane strain analyses, for each individual θ_k , is investigated in Fig. 4.24. This also includes deterministic solutions to both axisymmetric and plane strain conditions. It can be seen that for a certain combination of v_k and θ_k , the permeability matching procedures produced almost identical $\mu_{U(pp)}$ profiles. However, for a certain θ_k and at any particular consolidation time t , the estimated values of $\mu_{U(pp)}$ derived from the equivalent plane strain analysis are slightly lower than those obtained from the axisymmetric solution, for $v_k \geq 100\%$. The influence of θ_k on $\mu_{U(pp)}$ is illustrated

in Fig. 4.25 for each considered v_k in a sequential order. It can be seen that, in general, the effect of θ_k on $\mu_{U(pp)}$ is marginal from the matching point of view and both solutions give almost identical results. However, for any $v_k \geq 100\%$ and at any certain t , the plane strain solution gives slightly lower values of $\mu_{U(pp)}$ compared to the axisymmetric analysis, irrespective of the values of θ_k .

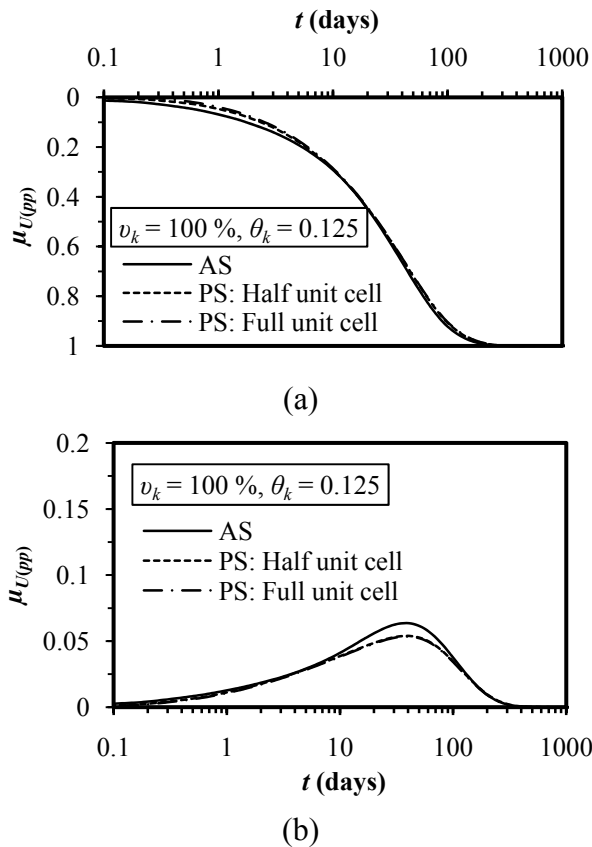


Figure 4.23: Comparison between the results from full and half unit cells

(a) $\mu_{U(pp)}$ and (b) $\sigma_{U(pp)}$, for $v_k = 100\%$, $\theta_k = 0.125$

Figs. 4.26 shows the effect of v_k on the agreement between $\sigma_{U(pp)}$ estimated via the axisymmetric and equivalent plane strain analyses, for all considered θ_k , one by one. It can be seen that the matching procedure gives identical results for both axisymmetric and plane strain when v_k is as low as 25%. As v_k increases, the discrepancy in $\sigma_{U(pp)}$ gradually increases particularly at and near the peak value of $\sigma_{U(pp)}$. The effects of θ_k on $\sigma_{U(pp)}$ are depicted sequentially in Fig. 4.27, for each individual θ_k . General speaking, the discrepancy in $\sigma_{U(pp)}$ obtained from the axisymmetric and equivalent plane strain analyses increases with the increase of θ_k . However this effect is noticeable only when $v_k \geq 100\%$.

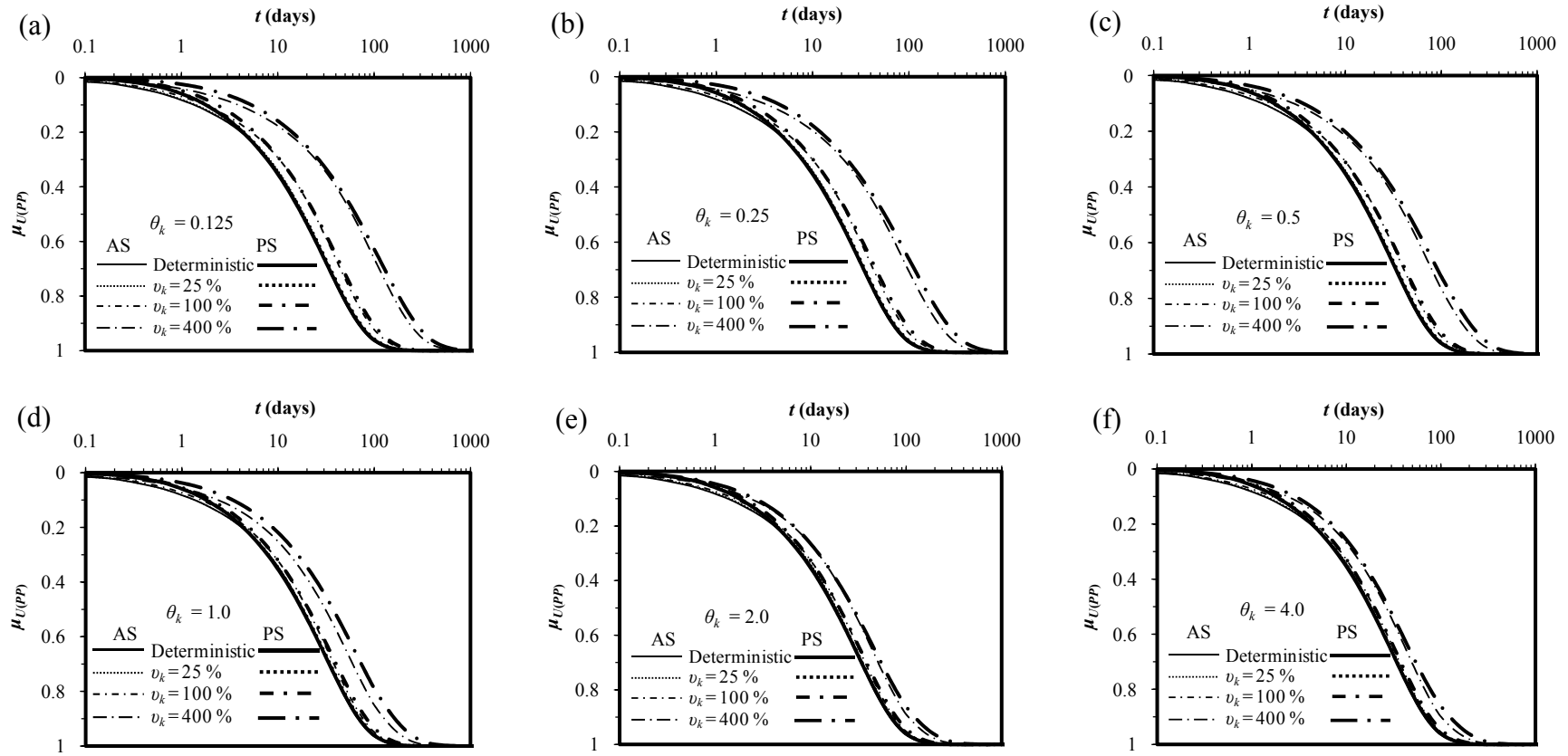


Figure 4.24: Matching comparison for the effect of v_k on $\mu_{U(pp)}$ at (a) $\theta_k = 0.125$; (b) $\theta_k = 0.5$; (c) $\theta_k = 0.5$; (d) $\theta_k = 1.0$; (e) $\theta_k = 2.0$; and (f) $\theta_k = 4.0$

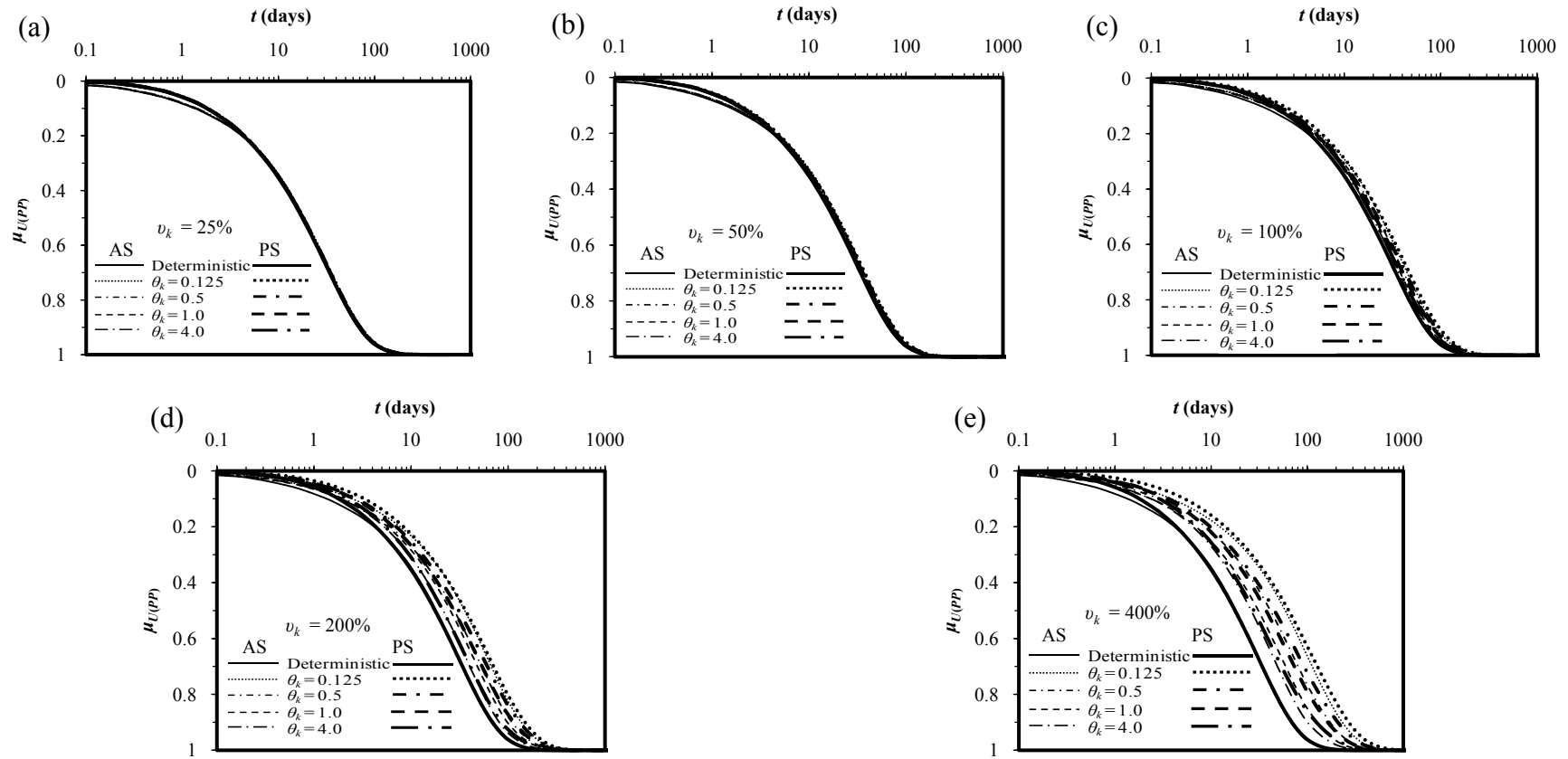


Figure 4.25: Matching comparison for the effect of θ_k on $\mu_{U(pp)}$ at (a) $v_k = 25\%$; (b) $v_k = 50\%$; (c) $v_k = 100\%$; (d) $v_k = 200\%$; and (e) $v_k = 400\%$

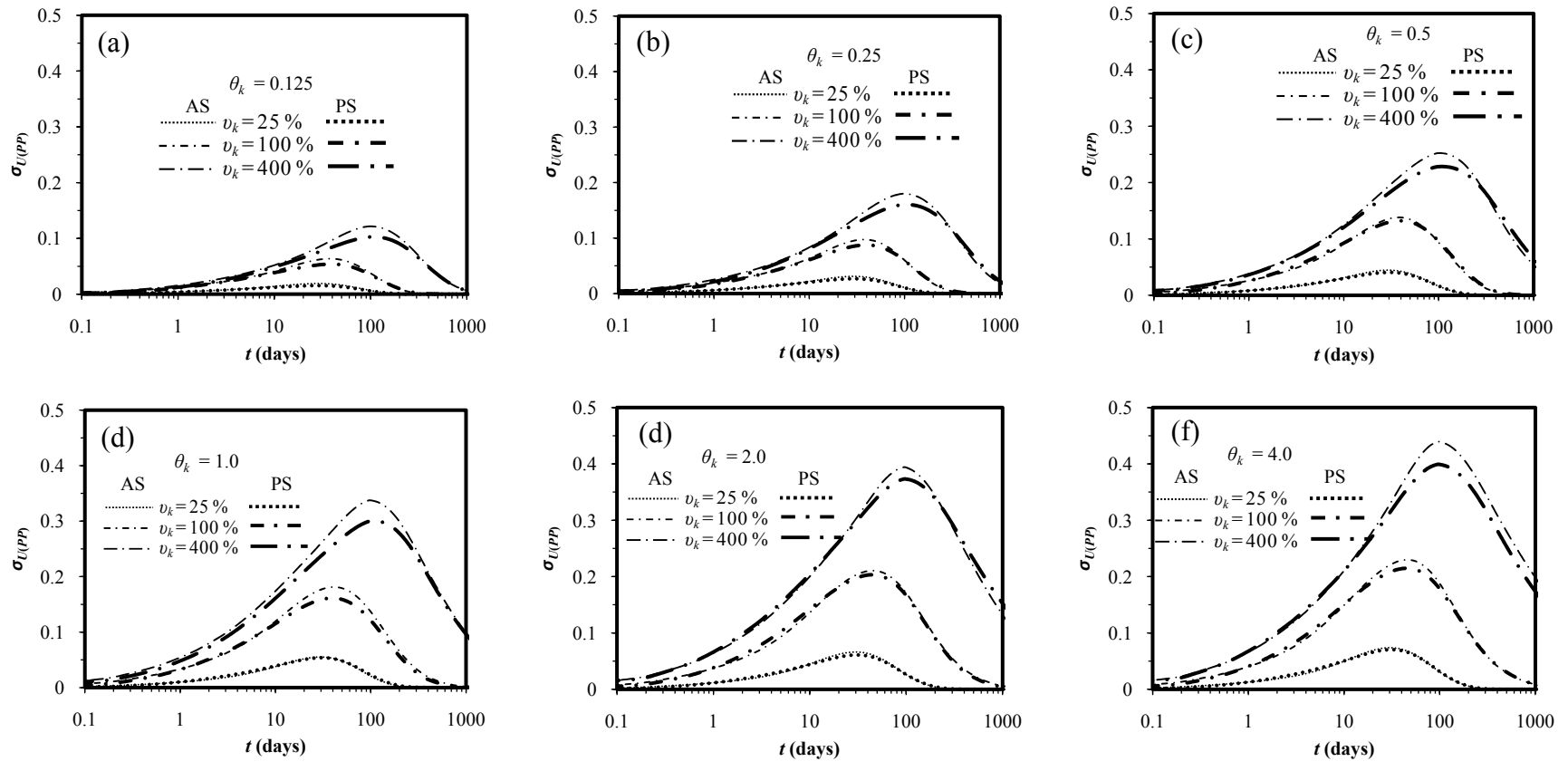


Figure 4.26: Matching comparison for the effect of v_k on $\sigma_{U(pp)}$ at (a) $\theta_k = 0.125$; (b) $\theta_k = 0.5$; (c) $\theta_k = 0.5$; (d) $\theta_k = 1.0$; (e) $\theta_k = 2.0$; and (f) $\theta_k = 4.0$

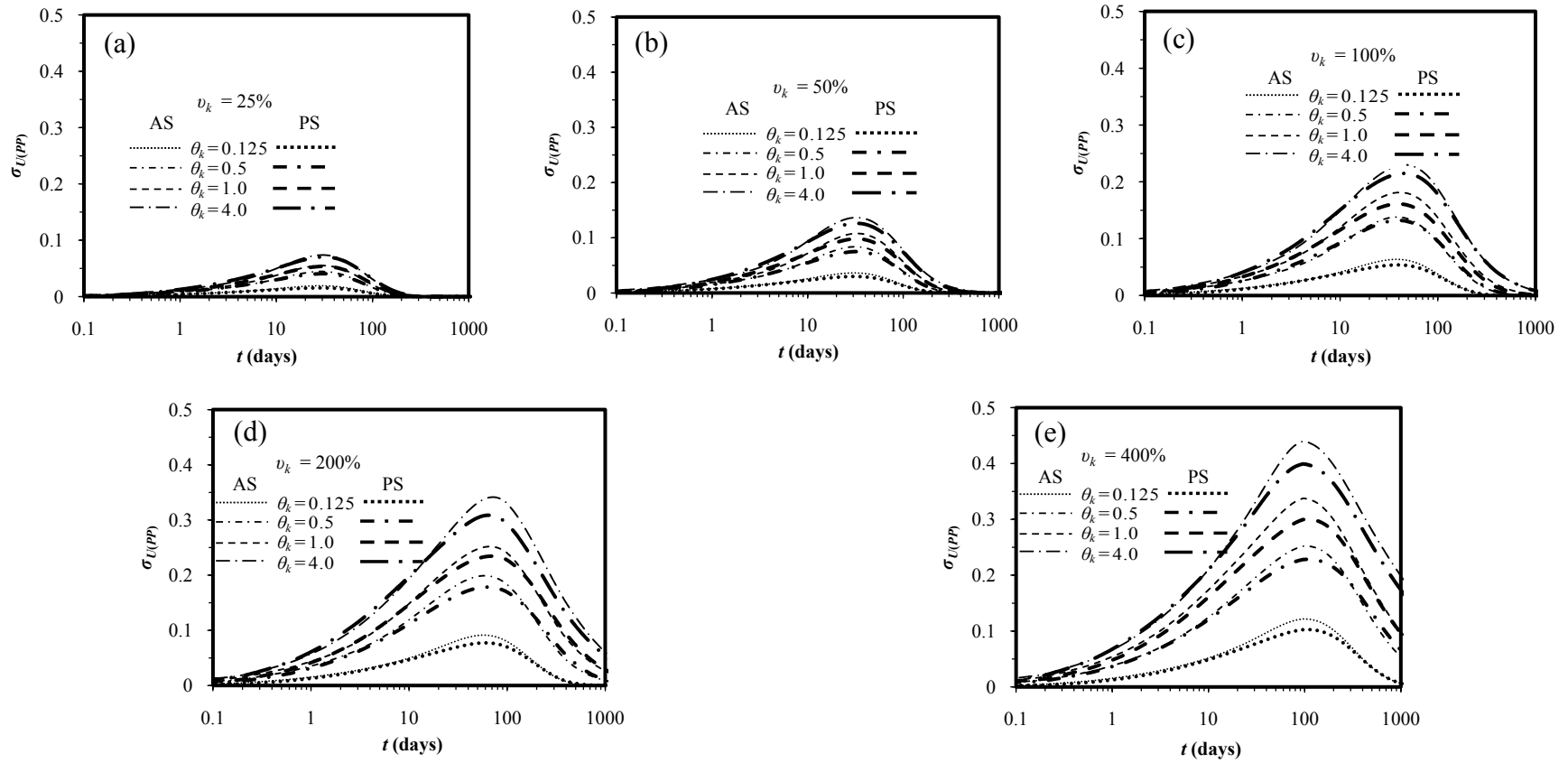


Figure 4.27: Matching comparison for the effect of θ_k on $\sigma_{U(pp)}$ at (a) $v_k = 25\%$; (b) $v_k = 50\%$; (c) $v_k = 100\%$; (d) $v_k = 200\%$; and (e) $v_k = 400\%$

- **Matching comparison for the effect of v_k and θ_k on the the probability of achieving 90% consolidation**

The equivalence between the axisymmetric and plane strain analyses is also assessed in terms of the probability of achieving 90% consolidation, $P[U \geq U_{90}]_{(pp)}$ in Figs. 4.28 and 4.29. Fig. 4.28 shows the effect of v_k on the matching between $P[U \geq U_{90}]_{(pp)}$ estimated via the axisymmetric and equivalent plane strain analyses over the range of selected θ_k in an ascending order. The overall observation that can be obtained by looking at each individual graph plotted for different θ_k is that the equivalent plane strain analysis gives lower values of $P[U \geq U_{90}]_{(pp)}$ compared to the axisymmetric solution, for all cases of v_k when $\theta_k \leq 1.0$. It can also be seen that the lower values of $P[U \geq U_{90}]_{(pp)}$ produced by the plane strain analysis become more prevailing as v_k increases. For any $\theta_k \geq 2.0$, $P[U \geq U_{90}]_{(pp)}$ from both solutions is identical for all values of v_k .

In Fig. 4.29, the variation of $P[U \geq U_{90}]_{(pp)}$ with the consolidation time is illustrated for various θ_k at a fixed value of v_k , sequentially increased from the lower limit to the upper limit. It can be observed that, in general, the equivalent plane strain analysis gives slightly lower values of $P[U \geq U_{90}]_{(pp)}$ than the axisymmetric solution, for all θ_k . However, the discrepancy between the plane strain and axisymmetric solutions become more significant for smaller θ_k . One particular note regarding Fig. 4.29 is that for any $\theta_k \geq 2.0$, both the axisymmetric and equivalent plane strain analyses give almost identical $P[U \geq U_{90}]_{(pp)}$, implying that the estimated $P[U \geq U_{90}]_{(pp)}$ from both conditions will be similar if the soil is homogeneous. The overall conclusion that can be derived by comparing the results of Figs. 4.28 and 4.29 is that for erratic soils (i.e. θ_k is small), the equivalent plane strain analysis gives lower $P[U \geq U_{90}]_{(pp)}$ than that of the axisymmetric solution.

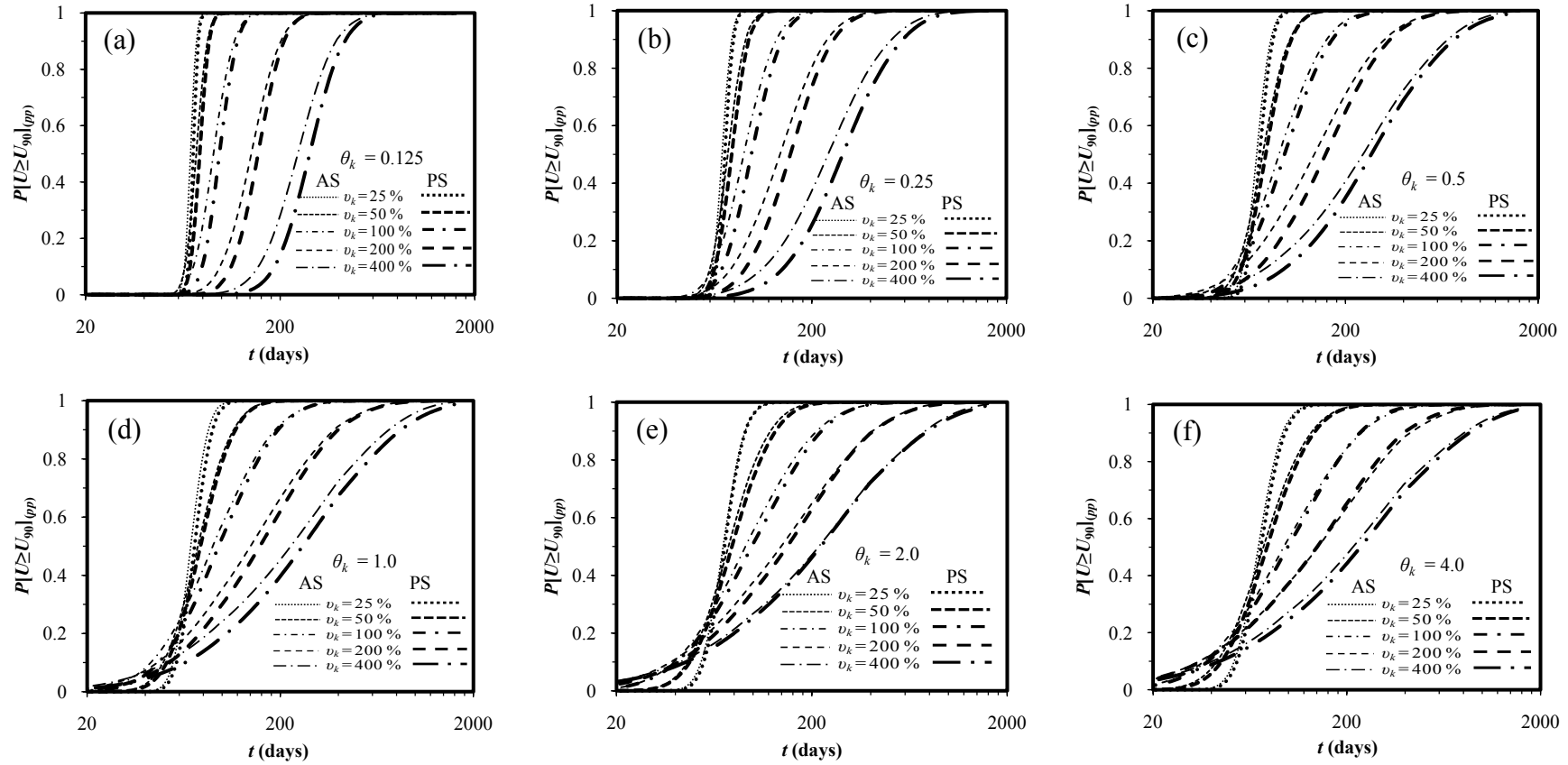


Figure 4.28: Matching comparison for the effect of v_k on $P[U \geq U_{90}]_{pp}$ at (a) $\theta_k = 0.125$; (b) $\theta_k = 0.5$; (c) $\theta_k = 0.5$; (d) $\theta_k = 1.0$; (e) $\theta_k = 2.0$; and (f) $\theta_k = 4.0$

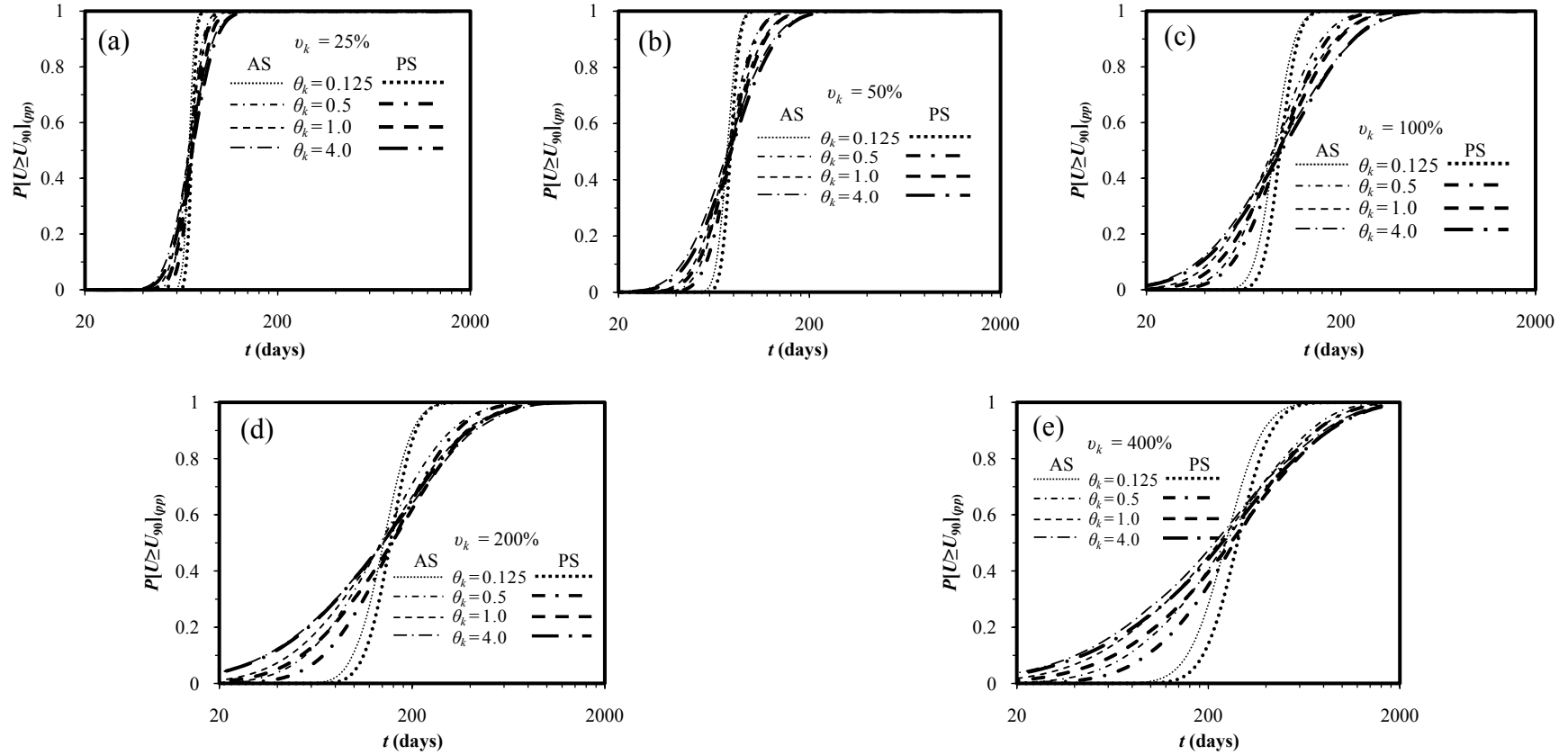


Figure 4.29: Matching comparison for the effect of θ_k on $P[U \geq U_{90}]_{pp}$ at (a) $v_k = 25\%$; (b) $v_k = 50\%$; (c) $v_k = 100\%$; (d) $v_k = 200\%$; and (e) $v_k = 400\%$

4.2.1.3 Probabilistic analysis of soil consolidation considering both permeability and volume compressibility as random variables

The results presented so far are based on the assumption that k is the only random variable and m_v remains constant across the soil mass. Although the COV of m_v (i.e. v_{m_v}) is typically quite low (it ranges from 25% to 30%) and much lower than that of v_k (which ranges from 200% to 300%), several researchers indicate that both k and m_v play important roles in the consolidation of heterogeneous soil. Accordingly, in this section, both k and m_v are treated as random variables. The following aspects are studied in this section:

- (a) The sensitivity of the statistics of the degree of consolidation and probability of achieving 90% consolidation is examined- to the statistically defined input data (i.e. v and θ) in relation to both k and m_v .
- (b) The degree of consolidation as defined by the excess pore water pressure is known to be different from that defined by settlement, when both k and m_v are treated as random variables (e.g. Lee et al. 1992). These differences are fully investigated in a probabilistic frame work.
- (c) The influence of cross correlation between the random variables k and m_v on soil consolidation is investigated through parametric studies.

In order to achieve the objectives set out above, random soil profiles are simulated by considering both k and m_v as random variables based on their prescribed statistical parameters, as shown in Table 4.2. It can be noticed that, although in reality v_k is much higher than that of v_{m_v} , the same range of v for both k and m_v is selected in this study for comparison purposes only. The range of θ (i.e. θ_k and θ_{m_v}) is also assumed to be the same for both k and m_v . This assumption is reasonable because, if one thinks that the spatial correlation structure of a soil is caused by changes in the constitutive nature of the soil over the ground, then both k and m_v would have similar correlation lengths. As shown in Table 4.2, two different types of random fields of k and m_v are used, including uncorrelated (i.e. $\rho = 0.0$) and perfectly positively correlated (i.e. $\rho = 1.0$). An isotropic scale of fluctuation is assumed throughout the analysis. Depending on the definite objective to be achieved, stochastic consolidation analyses are performed for many different arbitrarily selected sets of v , θ and ρ . For

each selected set of ν , θ and ρ , 1000 Monte Carlo simulations are performed. The obtained consolidation responses are then statistically analysed to estimate μ_U , σ_U and $P[U \geq U_{90}]$. It should be noted that since the general trends of μ_U , σ_U and $P[U \geq U_{90}]$ remain unaltered over the range of prescribed values of ν and θ , only the results of a few of the tests conducted are presented in this section.

Table 4.2: Ranges of statistical parameters used in the analyses

Parameter	Value
ν (%) (for both k and m_v)	25, 50, 100, 200, 400
θ (m) (for both k and m_v)	0.125, 0.25, 0.5, 1.0, 2.0, 4.0
Cross-correlation coefficient between k and m_v , ρ	0.0 and 1.0

4.2.1.3.1 Results of sensitivity analyses

It has been shown in Section 4.2.1.2 that the behaviour of soil consolidation is dependent on the magnitude of ν and θ of soil permeability. Different values of ν_k and θ_k have different implications for the estimated degree of consolidation. Accordingly, it is reasonable to expect that different ν and θ of k and m_v may lead to quite different conclusions relating to the estimated behaviour of soil consolidation. In this section, a series of axisymmetric consolidation analyses were performed to investigate the sensitivity of statistics of the degree of consolidation and the probability of achieving 90% consolidation over a range of ν and θ of k and m_v . No cross-correlation between k and m_v is assumed (i.e. $\rho = 0.0$). The influence of cross-correlation between k and m_v will be investigated and discussed later in Section 4.2.1.3.3. The sensitivity analyses carried out in this section are divided into two parts. In the first part, the COV of both k and m_v is assumed to be the same (i.e. $\nu_{m_v} = \nu_k$), whereas in the second part, the COV of m_v is selected from Table 4.2 in such a way that it turns out to be one quarter of the COV of k (i.e. $\nu_{m_v} = 0.25 \nu_k$). This is due to the fact that the variability of m_v is much smaller than that of k , as previously discussed in Chapter 2 (see Table 2.2). It should be noted that only the results computed based on the excess pore water pressure are presented in this section. As will be shown later in Section 4.2.1.3.2, the difference between the

excess pore water pressure and settlement results is insignificant, especially in the range of COV of m_v that is likely to be encountered in reality. The results obtained from each part of the study are described in order below.

4.2.1.3.1.1 Results of sensitivity analyses with $v_{m_v} = v_k$

The results of the sensitivity analyses in which v of both k and m_v are assumed to be the same are presented first. The effects of varying v and θ on μ_U and σ_U are investigated in Figs. 4.30 and 4.31, while their effects on $P[U \geq U_{90}]$ are investigated in Fig. 4.32.

- ***Effects of v and θ on the mean and standard deviation of U***

The effect of v on $\mu_{U(pp)}$ for a constant value of $\theta = 2.0$ is shown Fig. 4.30(a), whereas the effect of θ on $\mu_{U(pp)}$ for a fixed value of $v = 100\%$ is shown in Fig. 4.30(b). The deterministic solution of no soil variability is also included in both figures. It can be seen from Fig. 4.30(a) that, at any particular consolidation time, $\mu_{U(pp)}$ increases with the increase of v and the increasing rate of $\mu_{U(pp)}$ consistently increases as v increases. Fig. 4.30(a) also indicates that the $\mu_{U(pp)}$ curve of less heterogeneous soil of $v = 25\%$ is close to the deterministic U curve, but it gradually shifts to the left for more heterogeneous soils of higher v , implying an accelerated rate of consolidation. It should be noted that this observation is opposite to that found for the case where k was considered as the only random variable. At any certain time, an increase in $\mu_{U(pp)}$ with the increase of v can be explained by noting that a higher v makes the heterogeneous system more erratic, so that the low k values and even more lower compressible zones are bunched together in most of the simulations, resulting in an increase in the average coefficient of consolidation. Similar trend of $\mu_{U(pp)}$ is also obtained for the effect of θ , as shown in Fig. 4.30(b). It can be seen that at any particular consolidation time, t , there is a gradual increase in $\mu_{U(pp)}$ as θ increases. It is also interesting to see that for ragged random fields with a smaller θ , the $\mu_{U(pp)}$ curve approaches the deterministic curve. This behaviour is expected, as for small θ , both k and m_v with low and high values are distributed quite uniformly throughout the domain, implying an average coefficient of consolidation close to the

deterministic coefficient of consolidation. As the random fields become smooth with higher θ , high k values and comparatively lower m_v values tend to bunch together in most of the simulations (this is possibly because k and m_v are uncorrelated). Consequently, there is an increase in the average coefficient of consolidation compared to the deterministic coefficient of consolidation and in turn the $\mu_{U(pp)}$. From Fig. 4.30, it can also be seen that low variability (i.e. $v \leq 25\%$) and a small scale of fluctuation (i.e. $\theta \leq 0.25$) have little effect on $\mu_{U(pp)}$.

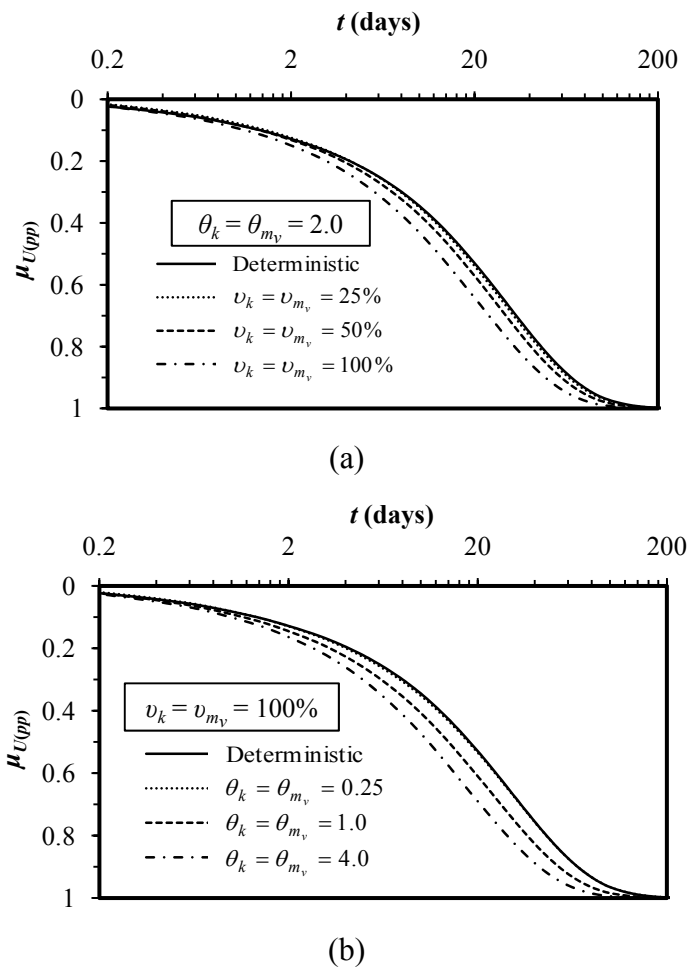
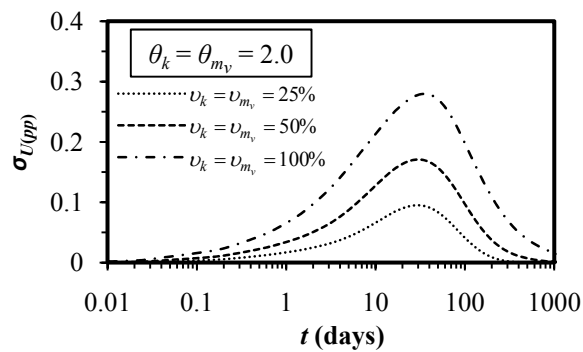


Figure 4.30: Effect of: (a) v on $\mu_{U(pp)}$ for $\theta = 2.0$; (b) θ on $\mu_{U(pp)}$ for $v = 100\%$

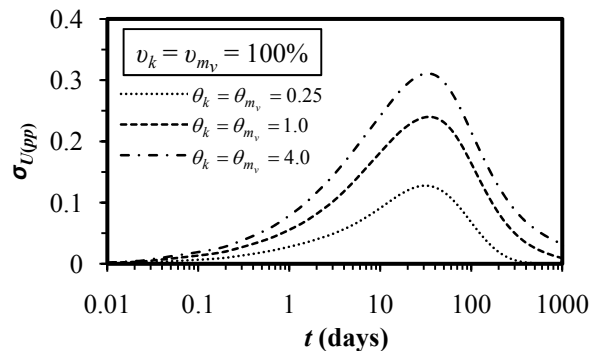
Fig. 4.31(a) shows the effect of v on $\sigma_{U(pp)}$ for a fixed value of $\theta = 2.0$. It can be seen that, as expected, at any particular t between 0 and ∞ , $\sigma_{U(pp)}$ increases with the increase of v . This behaviour is ‘intuitive’ due to the fact that the larger the value of v , the more chance is there for a low k to come with low m_v in one simulation and vice versa for another simulation. As a result, the potential coefficient of consolidation

value will be exaggerated. It should be noted that this observation is similar to that found for the case where k was the only random variable.

The effect of θ on $\sigma_{U(pp)}$ is illustrated in Fig. 4.31(b) for a constant value of $v = 100\%$. It can be seen that at any certain consolidation time, t , $\sigma_{U(pp)}$ increases with the increase of θ . As already discussed in Section 4.2.1.2.1, when the correlation length is large, $\sigma_{U(pp)}$ is also expected to be large as there is less averaging variance reduction within each realization.



(a)



(b)

Figure 4.31: Effect of: (a) v on $\sigma_{U(pp)}$ for $\theta = 2.0$; (b) θ on $\sigma_{U(pp)}$ for $v = 100\%$

- ***Effects of v and θ on the probability of achieving 90% consolidation***

The effects of the spatial variability of k and m_v on the probability of achieving 90% consolidation are shown in Fig. 4.32, in which $P[U \geq U_{90}]_{(pp)}$ is expressed as a function of consolidation time t . The deterministic time of achieving 90% consolidation, t_{D90} , is also shown in Fig. 4.32 by vertical solid lines to give $P[U \geq U_{90}]_{(pp)}$ at that time for any combination of v and θ .

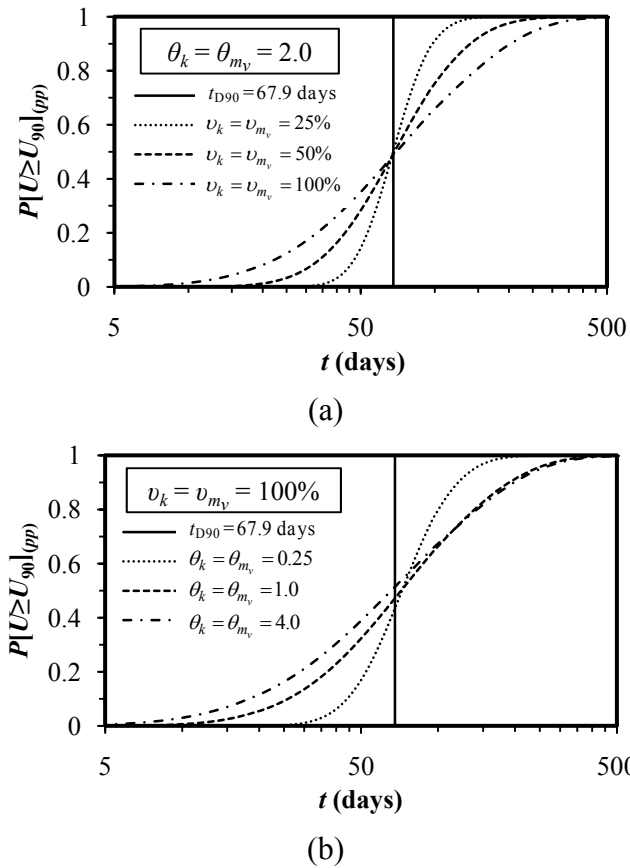


Figure 4.32: Effect of: (a) v on $P[U \geq U_{90}]_{(pp)}$ for $\theta = 2.0$; (b) θ on $P[U \geq U_{90}]$ for $v = 100\%$

Before discussing the results presented in Fig. 4.32, the legitimacy of the lognormal distribution hypothesis for $U^*(t)$ is examined once again as both k and m_v are random in this part of the study. Fig. 4.33 illustrates the typical histograms for $U^*(t)$ in the case of $v_k = v_{m_v} = 200\%$, $\theta_k = \theta_{m_v} = 0.5$ at 271.6 days, along with their fitted lognormal distributions. The goodness-of-fit test yielded p -value of 0.83, indicating strong agreement between the histogram and the fitted distribution. Therefore, the lognormal distribution is certainly an appropriate assumption to the distribution of the simulated $U^*(t)$ data even when both k and m_v are random variables.

Fig. 4.32(a) shows the variation of $P[U \geq U_{90}]_{(pp)}$ for various v at a fixed value of $\theta = 2.0$. It can be seen that, at any certain consolidation time, $P[U \geq U_{90}]_{(pp)}$ decreases with the increase of v . The exception to this trend occurs before the deterministic 90% consolidation time (i.e. t_{D90}) where the role of v has the opposite effect, with lower values of v tending to give the lowest values of $P[U \geq U_{90}]_{(pp)}$. This observation

is similar to that found for the case where k was assumed to be the only random variable. The similarity in the trends of $P[U \geq U_{90}]_{(pp)}$ for both cases suggests that the reason given for the case with random k is also applicable for this case.

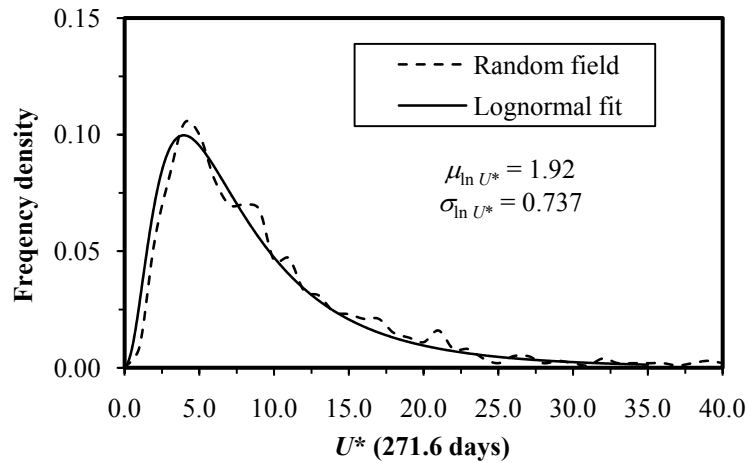


Figure 4.33: Typical example of frequency density histogram of simulated $U^*(t)$ with fitted lognormal distribution for $\nu_k = \nu_{m_v} = 200\%$, $\theta_k = \theta_{m_v} = 0.5$ at 271.6 days

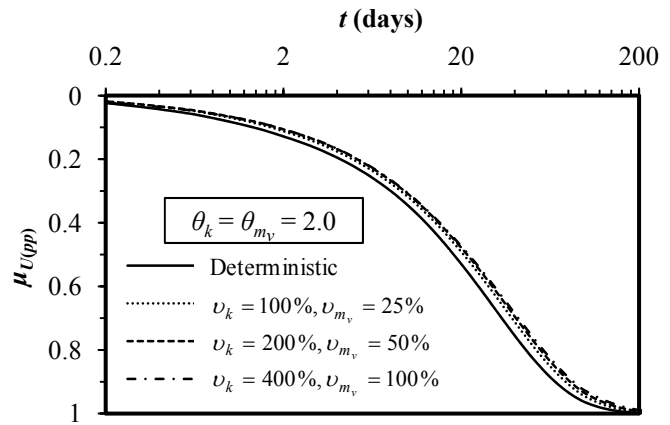
The effect of θ on $P[U \geq U_{90}]_{(pp)}$ for a constant value of $\nu = 100\%$ is investigated in Fig. 4.32(b). It can be seen that all curves crossover at a critical value of $P[U \geq U_{90}]_{(pp)} \approx 50\%$ and the effects of θ on $P[U \geq U_{90}]_{(pp)}$ are opposite before and after this crossover point. It should be noted that the behaviour of $P[U \geq U_{90}]_{(pp)}$ with respect to θ is similar to that obtained in Section 4.2.1.2.1 for the effect of θ_k alone. Accordingly, the same reasons as those explained the observed trend of $P[U \geq U_{90}]_{(pp)}$ with respect to θ_k are also valid for this case.

4.2.1.3.1.2 Results of sensitivity analyses with $\nu_{m_v} = 0.25 \nu_k$

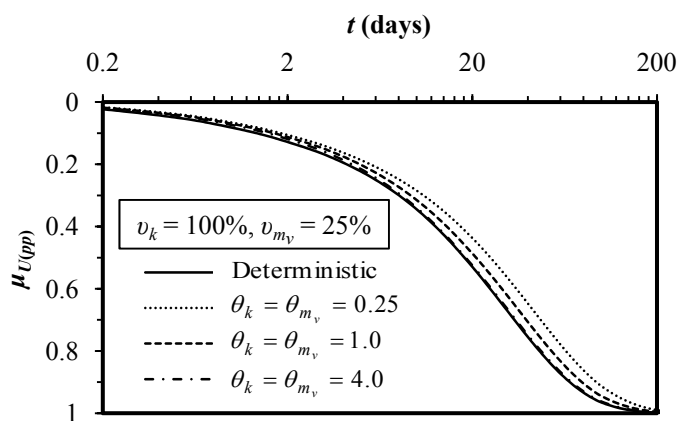
In this section, the results of the sensitivity analyses in which ν_{m_v} is assumed to be four times smaller than that of ν_k are presented in Figs. 4.34–4.36, in which $\mu_{U(pp)}$, $\sigma_{U(pp)}$ and $P[U \geq U_{90}]_{(pp)}$ are expressed as functions of the consolidation time t .

• **Effects of v and θ on the mean and standard deviation of U**

The effect of v on $\mu_{U(pp)}$ for a constant value of $\theta_k = \theta_{m_v} = 2.0$ is shown Fig. 4.34(a). It can be seen that at any particular consolidation time, $\mu_{U(pp)}$ decreases marginally with increasing v . This observation is opposite to that found for $v_{m_v} = v_k$ case (see Fig. 4.30(a)) and indicates that the variational trend of $\mu_{U(pp)}$ (i.e. decreases or increases with the increase of v) with respect to v depends on the ratio of v_k to v_{m_v} . The effect of θ on $\mu_{U(pp)}$ for a fixed value of $v_k = 100\%$ and $v_{m_v} = 25\%$ is shown in Fig. 4.34(b). It can be seen that at any particular consolidation time, $\mu_{U(pp)}$ increases with increasing θ . Qualitative comparison of the Figs. 4.30(b) and 4.34(b) reveal that the effect of increasing θ on $\mu_{U(pp)}$ is similar for both $v_{m_v} = v_k$ and $v_{m_v} = 0.25 v_k$ cases.



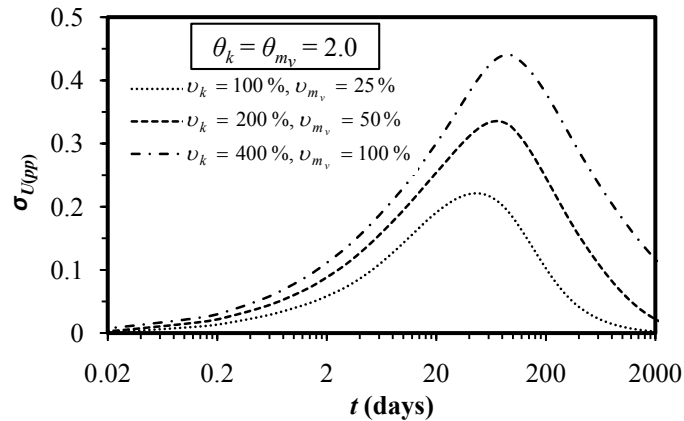
(a)



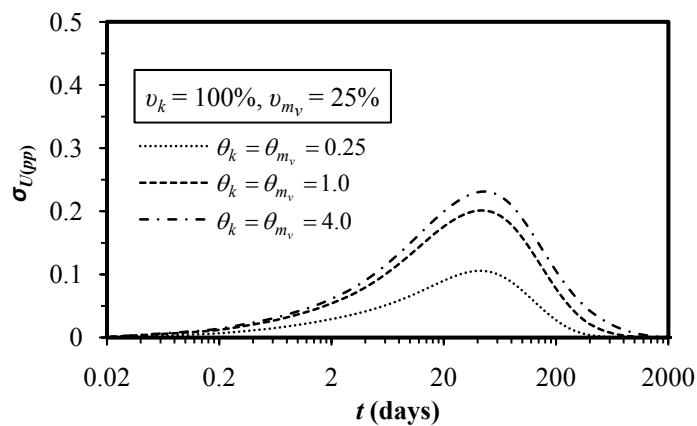
(b)

Figure 4.34: Effect of: (a) v on $\mu_{U(pp)}$ for $\theta = 2.0$; (b) θ on $\mu_{U(pp)}$ for $v_k = 100\%$, $v_{m_v} = 25\%$

The influence of increasing v and θ on $\sigma_{U(pp)}$ is investigated in Fig. 4.35. It can be seen that $\sigma_{U(pp)}$ increases with the increase of both v and θ , as shown in Figs. 4.35(a) and (b), respectively. Similar trend of $\sigma_{U(pp)}$ is also obtained for the effect of v and θ with $v_{m_v} = v_k$, as shown in Figs. 4.31(a) and (b), respectively.



(a)



(b)

Figure 4.35: Effect of: (a) v on $\sigma_{U(pp)}$ for $\theta = 2.0$; (b) θ on $\sigma_{U(pp)}$ for $v_k = 100\%$, $v_{m_v} = 25\%$

- ***Effects of v and θ on the probability of achieving 90% consolidation***

Fig. 4.36 illustrates the effect of varying v and θ on $P[U \geq U_{90}]_{(pp)}$. It can be seen that the observed trends of $P[U \geq U_{90}]_{(pp)}$ with respect to increasing v and θ , as shown in Figs. 4.36(a) and (b), remain similar to that obtained for the effect of v and θ with $v_{m_v} = v_k$, presented in Section 4.2.1.3.1.1.

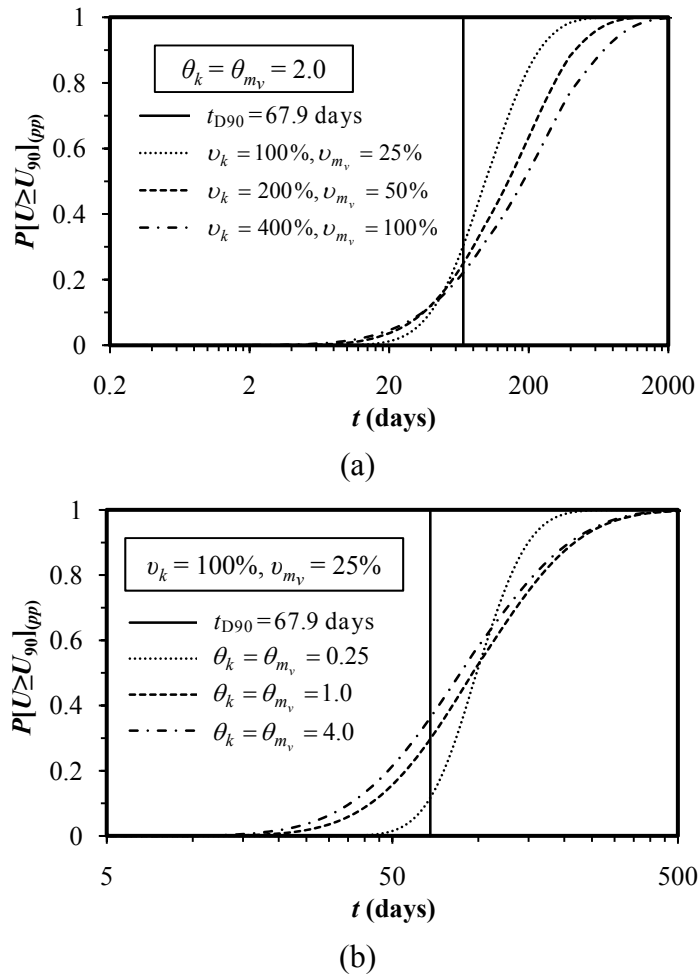


Figure 4.36: Effect of: (a) v on $P[U \geq U_{90}]_{(pp)}$ for $\theta = 2.0$; (b) θ on $P[U \geq U_{90}]_{(pp)}$ for $v_k = 100\%$, $v_{m_v} = 25\%$

The overall conclusion that can be drawn from the sensitivity analysis results presented in Sections 4.2.1.3.1.1 and 4.2.1.3.1.2 is that the effects of v and θ on $\sigma_{U(pp)}$ and $P[U \geq U_{90}]_{(pp)}$, and the effect of θ on $\mu_{U(pp)}$ are similar for both cases when $v_{m_v} = v_k$ and $v_{m_v} = 0.25 v_k$, and the only exception occurs for the effect of v on $\mu_{U(pp)}$. It is observed that $\mu_{U(pp)}$ increases with increasing v when $v_{m_v} = v_k$, whereas $\mu_{U(pp)}$ marginally decreases with increasing v for $v_{m_v} = 0.25 v_k$. This result indicates that the behaviour of $\mu_{U(pp)}$ with respect to v depends on the ratio of v_{m_v} / v_k .

4.2.1.3.2 Results based on excess pore water pressure and settlement

As stated earlier, when m_v differs from one location to another across the soil mass, the degree of consolidation as defined by the excess pore water pressure will be different from that defined by settlement. To assess this difference, in this section, the results based on the excess pore water pressure are compared with those obtained from settlement. For the convenience of comparison, the same values of v and θ are assumed for both k and m_v (i.e. $v_k = v_{m_v}$ and $\theta_k = \theta_{m_v}$).

- ***Comparison between statistics of U obtained from excess pore water pressure and settlement***

The comparison between the mean, μ_U , and standard deviation, σ_U , of the degree of consolidation, U , defined by the excess pore water pressure and settlement are shown in Figs. 4.37–4.40, in which μ_U and σ_U are expressed as functions of the consolidation time, t . It should be noted that, “*pp*” and “*set*” refer to the solutions based on the excess pore water pressure and settlement respectively, as mentioned earlier.

The relationship between μ_U and the consolidation time, t , for various v with constant $\theta = 1.0$ is illustrated in Fig. 4.37. The results obtained from random fields with no cross-correlation between k and m_v are shown in Fig. 4.37(a), which shows that the estimated μ_U profile derived from the excess pore water pressure is identical to that obtained from settlement, when v is as low as 100%. Noticeable difference between $\mu_{U(pp)}$ and $\mu_{U(set)}$ profiles can only be seen when v is as high as 200% and at any certain time, the estimated $\mu_{U(set)}$ is higher than $\mu_{U(pp)}$. Fig. 4.37(b) shows the results from cross-correlated random fields, which demonstrated that the estimated $\mu_{U(pp)}$ and $\mu_{U(set)}$ are identical for all values of v .

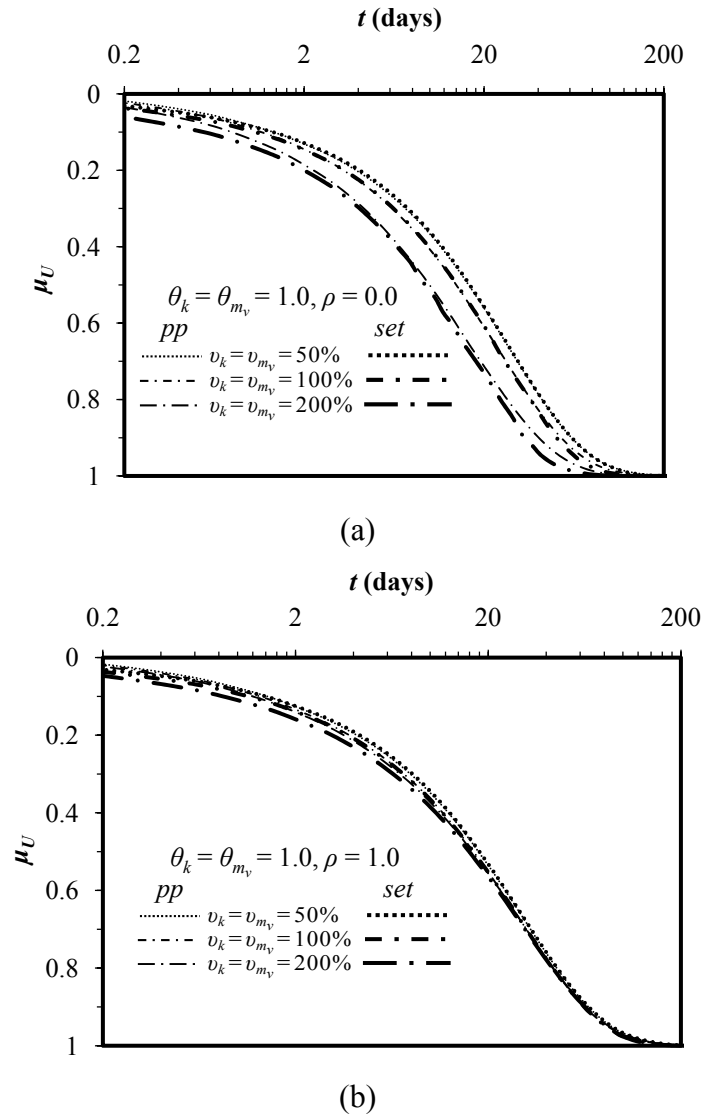


Figure 4.37: Comparison of the results defined by the excess pore water pressure and settlement for the effect of v on (a) μ_U at $\theta = 1.0, \rho = 0.0$ and (b) μ_U at $\theta = 1.0, \rho = 1.0$

The agreement between $\mu_{U(pp)}$ and $\mu_{U(set)}$ for various θ with constant $v = 100\%$ is shown in Fig. 4.38. As shown in Fig. 4.38(a), for random fields with no cross-correlation, the estimated μ_U defined by settlement is slightly higher than that defined by the excess pore water pressure, only when θ is as high as 2.0. On the other hand, in Fig. 4.38(b), μ_U is identical for any certain θ when the random fields become perfectly cross-correlated.

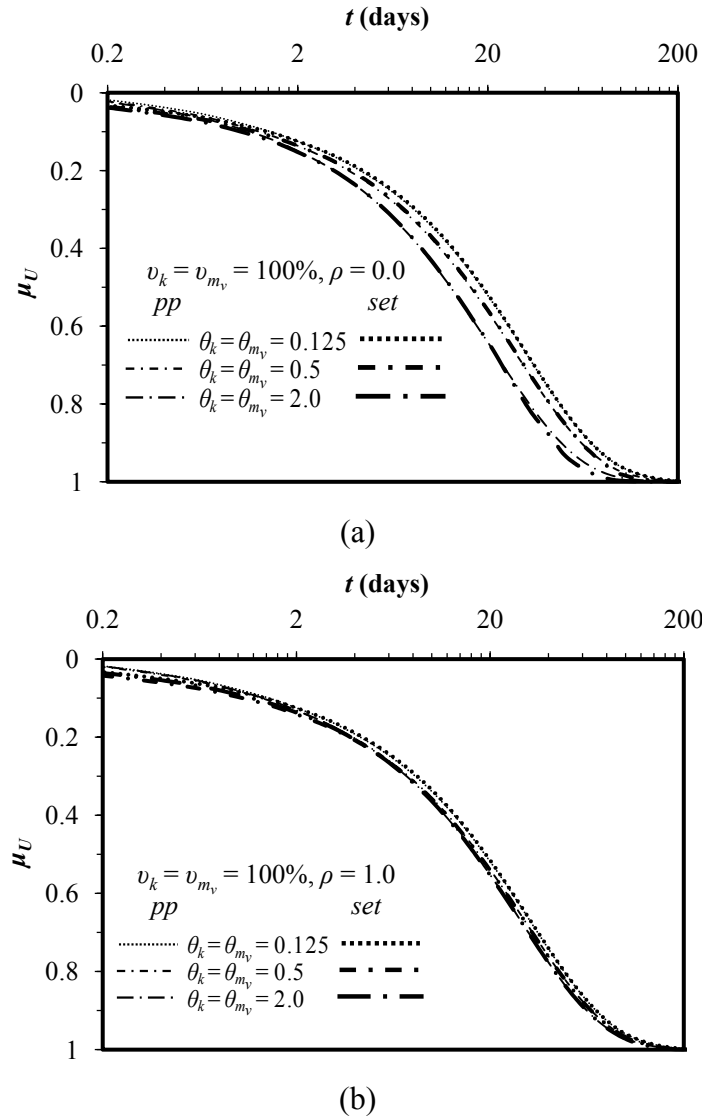
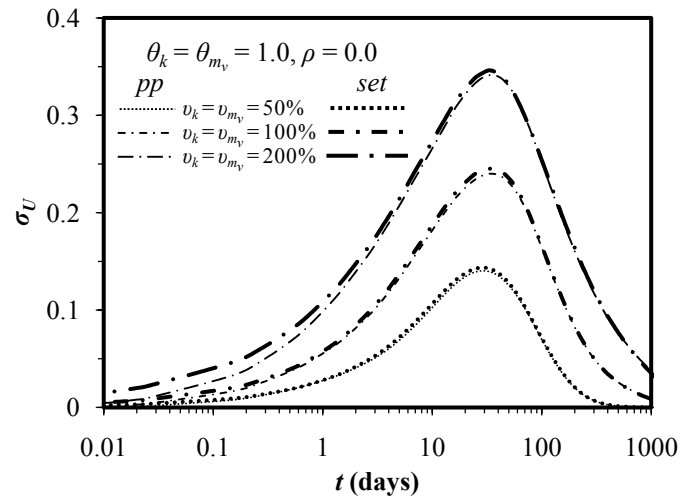
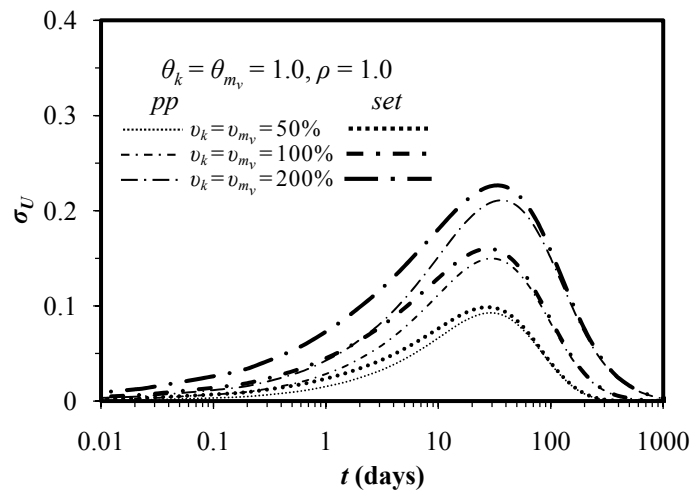


Figure 4.38: Comparison of the results defined by the excess pore water pressure and settlement for the effect of θ on (a) μ_U at $v = 100\%$, $\rho = 0.0$ and (b) μ_U at $v = 100\%$, $\rho = 1.0$

The estimated σ_U from the excess pore water pressure and settlement for various v with constant $\theta = 1.0$ are compared in Fig. 4.39. Results obtained from random fields with no cross-correlation are shown in Fig. 4.39(a), which from its visual inspection of the figure suggests that the difference between $\sigma_{U(pp)}$ and $\sigma_{U(set)}$ is negligible for any particular value of v . Fig. 4.39(b) illustrates the results from cross-correlated random fields, which shows that for any specific v , $\sigma_{U(set)}$ is higher than $\sigma_{U(pp)}$ and the discrepancy in σ_U increases with the increase of v .



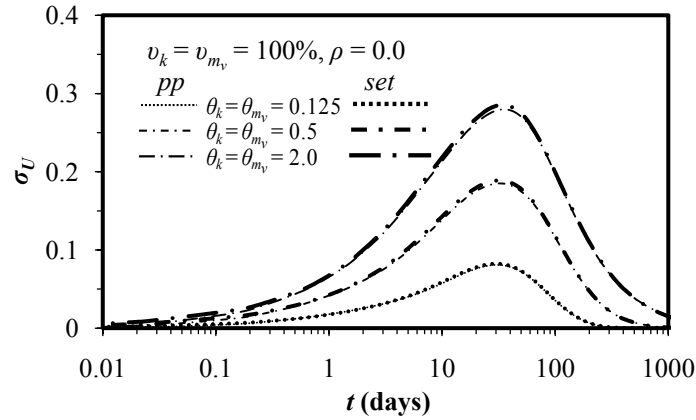
(a)



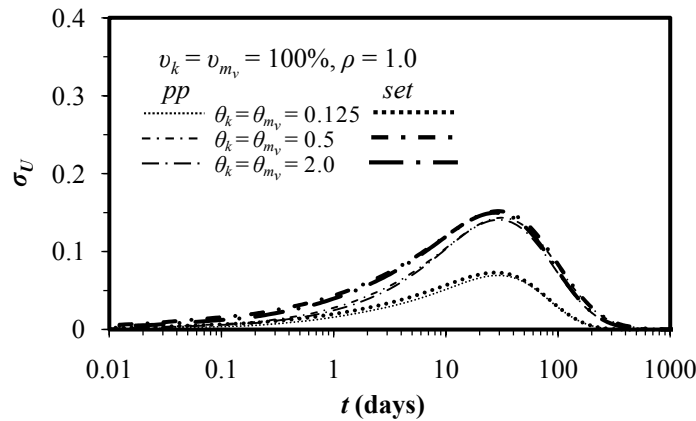
(b)

Figure 4.39: Comparison of the results defined by the excess pore water pressure and settlement for the effect of v on (a) σ_U at $\theta = 1.0, \rho = 0.0$ and (b) σ_U at $\theta = 1.0, \rho = 1.0$

The agreement between $\sigma_{U(pp)}$ and $\sigma_{U(set)}$ for various θ with constant $v = 100\%$ is investigated in Fig. 4.40. For no cross-correlation between k and m_v , as shown in Fig. 4.40(a), $\sigma_{U(pp)}$ and $\sigma_{U(set)}$ are identical for any specific θ . On the other hand, in Fig. 4.40(b), $\sigma_{U(set)}$ is higher than $\sigma_{U(pp)}$ for any individual θ .



(a)



(b)

Figure 4.40: Comparison of the results defined by the excess pore water pressure and settlement for the effect of θ on (a) σ_U at $v = 100\%$, $\rho = 0.0$ and (b) σ_U at $v = 100\%$, $\rho = 1.0$

- ***Comparison between the probability of achieving 90% consolidation obtained from excess pore water pressure and settlement***

The agreement between the obtained results based on the excess pore water pressure and settlement are also investigated in terms of the probability of achieving 90% consolidation, $P[U \geq U_{90}]$ in Figs. 4.41–4.42. The compliance between $P[U \geq U_{90}]_{(pp)}$ and $P[U \geq U_{90}]_{(set)}$ for various v with constant $\theta = 1.0$ is shown in Fig. 4.41. As shown in Fig. 4.41(a), for random fields with no cross-correlation, a slight discrepancy between $P[U \geq U_{90}]_{(pp)}$ and $P[U \geq U_{90}]_{(set)}$ profiles can only be seen when v is as high as 200%, particularly when $P[U \geq U_{90}] \geq 70\%$. It can also be seen that beyond the probability level of 70%, $P[U \geq U_{90}]_{(set)}$ is slightly higher than

$P[U \geq U_{90}]_{(pp)}$ for $v = 200\%$. This means that the excess pore water pressure gives a marginally conservative estimation of $P[U \geq U_{90}]$. The results from cross-correlated random fields are contrasted in Fig. 4.41(b), which shows that for any certain v , the estimated $P[U \geq U_{90}]_{(pp)}$ and $P[U \geq U_{90}]_{(set)}$ are identical.

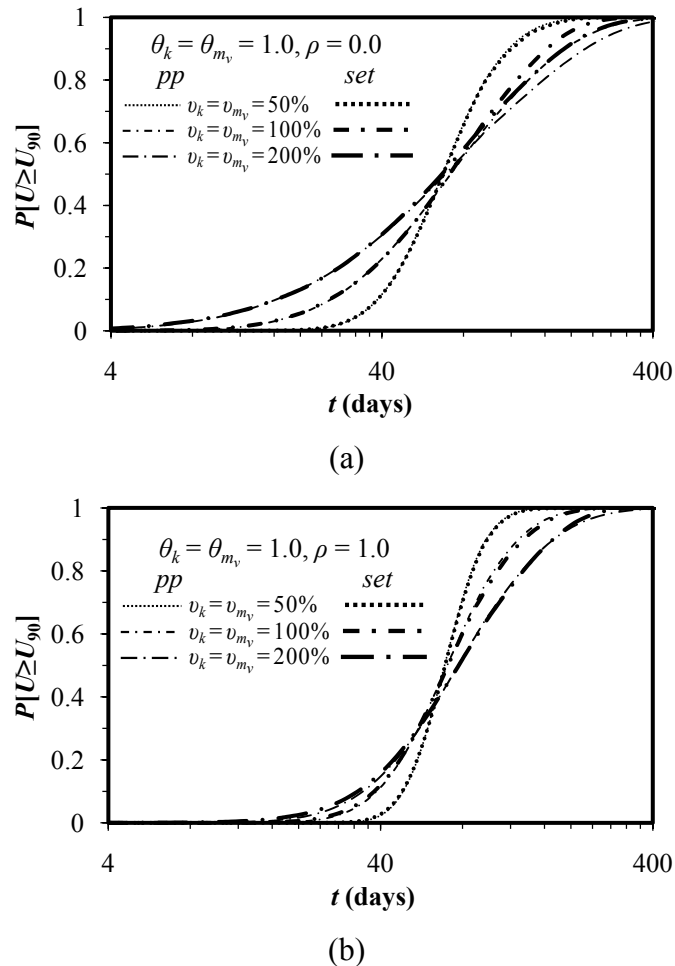


Figure 4.41: Comparison of the results defined by the excess pore water pressure and settlement for the effect of v on (a) $P[U \geq U_{90}]$ at $\theta = 1.0, \rho = 0.0$ and (b) $P[U \geq U_{90}]$ at $\theta = 1.0, \rho = 1.0$

The estimated $P[U \geq U_{90}]_{(pp)}$ and $P[U \geq U_{90}]_{(set)}$ for various θ with a constant $v = 100\%$ are compared in Fig. 4.42. The results obtained from random fields with no cross-correlation are shown in Fig. 4.42(a), which shows that, in general, for a definite θ , both the excess pore water pressure and settlement give almost identical solutions of $P[U \geq U_{90}]$. Little discrepancy, however, is observed between these two solutions when $\theta \geq 2.0$, especially at a higher probability level (for example, when

$P[U \geq U_{90}] \geq 70\%$). Fig. 4.42(b) illustrates the results from cross-correlated random fields, which illustrates that for any certain θ , the estimated $P[U \geq U_{90}]_{(pp)}$ and $P[U \geq U_{90}]_{(set)}$ are identical.

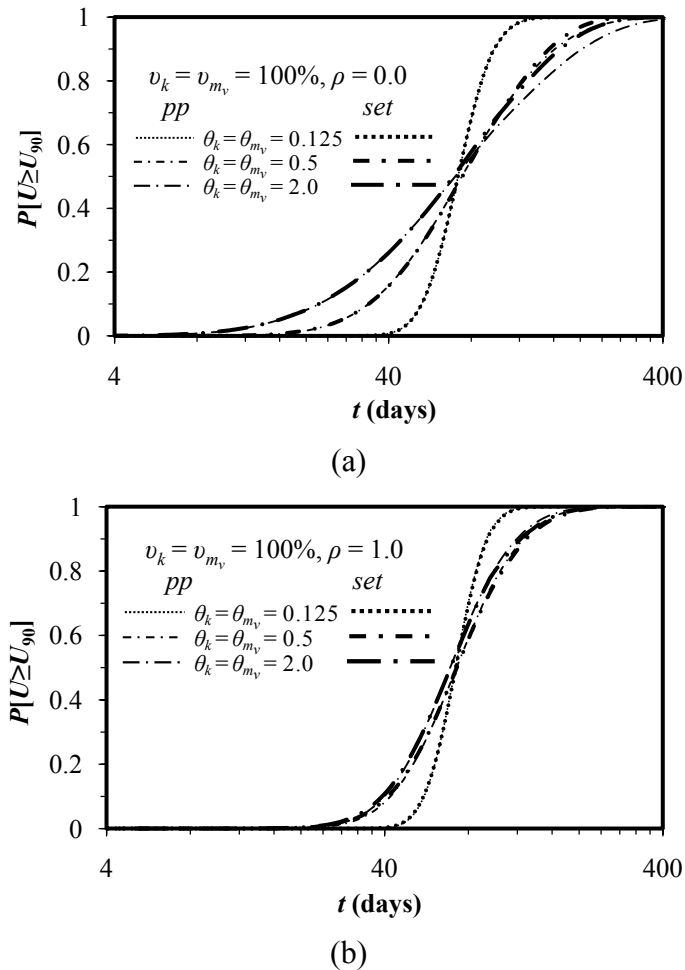


Figure 4.42: Comparison of the results defined by the excess pore water pressure and settlement for the effect of θ on (a) $P[U \geq U_{90}]$ at $v = 100\%$, $\rho = 0.0$ and (b) $P[U \geq U_{90}]$ at $v = 100\%$, $\rho = 1.0$

As shown in Figs. 4.37–4.42, the difference between the obtained results based on the excess pore water pressure and settlement are fully investigated in terms of μ_U , σ_U and $P[U \geq U_{90}]$. Although little discrepancies are observed in μ_U and $P[U \geq U_{90}]$ for random fields with no cross correlation when v is as high as 200%, and in σ_U for cross correlated k and m_v when $v \geq 100\%$, it appears that the overall difference between the excess pore water pressure and settlement is insignificant as far as natural soils is concerned. It should be noted that the difference between the excess

pore water pressure and settlement occurs only due to the spatially variable m_v , and $v_{m_v} \geq 100\%$ is unlikely to be encountered in real soil deposits, based on the published data shown in Table 2.2. Therefore, in the subsequent part of this thesis, only the results based on the excess pore water pressure are presented and the subscripts “ pp ” that was used to represent the results based on the excess pore water pressure is also omitted from the presented results.

4.2.1.3.3 Influence of cross-correlation between spatially variable soil permeability and coefficient of volume compressibility

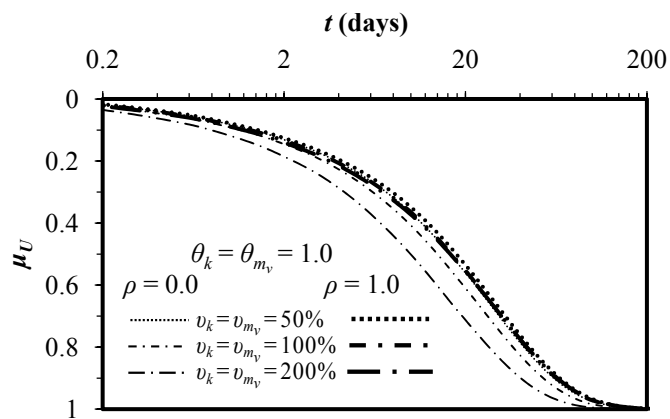
When dealing with more than one random variable, the uncertainties in one might be influenced by the uncertainties in the other, i.e. the random soil properties under consideration may be cross-correlated. In this section, analyses are performed to investigate the influence of cross-correlation between k and m_v . The cross-correlation between k and m_v is defined by the correlation coefficient, ρ , as previously discussed in Chapter 3 (Section 3.2.1.3). Although little is currently known about the level of correlation between k and m_v , it is often considered in soil mechanics that for the same soil, k and m_v are strongly positively correlated (Badaoui et al. 2007). Thus, a small magnitude of permeability corresponds to a small magnitude of compressibility. Strong positive correlation between k and m_v of fine-grained dredged materials has also been shown by Morris (2003). Accordingly, in this study, two correlation conditions of soil with $\rho = 0.0$ (i.e. uncorrelated) and 1.0 (i.e. perfectly positively correlated) are considered. The same values of v and θ are assumed for both k and m_v (i.e. $v_k = v_{m_v}$ and $\theta_k = \theta_{m_v}$) for purpose of comparison. The results obtained from these two correlation conditions are discussed below.

- **Comparison of statistics of U obtained by $\rho = 0.0$ and $\rho = 1.0$**

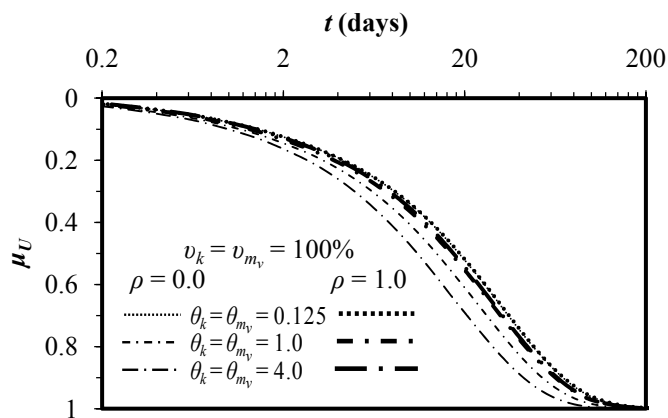
The computed values of μ_U and σ_U obtained for $\rho = 0.0$ and $\rho = 1.0$ are compared in Figs. 4.43–4.44. Fig. 4.43(a) shows the relationship between μ_U and the consolidation time, t , for various v at constant $\theta = 1.0$. It can be seen that at any certain t , the uncorrelated k and m_v lead to higher μ_U than that of perfectly correlated k and m_v . It can also be seen that for $\rho = 1.0$, μ_U is insensitive to v . Both behaviours can be

explained by noting that for $\rho = 0.0$, there is more chance of higher k values occurring with lower m_v values, while for $\rho = 1.0$, there is no such trend. When $\rho = 1.0$ in a given simulation, small k corresponds to small m_v and vice versa. As a result, μ_U remains almost identical in all cases of v .

The effect of θ on μ_U obtained with $\rho = 0.0$ and $\rho = 1.0$ is examined in Fig. 4.43 (b) for a fixed $v = 100\%$. It can be seen that similar trend of μ_U to that obtained for the effect of v is also obtained for the effect of θ . This is due to the same factors explained for Fig 4.43(a). However, it is interesting to note that in Fig. 4.43(b), for $\rho = 1.0$, there is a critical θ that leads to maximum values of μ_U .



(a)



(b)

Figure 4.43: Comparison of the results obtained by $\rho = 0.0$ and $\rho = 1.0$ for the effect of: (a) v on μ_U at $\theta = 1.0$ and (b) θ on μ_U at $v = 100\%$

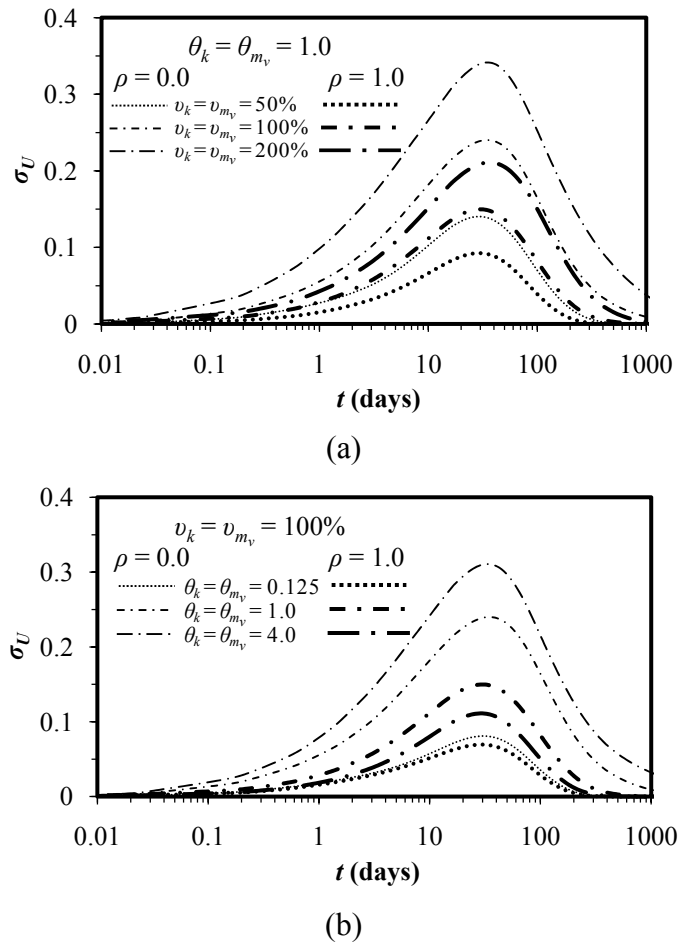


Figure 4.44: Comparison of the results obtained by $\rho = 0.0$ and $\rho = 1.0$ for the effect of: (a) v on σ_U at $\theta = 1.0$ and (b) θ on σ_U at $v = 100\%$

Fig 4.44 shows the comparison between σ_U calculated with $\rho = 0.0$ and $\rho = 1.0$. The effect of v on σ_U is examined in Fig. 4.44(a) for $\theta = 1.0$. It can be seen that for both $\rho = 0.0$ and $\rho = 1.0$, σ_U increases with increasing v , and at any certain t , uncorrelated k and m_v give higher σ_U than that of perfectly correlated k and m_v . Fig. 4.44(b) shows the effect of θ on σ_U for a fixed $v = 100\%$. It can be seen that, for any certain θ , the computed σ_U with $\rho = 0.0$ always higher than that computed with $\rho = 1.0$. One particular point to note in Fig. 4.44(b) is that there is a critical θ that leads to maximum values of σ_U for perfectly correlated k and m_v .

- **Comparison of probability of achieving 90% consolidation obtained for $\rho = 0.0$ and $\rho = 1.0$**

The comparison of $P[U \geq U_{90}]$ obtained for $\rho = 0.0$ and $\rho = 1.0$ is shown in Figs. 4.45. Fig. 4.45(a) illustrates the effect of v on $P[U \geq U_{90}]$ for $\theta = 1.0$, which clearly shows two trends in the results before and after the probability level of 0.5. For any particular v and at a certain t , the computed $P[U \geq U_{90}]$ with $\rho = 0.0$ always higher than that computed with $\rho = 1.0$ when $P[U \geq U_{90}] \leq 50\%$, whereas the role of v has the opposite effect when $P[U \geq U_{90}] \geq 50\%$. However, the effect of cross-correlation is not seen to be particularly large. If the positive cross-correlation indicated by Morris (2003) is correct, then the independent $\rho = 0.0$ case is conservative, having $P[U \geq U_{90}]$ somewhat less than the case of $\rho = 1.0$, provided that the target probability of achieving 90% consolidation is greater than 50%.

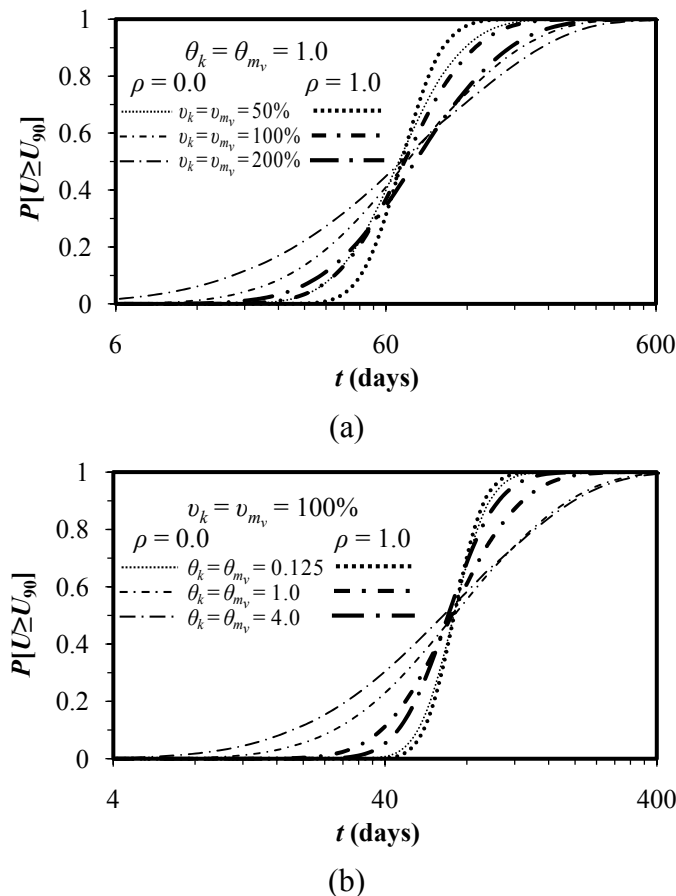


Figure 4.45: Comparison of the results obtained by $\rho = 0.0$ and $\rho = 1.0$ for the effect of: (a) v on $P[U \geq U_{90}]$ at $\theta = 1.0$ and (b) θ on $P[U \geq U_{90}]$ at $v = 100\%$

The estimated $P[U \geq U_{90}]$ for $\rho = 0.0$ and $\rho = 1.0$ are compared in Fig. 4.45(b) for various θ with constant $v = 100\%$. It can be seen that all curves crossover at a critical value of $P[U \geq U_{90}] \approx 50\%$. At any certain time prior to the crossover point, $P[U \geq U_{90}]$ increases with the increase of θ and the role of θ is to have the opposite effect after the crossover point. The only exception to this behaviour occurs for cross-correlated k and m_v when θ becomes larger than the critical θ . It can also be seen from Fig. 4.45(b) that for any particular v and at a certain t , the computed $P[U \geq U_{90}]$ for $\rho = 0.0$ always higher than that computed for $\rho = 1.0$ when $P[U \geq U_{90}] \leq 50\%$, whereas an opposite trend to this behaviour is observed when $P[U \geq U_{90}] \geq 50\%$.

Although the estimated behaviour of soil consolidation in terms of μ_U , σ_U and $P[U \geq U_{90}]$ is different based on the degree of correlation between k and m_v , the relationship or cross-correlation between k and m_v is poorly understood and no consensus is provided in the existing literature. The cross-correlation between soil properties is also strongly dependent on the particular soil being studied (Fenton and Griffiths 2003). Therefore, in the subsequent part of the thesis, the stochastic independence between k and m_v (i.e. $\rho = 0.0$) will be assumed rather than assuming any erroneous correlation.

4.3 Probabilistic Analysis of Soil Consolidation Considering Smear Effect

The smear effect that develops as a consequence of mandrel installation produces a disturbed zone of reduced soil permeability, k , and increased compressibility, m_v , known as the smear zone. As all expelled water must pass through this zone, even a small zone of reduced k and increased m_v close to the drain will significantly affect the rate of soil consolidation. Similar to the undisturbed zone, k and m_v in the smear zone are also inherently variable. However, due to the non-uniform spatial distribution of soil disturbance (which decreases with the increase of distance from the centre of the drain), the variability characteristics of the smeared soil may be significantly different from those of undisturbed soil. It is reasonable to expect that the COV of soil properties in the smear zone will be larger than those in the undisturbed zone; as the non-uniform disturbance of smeared soil may contribute some additional variability to its inherent spatial variability. Accordingly, the prediction of the behaviour of soil stabilised by PVDs, without considering the smear

effect would have little real application. In this section, the effect of the spatially variable k and m_v on the stochastic behaviour of soil consolidation by PVDs is examined with special consideration given to the smear effect.

4.3.1 Description of consolidation problem under consideration

To perform a stochastic analysis whilst considering the smear effect, the same axisymmetric unit cell as previously described in Section 4.2.1 is used. The only exception is that the unit cell is divided into two zones, namely the smear and undisturbed zones, as shown in Fig. 4.46. It has to be noted that the $0.05\text{m} \times 0.05\text{m}$ mesh, as previously shown in Fig. 4.2, is used in the analyses. The mean values of the spatially variable permeability and volume compressibility in the undisturbed zone are kept at fixed values equal to $\mu_{k_u} = 5 \times 10^{-10}$ m/sec and $\mu_{m_{v_u}} = 1.67 \times 10^{-4}$ m²/kN, respectively. In order to investigate the various aspects of stochastic soil consolidation by PVDs considering the smear effect, the mean value of k in the smear zone is varied using ratios of μ_{k_u} / μ_{k_s} equal to 1.5 and 2.0, while the mean value of m_v in the smear zone is varied using ratios of $\mu_{m_{v_s}} / \mu_{m_{v_u}}$ equal to 1.25 and 1.5. In addition, to investigate the effect of the smear zone ratio, $s = r_s / r_w$, on the behaviour of soil consolidation, three different s values of 5, 7 and 9 are considered, which correspond to r_s of 0.25m, 0.35m and 0.45m, respectively. It is worthy to note that the assumed values of r_s are slightly larger than the typical range of r_s mentioned in Chapter 2. This is to ensure that sufficient number of elements is available in the smear zone to produce stable statistics of the generated lognormally distributed permeability field, by the LAS technique. In addition, it will be shown later in this section that a reasonable change in r_s will not alter the general trends and observations derived from this study. All the geometric and soil properties used in the parametric study of this section are summarized in Table 4.3. Similar to the ‘no-smear’ case, the study carried out in this section is divided into two parts. In the first part, only soil permeability, k , is considered as random variable, while in the second part both k and m_v are selected to be random variables. It is to be noted that when only permeability is considered as random variable, a constant m_v equal to $\mu_{m_{v_u}}$ (i.e.

$1.67 \times 10^{-4} \text{ m}^2/\text{kN}$) is used for both the smear and undisturbed zones, i.e. $\mu_{m_{vs}} / \mu_{m_{vu}} =$

1.0. Details of each part of the study are described in order below.

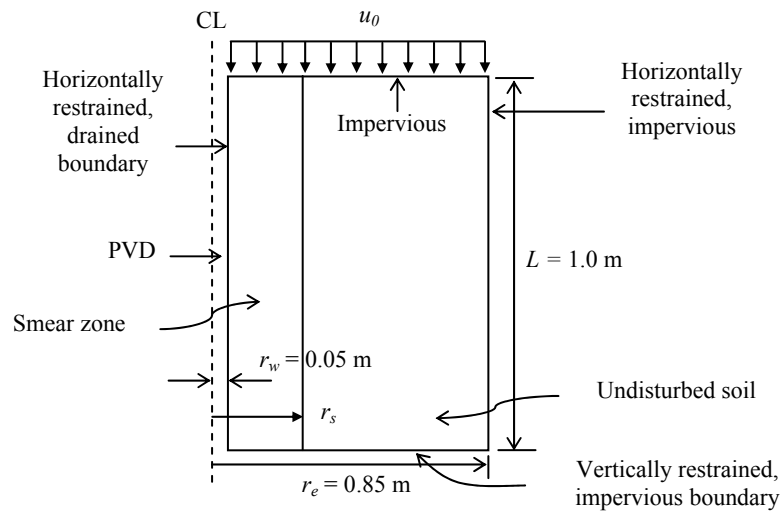


Figure 4.46: Geometry of the consolidation problem for the analysis considering smear

Table 4.3: Input parameters for parametric studies considering smear

Parameters	Input values
μ_{k_u} (m/sec)	5×10^{-10}
$\mu_{m_{vu}}$ (m^2/kN)	1.67×10^{-4}
μ_{k_u} / μ_{k_s}	1.5, 2.0
$\mu_{m_{vs}} / \mu_{m_{vu}}$	1.25, 1.5
s	5, 7, 9 (i.e. $r_s = 0.25\text{m}, 0.35\text{m}, 0.45\text{m}$)

4.3.1.1 Deterministic Solution

Prior to proceeding with the stochastic analyses, deterministic analyses are performed with different ratios of μ_{k_u} / μ_{k_s} and $\mu_{m_{vs}} / \mu_{m_{vu}}$. The deterministic analyses for each s listed in Table 4.3 are also conducted. In each analysis, respective constant

mean soil properties in the smear and undisturbed zones are used. The details of each deterministic analysis and the resulting t_{D90} are summarised in Table 4.4.

Table 4.4: Deterministic analyses under different smear zone parameters and the time required to achieve 90% consolidation

Test No.	Input smear zone parameters	Time required to achieve 90% consolidation, t_{D90} (days)
1	$\mu_{k_u} / \mu_{k_s} = 2.0, \mu_{m_{vs}} / \mu_{m_{vu}} = 1.0, s = 5$	117.6
2	$\mu_{k_u} / \mu_{k_s} = 2.0, \mu_{m_{vs}} / \mu_{m_{vu}} = 1.0, s = 7$	126.5
3	$\mu_{k_u} / \mu_{k_s} = 2.0, \mu_{m_{vs}} / \mu_{m_{vu}} = 1.0, s = 9$	131.25
4	$\mu_{k_u} / \mu_{k_s} = 1.5, \mu_{m_{vs}} / \mu_{m_{vu}} = 1.0, s = 7$	96.0
5	$\mu_{k_u} / \mu_{k_s} = 2.0, \mu_{m_{vs}} / \mu_{m_{vu}} = 1.25, s = 7$	129.3
6	$\mu_{k_u} / \mu_{k_s} = 2.0, \mu_{m_{vs}} / \mu_{m_{vu}} = 1.5, s = 7$	132.7

4.3.1.2 Probabilistic analysis of soil consolidation considering spatially random permeability

As mentioned earlier, soil permeability has the widest range of variation among all soil properties and is believed to have the most significant impact on soil consolidation. Therefore, it is worthwhile investigating the individual effect of a spatially variable k on the soil consolidation rate whilst considering the smear effect. The main focus of this section is as follows:

- Performing a sensitivity analysis to investigate the relative significance of the spatially variable smear permeability over undisturbed permeability.
- Carrying out an investigation into the effects of varying the ratio of the undisturbed zone mean permeability to the smear zone mean permeability, along with studying the effects of the smear zone ratio on the results obtained, using the same statistical parameters of k .

In order to perform a stochastic analysis considering the smear effect, two independent random fields of soil permeability are generated separately (one for the

smear zone and another for the undisturbed zone) based on their prescribed statistical parameters, as shown in Table 4.5. In such case, ν and θ of k are denoted ν_{k_u} and θ_{k_u} , respectively, for undisturbed zone, whereas they are denoted ν_{k_s} and θ_{k_s} , respectively, for the smear zone. Since little is currently known about the typical COVs and SOFs of soils in the smear zone, the same range of ν and θ are selected for both the smear and undisturbed zones. Both random fields are then mapped onto the corresponding grid in the finite element mesh, as illustrated in Figure 4.47. In Figure 4.47, RF- u and RF- s represent the random fields of the undisturbed and smear zones, respectively. The details of each part of the study and the obtained results are described below.

Table 4.5: Random field parameters for parametric studies

Parameter	Value
ν_k (%) (both for smear and undisturbed zone)	50, 100, 200
θ_k (m) (both for smear and undisturbed zone)	0.125, 0.5, 2.0

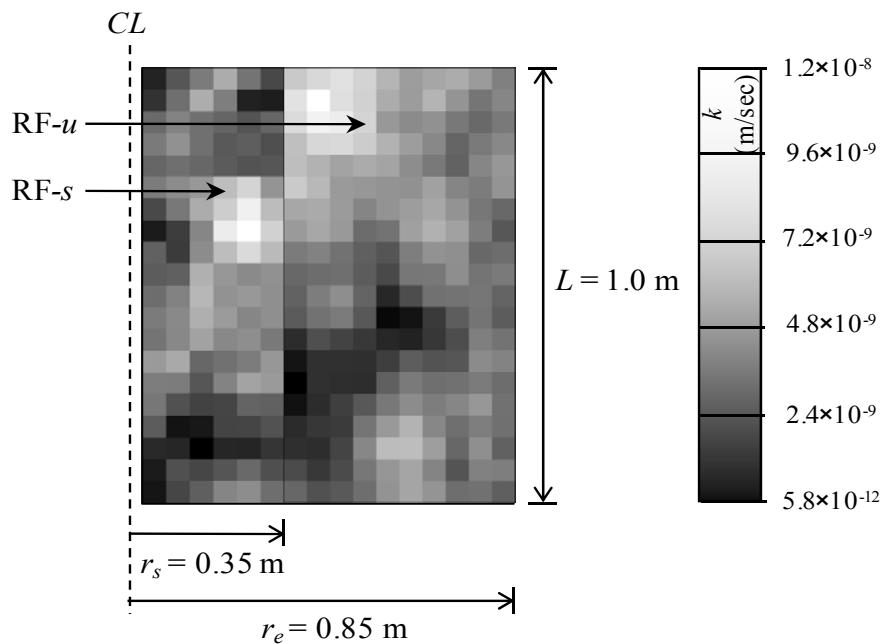


Fig. 4.47: Typical realization of a random permeability field for $\nu_{k_u} = 100\%$, $\nu_{k_s} = 50\%$, $\theta_{k_u} = 1.0$, $\theta_{k_s} = 0.5$ ($\mu_{k_u} = 5 \times 10^{-10}$ m/sec and $\mu_{k_s} = 2.5 \times 10^{-10}$ m/sec)

4.3.1.2.1 Results of parametric study

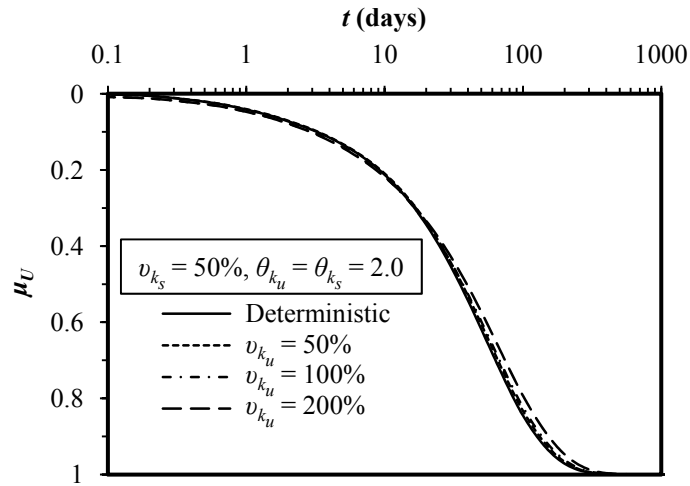
The input parameters μ_{k_u} / μ_{k_s} and s (shown in Table 4.3); v_k and θ_k (shown in Table 4.5) are varied systematically in the parametric study to investigate their influence on the estimated behaviour of soil consolidation. For each selected set of input parameters, 1000 Monte Carlo simulations are performed to estimate μ_U , σ_U and $P[U \geq U_{90}]$ from the consolidation response of each individual realization.

4.3.1.2.1.1 Effect of variation of v_k and θ_k on the mean and standard deviation of U and the probability of achieving 90% consolidation

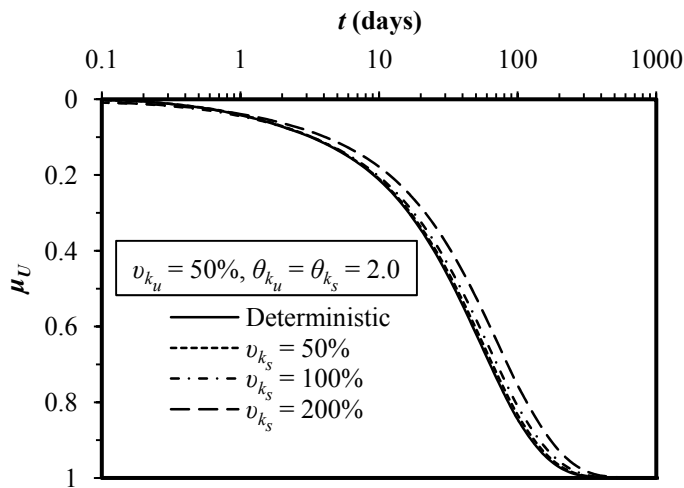
In this section, the ratio of μ_{k_u} / μ_{k_s} and s are held constant at 2.0 and 7, respectively. The effects of varying v_k and θ_k on μ_U , σ_U and $P[U \geq U_{90}]$ are investigated in Figs. 4.48–4.53. In Figs. 4.48–4.53, μ_U , σ_U and $P[U \geq U_{90}]$ are expressed as functions of the consolidation time t .

- *Effects of variation of v_k and θ_k on the mean of U*

Fig. 4.48 shows the effects of v_{k_u} and v_{k_s} on μ_U at a fixed value of $\theta_{k_u} = \theta_{k_s} = 2.0$, which also includes the deterministic solution of no soil variability. It can be seen from Fig. 4.48(a) that at any consolidation time, there is a slight reduction in μ_U for spatially varied soils compared to the deterministic case; however, in general, the effect of increasing v_{k_u} on μ_U remains marginal even when v_{k_u} is as high as 200%. The effect of v_{k_s} on μ_U at a fixed value of $v_{k_u} = 50\%$ is shown in Fig. 4.48(b), which shows that the varying values of v_{k_s} have a considerable impact on the estimated values of μ_U . At any certain consolidation time, μ_U decreases with the increase of v_{k_s} . The overall observation that can be derived from the comparison of the results in Fig.4.48 is that the decreasing rate of μ_U is higher for the increasing value of v_{k_s} than v_{k_u} , implying that the effect of v_{k_s} on μ_U is dominant.



(a)



(b)

Figure 4.48: Effect of v_{k_u} and v_{k_s} on μ_U for $\theta_{k_u} = \theta_{k_s} = 2.0$

The effect of varying θ_{k_u} and θ_{k_s} on μ_U at a fixed value of $v_{k_u} = v_{k_s} = 100\%$ is examined in Fig. 4.49. Virtually identical curves of μ_U in Fig. 4.49(a) for all θ_{k_u} with a fixed value of $\theta_{k_s} = 1.0$ indicate that μ_U is largely independent of θ_{k_u} . On the other hand, in Fig. 4.49(b), at any certain consolidation time, μ_U increases with the increase of θ_{k_s} . What this means is that the behaviour of μ_U is controlled by θ_{k_s} rather than θ_{k_u} .

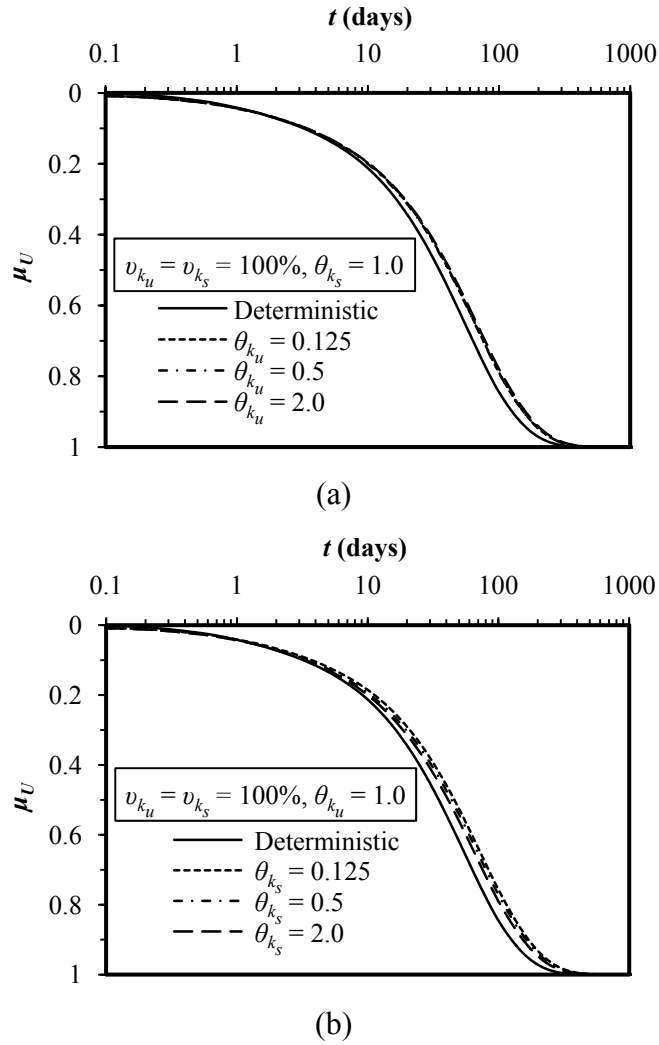
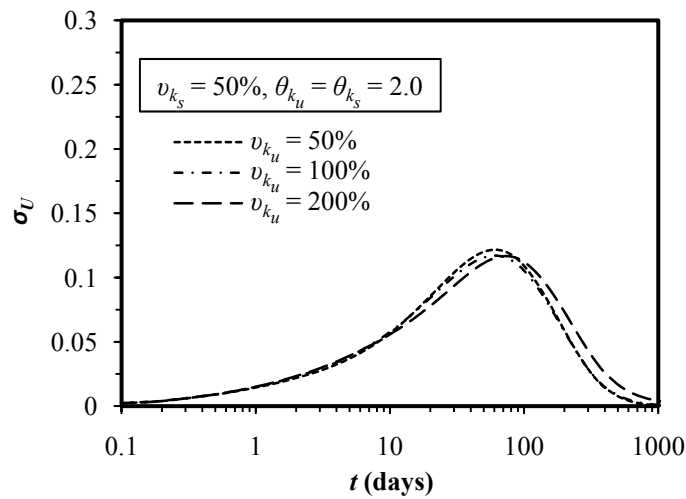


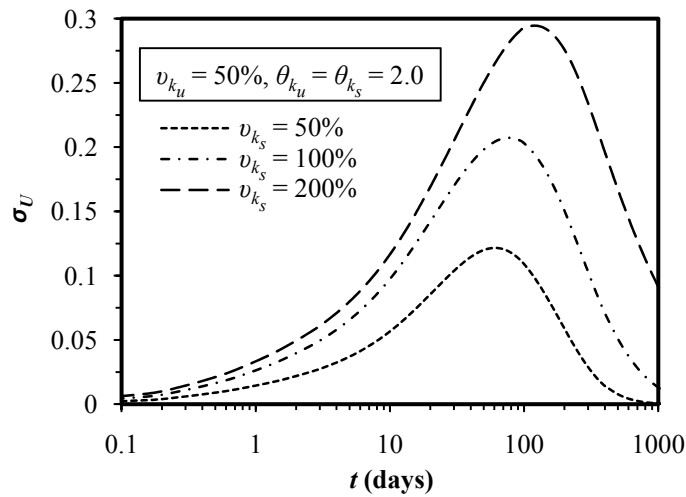
Figure 4.49: Effect of θ_{k_u} and θ_{k_s} on μ_U for $\nu_{k_u} = \nu_{k_s} = 100\%$

- ***Effects of variation of ν_k and θ_k on the standard deviation of U***

The influence of ν_{k_u} and ν_{k_s} on σ_U at a fixed value of $\theta_{k_u} = \theta_{k_s} = 2.0$ is highlighted in Fig. 4.50. As shown in Fig. 4.50(a), for a fixed value of ν_{k_s} (i.e. $\nu_{k_s} = 50\%$ in this case), increasing ν_{k_u} has little or no effect on σ_U . The effect of ν_{k_s} on σ_U at a fixed value of $\nu_{k_u} = 50\%$ is illustrated in Fig. 4.50(b). It can be seen that at any certain consolidation time, σ_U increases significantly with the increase of ν_{k_s} , implying the dominant effect of ν_{k_s} on the estimated values of σ_U .



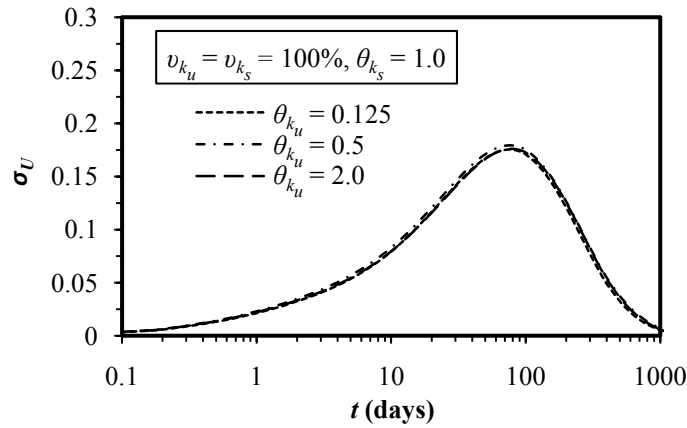
(a)



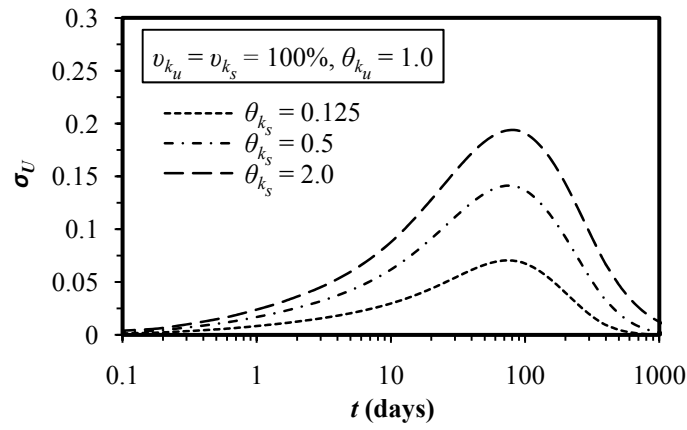
(b)

Figure 4.50: Effect of v_{k_u} and v_{k_s} on σ_U for $\theta_{k_u} = \theta_{k_s} = 2.0$

Fig. 4.51 illustrates the effects of varying θ_{k_u} and θ_{k_s} on σ_U for constant $v_{k_u} = v_{k_s} = 100\%$. In Fig. 4.51(a), it can be seen that, similar to the effect of θ_{k_u} on μ_U , σ_U remains almost identical for varying θ_{k_u} with a fixed value of $\theta_{k_s} = 1.0$. On the other hand, the estimated σ_U for different values of θ_{k_s} is plotted in Figure 4.51(b) at a fixed value of $\theta_{k_u} = 1.0$. It can be seen that, unlike θ_{k_u} , θ_{k_s} has a considerable impact on the estimated values of σ_U .



(a)



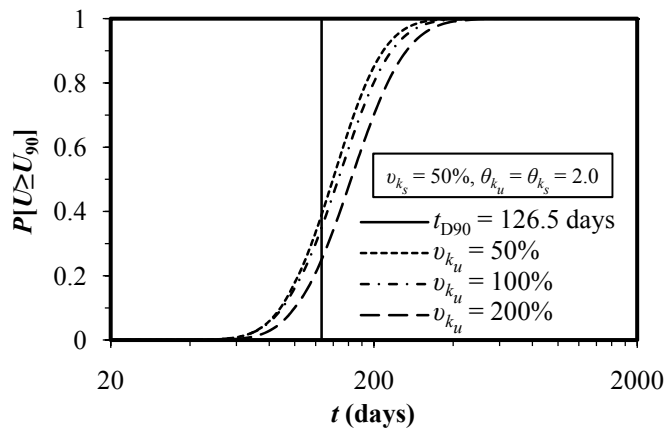
(b)

Figure 4.51: Effect of θ_{k_u} and θ_{k_s} on σ_U for $v_{k_u} = v_{k_s} = 100\%$

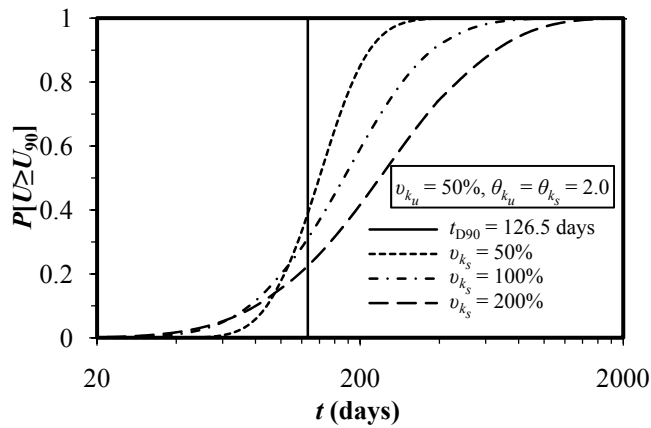
- ***Effects of variation of v_k and θ_k on the probability of achieving 90% consolidation***

The effects of spatially variable k on the probability of achieving 90% consolidation for the case considering the smear effect are shown in Figs. 4.52 and 4.53 (the deterministic time of achieving 90% consolidation, t_{D90} , is also shown in these figures by vertical solid lines that give $P[U \geq U_{90}]$ at that time for any combination of v_k and θ_k). For the smear case with spatially variable permeability, the rationality of the lognormal distribution for $U^*(t)$ is also assessed by the Chi-square test and Fig. 4.54 illustrates a typical example of the histogram of $U^*(t)$ for $v_u = 50\%$, $v_s = 100\%$, $\theta_u = \theta_s = 2.0$ at $t = 357$ days, along with their fitted lognormal distribution. The visual inspection of Fig. 4.54 suggests that the lognormal distribution fits the $U^*(t)$

histogram very well. The goodness-of-fit test using the Chi-square test yielded p -value of 0.73 implying that the lognormal distribution hypothesis for $U^*(t)$ is valid.



(a)

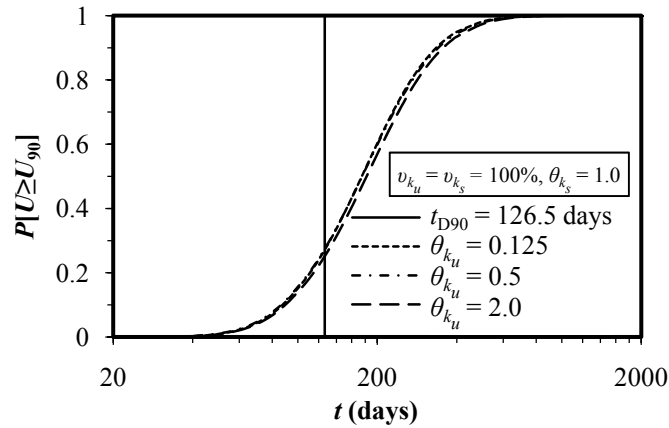


(b)

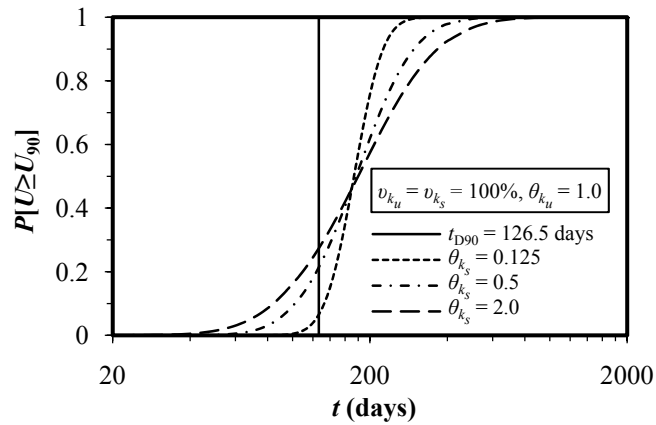
Figure 4.52: Effect of v_{k_u} and v_{k_s} on $P[U \geq U_{90}]$ for $\theta_{k_u} = \theta_{k_s} = 2.0$

The effects of v_{k_u} and v_{k_s} on $P[U \geq U_{90}]$ at a fixed value of $\theta_{k_u} = \theta_{k_s} = 2.0$ is investigated in Fig. 4.52. It can be seen from Fig. 4.52(a) that at any given consolidation time, $P[U \geq U_{90}]$ decreases as v_{k_u} increases (v_{k_s} is fixed at 50%); however, in general, the effect of increasing v_{k_u} on $P[U \geq U_{90}]$ remains marginal. The effect of v_{k_s} at a fixed value of $v_{k_u} = 50\%$ is shown in Fig. 4.52(b), which shows that the varying values of v_{k_s} have a considerable impact on the estimated values of $P[U \geq U_{90}]$. At any certain consolidation time, $P[U \geq U_{90}]$ decreases with the increase of v_{k_s} . The overall observation that can be derived from comparing the results in Fig. 4.52 is that, the decreasing rate of $P[U \geq U_{90}]$ is higher for the

increasing value of ν_{k_s} than ν_{k_u} , implying that the effect of ν_{k_s} on $P[U \geq U_{90}]$ is dominant.



(a)



(b)

Figure 4.53: Effect of θ_{k_u} and θ_{k_s} on $P[U \geq U_{90}]$ for $\nu_{k_u} = \nu_{k_s} = 100\%$

Fig. 4.53 illustrates the effects of θ_k on $P[U \geq U_{90}]$ at a fixed value of $\nu_{k_u} = \nu_{k_s} = 100\%$. In Fig. 4.53(a), the influence of θ_{k_u} on $P[U \geq U_{90}]$ is shown at $\theta_{k_s} = 1.0$, and the results yield almost identical curves indicating that θ_{k_u} has little or no impact on the probabilistic behaviour of the degree of consolidation. On the other hand, the estimated $P[U \geq U_{90}]$ for different values of θ_{k_s} is plotted in Fig. 4.53(b) at a fixed value of $\theta_{k_u} = 1.0$. It can be seen that, unlike θ_{k_u} , θ_{k_s} has a considerable impact on the estimated values of $P[U \geq U_{90}]$. The comparison between Figs. 4.53(a) and (b) reveals that the effect of θ_{k_s} on $P[U \geq U_{90}]$ is more significant than θ_{k_u} . It should be noted that the deterministic solution of this case yields $t_{D90} = 126.5$ days, and again it

is interesting to note that this deterministic solution yields $P[U \geq U_{90}] < 50\%$ for all combinations of values of ν_{k_u} , ν_{k_s} , θ_{k_u} and θ_{k_s} , as can be seen in Figs. 4.52 and 4.53.

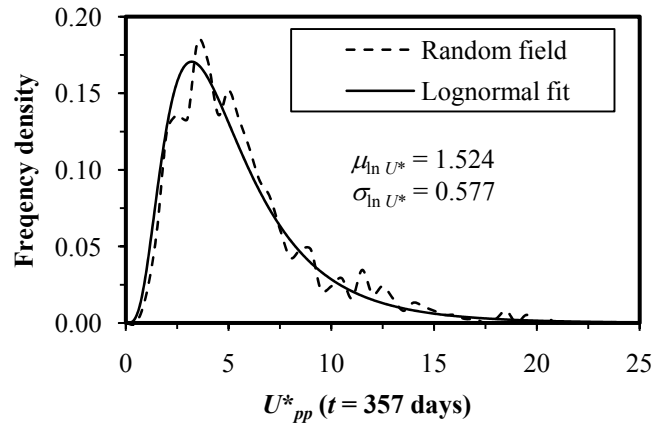


Figure 4.54: Typical example of frequency density histogram of simulated $U^*(t)$ with fitted lognormal distribution for $\nu_{k_u} = 50\%$, $\nu_{k_s} = 100\%$, $\theta_{k_u} = \theta_{k_s} = 2.0$

The overall conclusions that can be derived from all the results presented in Figs. 4.48–4.53 are that, the spatial variation of the smear zone permeability has a dominant effect on the probabilistic behaviour of soil consolidation. As discussed earlier, spatial variability in the smear zone will possibly be higher than that of the undisturbed zone. Under such circumstances, this observation has important implications in the sense that modelling soil consolidation with the same ν and θ for both the smear and undisturbed zones that are equal to the ν and θ of the smear zone does not significantly affect the final results.

4.3.1.2.1.2 Effects of variation of μ_{k_u} / μ_{k_s} and s on the mean and standard deviation of U and the probability of achieving 90% consolidation

As mentioned earlier in Chapter 2, depending on the type of drain, mandrel size, type of soil and installation procedures, the ratio of μ_{k_h} / μ_{k_s} and s can vary over several orders of magnitude. Therefore it is worthy, to investigate the effects of varying these parameters, i.e. how they impact upon the results of the spatially variable soil. In this section, ν_{k_u} and ν_{k_s} are held constant at 100% with the same θ_{k_u} and θ_{k_s} values of 1.0. The parameters μ_{k_u} / μ_{k_s} and s are varied systematically according to the values given

in Table. 4.3, and their effects on soil stabilisation by PVDs are illustrated in Figs. 4.55 and 4.56.

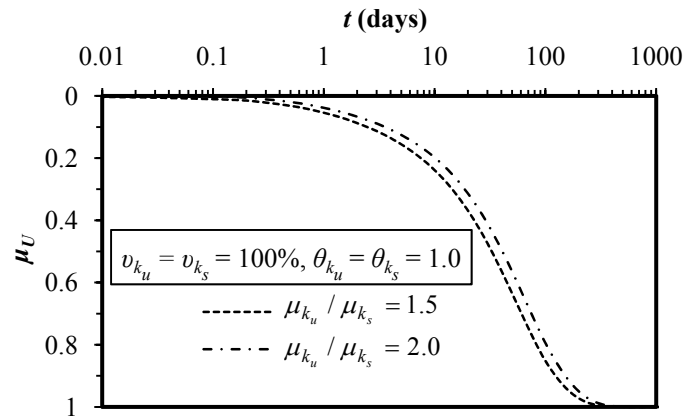
- ***Effects of variation of μ_{k_u} / μ_{k_s} on μ_U , σ_U and $P[U \geq U_{90}]$***

The influence of varying μ_{k_h} / μ_{k_s} on μ_U , σ_U and $P[U \geq U_{90}]$ is demonstrated in Fig. 4.55. Fig. 4.55(a) shows that any variation of the value of μ_{k_h} / μ_{k_s} has a considerable impact on the estimated values of μ_U . At any certain consolidation time, μ_U decreases with the increase of μ_{k_h} / μ_{k_s} . Since there is no change in v_k and θ_k , σ_U is shifted slightly to the right in the time axis with the increase of μ_{k_h} / μ_{k_s} , as shown in Fig. 4.55(b). The influence of μ_{k_h} / μ_{k_s} and $P[U \geq U_{90}]$ is illustrated in Fig. 4.55(c), which shows that, at any certain t , $P[U \geq U_{90}]$ decreases as μ_{k_h} / μ_{k_s} increases.

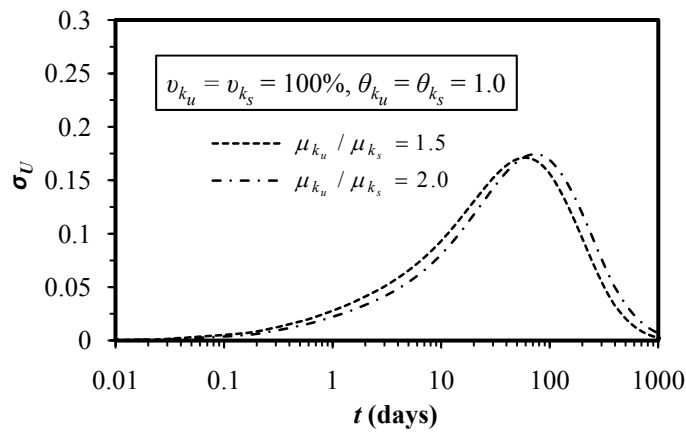
- ***Effects of variation of s on μ_U , σ_U and $P[U \geq U_{90}]$***

Fig. 4.56 highlights the effects of varying s on μ_U , σ_U and $P[U \geq U_{90}]$. The identical curves of μ_U in Fig. 4.56(a) indicate that the effect of increasing s on μ_U is marginal. Similar to the effect of μ_U , increasing s has a marginal effect on σ_U . However, at any certain time t , σ_U slightly increases with the increase of s as shown in Fig. 4.56(b).

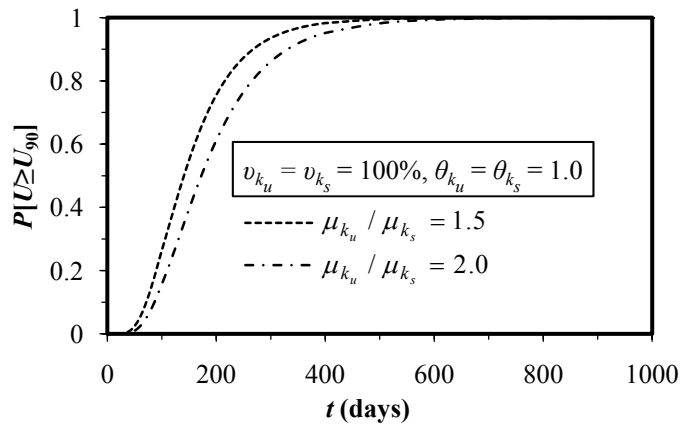
Fig. 4.56(c) investigates the effect of s on the estimated $P[U \geq U_{90}]$. Since increasing s has a minor effect on μ_U and σ_U , at any certain t , $P[U \geq U_{90}]$ slightly decreases with the increase of s . However, a comparison of Figs. 4.55(c) and 4.56(c) reveals that the effect of increasing s on $P[U \geq U_{90}]$ is not as significant as that of μ_{k_h} / μ_{k_s} . In general, the results presented in Figs. 4.55 and 4.56 imply that the determination of μ_{k_h} / μ_{k_s} should receive greater attention than that of s .



(a)

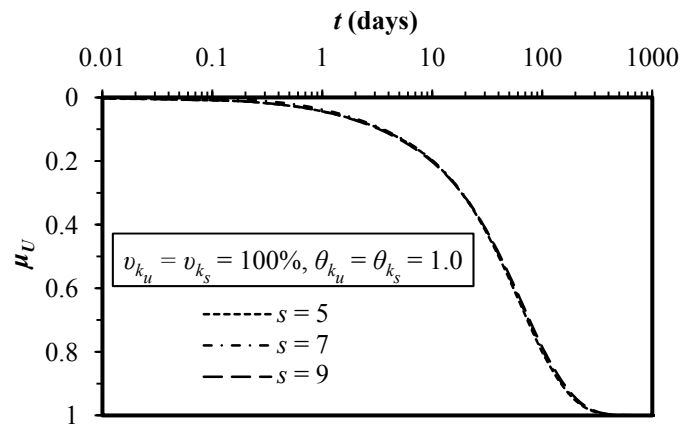


(b)

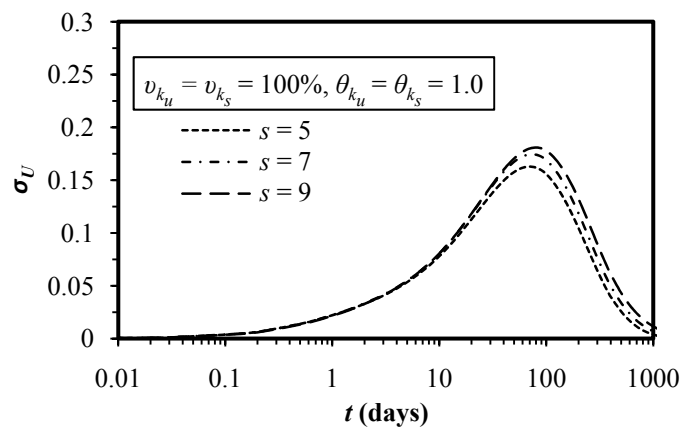


(c)

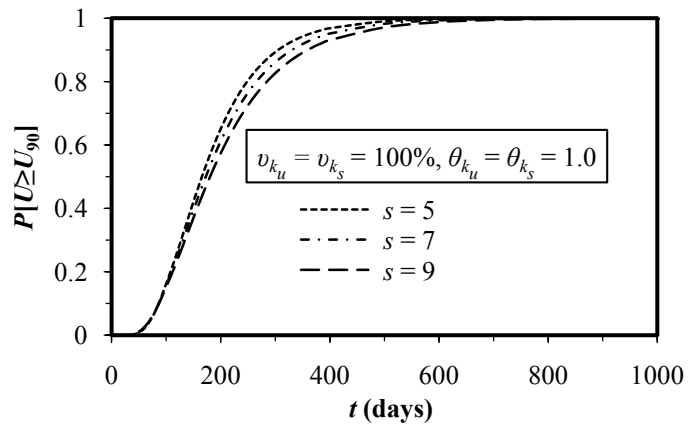
Figure 4.55: Effect of μ_{k_u} / μ_{k_s} on (a) μ_U (b) σ_U (c) $P[U \geq U_{90}]$ for $v_{k_u} = v_{k_s} = 100\%$, $\theta_{k_u} = \theta_{k_s} = 1.0$



(a)



(b)



(c)

Figure 4.56: Effect of smear ratio, s , on (a) μ_U (b) σ_U (c) $P[U \geq U_{90}]$ for $v_{k_u} = v_{k_s} = 100\%$, $\theta_{k_u} = \theta_{k_s} = 1.0$

4.3.1.3 Probabilistic analysis of soil consolidation considering both permeability and volume compressibility as random variables

As discussed in Section 2.6.3, the installation procedure of PVDs not only reduces the permeability but also increases the compressibility within the smear zone and this fact has been reported by several researchers (e.g. Arulrajah et al. 2004; Bergado et al. 2002; Saye 2001). The combined effects of reduced permeability and increased compressibility within the smear zone bring a different behaviour from that of the undisturbed soil, and the ignorance of increased compressibility in the smear zone may lead to a lack of precision in the analysis. Walker (2006) indicates that the value of the smear zone compressibility could increase by about 20% from that of the undisturbed zone, implying a 20% increase in the calculated ultimate settlement. In this section, both k and m_v are treated as random variables and stochastic analyses considering smear effect are performed. The main focus of this section is as follows:

- (d) A sensitivity analysis is performed to investigate the relative significance of the spatially variable smear zone parameters over undisturbed zone parameters.
- (e) The effect of varying undisturbed to smear zone mean compressibility ratio is investigated, using fixed values of statistical parameters of k and m_v .

In order to conduct the above mentioned investigations, random soil profiles are simulated by considering both k and m_v as random variables based on their prescribed statistical parameters, as shown in Table 4.6. Simulation of one soil profile considering both k and m_v as random variables in conjunction with smear effect involves generation of four independent random fields (two for each random variable). It should be noted that, similar to k described in Section 4.3.1.2, ν and θ of m_v are denoted $\nu_{m_{v_u}}$ and $\theta_{m_{v_u}}$, respectively, for undisturbed zone, whereas they are denoted $\nu_{m_{v_s}}$ and $\theta_{m_{v_s}}$, respectively, for the smear zone. To reflect the characteristics of natural soils, ν_{m_v} is selected so as to be one quarter of ν_k . However, the range of θ is assumed to be the same for both k and m_v . Since little is currently known about the typical COVs and SOFs for soils in the smear zone, the same range of ν and θ are selected for both smear and undisturbed zones. It is noted that no cross correlation

between k and m_v is considered and an isotropic scale of fluctuation is assumed throughout this section.

Table 4.6: Random field parameters for parametric studies

Parameter	Value
ν_k (%) (both for smear and undisturbed zone)	50, 100, 200
ν_{m_v} (%) (both for smear and undisturbed zone)	12.5, 25, 50
θ (m) (both for k and m_v , and smear and undisturbed zone)	0.125, 0.5, 2.0, 4.0

4.3.1.3.1 Results of parametric study

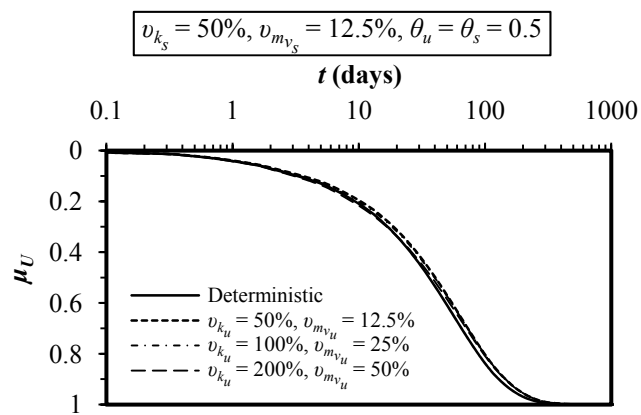
Depending on the definite objective that needs to be achieved, the input parameters $\mu_{m_{v_s}} / \mu_{m_{v_u}}$ (shown in Table 4.3); ν and θ (shown in Table 4.6) of both k and m_v are varied systematically in parametric study to investigate their influence on the estimated behaviour of soil consolidation. It is noted that the ratio of μ_{k_u} / μ_{k_s} and s are held constant at 2.0 and 7, respectively, throughout the parametric study. For each selected set of input parameters, 1000 Monte Carlo simulations are performed. The obtained consolidation responses from each individual realization are then statistically analysed to estimate μ_U , σ_U and $P[U \geq U_{90}]$.

4.3.1.3.1.1 Effect of variation of ν and θ on the mean and standard deviation of U and the probability of achieving 90% consolidation

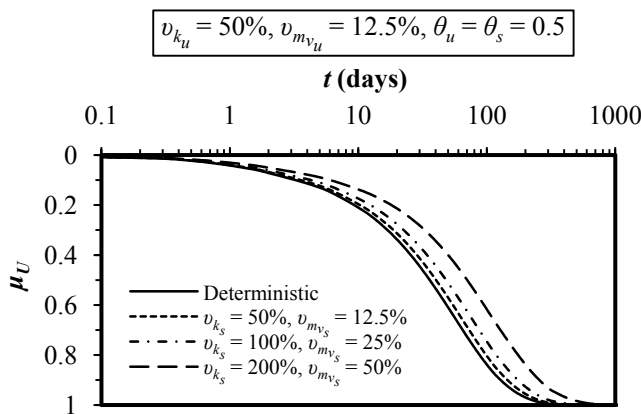
In this part of the parametric study, ν_{m_v} is chosen from Table 4.6 in such a way that it turns out to be one quarter of ν_k (i.e. $\nu_k = 4\nu_{m_v}$) and the ratio of $\mu_{m_{v_s}} / \mu_{m_{v_u}}$ is held constant at 1.25. The effect of varying ν and θ on μ_U and σ_U is illustrated in Figs. 4.57–4.60, while their effects on $P[U \geq U_{90}]$ are depicted in Figs. 4.61 and 4.62. In Figs. 4.57–4.60 and 4.61 and 4.62, μ_U , σ_U and $P[U \geq U_{90}]$ are expressed as functions of the consolidation time t .

- **Effect of variation of v and θ on the mean of U**

The effects of increasing v_u and v_s on μ_U at fixed value of $\theta_u = \theta_s = 0.5$ is examined in Fig. 4.57. In Fig. 4.57(a), it can be seen that at any consolidation time, there is a slight reduction in μ_U for spatially varied soils compared to the deterministic case. The identical curves for all cases of v_u (v_{k_s} and $v_{m_{v_s}}$ are fixed at 50% and 12.5% respectively) plotted in the figure indicate that the effect of increasing v_u on $\mu_{U(pp)}$ remains marginal.



(a)



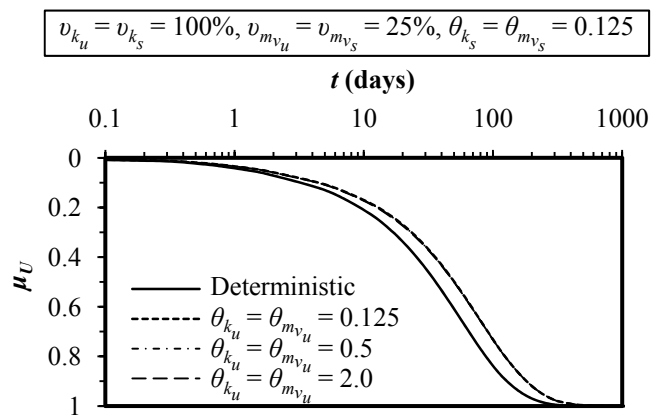
(b)

Figure 4.57: Effect of v_u and v_s on μ_U for $\theta_u = \theta_s = 0.5$

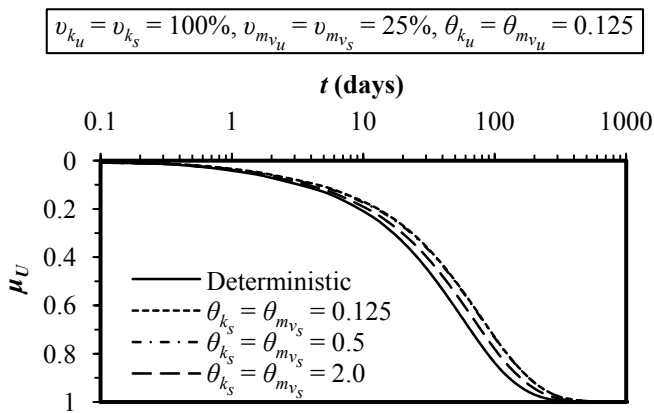
The effect of v_s on μ_U at fixed values of $v_{k_u} = 50\%$ and $v_{m_{v_u}} = 12.5\%$ is illustrated in Fig. 4.57(b), which shows that any change in v_s has a significant impact on the estimated values of μ_U . At any certain consolidation time, μ_U decreases with the increase of v_s , and the decreasing rate of μ_U consistently increases with the increase

of v_s . The comparison between Figs. 4.57(a) and (b) reveals that the effect of v_s on μ_U is dominant. It should be noted that this observation is similar to that found for the case that considered k as the only random variable.

Fig. 4.58 highlights the effects of increasing θ_u and θ_s on μ_U at fixed values of $v_{k_u} = v_{k_s} = 100\%$ and $v_{m_{v_u}} = v_{m_{v_s}} = 25\%$. Virtually, the identical curves of μ_U in Fig. 4.58(a) for all θ_u at a fixed value of $\theta_{k_s} = \theta_{m_{v_s}} = 0.125$, indicate that μ_U is more or less independent θ_u . On the other hand, in Fig. 4.58(b), it can be seen that at any certain consolidation time, μ_U increases with the increase of θ_s (θ_{k_u} and $\theta_{m_{v_u}}$ are fixed at 0.125). What this means is that the behaviour of μ_U is governed by θ_s rather than θ_u . This observation is also in agreement with that obtained for spatially variable k with smear effect.



(a)

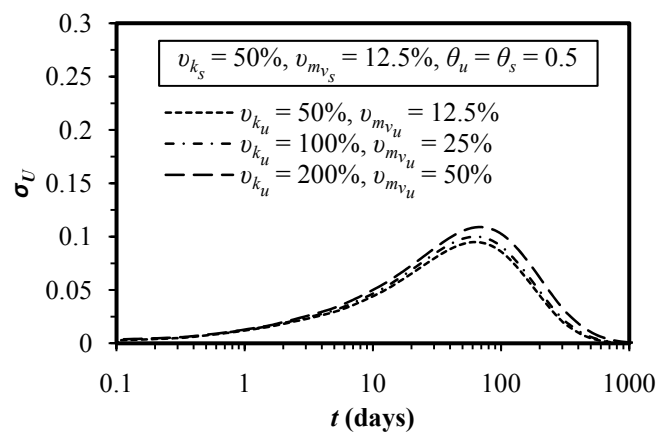


(b)

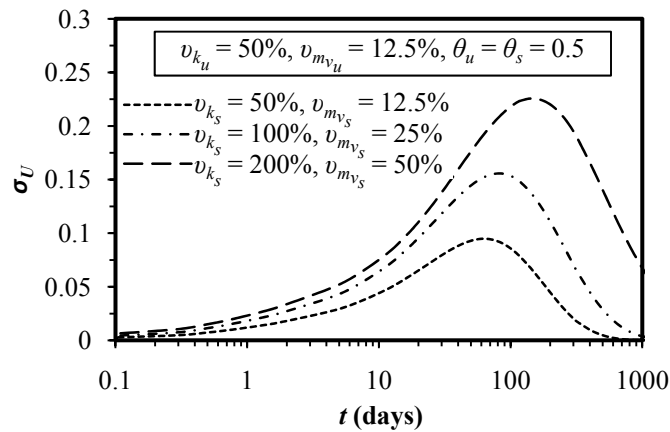
Figure 4.58: Effect of θ_u and θ_s on μ_U for $v_{k_u} = v_{k_s} = 100\%$, $v_{m_{v_u}} = v_{m_{v_s}} = 25\%$

- **Effect of variation of v and θ on the standard deviation of U**

The influence of v_u and v_s on σ_U at a fixed value of $\theta_u = \theta_s = 0.5$ is investigated in Fig. 4.59. For a fixed value of v_s (v_{k_s} and $v_{m_{v_s}}$ are, respectively, 50% and 12.5% in this case), increasing v_u has a marginal effect on σ_U , as shown in Fig. 4.59(a). Fig. 4.59(b) shows the effect of v_s on σ_U at fixed values of $v_{k_u} = 50\%$ and $v_{m_{v_u}} = 12.5\%$. It can be seen that at any certain consolidation time, σ_U increases significantly with the increase of v_s , implying the dominant effect of v_s on the estimated values of σ_U .



(a)



(b)

Figure 4.59: Effect of v_u and v_s on σ_U for $\theta_u = \theta_s = 0.5$

Fig. 4.60 illustrates the effect of varying θ_u and θ_s on σ_U at fixed values of $v_{k_u} = v_{k_s} = 100\%$ and $v_{m_{v_u}} = v_{m_{v_s}} = 25\%$. In Fig. 4.60(a), it can be seen that similar to the effect of θ_u on μ_U , σ_U remains almost identical for varying θ_u with a fixed value of $\theta_{k_s} =$

$\theta_{m_{vs}} = 0.125$. On the other hand, the estimated σ_U for different values of θ_s is plotted in Figure 4.60(b) at a fixed value of $\theta_{k_u} = \theta_{m_{vu}} = 0.125$. It can be seen that unlike θ_u , θ_s has a considerable impact on the estimated values of σ_U .

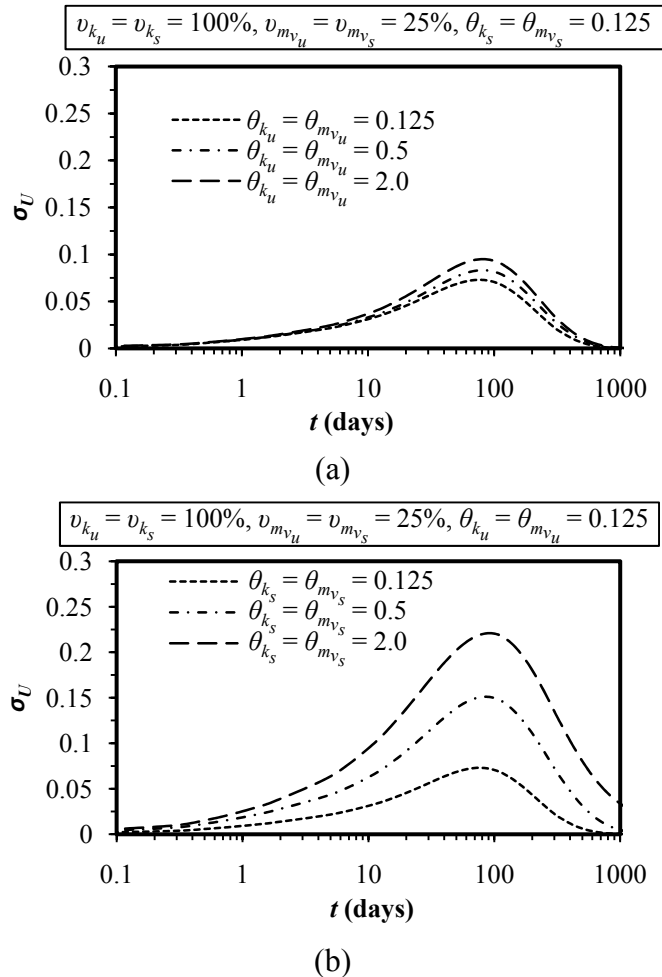


Figure 4.60: Effect of θ_u and θ_s on σ_U for $v_{k_u} = v_{k_s} = 100\%$, $v_{m_{vu}} = v_{m_{vs}} = 25\%$

- **Effect of variation of v and θ on the probability of achieving 90% consolidation**

Prior to presenting the results that investigate the effects of spatially variable of k and m_v on the probability of achieving 90% consolidation for the case considering the smear effect, the rationality of the lognormal distribution hypothesis for $U^*(t)$ is assessed by the Chi-square test. This process is performed for many combinations of v and θ at several different consolidation times. Fig. 4.63 illustrates the typical

histograms of $U^*(t)$ for the case of $\nu_{k_u} = 50\%$, $\nu_{k_s} = 100\%$, $\nu_{m_{v_u}} = 12.5\%$, $\nu_{m_{v_s}} = 25\%$, $\theta_{k_u} = \theta_{k_s} = \theta_{m_{v_u}} = \theta_{m_{v_s}} = 0.5$ at 129.3 days (note that the deterministic solution of the finite element code yields $t_{D90} = 129.3$ days for this consolidation problem, see also Table 4.4, Test no. 5) along with their fitted lognormal distributions. The goodness-of-fit test yielded p -value of 0.43, implying that the lognormal distribution hypothesis for $U^*(t)$ is valid even when both k and m_v are considered as random variables together with the smear effect.

The influence of the smear zone parameters over the undisturbed zone parameters are investigated in Figs. 4.61 and 4.62. The deterministic time of achieving 90% consolidation, t_{D90} , is also shown in the figures by vertical solid lines that give $P[U \geq U_{90}]$ at that time, for any combination of ν and θ .

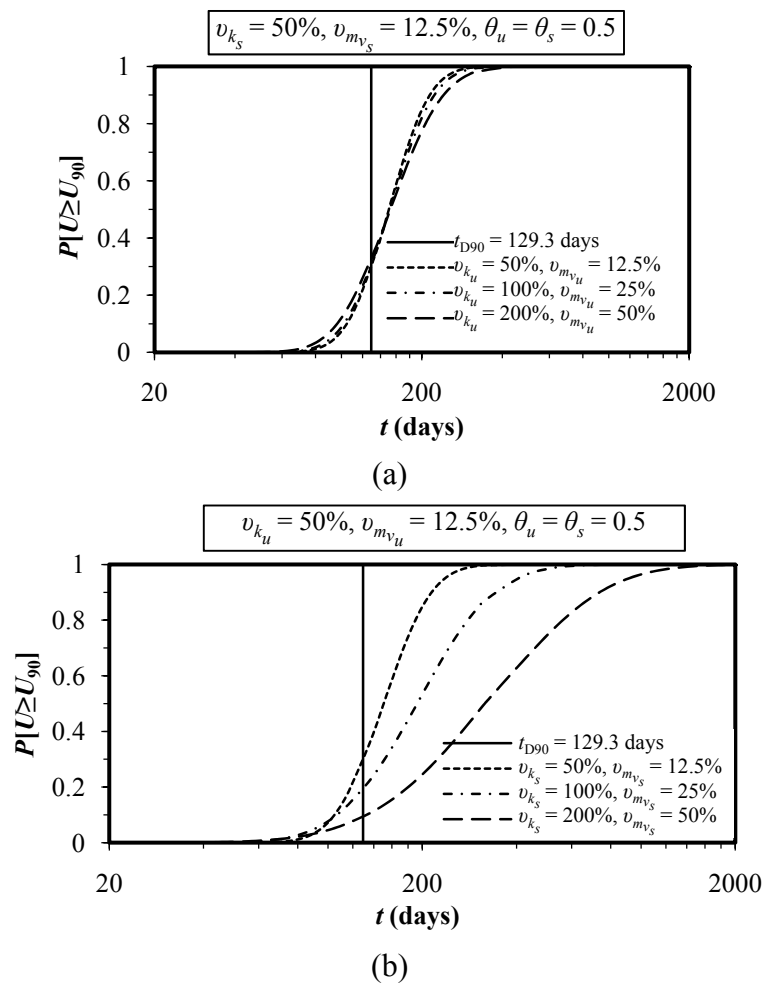
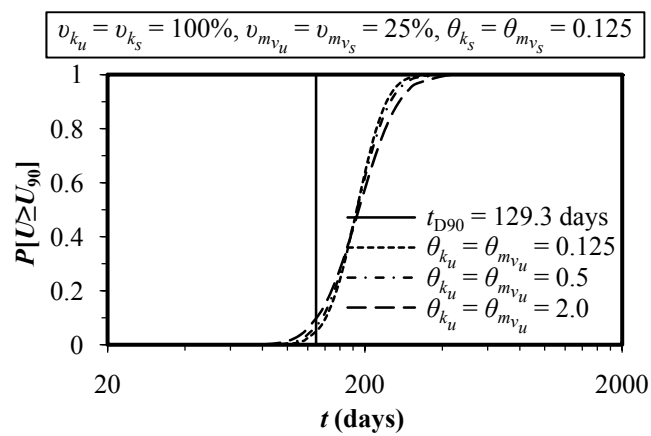
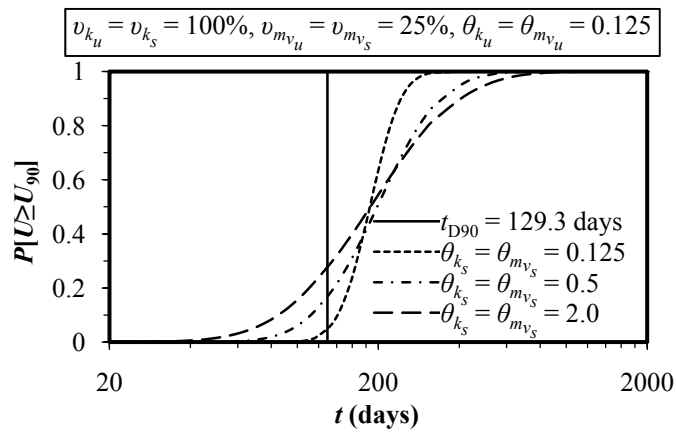


Figure 4.61: Effect of ν_u and ν_s on $P[U \geq U_{90}]$ for $\theta_u = \theta_s = 0.5$

Fig. 4.61 illustrates the effects of v_u and v_s on $P[U \geq U_{90}]$ at a fixed value of $\theta_u = \theta_s = 0.5$. It can be seen that, in general, the effect of increasing v_u (v_{k_s} and $v_{m_{v_s}}$ are fixed at 50% and 12.5%, respectively) on $P[U \geq U_{90}]$ remains marginal. The effect of v_s at fixed values of $v_{k_u} = 50\%$ and $v_{m_{v_u}} = 12.5\%$ is shown in Fig. 4.61(b), which shows that varying the values of v_s has a considerable impact on the estimated values of $P[U \geq U_{90}]$. At any certain consolidation time, $P[U \geq U_{90}]$ decreases with the increase of v_s . The overall observation that can be derived from comparing the results in Fig. 4.61 is that the effect of v_s on $P[U \geq U_{90}]$ is dominant.



(a)



(b)

**Figure 4.62: Effect of θ_u and θ_s on $P[U \geq U_{90}]$ for $v_{k_u} = v_{k_s} = 100\%$,
 $v_{m_{v_u}} = v_{m_{v_s}} = 25\%$**

Fig. 4.62 investigates the effects of θ on $P[U \geq U_{90}]$ at fixed values of $\nu_{k_u} = \nu_{k_s} = 100\%$ and $\nu_{m_{v_u}} = \nu_{m_{v_s}} = 25\%$. In Fig. 4.62(a), the influence of increasing θ_u on $P[U \geq U_{90}]$ is shown at $\theta_{k_s} = \theta_{m_{v_s}} = 0.125$, and the results yield almost identical curves indicating that varying the values of θ_u has little or no impact on the probabilistic behaviour of degree of consolidation. On the other hand, the estimated $P[U \geq U_{90}]$ for different values of θ_s is plotted in Fig. 4.62(b) at a fixed value of $\theta_{k_u} = \theta_{m_{v_u}} = 0.125$. It can be seen that unlike θ_u , θ_s has a considerable impact on the estimated values of $P[U \geq U_{90}]$. The comparison between Figs. 4.62(a) and (b) reveals that, the effect of θ_s on $P[U \geq U_{90}]$ is more significant than θ_u . It is interesting to know that the deterministic solution yields $P[U \geq U_{90}] < 50\%$ for all combinations of values of ν_u , ν_s , θ_u , and θ_s , as can be seen in Figs. 4.61 and 4.62.

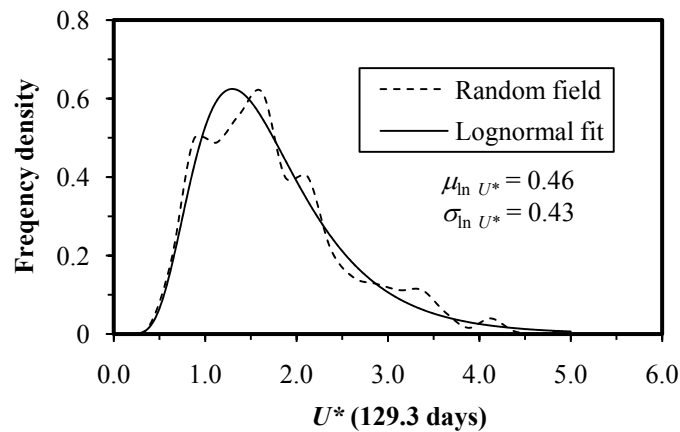


Figure 4.63: Typical example of frequency density histogram of simulated $U^*(t)$ with fitted lognormal distribution for $\nu_{k_u} = 50\%$, $\nu_{k_s} = 100\%$, $\nu_{m_{v_u}} = 12.5\%$,

$$\nu_{m_{v_s}} = 25\%, \theta_{k_u} = \theta_{k_s} = \theta_{m_{v_u}} = \theta_{m_{v_s}} = 0.5 \text{ at } 129.3 \text{ days}$$

The effects of ν and θ of the undisturbed and smear zones for both k and m_v on the estimated mean and standard deviation of the degree of consolidation and the probability of achieving 90% consolidation are found to follow the same trends as ν and θ of the undisturbed and smear zones for k alone. That is, in comparison ν and θ of the smear zone have a dominant effect on the probabilistic behaviour of soil consolidation even when both k and m_v are considered to be spatially random. This

observation reinforces the conclusion made earlier for the spatially variable k and spatially constant m_v together with the smear effect. That is, modelling soil consolidation with the same ν and θ for both zones (smear and undisturbed zones) that are equal to the ν and θ of the smear zone (i.e. ν_s and θ_s) does not significantly affect the final results.

4.3.1.3.1.2 Effects of variation of $\mu_{m_{v_s}} / \mu_{m_{v_u}}$ on the mean and standard deviation of U and the probability of achieving 90% consolidation

Similar to the ratio of μ_{k_h} / μ_{k_s} , the ratio of $\mu_{m_{v_s}} / \mu_{m_{v_u}}$ is also an uncertain parameter. The variation in $\mu_{m_{v_s}} / \mu_{m_{v_u}}$ depends on the type of drain, mandrel size, type of soil and installation procedures. Therefore, it is worthy to investigate the effects of varying this parameter, i.e. how it impacts upon the results of the spatially variable soil. To understand the effect of $\mu_{m_{v_s}} / \mu_{m_{v_u}}$, in this section, all the spatial variability parameters in the smear zone as well as in the undisturbed zone for both k and m_v are held at fixed values. The values of ν_{k_u} , $\nu_{m_{v_u}}$, ν_{k_s} and $\nu_{m_{v_s}}$ are held constant at 100%, while θ_{k_u} , $\theta_{m_{v_u}}$, θ_{k_s} and $\theta_{m_{v_s}}$ are held at a fixed value of 1.0. The parameter $\mu_{m_{v_s}} / \mu_{m_{v_u}}$ is varied systematically according to the values given in Table. 4.3, and its effects on soil stabilisation by PVDs are illustrated in Fig. 4.64.

- **Effects of variation of μ_{k_u} / μ_{k_s} on μ_U , σ_U and $P[U \geq U_{90}]$**

The influence of varying μ_{k_h} / μ_{k_s} on μ_U , σ_U and $P[U \geq U_{90}]$ is demonstrated in Figure 4.64. It can be seen that the varying values of μ_{k_h} / μ_{k_s} have little or no effect on μ_U , σ_U and $P[U \geq U_{90}]$. The comparison between Fig. 4.64 and Fig. 4.55 reveals that lower mean of permeability in the smear zone significantly affects the rate of soil consolidation and in contrast, an increased mean of compressibility in the smear zone does not largely affect soil consolidation. This result justifies the reason why the smear zone is traditionally described with reference to permeability changes alone, and the effect of compressibility changes is neglected.

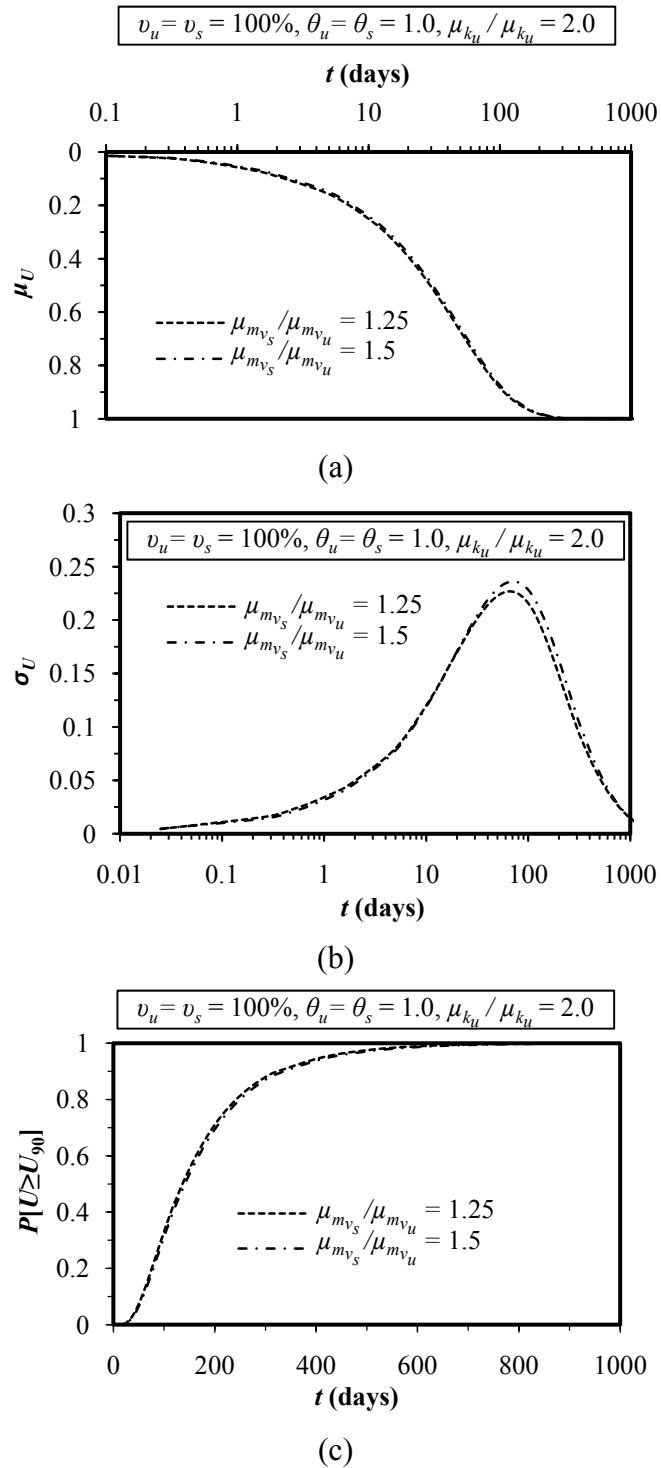


Figure 4.64: Effect of $\mu_{m_{v_s}} / \mu_{m_{v_u}}$ on (a) μ_U (b) σ_U (c) $P[U \geq U_{90}]$ for $v_u = v_s = 100\%$, $\theta_u = \theta_s = 1.0$ ($\mu_{k_h} / \mu_{k_s} = 2.0$)

4.4 Summary and Conclusions

The Random Field Theory and Finite Element Method were combined in a Monte Carlo framework to investigate the influence of soil spatial variability on soil stabilisation by prefabricated vertical drains (PVDs). The review of relevant literature indicate that, of all soil properties, soil permeability, k , and volume compressibility, m_v , have the most significant impact on soil consolidation by PVDs. Accordingly, k and m_v were modelled as random variables in the current study. The variability of both k and m_v was characterised by assuming that they follow a lognormal distribution. Parametric studies, based on the Monte Carlo simulation method, were conducted to investigate and quantify the effects of varying both the coefficient of variation, v , and scale of fluctuation, θ , with regard to their impacts on the mean, μ_U , standard deviation, σ_U , of the degree of soil consolidation and also on the probability of achieving 90% consolidation (i.e. $P[U \geq U_{90}]$), under various different conditions and situations. All numerical studies carried out in this chapter were divided into two parts. In the first part (described in Section 4.2), the smear effect was not considered, while the aspect of considering the smear effect was investigated in the second part (described in Section 4.3).

Section 4.2.1.2 described the results obtained from the no smear case with permeability as the only random variable. In this section, parametric studies were performed to investigate the sensitivity of statistics of the degree of consolidation and the probability of achieving 90% consolidation over a wide range v_k and θ_k . The effect of anisotropic θ_k over isotropic θ_k on the probabilistic behaviour of soil consolidation was investigated and discussed. At the end of this section, equivalent plane strain analyses to the axisymmetric analyses were conducted to make a matching comparison between the stochastic solutions obtained from these two conditions. The results of the sensitivity analysis indicated that both v_k and θ_k have a significant impact on the estimated μ_U , σ_U and $P[U \geq U_{90}]$. The conclusions are summarised as follows:

- When k was the only random variable and m_v was constant across the soil mass, the mean and standard deviation of the degree of consolidation defined by the

excess pore water pressure were identical with those defined by settlement. This result agrees with the observations made by Lee et al. (1992);

- The mean and standard deviation of the degree of consolidation were highly sensitive to the soil permeability variance. Increasing the permeability variance decreased the mean of the degree of consolidation but increased its standard deviation;
- The mean and standard deviation of the degree of consolidation were relatively less sensitive to the scale of fluctuation. Increasing the scale of fluctuation generally increased the mean and standard deviation of the degree of consolidation. However, for a scale of fluctuation $\theta_k \geq 2.0$, the influence of the scale of fluctuation on the mean and standard deviation of the degree of consolidation was marginal, particularly for a permeability variance $v_k \leq 25\%$;
- The interpretation of the results from the viewpoint of the reliability analysis indicated that the probability of achieving 90% consolidation at a consolidation time corresponding to the deterministically predicted 90% consolidation time always less than 50% over the range of the statistical parameters considered. This implies a risk of more than 50% for the deterministic prediction based on a single mean value of soil permeability coefficient;
- At a certain consolidation time, the probability of achieving 90% consolidation decreased with the increase of soil permeability variance, as expected. The probability of achieving 90% consolidation became independent of θ_k at a probability level of around 50%. Above 50% probability level and at a certain consolidation time, the probability of achieving 90% consolidation decreased as θ_k increases, and the role of θ_k was to have the opposite effect below this level. Moreover, the probability of achieving 90% consolidation became insensitive for $\theta_k \geq 2.0$;
- When θ_k became vanishingly small, the sharp increase in the probability of achieving 90% consolidation with respect to consolidation time suggested that the predicted mean degree of consolidation moved towards the true mean degree of consolidation, thus, the probability of achieving a desired degree of consolidation approached 100%.

Investigation into the effect of anisotropic θ_k over isotropic θ_k led to the following findings:

- An isotropic solution underestimated the mean degree of consolidation and this underestimation was marginal when the degree of anisotropy, ζ , was as low as 4.0. The amount by which isotropic assumption underestimated the mean degree of consolidation decreased with the decrease in both ζ and v_k . The effect of degree of anisotropy on the mean degree of consolidation was insignificant even for a high degree of anisotropy (e.g. $\zeta = 32$) when the coefficient of variation of soil permeability was as low as 50%;
- Anisotropic solutions always gave higher values of the standard deviation of the degree of consolidation than isotropic solutions. The difference in the standard deviation of the degree of consolidation obtained from anisotropic and isotropic conditions decreased with the decrease in both ζ and v_k . In other words, the difference in the standard deviation of the degree of consolidation obtained from anisotropic and isotropic conditions increased with the increase of both ζ and v_k ;
- The isotropic assumption always provided a conservative estimation of the probability of achieving 90% consolidation compared to the more realistic anisotropic condition, regardless of the degree of spatial variation. This result has a potential practical implication in the sense that the more realistic anisotropic condition will ensure improved economy in the reliability-based design of soil consolidation via PVDs. This was particularly so when the coefficient of variation of soil permeability was as high as 200% and the degree of anisotropy was as high as 32. However, it should be noted that this conclusion was true for almost all probability (confidence) levels but the difference between the isotropic and anisotropic solutions became less pronounced for high probability levels close to unity (i.e. at $P[U \geq U_{90}] \approx 95\sim 100\%$).

The comparison between the axisymmetric and equivalent plane strain analyses was assessed in terms of the statistical moments of the degree of consolidation and the probability of achieving a target degree of consolidation. This study yielded the following conclusions:

- The estimated values of the mean and standard deviation of the degree of consolidation derived from the equivalent plane strain analysis were slightly lower than those obtained from the axisymmetric solution, for $v_k \geq 100\%$;
- In general, the effect of the scale of fluctuation on the mean and standard deviation of the degree of consolidation was marginal from the matching point of view and both solutions gave almost identical results. However, for a any $v_k \geq 100\%$ and at any certain t , the plane strain solution gave slightly lower values of the mean and standard deviation of the degree of consolidation compared to the axisymmetric analysis irrespective of the values of θ_k ;
- The equivalent plane strain analysis gave lower values for the probability of achieving 90% consolidation compared to the axisymmetric solution, for all cases of v_k when $\theta_k \leq 1.0$. For any $\theta_k \geq 2.0$, the probabilities of achieving 90% consolidation obtained from axisymmetric and plane strain solutions were identical for all values of v_k ;
- In general, the equivalent plane strain analysis gave slightly lower values for the probability of achieving 90% consolidation than the axisymmetric solution, for all θ_k . However, the discrepancy between the plane strain and axisymmetric solutions became more significant for erratic soils (i.e. θ_k is small and v_k is large). For a large scale of fluctuation (e.g. $\theta_k \geq 2.0$), both axisymmetric and equivalent plane strain analyses gave almost identical probabilities of achieving 90% consolidation. This observation suggested that closely matching probabilities can only be found when the soil is homogeneous;
- The overall conclusion that can be derived from this section is that, the equivalent plane strain analysis always provided lower values of the mean and standard deviation of the degree of consolidation, and a lower probability of achieving a target degree of consolidation than the axisymmetric solution, regardless of the values of the statistical parameters. Satisfactory matching in terms of the probability of achieving a target degree of consolidation can only be obtained when the consolidated soil mass is more or less homogeneous (i.e. when θ_k is large). For erratic soils (i.e. when θ_k is small), the derived probability from the plane strain analysis is expected to be relatively lower than that of the axisymmetric solution.

Section 4.2.1.3 described the results obtained from the no-smear case with both permeability and volume compressibility as random variables. The sensitivity of statistics of the degree of consolidation and probability of achieving 90% consolidation with respect to the spatially variable k and m_v was examined over a range of parametric variations. The sensitivity analysis was divided into two parts. In the first part, the COV of both k and m_v was assumed to be the same, whereas in the second part, the COV of m_v was chosen in such a way that it constituted one quarter of the COV of k (i.e. $\nu_{m_v} = 0.25 \nu_k$). No cross correlation between k and m_v was considered for each part of the sensitivity analysis. Following the sensitivity analysis, the differences between the degree of consolidation defined by the excess pore water pressure and settlement were investigated in a probabilistic frame work. Finally, the influence of cross correlation between k and m_v on soil consolidation was investigated. The results obtained from the study carried out in this section led to the following findings:

- When ν_{m_v} was assumed to be the same as ν_k (i.e. $\nu_{m_v} = \nu_k$), increasing the input ν increased the mean of the degree of consolidation and this observation was opposite to that found for the case with $\nu_{m_v} = 0.25 \nu_k$ and also for the case where permeability was considered as the only random variable. The standard deviation of the degree of consolidation also increased with the increase of coefficient of variation for both cases of $\nu_{m_v} = \nu_k$ and $\nu_{m_v} = 0.25 \nu_k$. Similar trend in the standard deviation of the degree of consolidation was also found for increasing ν_k with spatially constant m_v ;
- Increasing the scale of fluctuation increased the mean and standard deviation of the degree of consolidation either for $\nu_{m_v} = \nu_k$ and $\nu_{m_v} = 0.25 \nu_k$. The spatial correlation length has little influence on the mean of the degree of consolidation when $\nu \leq 25\%$. A similar observation was also made in the case of random permeability;
- The behaviour of the probability of achieving 90% consolidation with respect to varying ν and θ of permeability and volume compressibility, for both cases with $\nu_{m_v} = \nu_k$ and $\nu_{m_v} = 0.25 \nu_k$, was similar to that of ν and θ of permeability alone. The probability of achieving 90% consolidation at a consolidation time corresponding to the deterministically predicted 90% consolidation time was

found to be always be less than 50% over the range of the statistical parameters considered. At a certain consolidation time, the probability of achieving 90% consolidation decreased with the increase in v of k and m_v , as expected. The probability of achieving 90% consolidation became independent of θ at a probability level of around 50%. Above the 50% probability level and at a certain consolidation time, the probability of achieving 90% consolidation decreased as θ increases and the role of θ had the opposite effect below this level;

- The mean and standard deviation of the degree of consolidation and the probability of achieving 90% consolidation defined by the excess pore water pressure and settlement was different only when the COV of volume compressibility was as high as 200% and when k and m_v were uncorrelated. The mean of the degree of consolidation and the probability of achieving 90% consolidation defined by the excess pore water pressure and settlement were almost identical when k and m_v are perfectly positively correlated;
- The mean and standard deviation of the degree of consolidation and the probability of achieving 90% consolidation were highly sensitive to uncorrelated k and m_v rather than positively correlated k and m_v . An uncorrelated k and m_v were more likely to give a higher mean and standard deviation of the degree of consolidation than a correlated k and m_v . The probability of achieving 90% consolidation followed an opposite trend before and after the probability level of 50% for both v and θ , irrespective of the level of cross-correlation between k and m_v . However, at any certain consolidation time, the estimated probability of achieving 90% consolidation with an correlated k and m_v was found to be always higher than that computed with the uncorrelated k and m_v when the probability of achieving 90% consolidation $\leq 50\%$, whereas an opposite trend to this behaviour was observed when the probability of achieving 90% consolidation was $\geq 50\%$.

The results obtained by considering the smear effect together with random permeability and constant compressibility were discussed in Sections 4.3.1.2. Initially a parametric study was performed to investigate the relative significance of the spatially variable smear permeability over undisturbed permeability. The effects of varying the ratio of the undisturbed zone mean permeability to the smear zone mean permeability, and the effects of varying the smear zone ratio on the behaviour

of soil consolidation were then investigated using the same statistical parameters of k . The specific conclusions derived from this study can be summarized as follows:

- The effect of ν and θ of the undisturbed zone permeability on the estimated mean and standard deviation of the degree of consolidation and probability of achieving 90% consolidation was found to remain marginal. On the other hand, the estimated mean and standard deviation of the degree of consolidation and the probability of achieving 90% consolidation were highly sensitive to ν and θ of the smear zone permeability. This result indicates that the probabilistic behaviour of soil consolidation is governed by the spatial variation of the smear zone permeability. Since the spatial variability of the smear zone will possibly be higher than that of the undisturbed zone, this observation has important implications in the sense that, modelling soil consolidation with the same ν and θ for both zones that are equal to the ν and θ of the smear zone does not significantly affect the final results.
- Increasing the mean permeability ratio of the undisturbed zone to smear zone was found to have a considerable impact on the stochastic behaviour of soil consolidation. On the other hand, increasing the smear zone ratio was found to have a marginal effect on the mean and standard deviation of the degree of consolidation and in turn on the probability of achieving 90% consolidation. This observation reveals that the effect of increasing the smear zone ratio on soil consolidation is not as significant as that of the mean permeability ratio of the undisturbed zone to the smear zone.

The results obtained by considering smear the effect together with both the permeability and volume compressibility as random variable were discussed in Sections 4.3.1.3. Initially a sensitivity analysis was performed to investigate the relative significance of the spatially variable smear zone parameters over the undisturbed zone parameters. The effect of varying the mean compressibility ratio of the undisturbed zone to the smear zone on the behaviour of soil consolidation was then investigated using fixed values of statistical parameters of k and m_v . This study yielded the following conclusions:

- The effects of v and θ of both the undisturbed and smear zones k and m_v on the estimated mean and standard deviation of the degree of consolidation and probability of achieving 90% consolidation were found to follow the same trends as those of v and θ of the undisturbed and smear zones k alone, respectively. In comparison to v and θ of the undisturbed zone, v and θ of the smear zone had a dominant effect on the probabilistic behaviour of soil consolidation even when both k and m_v were considered to be spatially random. This observation reinforces the conclusion made earlier for the spatially variable k and spatially constant m_v together with smear effect. That is, modelling soil consolidation with the same v and θ for both zones (smear and undisturbed zones) that are equal to v and θ of the smear zone does not significantly affect the final results.
- Increasing the mean compressibility ratio of the undisturbed zone to the smear zone had little or no impact on the stochastic behaviour of soil consolidation. This observation reveals that an increased mean compressibility in the smear zone does not largely affect the rate of soil consolidation.

In the following chapter, an approximate, easy to use reliability-based semi-analytical (RBSA) model for estimating the probability of achieving a target degree of consolidation will be developed and verified against the computationally intensive finite element Monte Carlo (FEMC) results.

Chapter 5

Reliability-Based Semi-Analytical Model for Soil Consolidation by Vertical Drains

5.1 Introduction

As mentioned in Chapter 2, in recent years, the use of the reliability-based design (RBD) methods that consider the uncertainty associated with soil spatial variability has been widely accepted by many geotechnical engineering codes around the world, e.g. Eurocode 7 and Australian Standards AS 4678. Although Zhou et al. (1999) presented a probabilistic design method of PVDs for soil stabilization considering the uncertainty in the coefficient of horizontal (radial) consolidation due to measurement errors, no solution (either in the form of equations or charts) has considered soil spatial variability. Therefore, there is a need for developing such a probabilistic design method. The reliability-based numerical computational schemes presented in Chapter 3 require a large number of simulations that are computationally intensive and time consuming. In this chapter, a simplified reliability-based semi-analytical (RBSA) model is developed for soil consolidation by PVDs considering spatial variations of both k and m_v . Special subroutine (code) that is written in ForTRAN is also developed to facilitate the use of the developed RBSA model in a routine design practice. The model is verified against the results of the finite-element Monte-Carlo (FEMC) analyses over the range of observed or suggested values of input statistical parameters of the random soil properties found in the literature. In the sections that follow, the detailed description of the RBSA model is demonstrated first, then the comparison between the FEMC approach and proposed RBSA model is presented and discussed.

5.2 Reliability-Based Semi-Analytical Model

As indicated earlier, the FEMC analyses are computationally intensive and time consuming. Accordingly, it is not uncommon that practicing engineers have neither the time nor the resources to perform full scale FEMC simulations of soil consolidation by PVDs with spatially random soil properties. In an effort to remedy

this situation, an approximate, easy to use RBSA model is developed from which direct estimates of the probability of achieving a certain degree of consolidation at a given consolidation time can be readily obtained. The estimation of such probability requires a performance function or a theoretical (deterministic) model. As mentioned in Chapter 3, consolidation of soil by PVDs can take place by simultaneous vertical and horizontal (radial) drainage of water. However, as the drainage length in the vertical direction is significantly higher than that of the horizontal direction and permeability in the horizontal direction is often much higher than that of the vertical direction (Hansbo 1981), soil consolidation due to vertical drainage is much less than that of the horizontal drainage and may be neglected without considerable reduction in the accuracy of predicted consolidation. Consequently, in the current study, only soil consolidation due to horizontal drainage is considered in the RBSA method (note that no vertical drainage is also permitted for the FEMC analyses presented in the previous chapter). The commonly used analytical solution for horizontal (radial) consolidation proposed by Hansbo (1981), which is given in Eq. 2.12 is used in this study as the performance function for the RBSA model. It should be noted that in principle, both the horizontal and vertical permeability coefficients may be modelled as random variables. However, since the permeability variance of even one of the direction is rarely known with any accuracy, the usual assumption is that the permeability is isotropic. Under such assumption and using the definition of $U^*(t)$ given in Section 3.3 (see Eq. 3.34), Eq. 2.12 can be written as:

$$U^*(t) = \frac{2t}{r_e^2 \gamma_w} \frac{k}{m_v \alpha} \quad (5.1)$$

The above conversion of Eq. 2.12 to Eq. 5.1 is necessary as it simplifies the process of obtaining a closed form solution for the mean and variance of the degree of consolidation function $U^*(t)$ directly from the statistically defined input data relating to k and m_v .

The reliability-based problem requires determination of a reasonable probability distribution of $U^*(t)$. Once determined, the statistical parameters (i.e. mean and variance) of the distribution of $U^*(t)$ are estimated. With regard to this, simple semi-analytical relationships are derived to assist the designer in estimating the statistical

parameters of the distribution of $U^*(t)$ directly from the random field parameters. The approach involves considering an approximate model where the geometric averages, \bar{k} and \bar{m}_v , of k and m_v , respectively, over the influence zone surrounding the PVD are used in Eq. 5.1. The geometric average is used due to the fact that it represents a “natural” average of the lognormal distribution. Moreover, the behaviour of soil consolidation by PVDs is dominated by the low coefficient of consolidation values at the vicinity of the PVD, which is in accordance with Fenton and Griffiths (2008) that the geometric averaging is appropriate if the behaviour of a geotechnical system is dominated by low values of soil properties. If the consolidating soil domain surrounding the PVD is termed D and discretized into an assembly of non-overlapping rectangular (or square) elements, \bar{k} and \bar{m}_v over D can then be approximated with reference to Eq. 3.18 as follows:

$$\bar{k} = \left[\prod_{i=1}^m k_i \right]^{1/m} = \exp \left[\frac{1}{m} \sum_{i=1}^m \ln k_i \right] = \exp(\mu_{\ln k} + \sigma_{\ln k} \bar{G}_k) \quad (5.2)$$

$$\bar{m}_v = \left[\prod_{i=1}^m m_{v_i} \right]^{1/m} = \exp \left[\frac{1}{m} \sum_{i=1}^m \ln m_{v_i} \right] = \exp(\mu_{\ln m_v} + \sigma_{\ln m_v} \bar{G}_{m_v}) \quad (5.3)$$

where: $i = 1, 2, \dots, m$ represents the element number and \bar{G}_k and \bar{G}_{m_v} are the arithmetic averages of $G_k(i)$ and $G_{m_v}(i)$, respectively, over the domain D . It should be noted that no cross-correlation between k and m_v is considered in the development of the RBSA model. Therefore, $G_k(i)$ and $G_{m_v}(i)$ are, respectively, the two independent standard normal random fields for the specified scales of fluctuation of permeability and volume compressibility. It should also be noted that k_i and m_{v_i} are assumed to be constant within each element. Before finding the distribution and statistical parameters (i.e. mean and variance) of $U^*(t)$, a brief discussion in regards to the underlying equivalent normally distributed mean and variance of a lognormally distributed soil property X (i.e. $\mu_{\ln \bar{X}}$ and $\sigma_{\ln \bar{X}}^2$) is essential, as follows.

The input parameters relating to the random fields are assumed to be defined at the point level. However, soil properties are rarely measured at a point, and most

engineering measurements concerned with soil properties are performed on samples of some finite volume. Therefore, measured soil properties are actually a local average over the sample volume. In order to obtain the true point statistics, the locally averaged properties (measured) need to be corrected by taking into account the sample size. If the point distribution of the soil property of interest is normally distributed, the local averaging process will lead to a reduction in the point variance but the mean will not be affected. For the lognormal distribution, however, both the mean and standard deviation will be reduced by the local averaging. This is because the mean of a lognormal distribution depends on both the mean and variance of the underlying normal distribution. Based on the above discussion, the mean of the underlying equivalent log-soil property field ($\ln X$), $\mu_{\ln \bar{X}}$, which is unaltered by the local averaging can be given by:

$$\mu_{\ln \bar{X}} = \mu_{\ln X} \quad (5.4)$$

Using Eqs. 3.2 and 3.3, $\mu_{\ln \bar{X}}$ can be expressed in terms of the input statistics of X , as follows:

$$\mu_{\ln \bar{X}} = \mu_{\ln X} = \ln \mu_X - \frac{1}{2} \ln(1 + v_X^2) \quad (5.5)$$

According to the local averaging theory (Vanmarcke 1984), the variance, $\sigma_{\ln \bar{X}}^2$, which is affected by the local averaging is given by:

$$\sigma_{\ln \bar{X}}^2 = \gamma(D) \sigma_{\ln X}^2 \quad (5.6)$$

where: $\gamma(D)$ is the “variance function” that defines the amount by which the variance is reduced as a result of the local (arithmetic) averaging over the domain D and is a function of the size of the averaging domain and correlation function. The detailed calculation procedure of the variance reduction factor from the correlation function can be found in the Appendix A. It should be noted that the 3D variance reduction function is also presented in Appendix A, along with the 2D variance reduction function due to the fact that the proposed RBSA model can readily be used for the

3D spatial variation only by calculating $\gamma(D)$ through 3D variance reduction function. However, since both k and m_v fields are being modelled by a 2D random field and the FEMC results are obtained by 2D FEM analysis, $\gamma(D)$ in this study is calculated using the 2D variance reduction function.

By substituting Eq. 3.3 into Eq. 5.6, $\sigma_{\ln \bar{X}}^2$ can be expressed in terms of the prescribed statistics of X , as follows:

$$\sigma_{\ln \bar{X}}^2 = \gamma(D) \ln(1 + \nu_X^2) \quad (5.7)$$

The RBSA model developed in this chapter is divided into two groups. In the first group, both k and m_v are considered as random variables, while only k is considered as random variable in the second group. For each group, three RBSA models are developed that comply with the cases of considering smear effect, no smear effect and special case of considering smear effect. Each RBSA model is described in detail below. All the RBSA models developed in this study, under various assumed ground conditions are summarized in Table 5.1. Special computer programs written in ForTRAN are developed for the RBSA models in order to facilitate the use of the models, and the code of these programs is given in Appendix B.

Table 5.1: Summary of the developed RBSA models

Group No.	Spatially Variable Soil Properties	Ground Conditions	Abbreviated Name of the RBSA Model
Group 1	k and m_v	Case1: Smear effect	G1C1
		Case1: No smear effect	G1C2
		Case1: Special case with smear effect	G1C3
Group 2	k	Case1: Smear effect	G2C1
		Case1: No smear effect	G2C2
		Case1: Special case with smear effect	G2C3

G1C1: RBSA model considering smear effect (both k and m_v are random)

In this case of RBSA, both k and m_v are considered as spatially variable in the smear zone as well as in the undisturbed zone. However, α parameter in Eq. 5.1 proposed by Hansbo (1981) disregards the increased compressibility in the smear zone. Therefore, the parameter, α_{m_v} , proposed by Walker (2006) for taking into account the increased m_v in the smear zone (see Eq. 2.27) is included in Eq. 5.1. As the smear effect is considered, permeability and compressibility of the undisturbed zone (e.g. k and m_v in Eq. 5.1) are simply denoted as k_u and m_{v_u} to explicitly represent the undisturbed zone permeability and compressibility, respectively. Using the values of \bar{k} and \bar{m}_v instead of k and m_v , Eq. 5.1 becomes:

$$U^*(t) = C \frac{\bar{k}_u}{\bar{m}_{v_u} \bar{\alpha} \alpha_{m_v}} \quad (5.8)$$

where:

$$C = \frac{2t}{r_e^2 \gamma_w} \quad (5.9)$$

$\bar{\alpha}$ and $\bar{\alpha}_{m_v}$ are, respectively, the equivalent α and α_{m_v} parameters of the spatially variable soil and can be expressed as follows:

$$\bar{\alpha} = \ln\left(\frac{n}{s}\right) - \frac{3}{4} + \frac{\bar{k}_u}{\bar{k}_s} \ln(s) + F_r' \quad (5.10)$$

and

$$\bar{\alpha}_{m_v} = \frac{n^2 - s^2}{n^2 - 1} + \frac{s^2 - 1}{n^2 - 1} \frac{\bar{m}_{v_s}}{\bar{m}_{v_u}} \quad (5.11)$$

where: \bar{k}_u and \bar{k}_s are, respectively, the geometric average of permeability for the undisturbed and smear zones; \bar{m}_{v_u} and \bar{m}_{v_s} are, respectively, the geometric average of compressibility for the undisturbed and smear zones. Since the random variation of well resistance effect is not considered in this study, F'_r in Eq. 5.10, representing the average well resistance effect over the entire drain length, can be estimated as follows (Rixner et al. 1986):

$$F'_r = \frac{2\pi L^2}{3} \frac{\mu_{k_u}}{q_w} \quad (5.12)$$

Assuming that: $\ln\left(\frac{n}{s}\right) - \frac{3}{4} + F'_r = a$; $\ln(s) = b$ and $\frac{\bar{k}_u}{\bar{k}_s} = W$, Eq. 5.10 becomes:

$$\bar{\alpha} = a + bW \quad (5.13)$$

Again assuming that: $\frac{n^2 - s^2}{n^2 - 1} = g$; $\frac{s^2 - 1}{n^2 - 1} = h$ and $\frac{\bar{m}_{v_s}}{\bar{m}_{v_u}} = V$, Eq. 5.11 becomes:

$$\bar{\alpha}_{m_v} = g + hV \quad (5.14)$$

Now a reasonable distribution for $U^*(t)$ can be found. Since k_u , k_s , m_{v_u} and m_{v_s} are lognormally distributed, \bar{k}_u , \bar{k}_s , \bar{m}_{v_u} and \bar{m}_{v_s} are also lognormally distributed (by the central limit theorem geometric average of a random variable tends to have a lognormal distribution). Therefore, $\bar{\alpha}$, $\bar{\alpha}_{m_v}$ and in turn $U^*(t)$ will also be at least approximately lognormally distributed. It should be noted that, in Section 3.3, $U^*(t)$ is assumed to be lognormally distributed. The legitimacy of the lognormal distribution hypothesis for $U^*(t)$ under this condition (i.e. when both k and m_v are considered as random together with smear effect) is examined with the help of Chi-square test in Section 4.3.1.3.1.1 of Chapter 4 and it was found that the distribution of $U^*(t)$ strongly agrees with lognormal distribution. As $U^*(t)$ is approximately lognormally distributed, Eq. 5.8 yields:

$$\ln U^*(t) = \ln C + \ln \bar{k}_u - \ln \bar{m}_{v_u} - \ln \bar{\alpha} - \ln \bar{\alpha}_{m_v} \quad (5.15)$$

The mean $\mu_{\ln U^*(t)}$ of $\ln U^*(t)$ can be obtained by taking expectation of Eq. 5.15, as follows:

$$\mu_{\ln U^*(t)} = \ln C + \mu_{\ln \bar{k}_u} - \mu_{\ln \bar{m}_{v_u}} - \mu_{\ln \bar{\alpha}} - \mu_{\ln \bar{\alpha}_{m_v}} \quad (5.16)$$

As the variance of k_u , k_s , m_{v_u} and m_{v_s} contribute to the variance of $\ln U^*(t)$ and as $\bar{\alpha}$ and $\bar{\alpha}_{m_v}$ involve all of them, assuming no cross-correlation between k and m_v , the variance $\sigma_{\ln U^*(t)}^2$ of $\ln U^*(t)$ can simply be estimated as follows:

$$\sigma_{\ln U^*(t)}^2 = \sigma_{\ln \bar{\alpha}}^2 + \sigma_{\ln \bar{\alpha}_{m_v}}^2 \quad (5.17)$$

In order to obtain $\mu_{\ln U^*(t)}$ and $\sigma_{\ln U^*(t)}^2$ in Eqs. 5.16 and 5.17 above, the six unknown parameters $\mu_{\ln \bar{k}_u}$, $\mu_{\ln \bar{m}_{v_u}}$, $\mu_{\ln \bar{\alpha}}$, $\mu_{\ln \bar{\alpha}_{m_v}}$, $\sigma_{\ln \bar{\alpha}}^2$ and $\sigma_{\ln \bar{\alpha}_{m_v}}^2$ must be obtained by expressing them in terms of the known statistical input parameters of k and m_v . In the following part, the statistical parameters in relation to spatially variable k , i.e. $\mu_{\ln \bar{k}_u}$, $\mu_{\ln \bar{\alpha}}$ and $\sigma_{\ln \bar{\alpha}}^2$ will be calculated first followed by the calculation of the parameters $\mu_{\ln \bar{m}_{v_u}}$, $\mu_{\ln \bar{\alpha}_{m_v}}$ and $\sigma_{\ln \bar{\alpha}_{m_v}}^2$ relating to the spatially variable m_v .

- **Calculation of $\mu_{\ln \bar{k}_u}$, $\mu_{\ln \bar{\alpha}}$ and $\sigma_{\ln \bar{\alpha}}^2$**

With reference to Eqs. 5.4 and 5.5, $\mu_{\ln \bar{k}_u}$ can be calculated as follows:

$$\mu_{\ln \bar{k}_u} = \mu_{\ln k_u} = \ln \mu_{k_u} - \frac{1}{2} \ln(1 + v_{k_u}^2) \quad (5.18)$$

The mean of $\bar{\alpha}$ (i.e. $\mu_{\bar{\alpha}}$) can be obtained by taking expectation of Eq. 5.13, as follows:

$$\mu_{\bar{\alpha}} = a + b\mu_W \quad (5.19)$$

The variance of $\bar{\alpha}$ (i.e. $\sigma_{\bar{\alpha}}^2$) is calculated as follows:

$$\sigma_{\bar{\alpha}}^2 = b^2 \sigma_W^2 \quad (5.20)$$

Since both \bar{k}_u and \bar{k}_s are lognormally distributed, W will also be approximately lognormally distributed. With reference to Eqs. 5.15 and 5.16, $\mu_{\ln W}$ is calculated as follows:

$$\mu_{\ln W} = \mu_{\ln \bar{k}_u} - \mu_{\ln \bar{k}_s} \quad (5.21)$$

Again, with reference to Eqs. 5.4 and 5.5, $\mu_{\ln W}$ can be expressed with the known parameters of k as follows:

$$\mu_{\ln W} = \left(\ln \mu_{k_u} - \frac{1}{2} \ln(1 + v_{k_u}^2) \right) - \left(\ln \mu_{k_s} - \frac{1}{2} \ln(1 + v_{k_s}^2) \right) \quad (5.22)$$

Assuming no cross-correlation between k_u and k_s , the variance $\sigma_{\ln W}^2$ of $\ln W$ is calculated as follows:

$$\sigma_{\ln W}^2 = \sigma_{\ln \bar{k}_u}^2 + \sigma_{\ln \bar{k}_s}^2 \quad (5.23)$$

Since k_u and k_s are pertinent only over the undisturbed soil domain, D_u , and the smear zone, D_s , the average variance of $\ln W$ over the entire soil domain can be estimated as follows:

$$\sigma_{\ln W}^2 = \frac{(\sigma_{\ln \bar{k}_u}^2)_D + (\sigma_{\ln \bar{k}_s}^2)_D}{2} \quad (5.24)$$

The subscript D in Eq. 5.24 implies that k_u and k_s are averaged over the entire soil domain. With reference to Eqs. 5.6 and 5.7, Eq. 5.24 can be written as:

$$\sigma_{\ln W}^2 = \frac{\gamma(D)_{k_u} \ln(1 + \nu_{k_u}^2) + \gamma(D)_{k_s} \ln(1 + \nu_{k_s}^2)}{2} \quad (5.25)$$

where: $\gamma(D)_{k_u}$ and $\gamma(D)_{k_s}$ are the variance reduction factor for k_u and k_s , respectively. If θ_{k_u} is different from that of θ_{k_s} , $\gamma(D)_{k_u}$ will be different from that of $\gamma(D)_{k_s}$. It should be noted that both $\mu_{\ln W}$ and $\sigma_{\ln W}^2$ are now known. With reference to Eqs. 3.4 and 3.5, μ_W and σ_W^2 are thus:

$$\mu_W = \exp\left(\mu_{\ln W} + \frac{1}{2}\sigma_{\ln W}^2\right) \quad (5.26)$$

$$\sigma_W^2 = \mu_W^2(\exp(\sigma_{\ln W}^2) - 1) \quad (5.27)$$

Although Eq. 5.27 can give correct σ_W^2 for the same variability parameters in the disturbed and undisturbed zones (i.e. $\nu_{k_u} = \nu_{k_s}$ and $\theta_{k_u} = \theta_{k_s}$), the true σ_W^2 will be somewhat different from the calculated σ_W^2 if the variability parameters in the disturbed and undisturbed zones are different. For this reason, Eq. 5.27 is empirically adjusted to obtain σ_W^2 with reasonable accuracy as follows:

$$\sigma_W^2 = \left(\frac{2\nu_{\bar{k}_s}}{\nu_{\bar{k}_u} + \nu_{\bar{k}_s}}\right) \mu_W^2 [\exp(\sigma_{\ln W}^2) - 1] \quad (5.28)$$

where: $\nu_{\bar{k}_u} = \sigma_{\bar{k}_u} / \mu_{\bar{k}_u}$ is the coefficient of variation of equivalent permeability in the undisturbed zone ($\sigma_{\bar{k}_u}$ and $\mu_{\bar{k}_u}$ are the standard deviation and mean of \bar{k}_u , respectively), $\nu_{\bar{k}_s} = \sigma_{\bar{k}_s} / \mu_{\bar{k}_s}$ is the coefficient of variation of equivalent permeability in the smear zone ($\sigma_{\bar{k}_s}$ and $\mu_{\bar{k}_s}$ are the standard deviation and mean of \bar{k}_s , respectively). The empirical adjustment of σ_W^2 is necessary because of the fact that the sum of two lognormally distributed random variables does not have a simple closed form solution. In addition, k_u and k_s are not distributed over the entire soil

domain and do not have the same influence on the behaviour of soil consolidation. The mean and standard deviation of \bar{k}_u can then be calculated with reference to Eqs. 3.4 and 3.5, using Eqs. 5.5 and 5.7 as follows:

$$\mu_{\bar{k}_u} = \exp\left(\mu_{\ln \bar{k}_u} + \frac{1}{2}\sigma_{\ln \bar{k}_u}^2\right) = \exp\left(\ln \mu_{k_u} - \frac{1}{2}\ln(1 + \nu_{k_u}^2) + \frac{1}{2}\gamma(D)_{k_u} \ln(1 + \nu_{k_u}^2)\right) \quad (5.29)$$

$$\sigma_{\bar{k}_u} = \mu_{\bar{k}_u} \sqrt{\left[\exp(\sigma_{\ln \bar{k}_u}^2) - 1\right]} = \mu_{\bar{k}_u} \sqrt{\left[\exp(\gamma(D)_{k_u} \ln(1 + \nu_{k_u}^2)) - 1\right]} \quad (5.30)$$

Similarly, the mean and standard deviation of \bar{k}_s can be calculated as follows:

$$\mu_{\bar{k}_s} = \exp\left(\mu_{\ln \bar{k}_s} + \frac{1}{2}\sigma_{\ln \bar{k}_s}^2\right) = \exp\left(\ln \mu_{k_s} - \frac{1}{2}\ln(1 + \nu_{k_s}^2) + \frac{1}{2}\gamma(D)_{k_s} \ln(1 + \nu_{k_s}^2)\right) \quad (5.31)$$

$$\sigma_{\bar{k}_s} = \mu_{\bar{k}_s} \sqrt{\left[\exp(\sigma_{\ln \bar{k}_s}^2) - 1\right]} = \mu_{\bar{k}_s} \sqrt{\left[\exp(\gamma(D)_{k_s} \ln(1 + \nu_{k_s}^2)) - 1\right]} \quad (5.32)$$

Substituting Eqs. 5.26 and 5.28 into Eqs. 5.19 and 5.20 gives:

$$\mu_{\bar{\alpha}} = a + b \left[\exp\left(\mu_{\ln W} + \frac{1}{2}\sigma_{\ln W}^2\right) \right] \quad (5.33)$$

$$\sigma_{\bar{\alpha}}^2 = \left(\frac{2\nu_{\bar{k}_s}}{\nu_{\bar{k}_u} + \nu_{\bar{k}_s}} \right) b^2 \mu_W^2 \left[\exp(\sigma_{\ln W}^2) - 1 \right] \quad (5.34)$$

Finally, the mean $\mu_{\ln \bar{\alpha}}$ and standard deviation $\sigma_{\ln \bar{\alpha}}^2$ of the underlying normally distributed $\ln \bar{\alpha}$ can be obtained with reference to Eqs. 3.2 and 3.3 as follows:

$$\sigma_{\ln \bar{\alpha}}^2 = \ln\left(1 + \frac{\sigma_{\bar{\alpha}}^2}{\mu_{\bar{\alpha}}^2}\right) \quad (5.35)$$

$$\mu_{\ln \bar{\alpha}} = \ln \mu_{\bar{\alpha}} - \frac{1}{2} \sigma_{\ln \bar{\alpha}}^2 \quad (5.36)$$

- **Calculation of $\mu_{\ln \bar{m}_{v_u}}$, $\mu_{\ln \bar{\alpha}_{m_v}}$ and $\sigma_{\ln \bar{\alpha}_{m_v}}^2$**

$\mu_{\ln \bar{m}_{v_u}}$, $\mu_{\ln \bar{\alpha}_{m_v}}$ and $\sigma_{\ln \bar{\alpha}_{m_v}}^2$ are calculated in a similar way as that followed for calculating $\mu_{\ln \bar{k}_u}$, $\mu_{\ln \bar{\alpha}}$ and $\sigma_{\ln \bar{\alpha}}^2$. With reference to Eqs. 5.18, $\mu_{\ln \bar{m}_{v_u}}$ can be calculated as follows:

$$\mu_{\ln \bar{m}_{v_u}} = \mu_{\ln m_{v_u}} = \ln \mu_{m_{v_u}} - \frac{1}{2} \ln(1 + \nu_{m_{v_u}}^2) \quad (5.37)$$

$\mu_{\bar{\alpha}_{m_v}}$ and $\sigma_{\bar{\alpha}_{m_v}}^2$ can be computed with reference to Eqs. 5.19 and 5.20, respectively, using Eq. 5.14 as follows:

$$\mu_{\bar{\alpha}_{m_v}} = g + h \mu_V \quad (5.38)$$

$$\sigma_{\bar{\alpha}_{m_v}}^2 = h^2 \sigma_V^2 \quad (5.39)$$

Again with reference to Eqs. 5.22 and 5.25, $\mu_{\ln V}$ and $\sigma_{\ln V}^2$, respectively, can be expressed with known parameters of m_v as follows:

$$\mu_{\ln V} = \left(\ln \mu_{m_{v_s}} - \frac{1}{2} \ln(1 + \nu_{m_{v_s}}^2) \right) - \left(\ln \mu_{m_{v_u}} - \frac{1}{2} \ln(1 + \nu_{m_{v_u}}^2) \right) \quad (5.40)$$

$$\sigma_{\ln V}^2 = \frac{\gamma(D)_{m_{v_u}} \ln(1 + \nu_{m_{v_u}}^2) + \gamma(D)_{m_{v_s}} \ln(1 + \nu_{m_{v_s}}^2)}{2} \quad (5.41)$$

where: $\gamma(D)_{m_{v_u}}$ and $\gamma(D)_{m_{v_s}}$ are the variance reduction factor for m_{v_u} and m_{v_s} , respectively. It should be noted that both $\mu_{\ln V}$ and $\sigma_{\ln V}^2$ are now known.

With reference to Eqs. 5.26 and 5.28, μ_V and σ_V^2 are thus:

$$\mu_V = \exp\left(\mu_{\ln V} + \frac{1}{2}\sigma_{\ln V}^2\right) \quad (5.42)$$

$$\sigma_V^2 = \left(\frac{2\nu_{\bar{m}_{v_s}}}{\nu_{\bar{m}_{v_u}} + \nu_{\bar{m}_{v_s}}}\right)\mu_V^2[\exp(\sigma_{\ln V}^2)-1] \quad (5.43)$$

where: $\nu_{\bar{m}_{v_u}} = \sigma_{\bar{m}_{v_u}} / \mu_{\bar{m}_{v_u}}$ is the coefficient of variation of equivalent compressibility in the undisturbed zone ($\sigma_{\bar{m}_{v_u}}$ and $\mu_{\bar{m}_{v_u}}$ are the standard deviation and mean of \bar{m}_{v_u} , respectively), $\nu_{\bar{m}_{v_s}} = \sigma_{\bar{m}_{v_s}} / \mu_{\bar{m}_{v_s}}$ is the coefficient of variation of equivalent compressibility in the smear zone ($\sigma_{\bar{m}_{v_s}}$ and $\mu_{\bar{m}_{v_s}}$ are the standard deviation and mean of \bar{m}_{v_s} , respectively).

The mean and standard deviation of \bar{m}_{v_u} and \bar{m}_{v_s} can be estimated with reference to Eqs. 5.29–5.32 as follows:

$$\mu_{\bar{m}_{v_u}} = \exp\left(\ln \mu_{m_{v_u}} - \frac{1}{2}\ln(1 + \nu_{m_{v_u}}^2) + \frac{1}{2}\gamma(D)_{m_{v_u}} \ln(1 + \nu_{m_{v_u}}^2)\right) \quad (5.44)$$

$$\sigma_{\bar{m}_{v_u}} = \mu_{\bar{m}_{v_u}} \sqrt{\left[\exp(\gamma(D)_{m_{v_u}} \ln(1 + \nu_{m_{v_u}}^2)) - 1\right]} \quad (5.45)$$

and

$$\mu_{\bar{m}_{v_s}} = \exp\left(\ln \mu_{m_{v_s}} - \frac{1}{2}\ln(1 + \nu_{m_{v_s}}^2) + \frac{1}{2}\gamma(D)_{m_{v_s}} \ln(1 + \nu_{m_{v_s}}^2)\right) \quad (5.46)$$

$$\sigma_{\bar{m}_{v_s}} = \mu_{\bar{m}_{v_s}} \sqrt{\left[\exp(\gamma(D)_{m_{v_s}} \ln(1 + \nu_{m_{v_s}}^2)) - 1\right]} \quad (5.47)$$

Substituting Eqs. 5.42 and 5.43 into Eqs. 5.38 and 5.39 gives:

$$\mu_{\bar{\alpha}_{m_v}} = g + h \left[\exp \left(\mu_{\ln V} + \frac{1}{2} \sigma_{\ln V}^2 \right) \right] \quad (5.48)$$

$$\sigma_{\bar{\alpha}_{m_v}}^2 = \left(\frac{2\nu_{\bar{m}_{v_s}}}{\nu_{\bar{m}_{v_u}} + \nu_{\bar{m}_{v_s}}} \right) h^2 \mu_V^2 \left[\exp(\sigma_{\ln V}^2) - 1 \right] \quad (5.49)$$

Finally, the mean $\mu_{\ln \bar{\alpha}_{m_v}}$ and standard deviation $\sigma_{\ln \bar{\alpha}_{m_v}}^2$ of the underlying normally distributed $\ln \bar{\alpha}_{m_v}$ can be obtained with reference to Eqs. 5.35 and 5.36 as follows:

$$\sigma_{\ln \bar{\alpha}_{m_v}}^2 = \ln \left(1 + \frac{\sigma_{\bar{\alpha}_{m_v}}^2}{\mu_{\bar{\alpha}_{m_v}}^2} \right) \quad (5.50)$$

$$\mu_{\ln \bar{\alpha}_{m_v}} = \ln \mu_{\bar{\alpha}_{m_v}} - \frac{1}{2} \sigma_{\ln \bar{\alpha}_{m_v}}^2 \quad (5.51)$$

All six parameters: $\mu_{\ln \bar{k}_u}$, $\mu_{\ln \bar{m}_{v_u}}$, $\mu_{\ln \bar{\alpha}}$, $\mu_{\ln \bar{\alpha}_{m_v}}$, $\sigma_{\ln \bar{\alpha}}^2$ and $\sigma_{\ln \bar{\alpha}_{m_v}}^2$ are now known and can be used in Eqs. 5.16 and 5.17 for the estimation of $\mu_{\ln U^*(t)}$ and $\sigma_{\ln U^*(t)}^2$. Using the developed semi-analytical relationship, the procedure for calculating $\mu_{\ln U^*(t)}$ and $\sigma_{\ln U^*(t)}^2$ can be summarized as follows:

1. Determine all constant parameters involved in the RBSA, i.e. C , a , b , g , h , $\gamma(D)_{k_u}$, $\gamma(D)_{k_s}$, $\gamma(D)_{m_{v_u}}$ and $\gamma(D)_{m_{v_s}}$;
2. Calculate $\mu_{\ln \bar{k}_u}$ and $\mu_{\ln \bar{m}_{v_u}}$ from Eqs. 5.18 and 5.37;
3. Calculate $\mu_{\ln W}$, $\sigma_{\ln W}^2$, μ_W , $\mu_{\ln V}$, $\sigma_{\ln V}^2$ and μ_V using Eqs. 5.22, 5.25, 5.26, 5.40, 5.41 and 5.42;
4. Calculate $\mu_{\bar{k}_u}$, $\sigma_{\bar{k}_u}$, $\mu_{\bar{k}_s}$, $\sigma_{\bar{k}_s}$, $\mu_{\bar{m}_{v_u}}$, $\sigma_{\bar{m}_{v_u}}$, $\mu_{\bar{m}_{v_s}}$ and $\sigma_{\bar{m}_{v_s}}$ using Eqs. 5.29, 5.30, 5.31, 5.32, 5.44, 5.45, 5.46 and 5.47, then determine $\nu_{\bar{k}_u}$, $\nu_{\bar{k}_s}$, $\nu_{\bar{m}_{v_u}}$ and $\nu_{\bar{m}_{v_s}}$;

5. Using the values of $\mu_{\ln W}$, $\sigma_{\ln W}^2$, μ_W , $\mu_{\ln V}$, $\sigma_{\ln V}^2$, μ_V , $U_{\bar{k}_u}$, $U_{\bar{k}_s}$, $U_{\bar{m}_u}$ and $U_{\bar{m}_s}$ obtained in Steps 3 and 4, calculate $\mu_{\bar{\alpha}}$, $\sigma_{\bar{\alpha}}^2$, $\mu_{\bar{\alpha}_{m_v}}$ and $\sigma_{\bar{\alpha}_{m_v}}^2$ from Eqs. 5.33, 5.34, 5.48 and 5.49;
6. Use Eqs. 5.35, 5.36, 5.50 and 5.51 to determine $\sigma_{\ln \bar{\alpha}}$, $\mu_{\ln \bar{\alpha}}$, $\sigma_{\ln \bar{\alpha}_{m_v}}^2$ and $\mu_{\ln \bar{\alpha}_{m_v}}$ from the obtained values of $\mu_{\bar{\alpha}}$, $\sigma_{\bar{\alpha}}^2$, $\mu_{\bar{\alpha}_{m_v}}$ and $\sigma_{\bar{\alpha}_{m_v}}^2$ in Step 5; and
7. Evaluate $\mu_{\ln U^*(t)}$ and $\sigma_{\ln U^*(t)}^2$ by substituting $\mu_{\ln \bar{k}_u}$, $\mu_{\ln \bar{m}_u}$, $\mu_{\ln \bar{\alpha}}$ and $\mu_{\ln \bar{\alpha}_{m_v}}$ in Eq. 5.16, and $\sigma_{\ln \bar{\alpha}}$ and $\sigma_{\ln \bar{\alpha}_{m_v}}^2$ in Eq. 5.17.

G1C2: RBSA model considering no smear (both k and m_v are random)

If smear effect is not considered, k_u and m_{v_u} in Eq. 5.8 can be simply replaced as k and m_v , respectively. In addition, α_{m_v} will be equal to 1.0, and α parameter will become constant. By applying these conditions, Eq. 5.8 becomes:

$$U^*(t) = C \frac{\bar{k}}{\bar{m}_v} \quad (5.52)$$

where:

$$C = \frac{2t}{r_e^2 \gamma_w \alpha} \quad (5.53)$$

and

$$\alpha = \ln(n) - \frac{3}{4} + F'_r \quad (5.54)$$

It has mentioned earlier that \bar{k} and \bar{m}_v are lognormally distributed (by the central limit theorem). Therefore, $U^*(t)$ will also be approximately lognormally distributed. The plotted histogram of the $U^*(t)$ data derived from the FEMC for this case also strongly support lognormal distribution, as shown in Section 4.2.1.3.1.1. As $U^*(t)$ is

approximately lognormally distributed, $\mu_{\ln U^*(t)}$ and $\sigma_{\ln U^*(t)}^2$ of $\ln U^*(t)$ can be estimated from Eq. 5.52 with reference to Eqs. 5.16 and 5.17, as follows:

$$\mu_{\ln U^*(t)} = \ln C + \mu_{\ln \bar{k}} - \mu_{\ln \bar{m}_v} \quad (5.55)$$

$$\sigma_{\ln U^*(t)}^2 = \sigma_{\ln \bar{k}}^2 + \sigma_{\ln \bar{m}_v}^2 \quad (5.56)$$

$\mu_{\ln \bar{k}}$ and $\mu_{\ln \bar{m}_v}$ in Eq. 5.55, can be evaluated with reference to Eq. 5.5 as follows:

$$\mu_{\ln \bar{k}} = \ln \mu_{k_h} - \frac{1}{2} \ln(1 + \nu_k^2) \quad (5.57)$$

$$\mu_{\ln \bar{m}_v} = \ln \mu_{m_v} - \frac{1}{2} \ln(1 + \nu_{m_v}^2) \quad (5.58)$$

With reference to Eq. 5.6, $\sigma_{\ln \bar{k}}^2$ and $\sigma_{\ln \bar{m}_v}^2$ can then be expressed with the specified statistical parameters of k and m_v as follows:

$$\sigma_{\ln \bar{k}}^2 = \gamma(D)_k (\ln(1 + \nu_k^2)) \quad (5.59)$$

$$\sigma_{\ln \bar{m}_v}^2 = \gamma(D)_{m_v} (\ln(1 + \nu_{m_v}^2)) \quad (5.60)$$

Now $\mu_{\ln U^*(t)}$ and $\sigma_{\ln U^*(t)}^2$ can be evaluated by substituting $\mu_{\ln \bar{k}}$ and $\mu_{\ln \bar{m}_v}$ in Eq. 5.55, and $\sigma_{\ln \bar{k}}^2$ and $\sigma_{\ln \bar{m}_v}^2$ in Eq. 5.56 as follows:

$$\mu_{\ln U^*(t)} = \ln C + \left[\ln \mu_k - \frac{1}{2} \ln(1 + \nu_k^2) \right] - \left[\ln \mu_{m_v} - \frac{1}{2} \ln(1 + \nu_{m_v}^2) \right] \quad (5.61)$$

$$\sigma_{\ln U^*(t)}^2 = \gamma(D)_k (\ln(1 + \nu_k^2)) + \gamma(D)_{m_v} (\ln(1 + \nu_{m_v}^2)) \quad (5.62)$$

G1C3: RBSA model for special case of considering smear (both k and m_v are random)

If both k and m_v (individually or in together) have the same v and θ in the undisturbed and smear zones (i.e. $v_u = v_s$ and $\theta_u = \theta_s$, of course μ_u and μ_s are different), this can be considered as a special no smear case. In other words, if the soil properties of a site under consideration varies spatially in such a way that it satisfies the condition $v_{k_u} = v_{k_s}$, $\theta_{k_u} = \theta_{k_s}$ and $v_{m_v_u} = v_{m_v_s}$, $\theta_{m_v_u} = \theta_{m_v_s}$ then it is a special no-smear case. This case is considered because it has shown in Chapter 4 that the stochastic behaviour of soil consolidation is governed by v and θ in the smear zone, and modelling soil consolidation with the same v and θ for both zones that are equal to the v and θ of the smear zone will not significantly affect the final results. For this case, $\mu_{\ln U^*(t)}$ and $\sigma_{\ln U^*(t)}^2$ can be estimated using Eqs. 5.61 and 5.62, respectively. However, in this case μ_k and μ_{m_v} in Eq. 5.61 represent, respectively, the mean values of permeability and volume compressibility of the undisturbed zone. The C parameter for this case is different from that obtained from the RBSA– G1C2 and can be calculated as follows:

$$C = \frac{2t}{r_e^2 \gamma_w \alpha \alpha_{m_v}} \quad (5.63)$$

where:

$$\alpha = \ln\left(\frac{n}{s}\right) - \frac{3}{4} + \frac{\mu_{k_u}}{\mu_{k_s}} \ln(s) + F'_r \quad (5.64)$$

and

$$\alpha_{m_v} = \frac{n^2 - s^2}{n^2 - 1} + \frac{s^2 - 1}{n^2 - 1} \frac{\mu_{m_{v_s}}}{\mu_{m_{v_u}}} \quad (5.65)$$

It should be noted that the problem described in the RBSA–G1C3 can also be solved using the RBSA–G1C1 model and the results will essentially be almost identical for both cases. The agreement between RBSA–G1C3 and RBSA–G1C1 will be examined later in the following section.

G2C1: RBSA model considering smear effect (only k is random)

As mentioned earlier, the typical variability in m_v ranges from 25% to 30% and it has shown in the previous chapter that any coefficient of variation of $m_v \leq 25\%$ has little impact on the stochastic behaviour of soil consolidation. Under such condition, m_v can be considered as spatially constant without significantly affecting the final results. Accordingly, the RBSA model by treating k as spatially random and m_v as spatially constant is also developed. Considering the smear effect with permeability as the only random variable, Eq. 5.8 becomes:

$$U^*(t) = C \frac{\bar{k}_u}{\bar{\alpha}} \quad (5.66)$$

where:

$$C = \frac{2t}{r_e^2 m_v \gamma_w} \quad (5.67)$$

As the lognormal distribution assumption for $U^*(t)$ also remains valid when k is considered as the only random variable together with the smear effect (see Section 4.3.1.2.1.1), $\mu_{\ln U^*(t)}$ and $\sigma_{\ln U^*(t)}^2$ can be obtained from Eq. 5.66 with reference to Eqs. 5.16 and 5.17, as follows:

$$\mu_{\ln U^*(t)} = \ln C + \mu_{\ln \bar{k}_u} - \mu_{\ln \bar{\alpha}} \quad (5.68)$$

$$\sigma_{\ln U^*(t)}^2 = \sigma_{\ln \bar{\alpha}}^2 \quad (5.69)$$

To obtain $\mu_{\ln U^{*(t)}}$ and $\sigma_{\ln U^{*(t)}}^2$ in Eqs. 5.68 and 5.69, the three unknown parameters $\mu_{\ln \bar{k}_u}$, $\mu_{\ln \bar{\alpha}}$ and $\sigma_{\ln \bar{\alpha}}^2$ in Eqs. 5.68 and 5.69 must be obtained by expressing them in terms of the known statistical input parameters of k . All three unknown parameters: $\mu_{\ln \bar{k}_u}$, $\mu_{\ln \bar{\alpha}}$ and $\sigma_{\ln \bar{\alpha}}^2$ are already determined earlier for the RBSA of G1C1 and can be readily used in Eqs. 5.68 and 5.69 for the estimation of $\mu_{\ln U^{*(t)}}$ and $\sigma_{\ln U^{*(t)}}^2$. As m_v is remained constant across the soil mass, no calculations of the parameters $\mu_{\ln \bar{m}_{v_u}}$, $\mu_{\ln \bar{\alpha}_{m_v}}$ and $\sigma_{\ln \bar{\alpha}_{m_v}}^2$ in relation to m_v are not required for this case. The C parameter for RBSA–G2C1 will also be different from RBSA–G1C1 and can be determined using Eq. 5.67. The procedure for calculating $\mu_{\ln U^{*(t)}}$ and $\sigma_{\ln U^{*(t)}}^2$ for the RBSA of G2C1 can be summarized as follows:

1. Determine all constant parameters involved in the RBSA, i.e. a , b , $\gamma(D)_{k_u}$ and $\gamma(D)_{k_s}$; and determine C using Eq. 5.67;
2. Calculate $\mu_{\ln \bar{k}_u}$ from Eqs. 5.18;
3. Calculate $\mu_{\ln W}$, $\sigma_{\ln W}^2$ and μ_W using Eqs. 5.22, 5.25 and 5.26, respectively;
4. Calculate $\mu_{\bar{k}_u}$, $\sigma_{\bar{k}_u}$, $\mu_{\bar{k}_s}$ and $\sigma_{\bar{k}_s}$ using Eqs. 5.29, 5.30, 5.31 and 5.32, respectively, then determine $\nu_{\bar{k}_u}$ and $\nu_{\bar{k}_s}$;
5. Using the values of $\mu_{\ln W}$, $\sigma_{\ln W}^2$, μ_W , $\nu_{\bar{k}_u}$ and $\nu_{\bar{k}_s}$ obtained in Steps 3 and 4, calculate $\mu_{\bar{\alpha}}$ and $\sigma_{\bar{\alpha}}^2$ from Eqs. 5.33 and 5.34, respectively;
6. Use Eqs. 5.35 and 5.36 to determine $\sigma_{\ln \bar{\alpha}}^2$ and $\mu_{\ln \bar{\alpha}}$, respectively, from the obtained values of $\mu_{\bar{\alpha}}$ and $\sigma_{\bar{\alpha}}^2$ in Step 5; and
7. Evaluate $\mu_{\ln U^{*(t)}}$ and $\sigma_{\ln U^{*(t)}}^2$ by substituting $\mu_{\ln \bar{k}_u}$ and $\mu_{\ln \bar{\alpha}}$ in Eq. 5.68, and $\sigma_{\ln \bar{\alpha}}^2$ in Eq. 5.69.

G2C2: RBSA model considering no smear (only k is random)

The RBSA–G2C2 model can be simply derived from the RBSA–G1C2 model by considering m_v as a constant parameter. For constant m_v , Eq. 5.52 can be written as:

$$U^*(t) = C\bar{k} \quad (5.70)$$

where:

$$C = \frac{2t}{r_e^2 m_v \gamma_w \alpha} \quad (5.71)$$

α will remain the same as that given in Eq. 5.54, i.e. $\alpha = \ln(n) - \frac{3}{4} + F'_r$.

As \bar{k} is lognormally distributed, $U^*(t)$ will also be approximately lognormally distributed. The plotted histogram of the $U^*(t)$ data derived from FEMC for this case also strongly supports lognormal distribution, as shown in Section 4.2.1.2.1. As $U^*(t)$ is approximately lognormally distributed, $\mu_{\ln U^*(t)}$ and $\sigma_{\ln U^*(t)}^2$ can be obtained from Eq. 5.70 with reference to Eqs. 5.55 and 5.56, as follows (note that m_v is constant across the soil mass):

$$\mu_{\ln U^*(t)} = \ln C + \mu_{\ln \bar{k}} \quad (5.72)$$

$$\sigma_{\ln U^*(t)}^2 = \sigma_{\ln \bar{k}}^2 \quad (5.73)$$

$\mu_{\ln \bar{k}}$ and $\sigma_{\ln \bar{k}}^2$ are already evaluated through Eqs. 5.57 and 5.59, and can be substituted in Eqs. 5.72 and 5.73 to obtain $\mu_{\ln U^*(t)}$ and $\sigma_{\ln U^*(t)}^2$ as follows:

$$\mu_{\ln U^*(t)} = \ln C + \ln \mu_k - \frac{1}{2} \ln(1 + \nu_k^2) \quad (5.74)$$

$$\sigma_{\ln U^*(t)}^2 = \gamma(D)_k \ln(1 + \nu_k^2) \quad (5.75)$$

G2C3: RBSA model for special case of considering smear (only k is random)

Similar to the RBSA–G1C3 model, if both k_u and k_s have the same ν and θ (of course μ_{k_u} and μ_{k_s} are different), this can be also considered as a special no-smear case (note that m_ν is a constant parameter for this case). For the RBSA model of G2C3, $\mu_{\ln U^*(t)}$ and $\sigma_{\ln U^*(t)}^2$ can be estimated using Eqs. 5.74 and 5.75, respectively, as presented for the RBSA model of G2C2. However, in this case μ_k in Eq. 5.74 represents the mean value of permeability of the undisturbed zone. Although, the expression for C parameter in this case will remain the same as that given in Eq. 5.71, the magnitude of C parameter will be different from that obtained from the RBSA–G2C2. This is due to the fact that α parameter (and in turn C parameter) for the RBSA model of G2C3 will be different from that of the RBSA–G2C2 and can be calculated using the expression of α given in Eq. 5.64, i.e.

$$\alpha = \ln\left(\frac{n}{s}\right) - \frac{3}{4} + \frac{\mu_{k_u}}{\mu_{k_s}} \ln(s) + F'_r .$$

It should be noted that the problem described in

RBSA–G2C3 can be also solved using the RBSA model of G2C1 and the results will be essentially identical for both cases. In the following section, the detailed comparison between the results obtained from the stochastic FEMC simulations and the proposed RBSA models are described and discussed.

5.2.1 Comparison between Finite-element Monte-Carlo approach and reliability-based semi-analytical model

Prior to presenting the comparison based results of the FEMC approach with those of the proposed RBSA model, the calculation procedure for the RBSA model of G1C1 is demonstrated by an illustrative example of a unit cell consolidation problem. The RBSA model of G1C1 is selected for demonstration as it considers both k and m_ν as random variables including the smear effect. The required input geometric and soil parameters are assumed to be: $L = 1.0$ m, $r_w = 0.05$ m, $r_e = 0.85$ m (i.e. $n = 17$), $r_s = 0.35$ m (i.e. $s = 7$), $\mu_{k_u} = 5 \times 10^{-10}$ m/sec, $\mu_{m_{\nu_u}} = 1.67 \times 10^{-4}$ m²/kN, $\mu_{k_u} / \mu_{k_s} = 2.0$ and $\mu_{m_{\nu_u}} / \mu_{m_{\nu_s}} = 1.25$, while the required input random filed parameters are assumed to be: $\nu_{k_u} = 50\%$, $\nu_{k_s} = 100\%$, $\nu_{m_{\nu_u}} = 12.5\%$, $\nu_{m_{\nu_s}} = 25\%$, $\theta_{k_u} = \theta_{k_s} = \theta_{m_{\nu_u}} = \theta_{m_{\nu_s}} = 0.5$. It is

also assumed that the probability of achieving 90% consolidation to be determined at 129.3 days (note that the deterministic solution of the finite element code yields $t_{D90} = 129.3$ days for the selected problem). With the above information, $\mu_{\ln U^*(t)}$ (see Eq. 5.16) and $\sigma_{\ln U^*(t)}^2$ (see Eq. 5.17) can be computed by following the steps described earlier in developing the RBSA model of G1C1, as follows:

1. The constant parameters involved in the RBSA are calculated as follows:

$$C = (2 \times 129.3) / (0.85^2 \times 9.8) = 36.523 \quad (5.76)$$

Since no well resistance effect is considered, the parameters a and b can be calculated as:

$$a = \ln(17/7) - 0.75 = 0.137 \quad \text{and} \quad b = \ln(7) = 1.946 \quad (5.77)$$

Using $n = 17$ and $s = 7$, the parameters g and h can be calculated as:

$$g = (17^2 - 7^2) / (17^2 - 1) = 0.833 \quad \text{and} \quad g = (7^2 - 1) / (17^2 - 1) = 0.167 \quad (5.78)$$

Since $\theta_{k_u} = \theta_{k_s} = \theta_{m_{v_u}} = \theta_{m_{v_s}}$, hence $\gamma(D)_{k_u} = \gamma(D)_{k_s} = \gamma(D)_{m_{v_u}} = \gamma(D)_{m_{v_s}}$. Using the algorithm presented in Appendix A, the variance reduction factor due to averaging over the consolidated depth L and width $(r_e - r_w)$ are given by:

$$\gamma(D)_{k_u} = \gamma(D)_{k_s} = \gamma(D)_{m_{v_u}} = \gamma(D)_{m_{v_s}} = \gamma((r_e - r_w), L) = 0.22047 \quad (5.79)$$

Note that, in the following calculations, μ_{k_u} and μ_{k_s} are expressed in m/day.

2. $\mu_{\ln \bar{k}_u} = \ln(4.32 \times 10^{-5}) - 0.5 \ln(1 + 0.5^2) = -10.161 \quad (5.80)$

$$\mu_{\ln \bar{m}_{v_u}} = \ln(1.67 \times 10^{-4}) - 0.5 \ln(1 + 0.125^2) = -8.708 \quad (5.81)$$

$$3. \mu_{\ln W} = \left(\ln(4.32 \times 10^{-5}) - 0.5 \ln(1 + 0.5^2) \right) - \left(\frac{\ln(2.16 \times 10^{-5})}{-0.5 \ln(1 + 1.0^2)} \right) = 0.928 \quad (5.82)$$

$$\mu_{\ln V} = \left(\ln(2.083 \times 10^{-4}) - 0.5 \ln(1 + 0.25^2) \right) - \left(\frac{\ln(1.67 \times 10^{-4})}{-0.5 \ln(1 + 0.125^2)} \right) = 0.2 \quad (5.83)$$

$$\sigma_{\ln W}^2 = \left[(0.22047 \ln(1 + 0.5^2)) + (0.22047 \ln(1 + 1.0^2)) \right] / 2.0 = 0.101 \quad (5.84)$$

$$\sigma_{\ln V}^2 = \left[(0.22047 \ln(1 + 0.125^2)) + (0.22047 \ln(1 + 0.25^2)) \right] / 2.0 = 0.0084 \quad (5.85)$$

$$\mu_W = \exp(0.928 + 0.5 \times 0.101) = 2.66 \quad (5.86)$$

$$\mu_V = \exp(0.2 + 0.5 \times 0.0084) = 1.226 \quad (5.87)$$

$$4. \mu_{\bar{k}_u} = \exp \left(\frac{\ln(4.32 \times 10^{-5}) - 0.5 \ln(1 + 0.5^2) +}{0.5 \times 0.22047 \ln(1 + 0.5^2)} \right) = 3.96 \times 10^{-5} \quad (5.88)$$

$$\sigma_{\bar{k}_u} = 3.96 \times 10^{-5} \sqrt{\exp(0.22047 \ln(1 + 0.5^2)) - 1} = 8.89 \times 10^{-6} \quad (5.89)$$

and

$$\mu_{\bar{k}_s} = \exp \left(\frac{\ln(2.16 \times 10^{-5}) - 0.5 \ln(1 + 1.0^2) +}{0.5 \times 0.22047 \ln(1 + 1.0^2)} \right) = 1.648 \times 10^{-5} \quad (5.90)$$

$$\sigma_{\bar{k}_s} = 1.648 \times 10^{-5} \sqrt{\exp(0.22047 \ln(1 + 1.0^2)) - 1} = 6.7 \times 10^{-6} \quad (5.91)$$

Similarly:

$$\mu_{\bar{m}_{vu}} = \exp \left(\frac{\ln(1.67 \times 10^{-4}) - 0.5 \ln(1 + 0.125^2) +}{0.5 \times 0.22047 \ln(1 + 0.125^2)} \right) = 1.656 \times 10^{-4} \quad (5.92)$$

$$\sigma_{\bar{m}_{v_u}} = 1.656 \times 10^{-4} \sqrt{\exp(0.22047 \ln(1 + 0.125^2)) - 1} = 9.69 \times 10^{-6} \quad (5.93)$$

and

$$\mu_{\bar{m}_{v_s}} = \exp\left(\frac{\ln(2.803 \times 10^{-4}) - 0.5 \ln(1 + 0.25^2)}{0.5 \times 0.22047 \ln(1 + 0.25^2)}\right) = 2.034 \times 10^{-4} \quad (5.94)$$

$$\sigma_{\bar{k}_u} = 2.034 \times 10^{-4} \sqrt{\exp(0.22047 \ln(1 + 0.25^2)) - 1} = 2.36 \times 10^{-5} \quad (5.95)$$

Therefore:

$$v_{\bar{k}_u} = 8.89 \times 10^{-6} / 3.96 \times 10^{-5} = 0.2245 \quad (5.96)$$

$$v_{\bar{k}_s} = 6.7 \times 10^{-6} / 1.648 \times 10^{-5} = 0.406 \quad (5.97)$$

and

$$v_{\bar{m}_{v_u}} = 9.69 \times 10^{-6} / 1.656 \times 10^{-4} = 0.0585 \quad (5.98)$$

$$v_{\bar{m}_{v_s}} = 2.36 \times 10^{-5} / 2.034 \times 10^{-4} = 0.116 \quad (5.99)$$

$$5. \mu_{\bar{\alpha}} = 0.137 + 1.946 \times \exp(0.928 + 0.5 \times 0.101) = 5.315 \quad (5.100)$$

$$\sigma_{\bar{\alpha}}^2 = (2 \times 0.406) / (0.2245 + 0.406) \times 1.946^2 \times 2.66^2 \times (\exp(0.101) - 1) = 3.67 \quad (5.101)$$

and

$$\mu_{\bar{\alpha}_{m_v}} = 0.833 + 0.167 \times \exp(0.2 + 0.5 \times 0.0084) = 1.038 \quad (5.102)$$

$$\begin{aligned}\sigma_{\bar{\alpha}_{m_v}}^2 &= (2 \times 0.116) / (0.0585 + 0.116) \times 0.167^2 \times 1.226^2 \times (\exp(0.0084) - 1) \\ &= 4.69 \times 10^{-4}\end{aligned}\quad (5.103)$$

$$6. \sigma_{\ln \bar{\alpha}}^2 = \ln\left(1 + \left(3.67 / 5.315^2\right)\right) = 0.122 \quad (5.104)$$

$$\mu_{\ln \bar{\alpha}} = \ln(5.315) - 0.5 \times 0.122 = 1.61 \quad (5.105)$$

and

$$\sigma_{\ln \bar{\alpha}_{m_v}}^2 = \ln\left(1 + \left(4.69 \times 10^{-4} / 1.038^2\right)\right) = 4.35 \times 10^{-4} \quad (5.106)$$

$$\mu_{\ln \bar{\alpha}_{m_v}} = \ln(1.038) - 0.5 \times 4.35 \times 10^{-4} = 0.037 \quad (5.107)$$

7. Finally:

$$\mu_{\ln U^*(t)} = \ln(36.523) + (-10.161) - (-8.708) - 1.61 - 0.037 = 0.498 \quad (5.108)$$

$$\sigma_{\ln U^*(t)}^2 = 0.122 + 4.35 \times 10^{-4} = 0.122435 \quad (5.109)$$

Therefore, $\sigma_{\ln U^*(t)} = 0.35$. The frequency density plot for the selected problem at time 129.3 days was presented in Fig 4.61. It can be seen that the estimated $\mu_{\ln U^*(t)}$ and $\sigma_{\ln U^*(t)}$ from the FEMC approach were 0.46 and 0.43, respectively, indicating reasonable agreement between the RBSA model and the FEMC approach. Using the computed values of $\mu_{\ln U^*(t)}$ and $\sigma_{\ln U^*(t)}$ in Eq. 3.41, the probability of achieving 90% consolidation from the RBSA solution is as follows:

$$P[U(t_{D90}) \geq 0.9] = 1 - \Phi\left(\frac{\ln(2.3026) - 0.498}{0.35}\right) = 0.17 \quad (5.110)$$

The FEMC approach of the above problem yields $P[U(t_{D90}) \geq 0.9] = 0.19$ (see Fig 4.61). Again, these results demonstrate an excellent agreement between the FEMC

approach and proposed RBSA model. The fact that the obtained agreement is so good is encouraging, since it indicates that Hanbo's solution for radial consolidation is applicable to spatially variable soils if the soil properties are taken from geometric averages.

Following the procedure set out above, all subsequent statistics of the underlying normally distributed $\ln U^*(t)$ (i.e. the mean, $\mu_{\ln U^*(t)}$, and standard deviation, $\sigma_{\ln U^*(t)}$) and the probabilities of achieving 90% consolidation with time are obtained for all six proposed RBSA models over a range of random field parameters (i.e. v and θ). A comparative study between the FEMC approach and proposed RBSA model are then made to assess the capability of the proposed RBSA model in reproducing the FEMC results. The results obtained from the comparative study between each of the proposed RBSA model and their corresponding FEMC analyses are described in order below.

5.2.1.1 Comparison between FEMC and RBSA–G1C1

Employing the same illustrative example of the unit cell consolidation problem described earlier in Section 5.2.1 (i.e. $L = 1.0$ m, $r_w = 0.05$ m, $r_e = 0.85$ m, $r_s = 0.35$ m, $\mu_{k_u} = 5 \times 10^{-10}$ m/sec, $\mu_{m_{v_u}} = 1.67 \times 10^{-4}$ m²/kN, $\mu_{k_u} / \mu_{k_s} = 2.0$ and $\mu_{m_{v_u}} / \mu_{m_{v_s}} = 1.25$), both FEMC and RBSA–G1C1 are performed over the range of statistical parameters shown in Table 5.2. The agreement between the mean and standard deviation of $\ln U^*(t)$ derived via FEMC simulation and predicted via RBSA–G1C1, respectively, are examined in Figs. 5.1–5.4, in which $\mu_{\ln U^*(t)}$ and $\sigma_{\ln U^*(t)}$ are expressed as functions of the consolidation time, t .

Table 5.2: Random field parameters for the comparative study between FEMC and RBSA–G1C1

Parameter	Value
v_k (%) (both for smear and undisturbed zone)	50, 100, 200
v_{m_v} (%) (both for smear and undisturbed zone)	12.5, 25, 50
θ (m) (both for k and m_v , and smear and undisturbed zone)	0.125, 0.5, 2.0

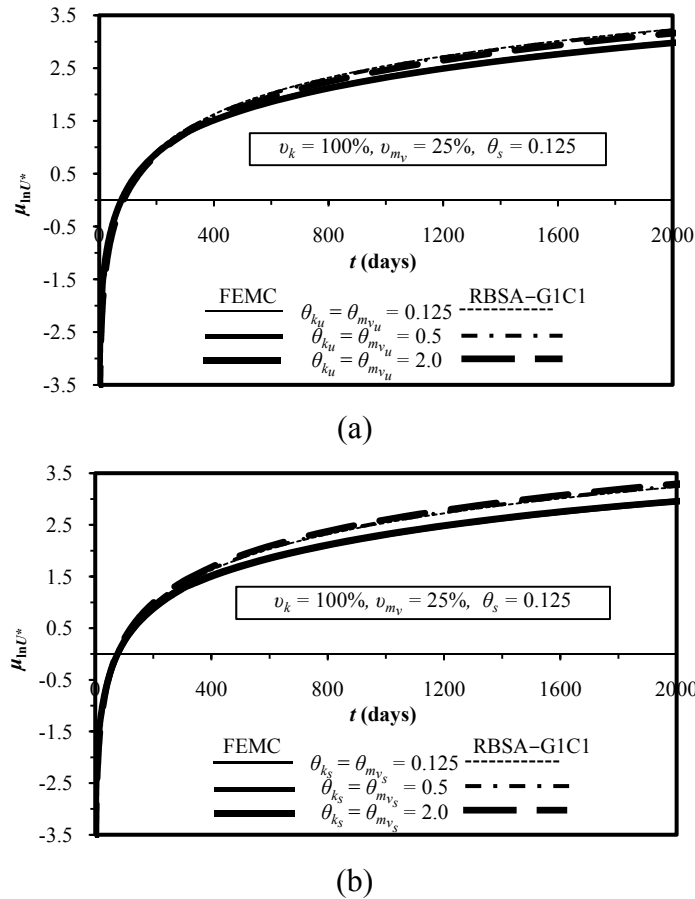


Figure 5.1: Comparison between FEMC and RBSA-G1C1 for the effect of: (a) θ_u on $\mu_{\ln U^*}$ at fixed value of $v_k = 100\%$, $v_{m_v} = 25\%$, $\theta_s = 0.125$; (b) θ_s on $\mu_{\ln U^*}$ at fixed value of $v_k = 100\%$, $v_{m_v} = 25\%$, $\theta_u = 0.125$

Fig. 5.1 shows the relationship between the estimated $\mu_{\ln U^*}$ versus the consolidation time, t , for various θ at constant $v_k = 100\%$ and $v_{m_v} = 25\%$. The effect of θ_u on $\mu_{U(pp)}$ for a constant value of $\theta_s = 0.125$ is shown Fig. 5.1(a), whereas the effect of θ_s on $\mu_{U(pp)}$ for a fixed value of $\theta_u = 0.125$ is shown in Fig. 5.1(b). It can be seen from Fig. 5.1 that the results obtained from both the FEMC approach and RBSA-G1C1 are almost identical. However, slight discrepancies in $\mu_{\ln U^*}$ obtained from these two solution approaches are found when the consolidation time t is as large as 400 days. In each solution method, it can be demonstrated that even though the values of $\mu_{\ln U^*}$ for various θ are drawn in the plot, they are represented by a single curve, implying that the obtained results at different θ are very close and cannot be distinguished. The virtually identical curves for all θ obtained from each method of analysis demonstrates that $\mu_{\ln U^*}$ is largely independent of θ . This is expected as in principle,

the correlation length θ does not affect the local average mean of the normally distributed process.

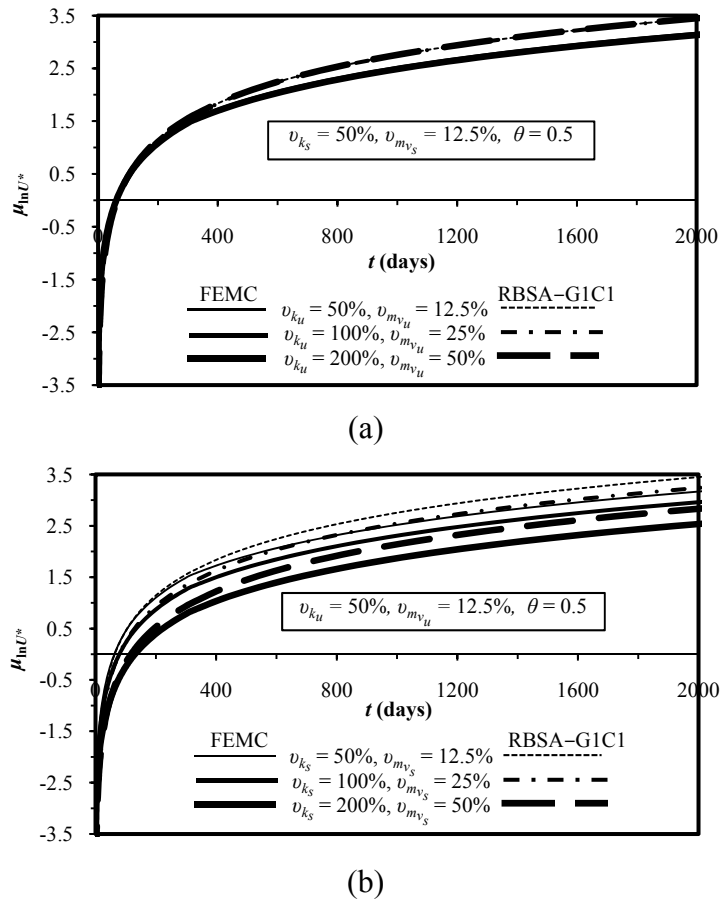
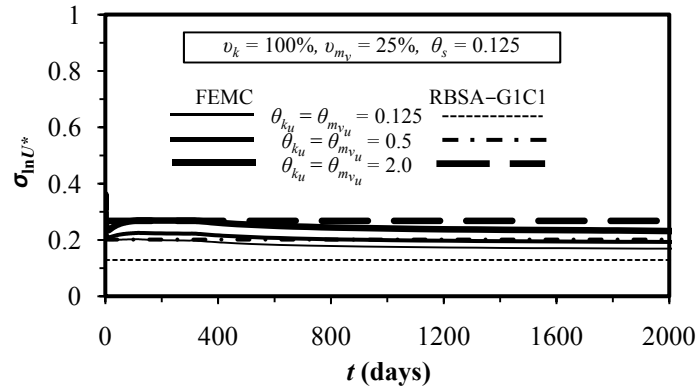


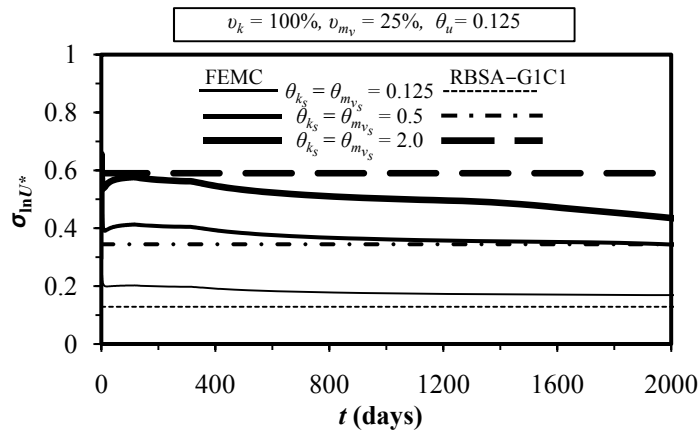
Figure 5.2: Comparison between FEMC and RBSA-G1C1 for the effect of: (a) v_u on $\mu_{\ln U^*}$ at fixed value of $v_{k_s} = 50\%$, $v_{m_{v_s}} = 12.5\%$, $\theta = 0.5$; (b) v_s on $\mu_{\ln U^*}$ at fixed value of $v_{k_u} = 50\%$, $v_{m_{v_u}} = 12.5\%$, $\theta = 0.5$

The influence of v on $\mu_{\ln U^*}$ is illustrated in Figs. 5.2(a) and (b) for a constant $\theta = 0.5$. It can be seen from Figs. 5.2 that, in general, the predicted values of $\mu_{\ln U^*}$ obtained from the RBSA model match those obtained from the FEMC approach reasonably well. In both methods, the estimated $\mu_{\ln U^*}$ decreases with the increase of v , as expected. However, the identical curves for all cases of v_u (v_{k_s} and $v_{m_{v_s}}$ are fixed at 50% and 12.5%, respectively) for both methods in Fig. 5.2(a) indicate that the effect of increasing v_u on $\mu_{\ln U^*}$ remains marginal. The effect of v_s on $\mu_{\ln U^*}$ at fixed value of $v_{k_u} = 50\%$ and $v_{m_{v_u}} = 12.5\%$ is illustrated in Fig. 5.2(b). It can be seen that, although

the agreement between the RBSA model of G1C1 and the FEMC approach is reasonable, the discrepancies in $\mu_{\ln U^*}$ obtained from these two solution approaches increase as t increases. The overall observation that can be derived from comparing the results in Figs. 5.2(a) and (b) is that, the decreasing rate of $\mu_{\ln U^*}$ is higher for an increase in v_s than v_u , implying the dominant effect of v_s on $\mu_{\ln U^*}$.



(a)



(b)

Figure 5.3: Comparison between FEMC and RBSA–G1C1 for the effect of: (a) θ_u on $\sigma_{\ln U^*}$ at fixed value of $v_k = 100\%$, $v_{m_v} = 25\%$, $\theta_s = 0.125$; (b) θ_s on $\sigma_{\ln U^*}$ at fixed value of $v_k = 100\%$, $v_{m_v} = 25\%$, $\theta_u = 0.125$

Fig. 5.3 illustrates the effect of varying θ_u and θ_s on $\sigma_{\ln U^*}$ at fixed values of $v_k = 100\%$ and $v_{m_v} = 25\%$. It can be seen that, in both methods, $\sigma_{\ln U^*}$ increases with the increase of θ , and the agreement between the FEMC approach and RBSA–G1C1 is excellent. However, the RBSA–G1C1 gives slightly lower values of $\sigma_{\ln U^*}$ than the FEMC when θ is as low as 0.5 and slightly higher values of $\sigma_{\ln U^*}$ when θ is as high as

2.0. In Fig. 5.3(a), it can be seen that similar to the effect of θ_u on $\mu_{\ln U^*}$, $\sigma_{\ln U^*}$ remains almost identical for varying θ_u with a fixed value of $\theta_{k_s} = \theta_{m_{v_s}} = 0.125$. On the other hand, the estimated $\sigma_{\ln U^*}$ for different values of θ_s is plotted in Figure 5.3(b) at a fixed value of $\theta_{k_u} = \theta_{m_{v_u}} = 0.125$. It can be seen that unlike θ_u , θ_s has a considerable impact on the estimated values of $\sigma_{\ln U^*}$.

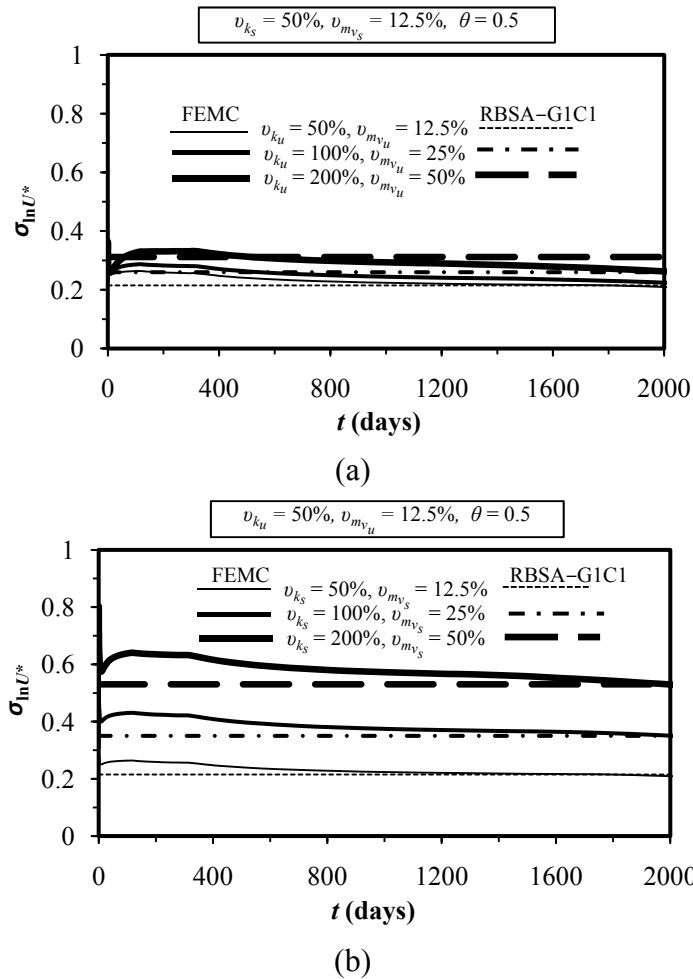


Figure 5.4: Comparison between FEMC and RBSA–G1C1 for the effect of: (a) v_u on $\sigma_{\ln U^*}$ at fixed value of $v_{k_s} = 50\%$, $v_{m_{v_s}} = 12.5\%$, $\theta = 0.5$; (b) v_s on $\sigma_{\ln U^*}$ at fixed value of $v_{k_u} = 50\%$, $v_{m_{v_u}} = 12.5\%$, $\theta = 0.5$

The effect of v on $\sigma_{\ln U^*}$ for a fixed value of $\theta = 0.5$ is shown in Fig. 5.4. It can be seen that, in general, $\sigma_{\ln U^*}$ increases with the increase of v and the agreement between the FEMC approach and RBSA model of G1C1 is extremely good. However, for a

certain v and at any particular consolidation time t , the estimated values of $\sigma_{\ln U^*}$ derived from the RBSA–G1C1 are slightly lower than those obtained from the FEMC approach. Moreover, the above observation is more accurate for v_s (Fig. 5.4(a)) than v_u (Fig. 5.4(b)). The comparison between Figs. 5.4(a) and (b) reveals that $\sigma_{\ln U^*}$ increases significantly with the increase of v_s , whereas there is only a slight increase in $\sigma_{\ln U^*}$ for the same amount of increase in v_u .

Having established, with reasonable accuracy, the distribution parameters of $\ln U^*(t)$ from the RBSA–G1C1 model, the capability of the derived parameters $\mu_{\ln U^*}$ and $\sigma_{\ln U^*}$ for accurately estimating the probability of achieving 90% consolidation, $P[U \geq U_{90}]$, at any specified time can be tested. The agreement between the probabilities of achieving 90% consolidation estimated via the FEMC simulation and predicted via RBSA–G1C1 are examined in Figs. 5.5–5.6, in which $P[U \geq U_{90}]$ is expressed as a function of the consolidation time, t .

In Fig 5.5, the FEMC approach and proposed RBSA–G1C1 model show good agreement for various θ_u and θ_s at constant values of $v_k = 100\%$ and $v_m = 25\%$. In both methods, it can be seen that all curves crossover at a critical value of $P[U \geq U_{90}] \approx 50\%$ where $P[U \geq U_{90}]$ becomes independent of θ . At a certain t past the crossover point, opposite behaviour for $P[U \geq U_{90}]$ with respect to the dependence on θ is observed. At a certain time prior to the crossover point, $P[U \geq U_{90}]$ increases with the increase of θ , whereas after the crossover point it decreases with the increase of θ . Although the overall agreement between the two solution methods in terms of estimated $P[U \geq U_{90}]$ is reasonably well, slight discrepancies in $P[U \geq U_{90}]$ are found when θ is as small as 0.5. For any $P[U \geq U_{90}] \geq 50\%$, the estimated values of $P[U \geq U_{90}]$ derived from the RBSA–G1C1 are slightly higher (unconservative) than those obtained from the FEMC approach.

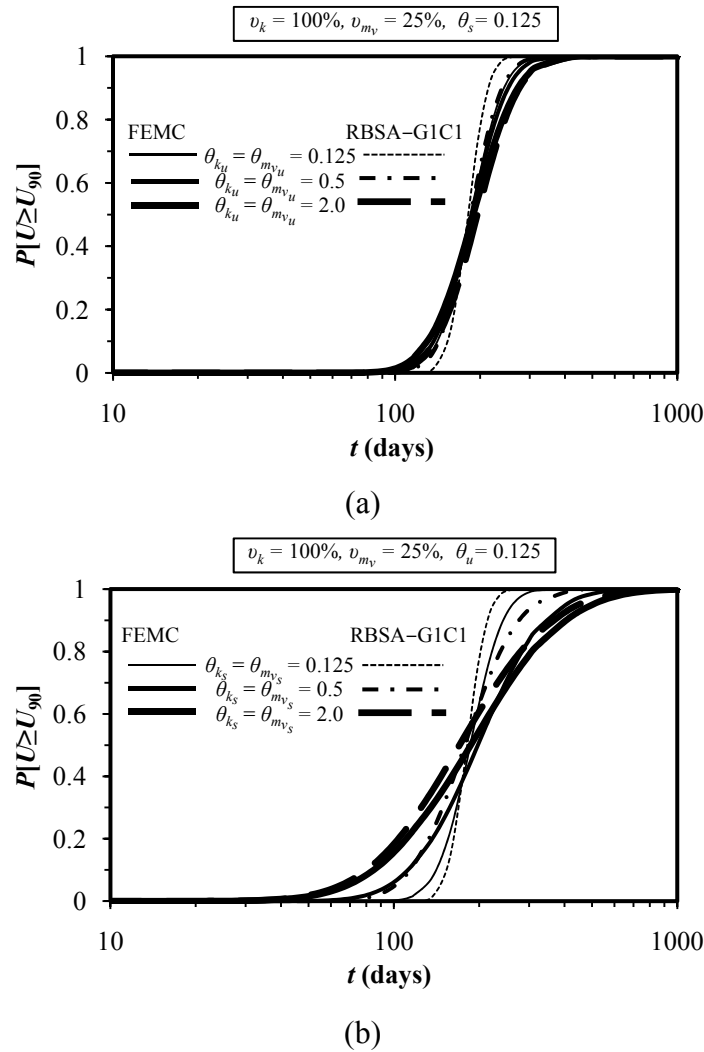
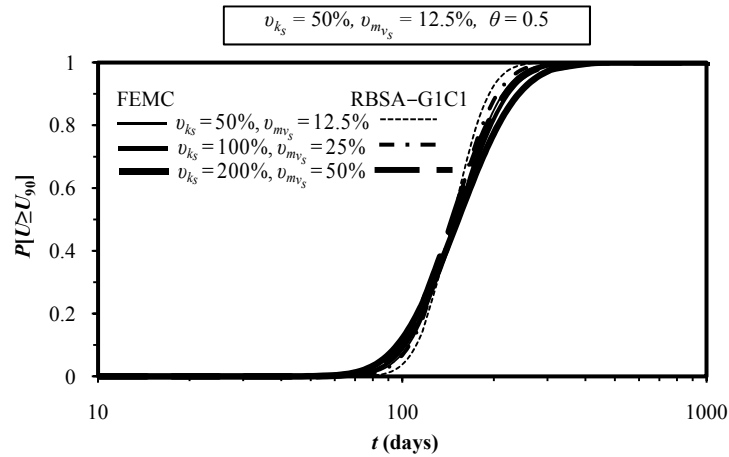


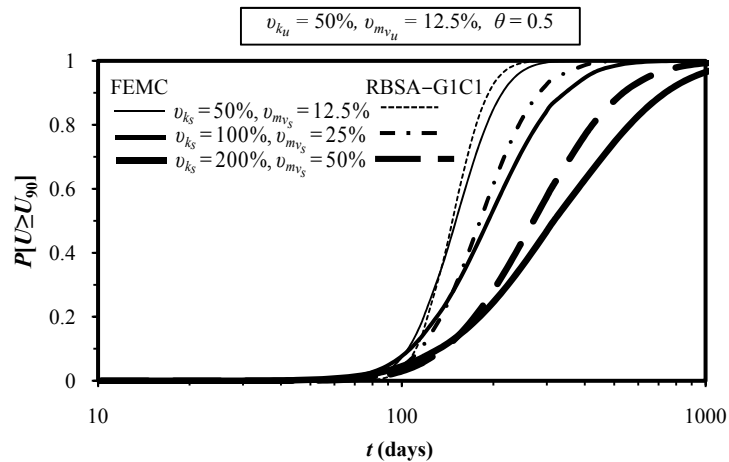
Figure 5.5: Comparison between FEMC and RBSA–G1C1 for the effect of: (a) θ_u on $P[U \geq U_{90}]$ at fixed value of $\nu_k = 100\%$, $\nu_{m_v} = 25\%$, $\theta_s = 0.125$; (b) θ_s on $P[U \geq U_{90}]$ at fixed value of $\nu_k = 100\%$, $\nu_{m_v} = 25\%$, $\theta_u = 0.125$

The effect of increasing ν_u on $P[U \geq U_{90}]$ at a fixed value of $\theta = 0.5$ is illustrated in Fig. 5.6(a). It can be seen that the predicted $P[U \geq U_{90}]$ obtained from the proposed RBSA–G1C1 agrees very well with those obtained from the FEMC approach for all cases of ν_u (ν_{k_s} and $\nu_{m_{v_s}}$ are fixed at 50% and 12.5%, respectively). The virtually identical curves of $P[U \geq U_{90}]$ in Fig. 5.6(a) for all ν_u indicate that $P[U \geq U_{90}]$ is largely independent of ν_u . Fig. 5.6(b) illustrates the effect of ν_s on $P[U \geq U_{90}]$ at a fixed value of $\theta = 0.5$. Although the overall agreement between the predicted $P[U \geq U_{90}]$ by RBSA–G1C1 and the obtained $P[U \geq U_{90}]$ by the FEMC approach is reasonable, the caveat, however, is that the proposed RBSA–G1C1 model gives

unconservative estimate of $P[U \geq U_{90}]$. This higher values of predicted $P[U \geq U_{90}]$ given by the proposed RBSA–G1C1 is due to the higher predicted $\mu_{\ln U^*}$, as shown in Fig. 5.2(b). Fig. 5.6 also illustrates that the increasing rate of $P[U \geq U_{90}]$ with respect to t decreases as v decreases and this effect is more pronounced for an increase in v_s than v_u . What this means is that the probabilistic behaviour of soil consolidation is governed by v_s rather than v_u .



(a)



(b)

Figure 5.6: Comparison between FEMC and RBSA–G1C1 for the effect of: (a) v_u on $P[U \geq U_{90}]$ at fixed value of $v_{k_s} = 50\%$, $v_{m_{v_s}} = 12.5\%$, $\theta = 0.5$; (b) v_s on $P[U \geq U_{90}]$ at fixed value of $v_{k_u} = 50\%$, $v_{m_{v_u}} = 12.5\%$, $\theta = 0.5$

5.2.1.2 Comparison between FEMC and RBSA–G1C2

As mentioned earlier, the proposed RBSA–G1C2 deals with both random k and m_v ; however, no smear effect is considered in this case. Accordingly, an illustrative example of a unit cell consolidation problem of $L = 1.0$ m, $r_w = 0.05$ m, $r_e = 0.85$ m, $\mu_k = 5 \times 10^{-10}$ m/sec and $\mu_{m_v} = 1.67 \times 10^{-4}$ m²/kN is considered to examine the degree of agreement between the proposed RBSA–G1C2 model and FEMC approach. Both the FEMC and RBSA–G1C2 are performed over the range of the statistical parameters shown in Table 5.3. The agreement between $\mu_{\ln U^*}$, $\sigma_{\ln U^*}$ and $P[U \geq U_{90}]$ derived via the FEMC simulation and predicted via the RBSA–G1C2 are examined in Figs. 5.7–5.9, in which $\mu_{\ln U^*}$, $\sigma_{\ln U^*}$ and $P[U \geq U_{90}]$ are expressed as functions of the consolidation time, t .

Table 5.3: Random field parameters for the comparative study between FEMC and RBSA–G1C2

Parameter	Value
v_k (%)	50, 100, 200
v_{m_v} (%)	12.5, 25, 50
θ (m) (both for k and m_v)	0.25, 1.0, 4.0

Fig. 5.7(a) shows the relationship between the estimated $\mu_{\ln U^*}$ versus the dimensionless consolidation time, t , for various θ at constant values of $v_k = 100\%$ and $v_{m_v} = 25\%$. In both methods, the estimated values of $\mu_{\ln U^*}$ are almost identical for all cases of θ , implying that $\mu_{\ln U^*}$ is largely independent of θ , which is in accordance with the random field theory. It can be seen that $\mu_{\ln U^*}$ obtained from both the FEMC approach and RBSA–G1C2 model are in a good agreement. However, the RBSA–G1C2 model gives slightly higher $\mu_{\ln U^*}$ than the FEMC when t is as high as 500 days.

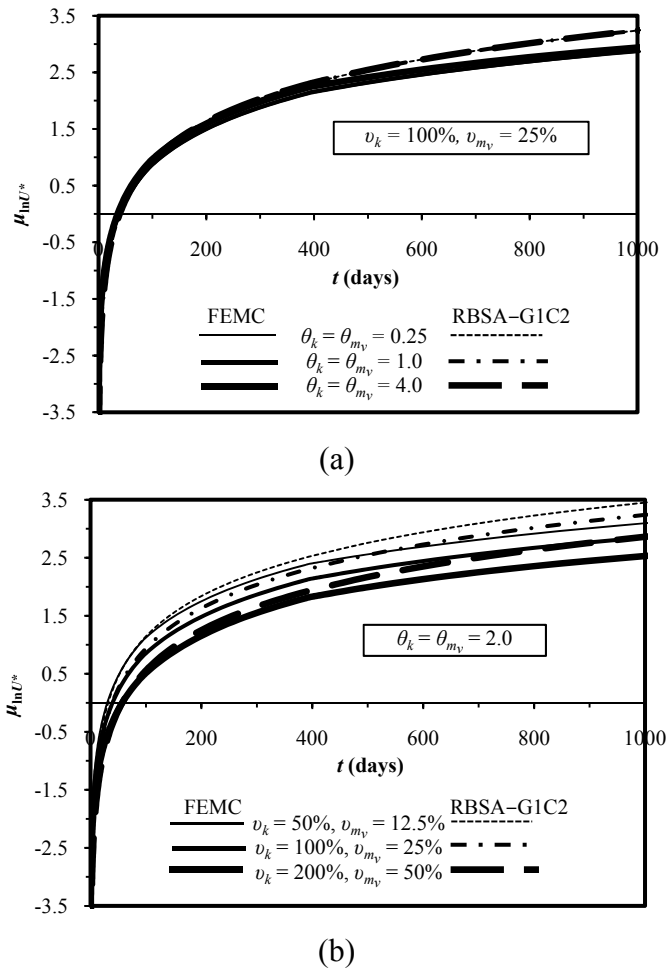


Figure 5.7: Comparison between FEMC and RBSA–G1C2 for the effect of: (a) θ on $\mu_{\ln U^*}$ for $v_k = 100\%$, $v_{m_v} = 25\%$; (b) v on $\mu_{\ln U^*}$ for $\theta = 2.0$

The effect of v on $\mu_{\ln U^*}$ for a constant value of $\theta = 2.0$ is shown Fig. 5.7(b). It can be seen that at any particular t , the estimated $\mu_{\ln U^*}$ decreases with the increase in v for both solution methods. In general, the predicted $\mu_{\ln U^*}$ by the RBSA–G1C2 is higher than the estimated $\mu_{\ln U^*}$ by the FEMC approach. However, it is interesting to see that the degree of agreement between the RBSA–G1C2 and the FEMC boost with increasing v . In other words, the discrepancy in $\mu_{\ln U^*}$ obtained from the two solution approaches decreases with increasing v .

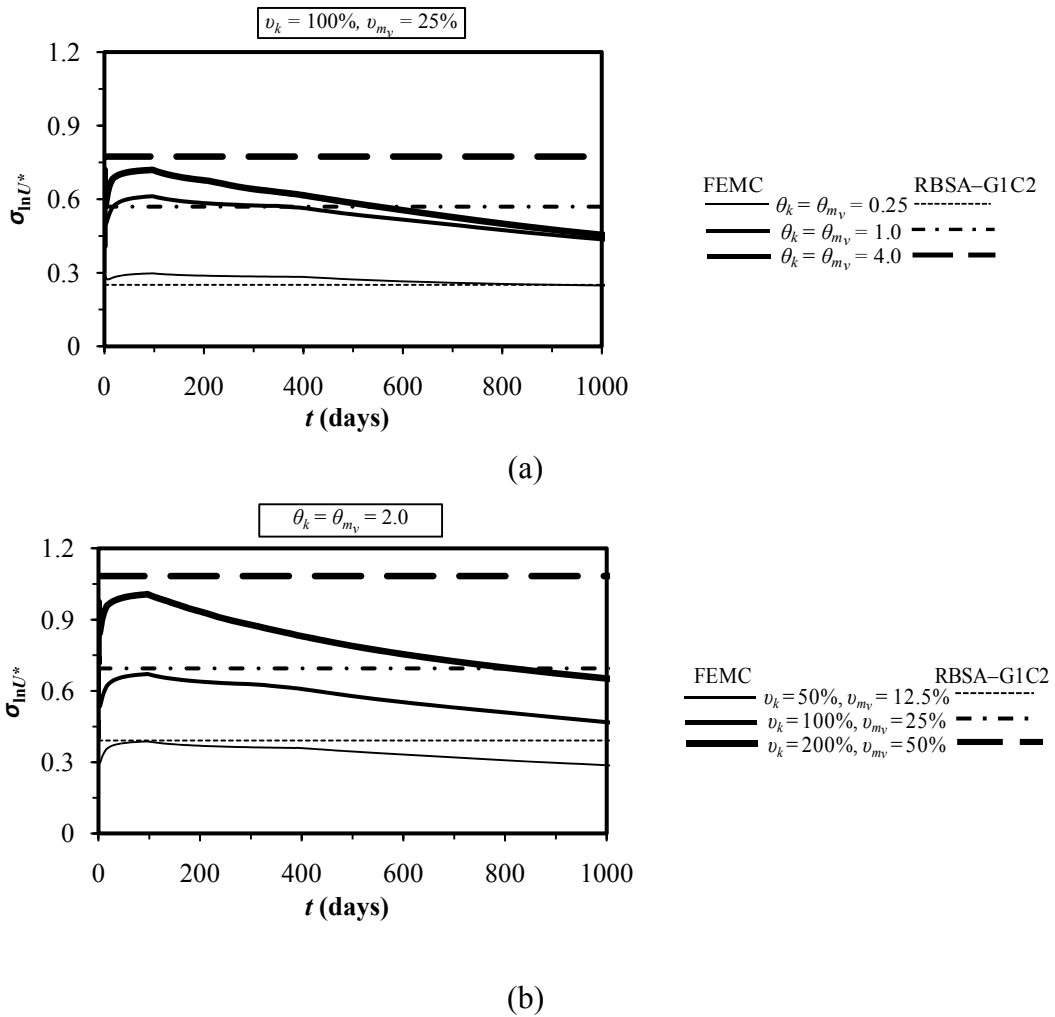


Figure 5.8: Comparison between FEMC and RBSA-G1C2 for the effect of: (a) θ on $\sigma_{\ln U^*}$ for $v_k = 100\%$, $v_{m_v} = 25\%$; (b) v on $\sigma_{\ln U^*}$ for $\theta = 2.0$

The agreement between the FEMC approach and RBSA-G1C2 model is further illustrated via matching the estimated $\sigma_{\ln U^*}$ at different values of θ and constant values of $v_k = 100\%$ and $v_{m_v} = 25\%$ (see Fig. 5.8(a)). It can be seen that $\sigma_{\ln U^*}$ increases with the increase of θ , and apart from some slight discrepancies for large θ (i.e. $\theta_k = \theta_{m_v} = 4.0$), the agreement between the FEMC approach and RBSA-G1C2 is reasonable. The effect of v on $\sigma_{\ln U^*}$ for a fixed value of $\theta = 2.0$ is shown in Fig. 5.8(b). It can be seen that, in general, $\sigma_{\ln U^*}$ increases with the increase of v and the agreement between the FEMC approach and RBSA-G1C2 is reasonably well. The considerable discrepancies in $\sigma_{\ln U^*}$ can be only found when $v_k = 200\%$ and $v_{m_v} = 50\%$.

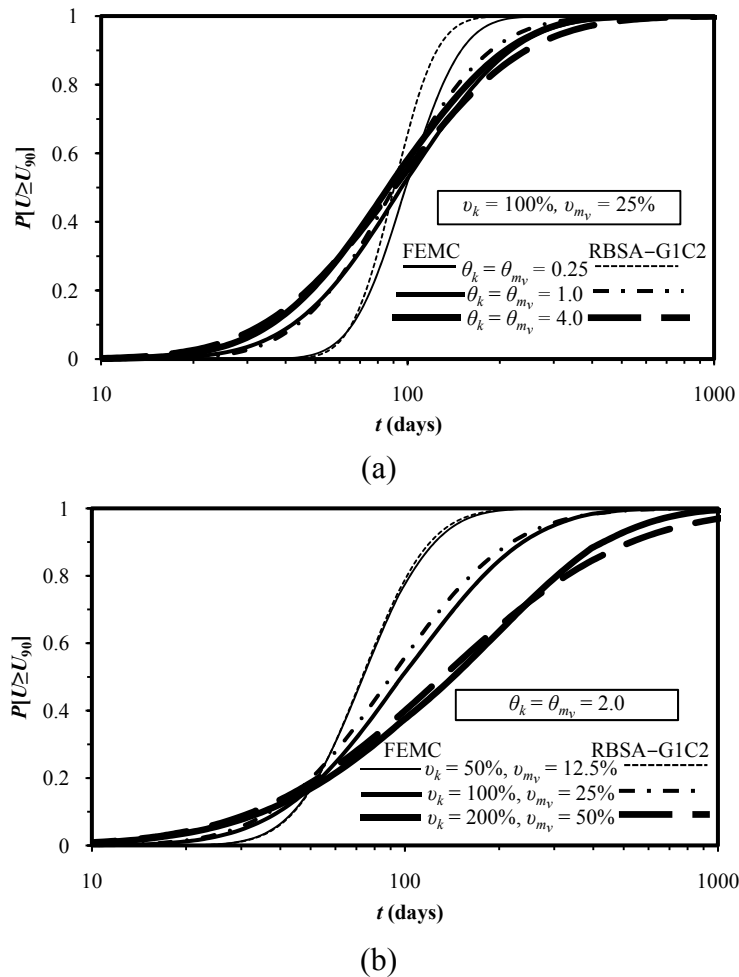


Figure 5.9: Comparison between FEMC and RBSA–G1C2 for the effect of: (a) θ on $P[U \geq U_{90}]$ for $v_k = 100\%$, $v_{m_v} = 25\%$; (b) v on $P[U \geq U_{90}]$ for $\theta = 2.0$

The agreement between the FEMC approach and RBSA of G1C2 model in terms of $P[U \geq U_{90}]$ is examined in Fig. 5.9. In general, the FEMC approach and proposed RBSA–G1C2 show good agreement for various θ at constant values of $v_k = 100\%$ and $v_{m_v} = 25\%$, as shown in Fig. 5.9(a). However, one particular note in this figure is that the RBSA–G1C2 model over-predicts $P[U \geq U_{90}]$ compared to the FEMC when θ is as low as 0.25. Fig. 5.9(b) highlights the effect of v on $P[U \geq U_{90}]$ at a fixed value of $\theta = 2.0$. It can be seen that the predicted $P[U \geq U_{90}]$ by the proposed RBSA–G1C2 agrees very well with those obtained from the FEMC approach.

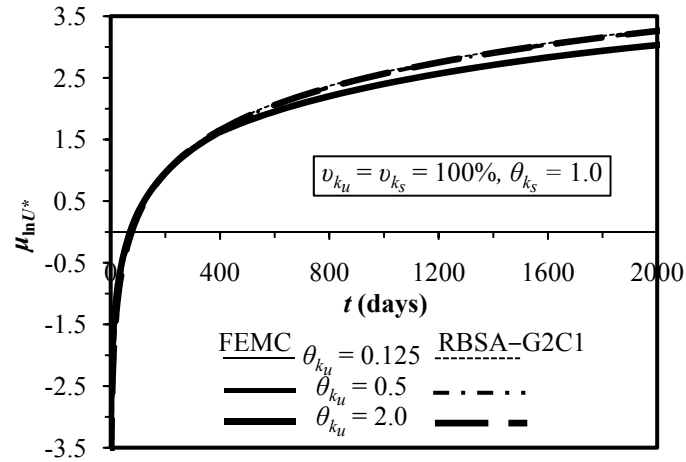
5.2.1.3 Comparison between FEMC and RBSA–G2C1

The proposed RBSA model of G2C1 deals with spatially variable k including the smear effect. In this case, it is assumed that m_v remains constant across the soil mass. In order to assess the capability of the proposed RBSA model G2C1 in reproducing the FEMC results, an illustrative example of an axisymmetric unit cell of $L = 1.0$ m, $r_w = 0.05$ m, $r_e = 0.85$ m, $r_s = 0.35$ m, $\mu_{k_u} = 5 \times 10^{-10}$ m/sec, $\mu_{k_u} / \mu_{k_s} = 2.0$ is considered. Constant m_v value of 1.67×10^{-4} m²/kN is used throughout the unit cell. Both the FEMC and RBSA–G2C1 are carried out over the range of the statistical parameters shown in Table 5.4. The agreement between $\mu_{\ln U^*}$, $\sigma_{\ln U^*}$ and $P[U \geq U_{90}]$ derived via the FEMC simulation and predicted using the RBSA–G2C1 are examined in Figs. 5.10–5.15.

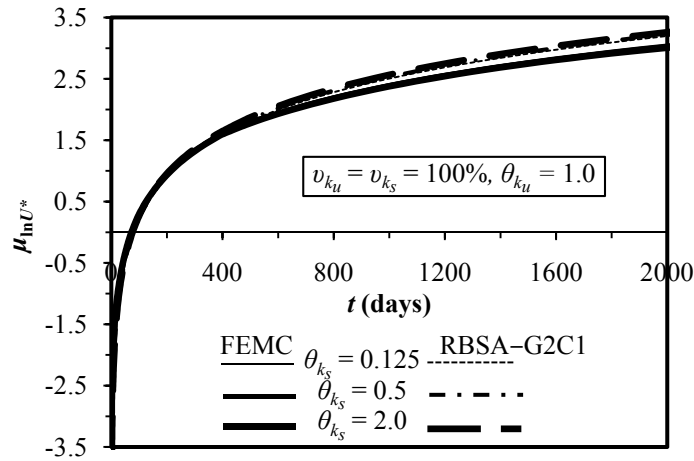
Table 5.4: Random field parameters for the comparative study between FEMC and RBSA–G2C1

Parameter	Value
ν_k (%) (both for undisturbed and smear zone)	50, 100, 200
θ_k (m) (both for undisturbed and smear zone)	0.25, 0.5, 1.0, 2.0

The effect of varying θ_{k_u} and θ_{k_s} on $\mu_{\ln U^*}$ at fixed values of $\nu_{k_u} = \nu_{k_s} = 100\%$ is examined in Fig. 5.10. It can be seen that $\mu_{\ln U^*}$ obtained from both the FEMC approach and RBSA–G2C1 model are almost identical, implying an excellent agreement between the two solution methods. In each solution approach, the single curve of $\mu_{\ln U^*}$ for all cases of θ_k indicates that the mean degree of consolidation, $\mu_{\ln U^*}$, is more or less independent of θ_k . A similar trend of $\mu_{\ln U^*}$ with respect to the dependence of θ is also obtained for the RBSA models of G1C1 and G1C2.



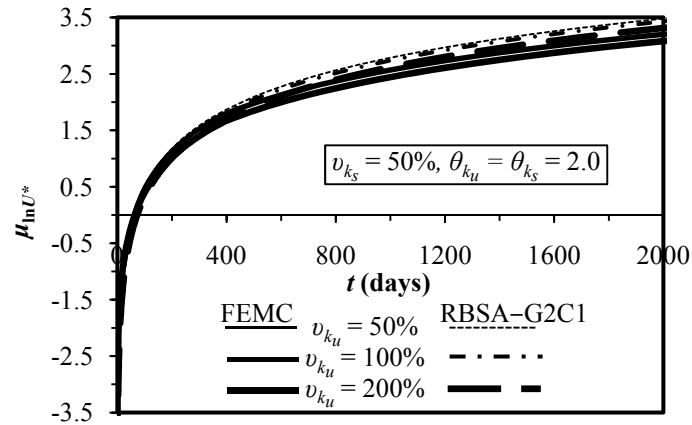
(a)



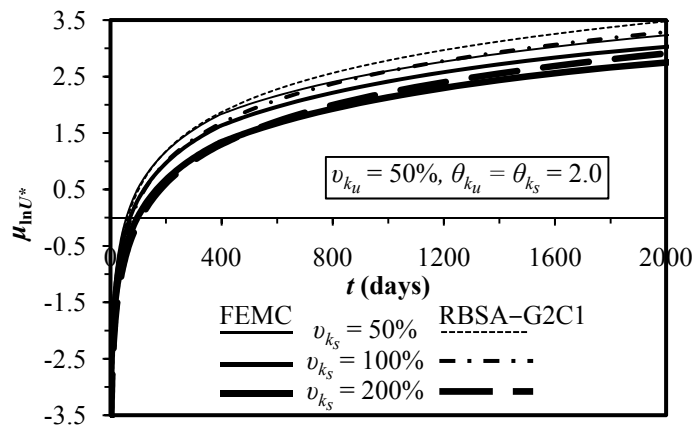
(b)

Figure 5.10: Comparison between FEMC and RBSA–G2C1 for the effect of: (a) θ_{k_u} on $\mu_{\ln U^*}$ at fixed value of $\nu_{k_u} = \nu_{k_s} = 100\%$, $\theta_{k_s} = 1.0$; (b) θ_{k_s} on $\mu_{\ln U^*}$ at fixed value of $\nu_{k_u} = \nu_{k_s} = 100\%$, $\theta_{k_u} = 1.0$

The influence of ν_k on $\mu_{\ln U^*}$ is illustrated in Figs 5.11(a) and (b) for a constant $\theta_{k_u} = \theta_{k_s} = 1.0$. It can be seen from Fig. 5.11 that, in general, the predicted values of $\mu_{\ln U^*}$ obtained from the RBSA model of G2C1 match those obtained from the FEMC approach very well. In both methods, the estimated $\mu_{\ln U^*}$ decreases with the increase of ν_{k_s} , as expected. However, the effect of increasing ν_{k_u} on $\mu_{\ln U^*}$ is marginal (see Fig. 5.11(a)), whereas the effect of increasing ν_{k_s} on $\mu_{\ln U^*}$ is significant (see Fig. 5.11(b)).



(a)



(b)

Figure 5.11: Comparison between FEMC and RBSA–G2C1 for the effect of: (a) v_{k_u} on $\mu_{\ln U^*}$ at fixed value of $v_{k_s} = 50\%$, $\theta_{k_u} = \theta_{k_s} = 2.0$; (b) v_{k_s} on $\mu_{\ln U^*}$ at fixed value of $v_{k_u} = 50\%$, $\theta_{k_u} = \theta_{k_s} = 2.0$

Fig. 5.12 demonstrates the agreement between $\sigma_{\ln U^*}$ estimated via the FEMC and RBSA model of G2C1, for various values of θ_{k_u} and θ_{k_s} at a fixed value of $v_{k_u} = v_{k_s} = 100\%$. In each solution approach, the single curve of $\sigma_{\ln U^*}$ in Fig. 5.12(a) for all cases of θ_{k_u} indicates that $\sigma_{\ln U^*}$ is very much independent of θ_k . It can also be concluded that the agreement between the FEMC approach and RBSA–G2C1 for the effect of θ_{k_u} on $\sigma_{\ln U^*}$ is very good. The effect of θ_{k_s} on $\sigma_{\ln U^*}$ at a fixed value of $\theta_{k_u} = 1.0$ is illustrated in Fig. 5.12(b). It can be seen that, although there is a slight discrepancy in $\sigma_{\ln U^*}$ obtained from the FEMC and RBSA–G2C1, the overall agreement between the two solution approaches is very good.

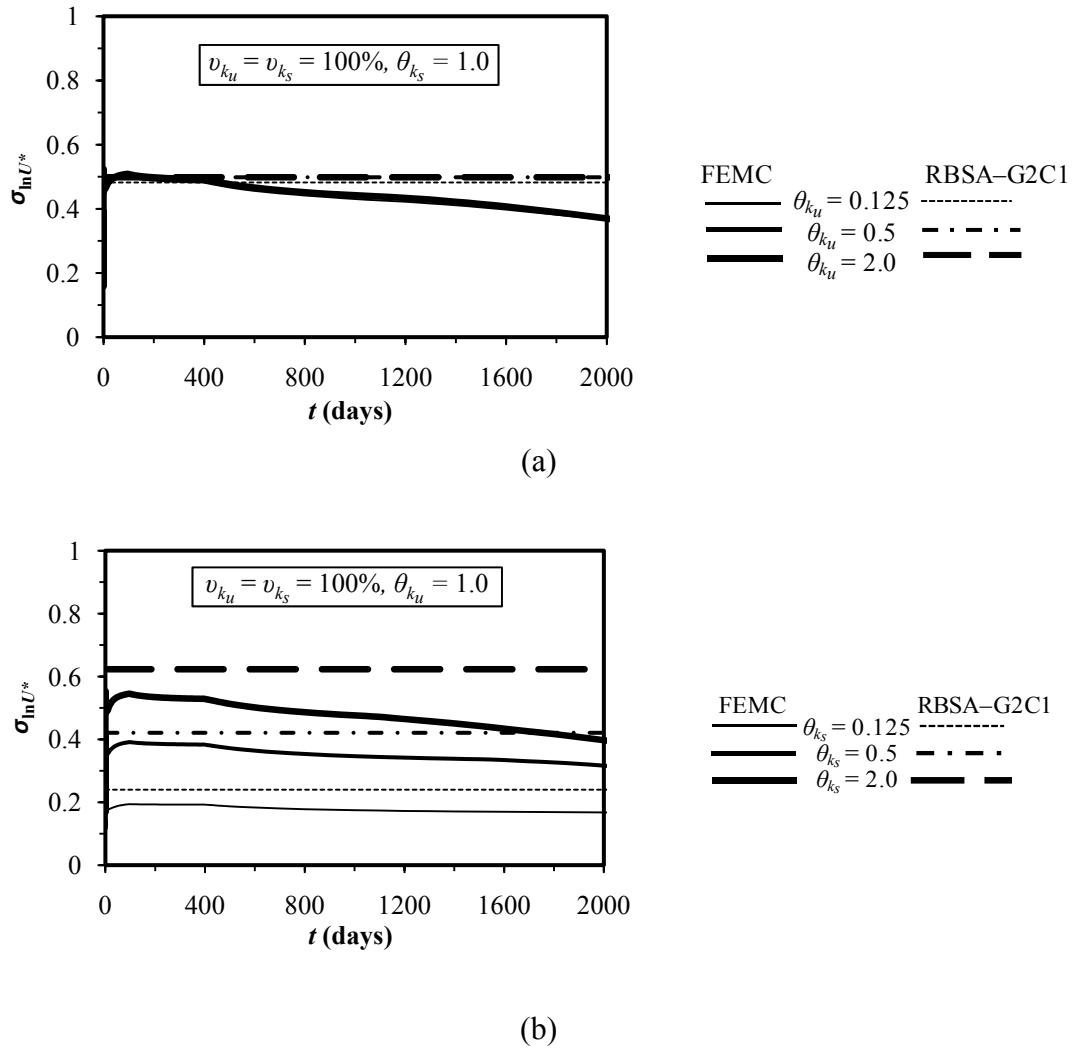
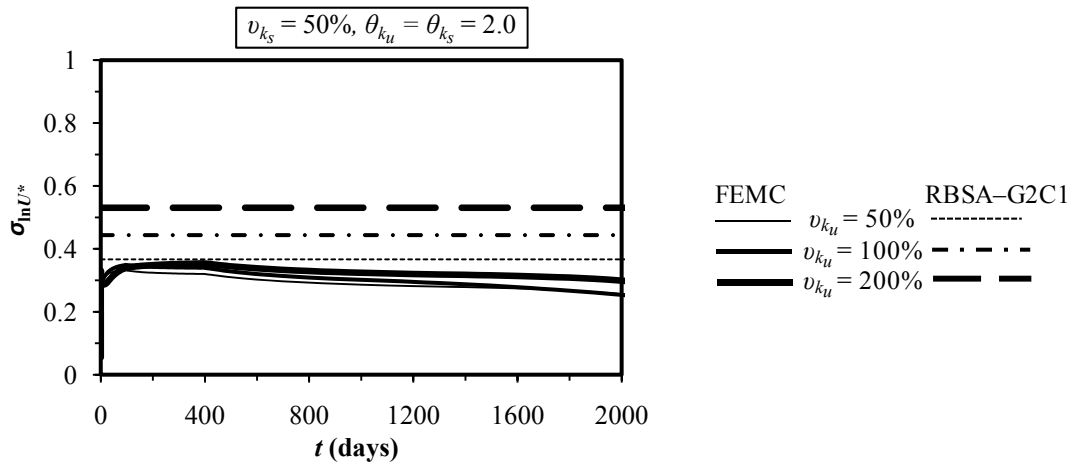


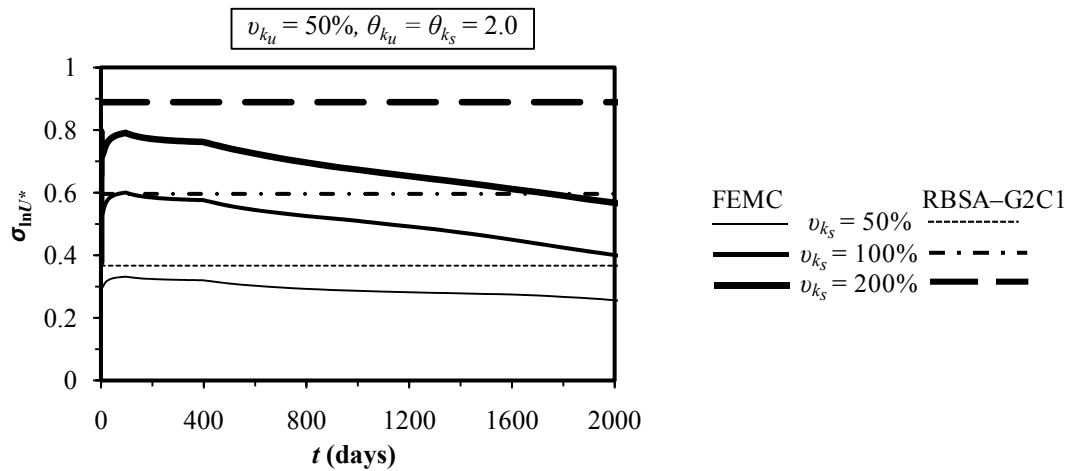
Figure 5.12: Comparison between FEMC and RBSA-G2C1 for the effect of: (a) θ_{k_u} on $\sigma_{\ln U^*}$ at fixed value of $\nu_{k_u} = \nu_{k_s} = 100\%$, $\theta_{k_s} = 1.0$; (b) θ_{k_s} on $\sigma_{\ln U^*}$ at fixed value of $\nu_{k_u} = \nu_{k_s} = 100\%$, $\theta_{k_u} = 1.0$

The influence of ν_{k_u} and ν_{k_s} on $\sigma_{\ln U^*}$ at a fixed value of $\theta_{k_u} = \theta_{k_s} = 2.0$ is highlighted in Fig. 5.13. For a fixed value of ν_{k_s} ($\nu_{k_s} = 50\%$ in this case), increasing ν_{k_u} has little to no effect on $\sigma_{\ln U^*}$, as shown in Fig. 5.13(a). This observation is particularly true for the FEMC approach. Unlike the FEMC approach, the predicted $\sigma_{\ln U^*}$ by the RBSA-G2C1 increases marginally with increasing ν_{k_u} . Accordingly, the discrepancy in $\sigma_{\ln U^*}$ obtained from the RBSA-G2C1 and FEMC increases with increasing ν_{k_u} . The effect of ν_{k_s} on $\sigma_{\ln U^*}$ at a fixed value of $\nu_{k_u} = 50\%$ is illustrated in Fig. 5.13(b). In both methods, it can be seen that, $\sigma_{\ln U^*}$ increases significantly with

the increase of ν_{k_s} . For each prescribed values of ν_{k_s} , the RBSA-G2C1 gives slightly higher values of $\sigma_{\ln U^*}$ than those obtained from the FEMC method. However, overall, the predicted $\sigma_{\ln U^*}$ is seen to be in good agreement with the estimated $\sigma_{\ln U^*}$ for all ν_{k_s} .



(a)



(b)

Figure 5.13: Comparison between FEMC and RBSA-G2C1 for the effect of: (a) ν_{k_u} on $\sigma_{\ln U^*}$ at fixed value of $\nu_{k_s} = 50\%$, $\theta_{k_u} = \theta_{k_s} = 2.0$; (b) ν_{k_s} on $\sigma_{\ln U^*}$ at fixed value of $\nu_{k_u} = 50\%$, $\theta_{k_u} = \theta_{k_s} = 2.0$

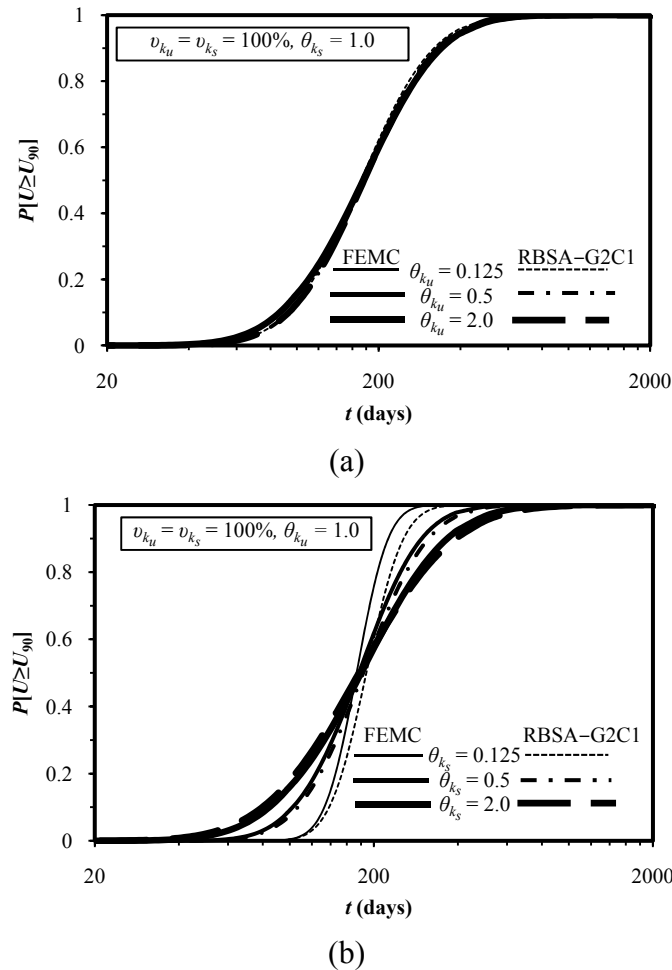
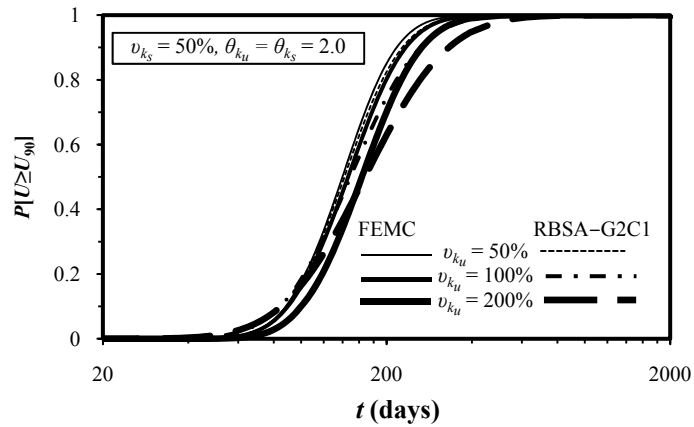


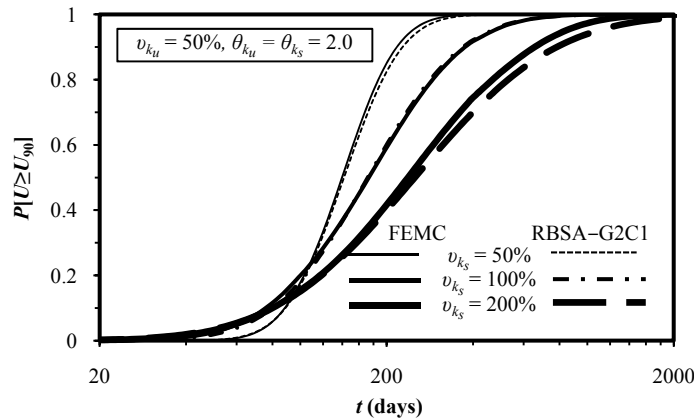
Figure 5.14: Comparison between FEMC and RBSA-G2C1 for the effect of: (a) θ_{k_u} on $P[U \geq U_{90}]$ at fixed value of $v_{k_u} = v_{k_s} = 100\%$, $\theta_{k_s} = 1.0$; (b) θ_{k_s} on $P[U \geq U_{90}]$ at fixed value of $v_{k_u} = v_{k_s} = 100\%$, $\theta_{k_u} = 1.0$

Fig. 5.14 illustrates the effects of θ_k on $P[U \geq U_{90}]$ at a fixed value of $v_{k_u} = v_{k_s} = 100\%$. In Fig. 5.14(a), the influence of θ_{k_u} on $P[U \geq U_{90}]$ is shown at $\theta_{k_s} = 1.0$. In both methods, almost identical curves of $P[U \geq U_{90}]$ for all θ_{k_u} are obtained indicating that θ_{k_u} has little or no impact on the probabilistic behaviour of the degree of consolidation. The results also indicate that the FEMC approach and the proposed RBSA model of G2C1 show good agreement for various θ_{k_u} . On the other hand, the estimated $P[U \geq U_{90}]$ for different values of θ_{k_s} is plotted in Fig. 5.14(b) at a fixed value of $\theta_{k_u} = 1.0$. It can be seen that, unlike θ_{k_u} , θ_{k_s} has a considerable impact on the estimated values of $P[U \geq U_{90}]$. The agreement between the two solution

methods in terms of estimated $P[U \geq U_{90}]$ is exceptionally good when θ_{k_s} is as high as 0.5. However, slight discrepancies in $P[U \geq U_{90}]$ obtained from the two solution approaches are found when θ_{k_s} is as small as 0.125. For any $P[U \geq U_{90}] \geq 50\%$, the estimated values of $P[U \geq U_{90}]$ derived from the RBSA–G2C1 are slightly lower (conservative) than those obtained from the FEMC approach.



(a)



(b)

Figure 5.15: Comparison between FEMC and RBSA–G2C1 for the effect of: (a) v_{k_u} on $P[U \geq U_{90}]$ at fixed value of $v_{k_s} = 50\%$, $\theta_{k_u} = \theta_{k_s} = 2.0$; (b) v_{k_s} on $P[U \geq U_{90}]$ at fixed value of $v_{k_u} = 50\%$, $\theta_{k_u} = \theta_{k_s} = 2.0$

The effect of increasing v_k on $P[U \geq U_{90}]$ at a fixed value of $\theta_{k_u} = \theta_{k_s} = 2.0$ is investigated in Fig. 5.15. It can be seen that the predicted $P[U \geq U_{90}]$ by the proposed RBSA–G2C1 agrees very well with those obtained from the FEMC approach, for all cases of v_{k_u} (see Fig. 5.15(a)) and v_{k_s} (see Fig. 5.15(b)). However, slight

discrepancies in $P[U \geq U_{90}]$ obtained from the two solution approaches are found only when v_k is as high as 200%. This observation is particularly true for v_{k_u} in Fig. 5.15(a) rather than v_{k_s} in Fig. 5.15(b).

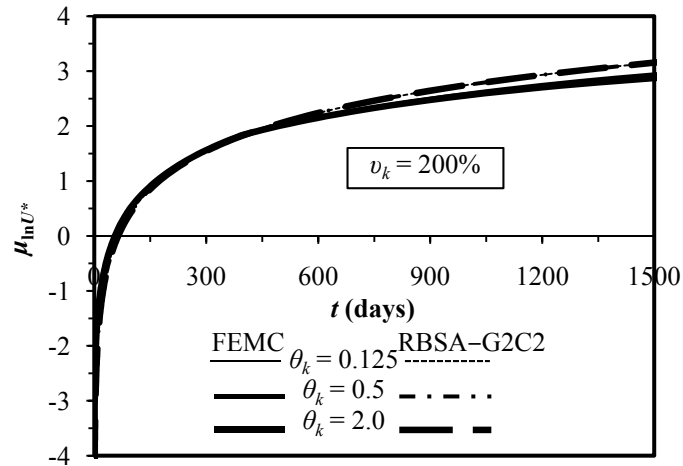
5.2.1.4 Comparison between FEMC and RBSA–G2C2

In the proposed RBSA model of G2C2, the smear effect is excluded and only k is considered as spatially random. For the purpose of comparing the proposed RBSA–G2C2 with the FEMC, an illustrative example of an axisymmetric unit cell consolidation problem of $L = 1.0$ m, $r_w = 0.05$ m, $r_e = 0.85$ m and $\mu_k = 5 \times 10^{-10}$ m/sec is considered. Constant m_v value of 1.67×10^{-4} m²/kN is provided across the soil mass. Both the FEMC and RBSA–G2C2 are performed over the range of the statistical parameters as shown in Table 5.5. The agreement between $\mu_{\ln U^*}$, $\sigma_{\ln U^*}$ and $P[U \geq U_{90}]$ estimated by FEMC simulation and predicted by RBSA–G2C2 are investigated in Figs. 5.16–5.18.

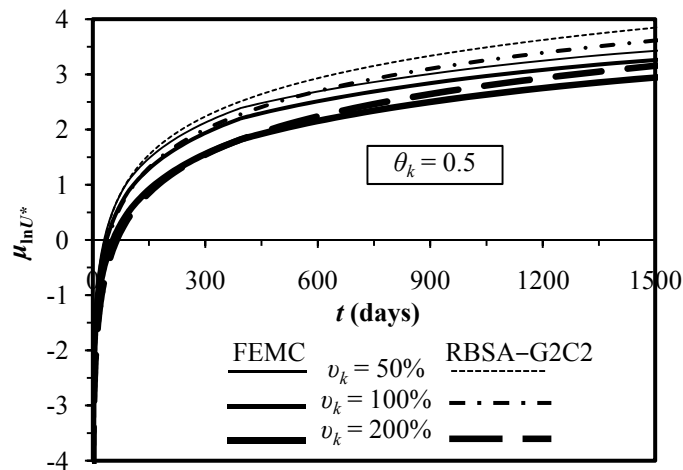
Table 5.5: Random field parameters for the comparative study between FEMC and RBSA–G2C2

Parameter	Value
v_k (%)	50, 100, 200
θ_k (m)	0.25, 0.5, 2.0

Fig. 5.16(a) investigates the effect of increasing θ_k on $\mu_{\ln U^*}$ at a fixed value of $v_k = 100\%$. It can be seen that $\mu_{\ln U^*}$ obtained from both the FEMC approach and RBSA–G2C2 model are almost identical and show an excellent agreement. The influence of v_k on $\mu_{\ln U^*}$ is illustrated in Fig. 5.16(b) for constant $\theta_k = 0.5$. It can be seen that, in general, the predicted values of $\mu_{\ln U^*}$ obtained from the RBSA–G2C2 model match those obtained from the FEMC approach reasonably well. However, the RBSA–G2C2 slightly over-predicts $\mu_{\ln U^*}$, and this over-prediction becomes less pronounced as v_k increases. In both methods, the estimated $\mu_{\ln U^*}$ decreases with the increase of v_k , as expected.



(a)



(b)

Figure 5.16: Comparison between FEMC and RBSA–G2C2 for the effect of: (a) θ on $\mu_{\ln U^*}$ for $v_k = 200\%$; (b) v on $\mu_{\ln U^*}$ for $\theta = 0.5$

The agreement between the FEMC approach and RBSA–G2C2 model in terms of the estimated $\sigma_{\ln U^*}$ at different values of θ_k and v_k is shown in Fig. 5.17. It can be seen that, apart from the considerable discrepancy in Fig. 5.17(a) for $\theta_k = 2.0$, the agreement between the FEMC approach and RBSA–G2C2 model is reasonably well and shows good compliance.

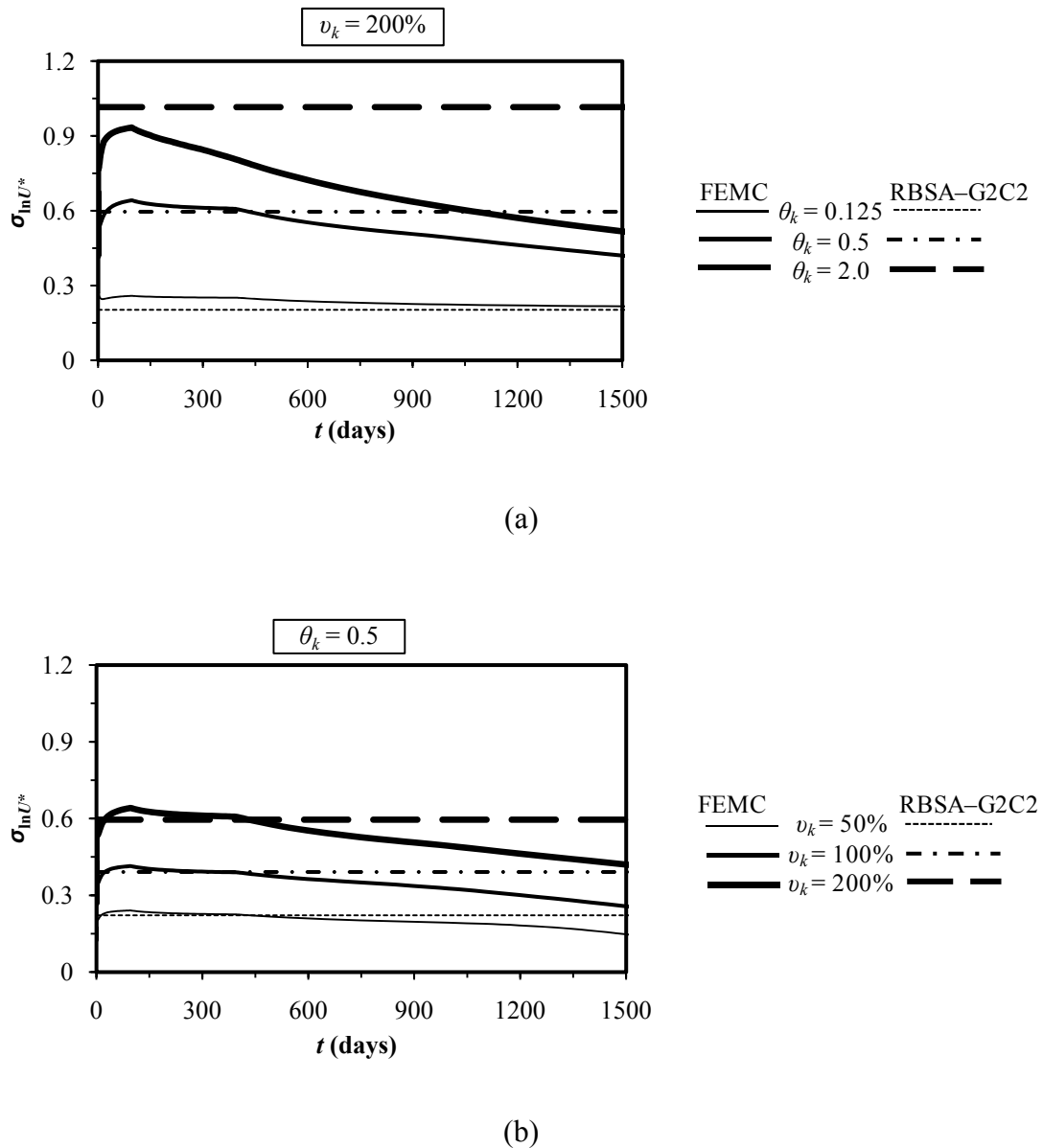


Figure 5.17: Comparison between FEMC and RBSA-G2C2 for the effect of: (a) θ on $\sigma_{\ln U^*}$ for $v_k = 200\%$; (b) v on $\sigma_{\ln U^*}$ for $\theta = 0.5$

Fig. 18(a) depicts the compliance between the FEMC approach and proposed RBSA-G2C2 model for various θ_k with constant $v_k = 100\%$, and the results show good agreement. One particular note in Fig. 18(a) is that, at any $P[U \geq U_{90}] \geq 50\%$, the RBSA-G2C2 model tends to give unconservative estimates of $P[U \geq U_{90}]$ when θ_k is too small (e.g. $\theta_k = 0.125$), while it gives conservative estimates of $P[U \geq U_{90}]$ when θ_k is large (e.g. $\theta_k = 2.0$). It should be noted that this observation is also true for all RBSA modes described earlier. The effect of v_k on $P[U \geq U_{90}]$ is expressed at a fixed value of $\theta_k = 0.5$ and the results are shown in Fig. 18(b). It can be seen that the

predicted $P[U \geq U_{90}]$ by the RBSA-G2C2 model agrees very well with those obtained from the FEMC approach, for all prescribed values of v_k . Some slight discrepancy is though observed for $v_k = 200\%$ particularly at low probability level of $P[U \geq U_{90}] \leq 50\%$, however, the overall agreement is encouraging.

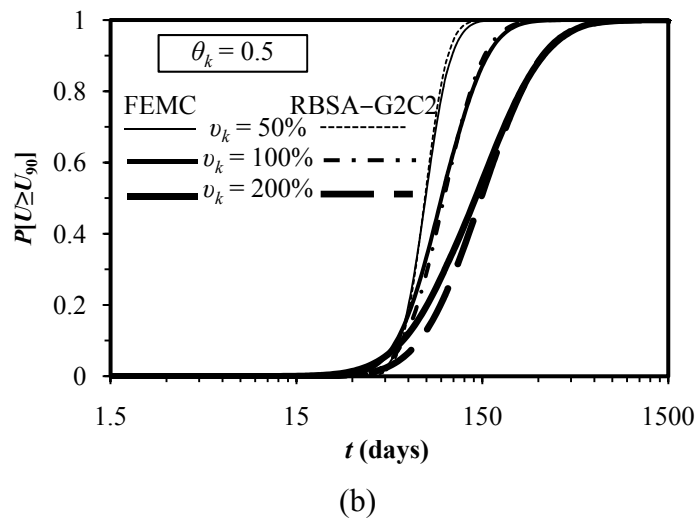
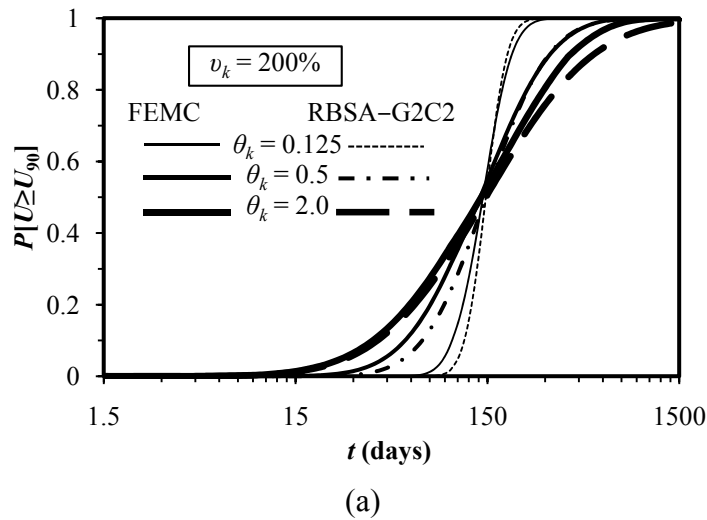


Figure 5.18: Comparison between FEMC and RBSA-G2C2 for the effect of: (a) θ on $P[U \geq U_{90}]$ for $v_k = 200\%$; (b) v on $P[U \geq U_{90}]$ for $\theta = 0.5$

5.2.1.5 Comparison between RBSA-G1C1 and RBSA-G1C3

As mentioned earlier, if both k and m_v (individually or in together) have the same v and θ in the undisturbed and smear zones, $\mu_{\ln U^*}$, $\sigma_{\ln U^*}$ and in turn $P[U \geq U_{90}]$ can be estimated using the RBSA model of either G1C1 or G1C3. Therefore, it is necessary to confirm that both models of G1C1 and G1C3 produce identical $\mu_{\ln U^*}$, $\sigma_{\ln U^*}$ and

$P[U \geq U_{90}]$, for any given consolidation problem. In order to make comparison between the RBSA models of G1C1 and G1C3, a more practical illustrative example of an axisymmetric unit cell of $L = 5.0$ m, $r_w = 0.05$ m, $r_e = 1.05$ m, $r_s = 0.25$ m, $\mu_{k_u} = 5 \times 10^{-10}$ m/sec, $\mu_{m_{v_u}} = 1.67 \times 10^{-4}$ m²/kN, $\mu_{k_u} / \mu_{k_s} = 2.0$ and $\mu_{m_{v_u}} / \mu_{m_{v_s}} = 1.25$ is considered. Both models of RBSA–G1C1 and RBSA–G1C3 are performed with $\nu_{k_u} = \nu_{k_s} = 100\%$, $\theta_{k_u} = \theta_{k_s} = 1.0$ and $\nu_{m_{v_u}} = \nu_{m_{v_s}} = 25\%$, $\theta_{m_{v_u}} = \theta_{m_{v_s}} = 1.0$. The comparison between the RBSA–G1C1 model and RBSA–G1C3 model is shown in Fig. 5.19. The FEMC solution of the above problem is also included in the figure to compare with those obtained from the two RBSA models.

It can be seen from Fig. 5.19(a) that the RBSA model of both G1C1 and G1C3 give identical $\mu_{\ln U^*}$. However, Fig. 19(b) shows that there is a slight discrepancy in the estimated $\sigma_{\ln U^*}$ between the RBSA model of G1C1 and G1C3, which is due to the fact that k_u and k_s ; and m_{v_u} and m_{v_s} were averaged over the entire soil domain to obtain a reasonable approximation of the parameter $\sigma_{\ln W}^2$ (see Eq. 5.25) and $\sigma_{\ln V}^2$ (see Eq. 5.41), although they were not distributed over the entire area of the unit cell. As the variance decreases with the increase in the averaging domain, the RBSA–G1C1 model gives slightly lower value of $\sigma_{\ln U^*}$ than the RBSA–G1C3 model. The comparison between the calculated $P[U \geq U_{90}]$ from the FEMC, G1C1 and G1C3 of RBSA models is presented in Fig. 5.19 (c). It can be seen that both G1C1 and G1C3 of RBSA models give almost identical $P[U \geq U_{90}]$. As the RBSA–G1C3 model gives slightly conservative (lower) estimate of $\sigma_{\ln U^*}$ and $P[U \geq U_{90}]$ than the RBSA–G1C1 model, it is recommended to use the RBSA–G1C3 instead of the RBSA–G1C1 model if both k and m_v (individually or in together) have the same ν and θ in the undisturbed and smear zones.

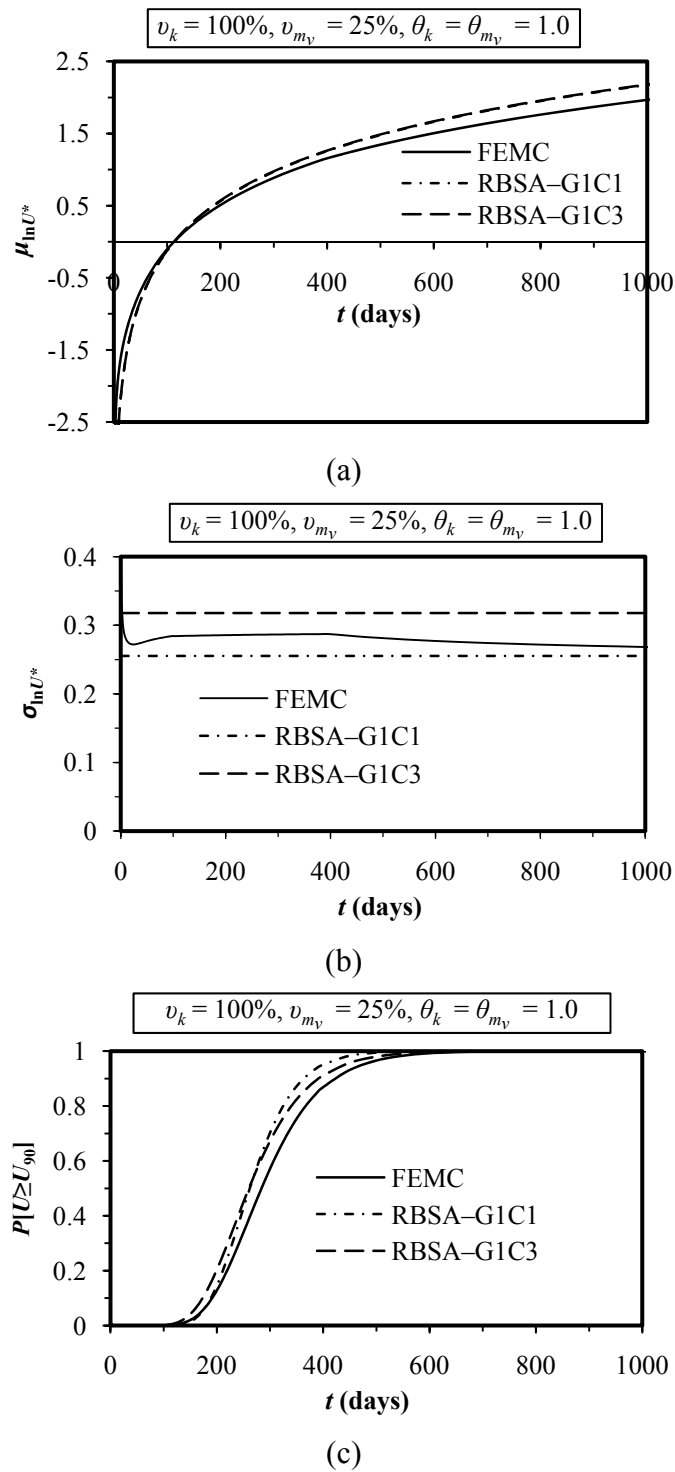


Figure 5.19: Comparison between (a) $\mu_{\ln U^*}$ (b) $\sigma_{\ln U^*}$ and (c) $P[U \geq U_{90}]$ obtained from FEMC, RBSA-G1C1 and RBSA-G1C3 for $v_{k_u} = v_{k_s} = 100\%$, $v_{m_{v_u}} = v_{m_{v_s}} = 25\%$, $\theta_{k_u} = \theta_{k_s} = \theta_{m_{v_u}} = \theta_{m_{v_s}} = 1.0$

5.2.1.6 Comparison between RBSA–G2C1 and RBSA–G2C3

As indicated earlier, when k is considered as the only random variable and has the same values of ν and θ in the undisturbed and smear zones, $\mu_{\ln U^*}$, $\sigma_{\ln U^*}$ and in turn $P[U \geq U_{90}]$ can be estimated using the RBSA model of either G2C1 or G2C3. In this section, a comparison between RBSA–G2C1 and RBSA–G2C3 models is carried out to ensure that they produce identical $\mu_{\ln U^*}$, $\sigma_{\ln U^*}$ and $P[U \geq U_{90}]$ for any given consolidation problem. The same axisymmetric unit cell, as previously described in Section 5.2.1.4, is used to perform the comparison. As both RBSA–G2C1 and RBSA–G2C3 models consider only k as spatially variable soil property and m_v is constant, the required input geometric and soil properties are assumed to be as follows: $L = 5.0$ m, $r_w = 0.05$ m, $r_e = 1.05$ m, $r_s = 0.25$ m, $\mu_{k_u} = 5 \times 10^{-10}$ m/sec and $\mu_{k_u} / \mu_{k_s} = 2.0$. Constant m_v value of 1.67×10^{-4} m²/kN is used throughout the unit cell. Both the RBSA–G2C1 and RBSA–G2C3 models are performed with $\nu_{k_u} = \nu_{k_s} = 100\%$ and $\theta_{k_u} = \theta_{k_s} = 1.0$. The comparison between the RBSA–G2C1 and RBSA–G2C3 models is shown in Fig. 5.20. The FEMC solution of the above problem is also included in the figure to investigate the agreement between the RBSA models and FEMC approach.

The RBSA model of both G2C1 and G2C3 give identical $\mu_{\ln U^*}$, as shown in Fig. 5.20(a). However, Fig. 20(b) shows that there is a slight discrepancy in the estimated $\sigma_{\ln U^*}$ between the RBSA models of G2C1 and G2C3, which is attributed to the fact that both k_u and k_s were averaged over the entire soil domain in estimating the parameter $\sigma_{\ln w}^2$ (see Eq. 5.25), although they were not distributed over the entire area of the unit cell. The agreement between the calculated $P[U \geq U_{90}]$ from the FEMC, G2C1 and G2C3 of RBSA models is illustrated in Fig. 5.20(c). It can be seen that both G2C1 and G2C3 of RBSA models give almost identical $P[U \geq U_{90}]$ compared to the FEMC approach. It is recommended to use RBSA–G2C3 model instead of RBSA–G2C1 model if k has the same values of ν and θ in the undisturbed and smear zones as the RBSA–G2C3 model will provide somewhat conservative estimate of $P[U \geq U_{90}]$ compared to the RBSA–G2C1 model.

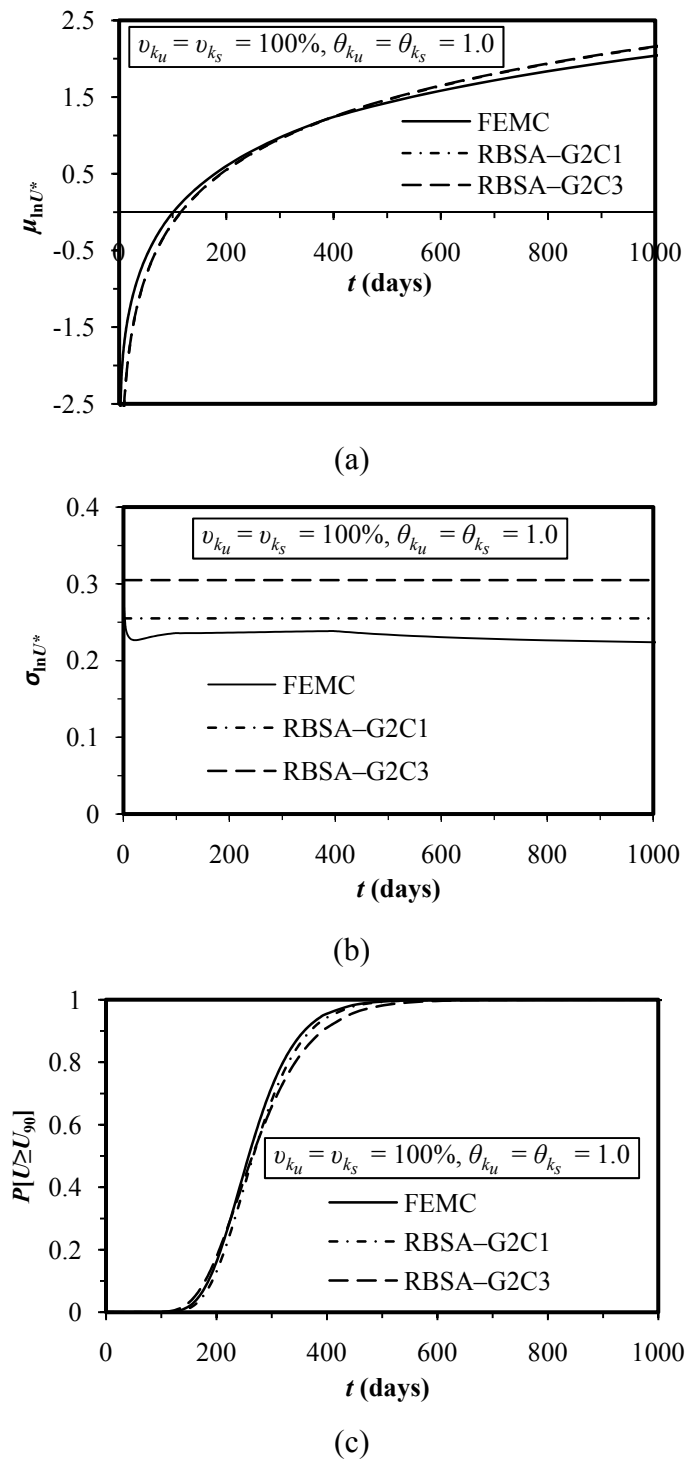


Figure 5.20: Comparison between (a) $\mu_{\ln U^*}$ (b) $\sigma_{\ln U^*}$ and (c) $P[U \geq U_{90}]$ obtained from FEMC, RBSA-G2C1 and RBSA-G2C3 for $v_{k_u} = v_{k_s} = 100\%$, $\theta_{k_u} = \theta_{k_s} =$

1.0

5.3 Summary and Discussions

In this chapter, a reliability-based semi-analytical (RBSA) model was developed to estimate the probability of achieving a target degree of consolidation by PVDs, allowing designers to avoid the full-scale finite-element Monte-Carlo (FEMC) simulations described in Chapter 4. The proposed RBSA model accounts for soil spatial variability using the geometric averages of soil permeability and volume compressibility, that were deemed to be the most significant spatial random variable affecting soil consolidation by PVDs. The performance function of the proposed RBSA model was based on the well-known deterministic equation proposed by Hansbo (1981), which considers soil consolidation due to horizontal drainage. Soil consolidation due to vertical drainage is usually much less than that of the vertical drainage and thus was not considered in development of the current RBSA model. Both the FEMC simulations and RBSA calculations were performed over a range of different combinations of the coefficients of variation and scales of fluctuation of soil permeability and volume compressibility using an axisymmetric unit cell. A comparison between the results obtained from the proposed RBSA model and those obtained from the full-scale FEMC simulations was conducted to assess the capability of the proposed RBSA model in reproducing the FEMC results in various situations. The comparative study between the proposed RBSA model and FEMC simulations led to the following findings:

- The proposed RBSA model slightly over-predicted $\mu_{\ln U^*}$ for all combinations of v and θ . This over prediction became more prevailing when both k and m_v were considered as spatially variable.
- The discrepancy in $\sigma_{\ln U^*}$ estimated via FEMC simulation and predicted by RBSA model increased with the increase in v and θ .
- At any certain time and for a certain value v , the proposed RBSA model tended to give unconservative estimate of $P[U \geq U_{90}]$ when θ was too small in comparison to the dimensions of the averaging domain. On the other hand, for significantly large θ , the proposed RBSA model tended to give conservative estimate of $P[U \geq U_{90}]$. The above observations were particularly true for $P[U \geq U_{90}] > 50\%$. When θ was of the order of the influence zone dimensions, the proposed RBSA model gave almost identical $P[U \geq U_{90}]$ to that obtained by the FEMC approach.

The RBSA model presented in this thesis also has some limitations which can be noted as follows:

- As the proposed RBSA model was developed based on the Hansbo's (1981) horizontal (radial) consolidation equation, it only considers soil consolidation due to horizontal drainage. However as explained earlier, soil consolidation due to vertical drainage is marginal and can be neglected without considerable impact on soil consolidation.
- No cross-correlation between k and m_v was assumed, i.e. k and m_v were assumed independent. However, the FEMC analyses using cross-correlated random fields of k and m_v revealed that the effect of non-zero correlation of k and m_v on the probability of achieving degree of consolidation is quite minor.

Overall, the results demonstrated in this chapter indicated that the geometric averaging model is a reasonable approach to estimate the statistics of the degree of consolidation and in turn the probability of achieving a target degree of consolidation. The results also indicated that, for a given coefficient of variation of soil property of interest, the stochastic response of soil consolidation by PVDs is dependent only on the ratio of the influence zone dimensions surrounding the PVD to the scale of fluctuation, which can be readily taken into account by the use of a variance reduction function. Specifically, the variance function gives an amount that the log-soil property (k or m_v or both) variance is reduced when its random field is averaged over a region equal to $(r_e - r_w)L$. Since the proposed RBSA model tended to give unconservative estimate of $P[U \geq U_{90}]$ for very small θ , particularly when $P[U \geq U_{90}] > 50\%$ (note that the probability of achieving a target degree of consolidation of usual interest is greater than 50%, as any $P[U \geq U_{90}] < 50\%$ is unconservative), a tentative recommendation is to use L no more than $5\theta^2 / (r_e - r_w)$. This is equivalent to taking θ larger than the original, accordingly will yield a conservative estimate of $P[U \geq U_{90}]$. There is, at this time, little justification for such a recommendation and future research into this problem is needed. However, if the vertical drain is inserted into a much deeper soil mass, one would not expect to average over the entire depth due to the reduction of applied surcharge load with depth and a reduction in the discharge capacity of drain with depth due to high lateral stress.

In the event that the soil is statistically anisotropic, that is, the scale of fluctuations differ in the vertical and horizontal directions, the proposed RBSA model can still be used simply by differing the vertical and horizontal scales of fluctuation in calculating the variance reduction factor using the algorithm given in Appendix A. Therefore, the proposed RBSA model can be confidently employed to assess the reliability of any PVD consolidation problem of arbitrary dimensions, geometries and having different mean soil properties. The overall results confirm that there is a good agreement between the proposed RBSA model and FEMC simulations, indicating that the simpler RBSA model negates the need for the computationally intensive FEMC technique for soil consolidation by PVDs.

Chapter 6

Summary, Conclusions and Recommendations

6.1 Summary

In this study, the effects of soil spatial variability on the behaviour of soil consolidation by PVDs was examined and quantified by combining the local average subdivision (LAS) technique (Fenton and Vanmarcke 1990) and finite element method into a Monte Carlo framework. The results obtained from the random finite-element Monte-Carlo (FEMC) analyses indicated that soil spatial variability has a significant effect on the estimated mean and standard deviation of the degree of consolidation and in turn on the probability of achieving 90% consolidation. An approximate, easy-to-use reliability-based semi-analytical (RBSA) model was also presented as an alternative tool to the FEMC approach from which direct estimates of the probability of achieving any target degree of consolidation at a given time can be readily obtained. A comparison between the results obtained from the proposed RBSA model and those obtained from the full-scale FEMC simulations was conducted to assess the capability of the proposed RBSA model in reproducing the FEMC results. It was found that predictions of the probability of achieving 90% consolidation from the RBSA model are in good agreement with those obtained from the FEMC.

Chapter 2 detailed the more important features associated with probabilistic modelling of soil consolidation by PVDs. This includes the theories related to soil consolidation, different elements of soil inherent spatial variability and averaging domain-variance relationships. It was discussed that typical values of soil property variation from one site should not be used blindly for another site while conducting a reliability analysis. In practice, soil variability measures should always be based on site-specific data due to the fact that the data reported in the literature often compounds real variability with testing errors. This chapter also described some of the most commonly used methods to perform stochastic soil consolidation analyses. A brief discussion regarding the accuracy and limitations of those methods was also provided. Finally, it was discussed that no or very little effort has been made

previously to quantify the effect of soil spatial variability on soil consolidation by PVDs. In addition, no attempt has been previously made to provide a rational reliability-based analytical PVD design model to properly deal with the uncertainty associated with soil spatial variability. Therefore, any attempt to address this issue would undoubtedly be beneficial.

Chapter 3 described the formulation and implementation of the proposed stochastic approach in evaluating the behaviour of soil consolidation by PVDs due to the effect of soil spatial variability. It was argued that both permeability and compressibility can be modelled by assuming lognormally distributed and the LAS method (Fenton and Vanmarcke 1990) is the most viable choice for the simulation of spatially random soil profiles. The formulation and validation of the finite element consolidation analysis model was discussed in some detail in this chapter. The chapter also described the procedure for estimating the mean and standard deviation of the degree consolidation using the consolidation responses obtained from the suite of Monte-Carlo simulations. In the same chapter, an approximate method to obtain the probability of achieving a desired degree of consolidation was presented and discussed. Prior to commencing the probabilistic analysis, initial investigations were undertaken to determine the minimum number of realisations and optimum mesh density required to produce reliable result from the finite element analysis. It was shown that 1000 Monte Carlo simulations and a mesh with an element size of $0.1 \text{ m} \times 0.1 \text{ m}$ were deemed to give reasonable precision in the stochastic consolidation analysis.

In Chapter 4, extensive parametric studies were conducted to examine the influence of the coefficient of variation (COV), v , and scale of fluctuation (SOF), θ , of soil permeability, k , and volume compressibility, m_v , on the estimated degree of consolidation, including the smear effect. The complete study presented in this chapter was divided into two parts. In the first part, the smear effect was excluded, however, it was investigated in the second and final part. Each part of the study was then further subdivided into two ‘groups’. In the first group, only soil permeability, k , was considered as the random variable, while in the second group both k and m_v were selected as random variables. The parametric studies carried out in this chapter yielded the following specific observations:

- Increasing the input variance of either k only or both k and m_v generally decreased the mean of the degree of consolidation. The exception to this trend was found only when v of both k and m_v were equal (i.e. $v_k = v_{m_v}$).
- Increasing the input variance of either k only or both k and m_v always increased the standard deviation of the degree of consolidation.
- Increasing the SOF generally increased the mean and standard deviation of the degree of consolidation. However, for large θ (e.g. $\theta \geq 2.0$), the influence of θ on the mean and standard deviation of the degree of consolidation was marginal. The scale of fluctuation has little influence on the mean and standard deviation of the degree of consolidation when the input variance of either k only or both k and m_v was small ($v \leq 25\%$).
- At a certain consolidation time, the probability of achieving 90% consolidation decreased with the increase in v of either k only or both k and m_v , as expected. The probability of achieving 90% consolidation became independent of θ at a probability level of around 50%. Above the 50% probability level and at a certain consolidation time, the probability of achieving 90% consolidation decreased as θ increased and the role of θ had the opposite effect below this level. In addition, the probability of achieving 90% consolidation became insensitive for larger θ (e.g. $\theta \geq 2.0$). The probability of achieving 90% consolidation at a consolidation time corresponding to the deterministically predicted 90% consolidation time was found to be always less than 50% for all combinations of values of v and θ . That is, the deterministic solution based on the mean soil properties always led to unconservative estimate of the degree of consolidation (i.e. $P[U \geq U_{90}] < 50\%$). These results were reassured from the design viewpoint because they indicated that the traditional approach of design of soil consolidation by PVDs leads to unconservative estimate of the true degree of consolidation and the more variable the soil is, the more unconservative the solution.
- When k was the only random variable and m_v was constant across the soil mass, the mean and standard deviation of the degree of consolidation defined by the excess pore water pressure were identical to those defined by settlement. This result agrees with the observations made by Lee et al. (1992);
- The mean and standard deviation of the degree of consolidation and the probability of achieving 90% consolidation defined by the excess pore water

pressure and settlement were different only when the COV of volume compressibility was as high as 200% and when k and m_v were uncorrelated. The mean of the degree of consolidation and the probability of achieving 90% consolidation defined by the excess pore water pressure and settlement were almost identical when k and m_v were perfectly positively correlated;

- The mean and standard deviation of the degree of consolidation and the probability of achieving 90% consolidation were highly sensitive to uncorrelated k and m_v rather than positively correlated k and m_v . Uncorrelated k and m_v were more likely to give higher mean and standard deviation of the degree of consolidation than the correlated k and m_v . The probability of achieving 90% consolidation followed an opposite trend before and after the probability level of 50% for both v and θ , irrespective of the level of cross-correlation between k and m_v . However, at any certain consolidation time, the estimated probability of achieving 90% consolidation with correlated k and m_v was found to be always higher than that computed with the uncorrelated k and m_v when the probability of achieving 90% consolidation $\leq 50\%$, whereas an opposite trend to this behaviour was observed when the probability of achieving 90% consolidation was $\geq 50\%$.
- The effect of v and θ of the undisturbed zone soil properties (either k only or both k and m_v) on the estimated mean and standard deviation of the degree of consolidation and probability of achieving 90% consolidation was found to remain marginal. On the other hand, the estimated mean and standard deviation of the degree of consolidation and the probability of achieving 90% consolidation were highly sensitive to v and θ of the soil properties of the smear zone. This result indicates that the probabilistic behaviour of soil consolidation is governed by the spatial variation of the soil properties of the smear zone. Since the spatial variability of the smear zone will possibly be higher than that of the undisturbed zone, this observation has important implications in the sense that, modelling soil consolidation with the same v and θ for both zones (i.e. undisturbed and smear) that are equal to the v and θ of the smear zone does not significantly affect the final results.
- Increasing the mean permeability ratio of the undisturbed zone to smear zone was found to have a considerable impact on the stochastic behaviour of soil consolidation. On the other hand, increasing the smear zone ratio was found to have a marginal effect on the mean and standard deviation of the degree of

consolidation and in turn on the probability of achieving 90% consolidation. This observation reveals that the effect of increasing the smear zone ratio on soil consolidation is not as significant as that of the mean permeability ratio of the undisturbed zone to the smear zone.

- Increasing the mean compressibility ratio of the undisturbed zone to the smear zone had little or no impact on the stochastic behaviour of soil consolidation. This observation reveals that an increased mean compressibility in the smear zone does not largely affect the rate of soil consolidation.

Investigation into the effect of anisotropic over isotropic scales of fluctuation of spatially variable soil permeability led to the following findings:

- An isotropic solution underestimated the mean degree of consolidation and this underestimation was marginal when the degree of anisotropy, ζ , was as low as 4.0. The amount by which isotropic assumption underestimated the mean degree of consolidation decreased with the decrease in both ζ and v_k . The effect of degree of anisotropy on the mean degree of consolidation was insignificant even for a high degree of anisotropy (e.g. $\zeta = 32$) when the coefficient of variation of soil permeability was as low as 50%;
- Anisotropic solutions always gave higher values of the standard deviation of the degree of consolidation than isotropic solutions. The difference in the standard deviation of the degree of consolidation obtained from anisotropic and isotropic conditions decreased with the decrease in both ζ and v_k . In other words, the difference in the standard deviation of the degree of consolidation obtained from anisotropic and isotropic conditions increased with the increase of both ζ and v_k ;
- The isotropic assumption always provided a conservative estimation of the probability of achieving 90% consolidation compared to the more realistic anisotropic condition, regardless of the degree of spatial variation. This result has a potential practical implication in the sense that the more realistic anisotropic condition will ensure improved economy in the reliability-based design of soil consolidation via PVDs. This was particularly true when the coefficient of variation of soil permeability was as high as 200% and the degree of anisotropy was as high as 32. However, it should be noted that this conclusion was true for almost all probability (confidence) levels but the difference between the isotropic

and anisotropic solutions became less pronounced for high probability levels close to unity (i.e. at $P[U \geq U_{90}] \approx 95\sim 100\%$).

In Chapter 4, stochastic analyses were also performed for both axisymmetric and equivalent plane strain conditions (using permeability matching theory), considering soil permeability as the only random variable. The comparison between the axisymmetric and equivalent plane strain analyses yielded the following conclusions:

- The equivalent plane strain analysis always provided lower values of the mean and standard deviation of the degree of consolidation, and a lower probability of achieving a target degree of consolidation than the axisymmetric solution, regardless of the values of the statistical parameters. Satisfactory matching in terms of the probability of achieving a target degree of consolidation can only be obtained when the consolidated soil mass is more or less homogeneous (i.e. when θ_k is large). For erratic soils (i.e. when θ_k is small), the derived probability from the plane strain analysis is expected to be relatively lower than that of the axisymmetric solution.

In Chapter 5, an approximate reliability-based semi-analytical model (RBSA) for estimating the probability of achieving a target degree of soil consolidation by PVDs was developed. In the proposed RBSA model, semi-analytical relationships for the statistical parameters (i.e. mean and standard deviation) of a degree of consolidation function, U^* , (note that U^* is an alternative representing form that was used to replace the degree of consolidation, U , and is defined as $U^* = \ln [1/(1-U)]$) were derived directly from the specified statistical parameters of the spatially variable soil properties by employing the theory of statistics and random field theory (Vanmarcke 1984). The reason for using U^* instead of U was that as it simplifies the process of obtaining a closed form solution for the mean and variance of the degree of consolidation function U^* directly from the statistically defined input data relating to spatially variable soil properties. In addition, unlike U , U^* provided sufficiently reasonable approximation to the probability distribution function that is necessary to estimate the probability of achieving a target degree of consolidation. The performance function of the proposed RBSA model was based on the well-known deterministic equation of horizontal (radial) consolidation proposed by Hansbo

(1981), accordingly the proposed model considers soil consolidation due to horizontal drainage only. However, as explained in the thesis, soil consolidation due to horizontal drainage is prevailing while consolidation due to vertical drainage is marginal and can be neglected without considerable reduction in soil consolidation. The proposed RBSA model accounts for soil spatial variability using the geometric averages of soil permeability and volume compressibility, including the smear effect. It was shown that U^* is approximately lognormally distributed at any time of the consolidation process and any combination of COV and SOF of the spatially variable soil properties. The computed distribution parameters of U^* at any given consolidation time from the RBSA model were then used to estimate the probability of achieving a target degree of consolidation at that time using Eq. 3.41. In the same chapter, a comparison between the results obtained from the proposed RBSA model and those obtained from the full-scale FEMC simulations was also conducted to assess the capability of the proposed RBSA model in reproducing the FEMC results. The comparative study between the proposed RBSA model and FEMC simulations led to the following findings:

- The results demonstrated that the geometric averaging model is a reasonable approach to estimate the statistics of the degree of consolidation and in turn the probability of achieving a target degree of consolidation. Furthermore, for a given coefficient of variation of soil permeability, the stochastic response of soil consolidation by PVDs is dependent only on the ratio of the scale of fluctuation to the influence zone dimensions surrounding the PVD, which can be readily taken into account by the use of a variance reduction function. Therefore, the proposed RBSA model can be confidently employed to assess the reliability of any PVD consolidation problem of arbitrary dimensions, geometries and having different mean soil properties. The overall results confirmed that there was a good agreement between the proposed RBSA model and FEMC simulations, indicating that the simpler RBSA model negates the need for the computationally intensive FEMC technique for soil consolidation by PVDs.

6.2 Conclusions

The work presented in this thesis explores the importance of considering the associated uncertainty due to soil spatial variability in the analysis and design of soil improvement by PVDs. For this purpose, a stochastic approach was developed using the random field theory and finite element modelling into a Monte Carlo framework. A parametric study was carried out to investigate the implications of statistical parameters of spatial variability of soil permeability and volume compressibility in terms of the mean, standard deviation and correlation length on soil improvement by PVDs. The study also introduced a reliability-based semi-analytical (RBSA) design method that was developed to estimate the probability of achieving any target degree of consolidation by PVDs, allowing designers to avoid the full-scale computationally intensive finite-element Monte-Carlo (FEMC) procedure.

The results clearly demonstrated the potential of using the proposed probabilistic context in providing valuable insights into the impact of soil spatial variability on soil improvement by PVDs. It was shown that spatial variation of soil permeability and volume compressibility within an affected soil mass significantly influences the degree of consolidation achieved via PVDs and thus the amount of soil improvement obtained. It was also shown that predictions from the RBSA model are in good agreement with those obtained from the FEMC, implying that the developed RBSA is reliable and can be used with confidence for design of soil improvement by PVDs and negating the need for the computationally intensive FEMC procedure. The overall results urge the use of probabilistic techniques in routine design practice of soil improvement by PVDs.

6.3 Recommendations for Future Work

Although this thesis has provided a significant contribution in regards to the stochastic soil consolidation via PVDs, further analytical and numerical studies associated with the consolidation behaviour of soil deposits with spatially variable properties are recommended. Future work should focus on the following aspects:

1. The consolidation analyses conducted in this research have assumed that the soil is linear elastic, i.e. the aspect of material non-linearity was not considered in this work. For more realistic non-linear material, the degree of consolidation based on pore water pressure and settlement will be different even in a deterministic context (Walker 2006). Therefore it is worthwhile to investigate the effect of nonlinear constitutive behaviour of soil on the outcome of statistical analyses.
2. The permeability, k , and volume compressibility, m_v , are related to changes in void ratio and effective stresses during the consolidation process and such changes in k and m_v can affect the generation and dissipation of excess pore-water pressure and rate of soil consolidation (Huang et al. 2010). In addition, in the field, the different subsoil stress histories (normally consolidated or over-consolidated) result in different consolidation responses (Seah and Juirnarongit 2003). Consequently, further research considering these aspects is desirable as it may provide further insights into the impact of soil spatial variability on soil consolidation by PVDs.
3. Although the consolidation around vertical drains is truly three dimensional (3D), in this study, the effect of soil spatial variability on the behaviour of soil consolidation was investigated employing 2D finite element (FE) model and the random soil properties (i.e. k and m_v) were modelled by a 2D random field. This means that the soil properties in the circumferential direction and normal to the plane of paper direction were respectively constant under the axisymmetric and plane strain conditions. In other words, there were concentric rings and blocks of constant soil properties under axisymmetric and plane strain conditions. However, due to the nature of the horizontal (radial) drainage to a PVD, small changes in k and m_v in any direction close to the drain may have an impact on the rates of consolidation. Hence, it is worthwhile to perform full 3D FEM consolidation analyses considering 3D soil variability. A proper 3D FEM analysis with 3D spatial variation may be computationally too intensive but certainly desirable. However, it should be noted that the developed RBSA models can handle 3D spatial variability analyses but it is recommended that their 3D solutions be verified first with full 3D FEM so that they can be used with confidence.

4. Although the lognormal distribution was used to model k and m_v , several other probability distributions, namely normal (e.g. Athanasiou-Grivas and Harr 1978), gamma (e.g. Chang 1985), Weibul (e.g. Zhou et al. 1999) may be adopted to model k and m_v . Therefore, the sensitivity of the of the degree of consolidation with respect to the probability distribution types is also necessary to be investigated for providing more insight. In addition, further investigation on the effect of employing different types of correlation structures (in this study an exponentially decaying Marcovian correlation function was used) in modelling random soil property field would be beneficial.

References

- Arulrajah, A., Nikraz, H. R., and Bo, M. W. (2004). "Factors affecting field instrumentation assessment of marine clay treated with prefabricated vertical drains." *Geotextiles and Geomembranes*, 22, 415-437.
- Athanasiou-Grivas, D., and Harr, M. E. (1978). "Consolidation-probability approach." *Journal of the Engineering Mechanics Division*, 104, 681-690.
- Badaoui, M., Nour, A., Slimani, A., and Berrah, M. K. (2007). "Consolidation statistics investigation via thin layer method analysis." *Transport in Porous Media*, 67(1), 69-91.
- Barron, R. A. (1948). "Consolidation of fine-grained soils by drain wells." *Transactions of the American Society of Civil Engineering*, 113, 718-754.
- Beacher, G. B., and Christian, J. T. (2003). *Reliability and Statistics in Geotechnical Engineering*, John Wiley & Sons, Chichester, England.
- Beacher, G. B., and Ingra, T. S. (1981). "Stochastic FEM in settlement predictions." *Journal of the Geotechnical Engineering Division*, 107(GT4), 449-463.
- Benjamin, J. R., and Cornell, C. A. (1970). *Probability, statistics, and decision for civil engineers*, McGraw-Hill, New York.
- Bergado, D. T., Asakami, H., Alfaro, M. C., and Balasubramaniam, A. S. (1991). "Smear effects of vertical drains on soft Bangkok clay." *Journal of Geotechnical Engineering, ASCE*, 117(10), 1509-1530.
- Bergado, D. T., Balasubramaniam, A. S., Fannin, R. J., and Holtz, R. D. (2002). "Prefabricated vertical drains (PVDs) in soft Bangkok clay: a case study of the new Bangkok International Airport project." *Canadian Geotechnical Journal*, 39(2), 304-315.
- Biot, M. A. (1941). "General theory of three-dimensional consolidation." *Journal of Applied Physics*, 12, 155-164.
- Bo, M. W., Chu, J., Low, B. K., and Choa, V. (2003). *Soil Improvement: Prefabricated Vertical Drain Techniques*, Thomson Learning, Singapore.
- Brockwell, P. J., and Davis, R. A. (1987). *Time Series: Theory and Methods*, Springer Verlag, New York.
- Cafaro, F., and Cherubini, C. (2002). "Large sample spacing in evaluation of vertical strength variability of clayey soil." *Journal of Geotechnical and Geoenvironmental Engineering*, 128(7), 558-568.

- Carillo, N. (1942). "Simple two- and three-dimensional cases in the theory of consolidation of soil." *Journal of Mathematics Physicals*, 21(1), 1-5.
- Carter, J. P., and Balaam, N. P. (1995). "Program AFENA - A general finite element algorithm: Users' Manual." Centre for Geotechnical Research, University of Sydney, Sydney.
- Casagrande, A. (1936) "The determination of the pre-consolidation load and its practical significance." *Proceedings of the 1st International Soil Mechanics and Foundation Engineering Conference*, Graduate School of Engineering, Harvard University, Cambridge, Massachusetts, 60-64.
- Chai, J. C., and Miura, N. (1999). "Investigation of factors affecting vertical drain behavior." *Journal of Geotechnical and Geoenvironmental Engineering*, 125(3), 216-226.
- Chang, C. S. (1985). "Uncertainty of one-dimensional consolidation analysis." *Journal of Geotechnical Engineering*, 111(12), 1411-1424.
- Christian, J. T., and Beacher, G. B. (1999). "Point estimate method as numerical quadrature." *Journal of Geotechnical and Geoenvironmental Engineering*, 125(GT9), 779-786.
- Corotis, R. B., Krizec, R. J., and El-Moursi, H. H. (1975). "Probabilistic approach to prediction of consolidation settlement." *Transportation Research Record*, 548, 47-61.
- Dagan, G. (1989). *Flow and transport in porous media*, Springer, New York.
- DeGroot, D. J., and Baecher, G. B. (1993). "Estimating autocovariance of in-situ soil properties." *Journal of Geotechnical Engineering*, 119(1), 147.
- Duncan, M. D. (2000). "Factors of safety and reliability in geotechnical engineering." *Journal of Geotechnical and Geoenvironmental Engineering*, 126(4), 307-316.
- Elachachi, S. M., Breyse, D., and Houy, L. (2004). "Longitudinal variability of soils and structural response of sewer networks." *Computers and Geotechnics*, 31, 625-641.
- Elkateb, T., Chalaturnyk, R., and Robertson, P. (2002). "An overview of soil heterogeneity: quantification and implications on geotechnical field problems." *Canadian Geotechnical Journal*, 40, 1-15.
- Eriksson, U., Hansbo, S., and Torstensson, B. A. (2000). "Soil improvement at Stockholm-Arlanda Airport." *Ground Improvement*, 4(2), 73-80.

- Fenton, G., and Griffiths, D. V. (2002). "Probabilistic foundation settlement on spatially random soil." *Journal of Geotechnical and Geoenvironmental Engineering*, 128(5), 381-390.
- Fenton, G. A. (1990). "Simulation and analysis of random fields," Princeton University, New Jersey.
- Fenton, G. A., and Griffiths, D. V. (1996). "Statistics of free surface flow through stochastic earth dam." *Journal of Geotechnical Engineering*, 122(6), 427-436.
- Fenton, G. A., and Griffiths, D. V. (2003). "Bearing-capacity prediction of spatially random $c-\phi$ soils." *Canadian Geotechnical Journal*, 40(1), 54-65.
- Fenton, G. A., and Griffiths, D. V. (2005). "Three-dimensional probabilistic foundation settlement." *Journal of geotechnical and geoenvironmental engineering*, 131(2), 232-239.
- Fenton, G. A., and Griffiths, D. V. (2008). *Risk assessment in geotechnical engineering*, Wiley, New York.
- Fenton, G. A., and Vanmarcke, E. H. (1990). "Simulation of random fields via local average subdivision." *Journal of Engineering Mechanics*, 116(8), 1733-1749.
- Fenton, G. A., and Vanmarcke, E. H. (1998). "Spatial variation in liquefaction risk." *Géotechnique*, 48(6), 819-831.
- Fenton, G. A., Zhang, X. Y., and Griffiths, D. V. (2007). "Reliability of shallow foundations designed against bearing failure using LRFD." *Georisk*, 1(4), 202--215.
- Freeze, R. A. (1977). "Probabilistic one-dimensional consolidation." *Journal of Geotechnical Engineering Division*, 103(GT7), 725-742.
- Gelhar, L. W. (1993). *Stochastic Subsurface Hydrology*, Prentice Hall, Englewood Cliffs, New Jersey.
- Griffiths, D. V., and Fenton, G. A. (1993). "Seepage beneath water retaining structures founded on spatially random soil." *Géotechnique*, 43(4), 577-587.
- Griffiths, D. V., and Fenton, G. A. (1997). "Three-dimensional seepage through spatially random soil." *Journal of geotechnical and geoenvironmental engineering*, 123(2), 153-160.
- Griffiths, D. V., and Fenton, G. A. (2004). "Probabilistic slope stability analysis by finite elements." *Journal of geotechnical and geoenvironmental engineering*, 130(5), 507-518.
- Griffiths, D. V., and Fenton, G. A. (2009). "Probabilistic settlement analysis by

- stochastic and random finite-element methods." *Journal of geotechnical and geoenvironmental engineering*, 135(11), 1629-1637.
- Griffiths, D. V., Fenton, G. A., and Lemons, C. B. (2002). "Probabilistic analysis of underground pillar stability." *International Journal for Numerical and Analytical Methods in Geomechanics*, 26(8), 775-791.
- Griffiths, D. V., Fenton, G. A., and Denavit, M. D. (2009). "Influence of spatial variability on slope reliability using 2-D random fields." *Journal of geotechnical and geoenvironmental engineering*, 135(10), 1367-1378.
- Hahn, G. J., and Shapiro, S. S. (1967). *Statistical model in engineering*, Wiley, New York.
- Haldar, S., and Sivakumar Babu, G. L. (2008). "Effect of soil spatial variability on the response of laterally loaded pile in undrained clay." *Computers and Geotechnics*, 35(4), 537-547.
- Hansbo, S. (1979). "Consolidation of clay by band-shaped prefabricated drains." *Ground Engineering*, 12(5), 16-18.
- Hansbo, S. (1981) "Consolidation of fine-grained soils by prefabricated drains." *Proceedings of the 10th International Conference on Soil Mechanics and Foundation Engineering*, Stockholm, Sweden, 677-682.
- Harada, T., and Shinozuka, M. (1986). "The scale of correlation for stochastic fields- Technical Report." Department of Civil Engineering and Engineering Mechanics, Columbia University, New York.
- Harr, M. E. (1987). *Reliability-based design in civil engineering* McGraw-Hill Book Company, New York.
- Hicks, M. A., and Onisiphorou, C. (2005). "Stochastic evaluation of static liquefaction in a predominantly dilative sand fill." *Géotechnique*, 55(2), 123-133.
- Hird, C. C., and Moseley, V. J. (2000). "Model study of seepage in smear zones around vertical drains in layered soil." *Géotechnique*, 50(1), 89-97.
- Hird, C. C., Pyrah, I. C., and Russel, D. (1992). "Finite element modelling of vertical drains beneath embankments on soft ground." *Géotechnique*, 42(3), 499-511.
- Hoeksema, R. J., and Kitanidis, P. K. (1985). "Analysis of the spatial structure of properties of selected aquifers." *Water Resources Research*, 21(4), 563-572.
- Holtz, R. D., Jamiolkowski, M., Lancellotta, R., and Pedroni, S. (1989) "Behaviour of bent prefabricated vertical drains." *Proceedings of the 12th International*

- Conference of Soil Mechanics and Foundation Engineering*, Rio De Janeiro, 1657-1660.
- Hong, H. P. (1992). "One-dimensional consolidation with uncertain properties." *Canadian Geotechnical Journal*, 29(1), 161-165.
- Hong, H. P., and Shang, J. Q. (1998). "Probabilistic analysis of consolidation with prefabricated vertical drains for soil improvement." *Canadian Geotechnical Journal*, 35(4), 666-677.
- Huang, J., and Griffiths, D. V. (2010). "One-dimensional consolidation theories for layered soil and coupled and uncoupled solutions by finite-element method." *Géotechnique*, 60(9), 709-713.
- Huang, J., Griffiths, D. V., and Fenton, G. A. (2010). "Probabilistic analysis of coupled soil consolidation." *Journal of Geotechnical and Geoenvironmental Engineering*, 136(3), 417-430.
- Hwang, D., and Witczak, M. W. (1984). "Multidimensional probabilistic consolidation." *Journal of Geotechnical Engineering*, 110(8), 1059-1077.
- Indraratna, B., Bamunawita, C., Redana, I. W., and McIntosh, G. (2003). "Modelling of prefabricated vertical drains in soft clay and evaluation of their effectiveness in practice." *Ground Improvement*, 7(3), 127-137.
- Indraratna, B., and Redana, I. W. (1997). "Plane-strain modeling of smear effects associated with vertical drains." *Journal of Geotechnical and Geoenvironmental Engineering*, 123(5), 474-478.
- Indraratna, B., and Redana, I. W. (1998). "Laboratory determination of smear zone due to vertical drain installation." *Journal of Geotechnical and Geoenvironmental Engineering, ASCE*, 124(2), 180-185.
- Indraratna, B., and Redana, I. W. (2000). "Numerical modeling of vertical drains with smear and well resistance installed in soft clay." *Canadian Geotechnical Journal*, 37(1), 132-145.
- Jaksa, M. B. (1997). "Inaccuracies associated with estimating random measurement errors." *Journal of geotechnical and geoenvironmental engineering*, 123(5), 393-401.
- Jaksa, M. B. (2000). "Geostatistical risk and inadequate site investigations: a case study." *Australian Geomechanics* 35(2), 39-46.
- Jaksa, M. B., Kaggwa, W. S., and Brooker, P. I. (1999) "Experimental evaluation of the scale of fluctuation of a stiff clay." *8th International Conference on the*

- Application of Statistics and Probability*, A. A. Balkema, Rotterdam, Sydney, 415-422.
- Jaksa, M. B., Yeong, K. S., Wong, K. T., and Lee, S. L. (2004) "Horizontal spatial variability of elastic modulus in sand from dilatometer." *9th Australia New Zealand Conference on Geomechanics*, Aucland, 289-294.
- Jamiolkowski, M., and Lancellotta, R. (1981). "Consolidation by vertical drains - uncertainties involved in prediction of settlement rates." Proceedings of the 10th International Conference on Soil Mechanics and Foundation Engineering, Stockholm, 345-451.
- Journel, A. G., and Huijbregts, C. J. (1978). *Mining Geostatistics*, Academic Press, London.
- Kjellman, W. (1948). "Accelerating consolidation of fine grain soils by means of cardboard wicks." Proceedings of the 2nd International Conference on Soil Mechanics and Foundation Engineering, 302-305.
- Kulhawy, F. H. (1992). "On evaluation of static soil properties " *Stability and Performance of Slopes and Embankments II*, Geotechnical Special Publication No. 31, 95-115.
- Kulhawy, F. H., Roth, M. J. S., and Grigoriu, M. D. (1991). "Some statistical evaluations of geotechnical properties." Proceedings of the 6th International Conference on Applied Statistical Problems in Civil Engineering (ICASP6), Mexico City, 705-712.
- Kuo, Y. L., Jaksa, M. B., Kaggwa, W. S., Fenton, G. A., Griffiths, D. V., and Goldsworthy, J. S. (2004) "Probabilistic analysis of multy-layered soil effects on shallow foundation settlement." *9th Australia New Zealand Conference on Geomechanics*, Auckland, 541-547.
- Lacasse, S., and Nadim, F. (1996) "Uncertainties in characterising soil properties." *Proceedings of the Uncertainty in Geologic Environment: From Theory to Practice*, Madison, Wisconsin, 49-75.
- Lambe, T. W., and Whitman, R. V. (1969). *Soil Mechanics*, John Wiley & Sons, Newyork.
- Lee, I. K., White, W., and Ingles, O. G. (1983). *Geotechnical engineering*, Pitman, London.
- Lee, P. K., Xie, K. H., and Cheung, Y. K. (1992). "A study on one-dimensional consolidation of layered systems." *International Journal of Numerical and*

- Analytical Methods in Geomechanics*, 16(11), 815-831.
- Lo, D. (1998). "Vertical drain performance: myths and facts." *Transactions, Hong Kong Institute of Engineering*, 5(1), 34-50.
- Mesri, G., and Choi, Y. K. (1985). "Settlement analysis of embankment on soft clays." *Journal of Geotechnical Engineering*, 3(4), 441-464.
- Morris, P. H. (2003). "Compressibility and permeability correlations for fine-grained dredged materials." *Journal of waterway, port, coastal, and ocean engineering*, 129(4), 188-191.
- Paice, G. M., Griffiths, D. V., and Fenton, G. A. (1994). "Influence of spatially random soil stiffness on foundation settlements." *ASCE Geotechnical Special Publication*, 1(40), 628-639.
- Paice, G. M., Griffiths, D. V., and Fenton, G. A. (1996). "Finite element modeling of settlements on spatially random soil." *Journal of Geotechnical and Geoenvironmental Engineering*, 122(9), 777-779.
- Phoon, K.-K. (1995). "Reliability-Based Design of Foundations for Transmission Line Structures." Cornell University, Ithaca, New York.
- Phoon, K.-K., and Kulhawy, F. H. (1999). "Characterization of geotechnical variability." *Canadian Geotechnical Journal*, 36(4), 612-624.
- Phoon, K.-K., Quek, S. T., and An, P. (2003). "Identification of statistically homogeneous soil layers using modified Bartlett statistics." *Journal of Geotechnical and Geoenvironmental Engineering*, 129(7), 649-659.
- Popescu, R., Deodatis, G., and Prevost, J. H. (2002) "Bearing capacity of heterogenous soils-a probabilistic approach." *55th Canadian Geotechnical and 3rd Joint LAH-CNC and CGS Ground Water Specialty Conference*, Niagra falls, Ontario, 1021-1027.
- Popescu, R., Prevost, J. H., and Deodatis, G. (1997). "Effects of spatial variability on soil liquefaction: some design recommendations." *Géotechnique*, 47(5), 1019-1036.
- Popescu, R., Prevost, J. H., and Deodatis, G. (2005). "3D effects in seismic liquefaction of stochastically variable soil deposits." *Géotechnique*, 55(1), 21-31.
- Pyrah, I. C. (1996). "One-dimensional consolidation of layered soils." *Géotechnique*, 46(3), 555-560.
- Rankine, B., Sivakugan, N., and Wijeyakulasuriya, V. (2005) "Observed and

- predicted behaviour of clay foundation response under the Sunshine Motorway Trial Embankment." *16th International Society of Soil Mechanics and Geotechnical Engineering Conference*, Osaka, Japan, 951-954.
- Rixner, J. J., Kraemer, S. R., and Smith, A. D. (1986). "Prefabricated vertical drains, Vol. I: Engineering guidelines." *FHWA/RD-86/168*, Federal Highway Administration, Washington D. C.
- Rosenblueth, E. (1975). "Point estimate for probability moments." *Proceedings of the National Academy of Sciences of the United States of America*, 72(10), 3812-3814.
- Rowe, P. W. (1972). "The relevance of soil fabric to site investigation practice." *Géotechnique*, 22(2), 195-300.
- Rowe, R. K., and Hinchberger, S. D. (1998). "The significance of rate effects in modelling the Sackville test embankment." *Canadian Geotechnical Journal*, 35(3), 500-516.
- Rowe, R. K., and Li, A. L. (2002). "Behaviour of reinforced embankments on soft rate-sensitive soils." *Géotechnique*, 52(1), 29-40.
- Saye, S. R. (2001). "Assessment of soil disturbance by the installation of displacement sand drains and prefabricated vertical drains." *Geotechnical Special Publication, #119, ASCE*, 325-362.
- Saye, S. R. (2003). "Assessment of soil disturbance by the installation of displacement sand drains and prefabricated vertical drains." *Geotechnical Special Publication #119, ASCE*, 325-362.
- Seah, T. H., and Juirnarongit, T. (2003). "Constant rate of strain consolidation with radial drainage." *Geotechnical Testing Journal*, 26(4), 1-12.
- Sharma, J. S., and Xiao, D. (2000). "Characterization of a smear zone around vertical drains by large-scale laboratory tests." *Canadian Geotechnical Journal*, 37(6), 1265-1271.
- Shogaki, T., Moro, M. H., Kaneko, M. M., Kogure, K., and Sudho, T. (1995) "Effect of sample disturbance on consolidation parameters of anisotropic clays." *International Symposium on Compression and Consolidation of Clayey Soils*, Hiroshima, Japan, 561-566.
- Sudicky, E. A. (1986). "A natural gradient experiment on solute transport in a sand aquifer: spatial variability of hydraulic conductivity and its role in the dispersion process." *Water Resources Research*, 22(13), 2069-2082.

- Tavenas, F., Jean, P., and Leroueil, S. (1983). "The permeability of natural soft clays; Part II, Permeability characteristics." *Canadian Geotechnical Journal*, 20(4), 645-660.
- Taylor, D. W. (1948). *Fundamentals of soil mechanics*, Wiley, New York.
- Terzaghi, K. (1943). *Theoretical soil mechanics*, John Wiley & Sons, New York.
- Vanmarcke, E. H. (1977). "Probabilistic modelling of soil profiles." *Journal of Geotechnical Engineering Division*, 103(11), 1227-1246.
- Vanmarcke, E. H. (1984). *Random fields: analysis and synthesis*, The MIT Press, Massachusetts.
- Walker, R. (2006). "Analytical solutions for modeling soft soil consolidation by vertical drains," University of Wollongong, Wollongong, Australia.
- Welker, A. L., Gilbert, R. B., and Bowders, J. J. (2000). "Using a reduced equivalent diameter for a prefabricated vertical drain to account for smear." *Geosynthetics International*, 7(1), 47-57.
- Wolff, T. F. (1996) "Probabilistic slope stability in theory and practice." *Proceedings of the Uncertainty in Geologic Environment*, Madison, Wisconsin, 419-433.
- Yegian, M. K., and Whitman, R. V. (1978). "Risk analysis for ground failure by liquefaction." *Journal of the Geotechnical Engineering Division*, 104(GT7), 921-937.
- Zeitoun, D. G., and Baker, R. (1992). "A stochastic approach for settlement predictions of shallow foundations." *Géotechnique*, 42(4), 617-629.
- Zhou, W., Hong, H. P., and Shang, J. Q. (1999). "Probabilistic design method of prefabricated vertical drains for soil improvement." *Journal of Geotechnical and Geoenvironmental Engineering*, 125(8), 659-664.

Appendix A

Variance Reduction Function

Three-dimensional (3D) Variance Reduction Function

The amount by which the variance is reduced from the point variance as a result of local averaging over the domain D is estimated from the variance function $\gamma(D)$. If D is a cube of dimension $X \times Y \times Z$, then γ corresponding to the Markov correlation function of:

$$\rho(\tau_1, \tau_2, \tau_3) = \exp[-\sqrt{(2\tau_1 / \theta_x)^2 + (2\tau_2 / \theta_y)^2 + (2\tau_3 / \theta_z)^2}] \quad (\text{A1})$$

can be defined as (Fenton and Griffiths 2008):

$$\gamma(X, Y, Z) = \frac{1}{X^2 Y^2 Z^2} \times \int_0^X \int_0^X \int_0^Y \int_0^Y \int_0^Z \int_0^Z \rho(\zeta_1 - \xi_1, \zeta_2 - \xi_2, \zeta_3 - \xi_3) d\zeta_1 d\xi_1 d\zeta_2 d\xi_2 d\zeta_3 d\xi_3 \quad (\text{A2})$$

In Eq. A1, θ_x , θ_y and θ_z are the scales of fluctuation in the X , Y and Z directions, respectively, where X , Y and Z represent the horizontal, normal to the plane of paper and vertical directions, respectively.

The sixfold integration in Eq. A2 can be condensed to a threefold integration by taking advantage of the quadrant symmetry ($\rho(\tau_1, \tau_2, \tau_3) = \rho(-\tau_1, \tau_2, \tau_3) = \rho(\tau_1, -\tau_2, \tau_3) = \rho(\tau_1, \tau_2, -\tau_3) = \rho(-\tau_1, -\tau_2, \tau_3) = \rho(-\tau_1, \tau_2, -\tau_3) = \rho(\tau_1, -\tau_2, -\tau_3) = \rho(-\tau_1, -\tau_2, -\tau_3)$) of the correlation function in Eq. A1 and can be expressed as follows: (Fenton and Griffiths 2008):

$$\gamma(X, Y, Z) = \frac{8}{X^2 Y^2 Z^2} \times \int_0^X \int_0^Y \int_0^Z (X - \tau_1)(Y - \tau_2)(Z - \tau_3) \rho(\tau_1, \tau_2, \tau_3) d\tau_1 d\tau_2 d\tau_3 \quad (\text{A3})$$

Eq. A3 can be computed numerically with reasonable accuracy using sixteen-point Gaussian quadrature integration scheme as follows (Fenton and Griffiths 2008):

$$\gamma(X, Y, Z) = \frac{1}{8} \sum_{i=1}^{16} \omega_i (1 - \psi_i) \sum_{j=1}^{16} \omega_j (1 - \psi_j) \sum_{k=1}^{16} \omega_k (1 - \psi_k) \rho(\zeta_i, \xi_j, \vartheta_k) \quad (\text{A4})$$

where:

$$\zeta_i = \frac{X}{2} (1 + \psi_i), \xi_j = \frac{Y}{2} (1 + \psi_j), \vartheta_k = \frac{Z}{2} (1 + \psi_k) \quad (\text{A5})$$

Two-dimensional (2D) Variance Reduction Function

If D is a rectangle of dimension $X \times Z$, then γ in Eq. A4 reduces to:

$$\gamma(X, Z) = \frac{1}{4} \sum_{i=1}^{16} \omega_i (1 - \psi_i) \sum_{k=1}^{16} \omega_k (1 - \psi_k) \rho(\zeta_i, \vartheta_k) \quad (\text{A6})$$

The weights, ω_i , and the Gauss points, ψ_i , are as follows:

i	ω_i	ψ_i
1	0.0271524594117540	-0.9894009349916490
2	0.0622535239386478	-0.9445750230732320
3	0.0951585116824927	-0.8656312023878310
4	0.1246289712555330	-0.7554044083550030
5	0.1495959888165760	-0.6178762444026430
6	0.1691565193950020	-0.4580167776572270
7	0.1826034150449230	-0.2816035507792580
8	0.1894506104550680	-0.0950125098376374
9	0.1894506104550680	0.0950125098376374
10	0.1826034150449230	0.2816035507792580
11	0.1691565193950020	0.4580167776572270
12	0.1495959888165760	0.6178762444026430
13	0.1246289712555330	0.7554044083550030
14	0.0951585116824927	0.8656312023878310
15	0.0622535239386478	0.9445750230732320
16	0.0271524594117540	0.9894009349916490

Appendix B

ForTRAN Code for the Developed RBSA Models

```
c-----  
c                               Program RBSA_PVD  
c-----  
c  Written by Md. Wasiul Bari  
c  PURPOSE: To compute the the probability of achieving  
c           a targrt degree of consolidation using RBSA model.  
c-----  
      Program RBSA_PVD  
      real kmn, ksd, kmne, ksde, scale, mvmn, ksmn, mvsmn, kssd  
      real mvsd, mvssd  
      logical lsck, lwellr, ldetrm, lstoch, lkhmv  
      character sub2*128, job*80, sub1*80, progm*32, rdate*24  
      character varfnc*6, base*64, outfl*70  
      external lnblnk  
      common/dbgrfl/ istat, debug  
  
      data progm/'This is RBSA_PVD (Version 1.0):'/  
c      constants  
      data zero/0.0/, one/1.0/  
  
      1 format(3a)  
      3 format()  
c      set input/output units  
      iin  = 5  
      istat = 10  
  
c      open the job data file  
      call openin( iin, base, ib )  
  
c      open output file  
      outfl = base(1:ib)  
      outfl(ib+1:ib+7) = 'out.stt'  
      open( istat, file = outfl, status = 'UNKNOWN' )  
  
c      read the job data file  
  
      call readdata(iin,istat,job,ldetrm,lstoch,re,lkhsv,lsmok,rw,  
>      lsck,lwellr,lkhmv,lsckmv,rs,dl,qw,kmn,mvmn,ksmn,mvsmn,  
>      ksd,mvsd,kssd,mvssd,thxku,thyku,thxks,thyks,thxmvu,  
>      thymvu,thxmvs,thymvs,ctime,uravg,varfnc)  
  
c      compute probability of achieving degree of consolidation  
  
      call statcons(iin,istat,job,ldetrm,lstoch,re,lkhsv,lsmok,rw,  
>      lsck,lwellr,lkhmv,lsckmv,rs,dl,qw,kmn,mvmn,ksmn,mvsmn,  
>      ksd,mvsd,kssd,mvssd,thxku,thyku,thxks,thyks,thxmvu,  
>      thymvu,thxmvs,thymvs,ctime,uravg,varfnc)  
  
      close (istat)  
      stop  
      end
```

```

c-----
c               subroutine readdata
c-----
c  Written by Md Wasiul Bari
c  PURPOSE:  Reads the input file for RBSA_PVD.
c-----
      subroutine readdata(iin,istat,job,ldetrm,lstoch,re,lkhsv,
>          lsmok,rw,lsck,lwellr,lkkmv,lsckmv,rs,dl,qw,kmn,
>          mvmn,ksmn,mvsmn,ksd,mvsv,kssd,mvssd,thxku,thyku,
>          thxks,thyks,thxmvu,thymvu,thxmvsv,thymvsv,
>          ctime,uravg,varfnc)

      parameter ( IT = 50 )
      real kmn, ksd, mvmn, ksmn, mvsmn, kssd, mvsv, mvssd
      real tmp(2)
      character*128 str
      character*(*) job, varfnc
      logical lsckmv,lkhsv, lsmok, ldetrm, lsck, lwellr, lkkmv,
      logical lstoch
      logical ltmp(2)
      external lnblnk

1  format(a)
2  format(a,3i5)
3  format(a,3e14.5)
4  format(a,15)
5  format(a,a)
6  format(e14.5)
7  format(a//)
c          1 read job title
      read(iin,1) job
      write(istat,7)job
      write(istat,7)'Input parameters'

c          2 Deterministic design ?
      read(iin,1) str
      if( nrdlog(str(IT:),ldetrm,1) .lt. 1 ) go to 100
      write(istat,4)'Deterministic analysis by
> Hansbo (1981) Eq.= ',ldetrm

c          3 Stochastic design ?
      read(iin,1) str
      if( nrdlog(str(IT:),lstoch,1) .lt. 1 ) go to 100
      write(istat,4)'Stochastic analysis= ',lstoch

c          4 Radius of influence zone
      read(iin,1) str
      if( nrdfp(str(IT:),re,1) .lt. 1 ) go to 100
      write(istat,3)'Radius of influence zone (m)= ',re

c          5 Radius of drain
      read(iin,1) str
      if( nrdfp(str(IT:),rw,1) .lt. 1 ) go to 100
      write(istat,3)'Radius of drain (m)= ',rw

c          6 Consider smear effect ?
      read(iin,1) str
      if( nrdlog(str(IT:),lsmok,1) .lt. 1 ) go to 100
      write(istat,4)'Consider smear effect= ',lsmok

```

```
c          7 Consider both horizontal permeability and
c          coeff. of volume compressibility spatial variable ?

      read(iin,1) str
      if( nrdlog(str(IT:),lkhmv,1) .lt. 1 ) go to 100
      write(istat,4)'Consider both horizontal permeability and
> coeff. of volume compressibility spatial variable= ',lkhmv

c          8 Consider only permeability spatially variable ?
      read(iin,1) str
      if( nrdlog(str(IT:),lkhsv,1) .lt. 1 ) go to 100
      write(istat,4)'Consider permeability is the only spatial
> variable= ',lkhsv

c          9 Special case with permeability and
c          coeff. of volume compressibility?

      read(iin,1) str
      if( nrdlog(str(IT:),lsckmv,1) .lt. 1 ) go to 100
      write(istat,4)'Special case with both permeability and
> coeff. of volume compressibility= ',lsckmv

c          10 Special case with only permeability ?
      read(iin,1) str
      if( nrdlog(str(IT:),lsck,1) .lt. 1 ) go to 100
      write(istat,4)'Special case with only
> permeability= ',lsck

c          11 Consider well resistance effect ?
      read(iin,1) str
      if( nrdlog(str(IT:),lwellr,1) .lt. 1 ) go to 100
      write(istat,4)'Consider well resistance effect
> (spatially constant) = ',lwellr

c          12 Radius of smear zone
      read(iin,1) str
      if( nrdfp(str(IT:),rs,1) .lt. 1 ) go to 100
      write(istat,3)'Radius of smear zone (m)= ',rs

c          13 Length of drain
      read(iin,1) str
      if( nrdfp(str(IT:),dl,1) .lt. 1 ) go to 100
      write(istat,3)'Length of the drain (m)= ',dl

c          14 Discharge capacity of drain
      read(iin,1) str
      if( nrdfp(str(IT:),qw,1) .lt. 1 ) go to 100
      write(istat,3)'Discharge capacity of drain (qubm/day)= ',qw

c          15 Horizontal permeability mean
      read(iin,1) str
      if( nrdfp(str(IT:),kmn,1) .lt. 1 ) go to 100
      write(istat,3)'Undisturbed permeability mean (m/day)= ',kmn

c          16 Coefficient of volume compress. mean
      read(iin,1) str
      if( nrdfp(str(IT:),mvmn,1) .lt. 1 ) go to 100
      write(istat,3)'Undisturbed compressibility
> mean (sq.m/kN)= ',mvmn
```

```
c          17 Smear permeability mean
read(iin,1) str
if( nrdfp(str(IT:),ksmn,1) .lt. 1 ) go to 100
write(istat,3)'Smear permeability mean (m/day)= ',ksmn

c          18 Smear compressibility mean
read(iin,1) str
if( nrdfp(str(IT:),mvsmn,1) .lt. 1 ) go to 100
write(istat,3)'Smear compressibility mean (sq.m/kN)= ',mvsmn

c          19 Horizaontal permeability standard dev.
read(iin,1) str
if( nrdfp(str(IT:),ksd,1) .lt. 1 ) go to 100
write(istat,3)'Undisturbed permeability standard
> dev. (m/day)= ',ksd

c          20 Coefficient of volume compressibility standard dev.
read(iin,1) str
if( nrdfp(str(IT:),mvsd,1) .lt. 1 ) go to 100
write(istat,3)'Undisturbed compressibility
> standard dev. (sq.m/kN)= ',mvsd

c          21 Smear permeability standard dev.
read(iin,1) str
if( nrdfp(str(IT:),kssd,1) .lt. 1 ) go to 100
write(istat,3)'Smear permeability standard dev.(m/day)= ',kssd

c          22 Coefficient of volume compressibility standard dev.
read(iin,1) str
if( nrdfp(str(IT:),mvssd,1) .lt. 1 ) go to 100
write(istat,3)'Smear compressibility
> standard dev. (sq.m/kN)= ',mvssd

c          23 scale(s) of fluctuation of undisturbed permeability
read(iin,1) str
n = nrdfp(str(IT:),tmp,2)
if( n .lt. 1 ) go to 100
thxku = tmp(1)
thyku = tmp(n)
write(istat,3)'Undisturbed permeability scale of fluctuation,
> X and Y directions (m)= ',thxku,thyku

c          24 scale(s) of fluctuation of smear permeability
read(iin,1) str
n = nrdfp(str(IT:),tmp,2)
if( n .lt. 1 ) go to 100
thxks = tmp(1)
thyks = tmp(n)
write(istat,3)'Smear permeability scale of fluctuation,
> X and Y directions (m)= ',thxks,thyks

c          25 scale(s) of fluctuation of undisturbed
c > compressibility
read(iin,1) str
n = nrdfp(str(IT:),tmp,2)
if( n .lt. 1 ) go to 100
thxmvu = tmp(1)
thymvu = tmp(n)
write(istat,3)'Undisturbed compressibility scale of
> fluctuation, X and Y directions (m)= ',thxmvu,thymvu
```

```

c          26 scale(s) of fluctuationof smear compressibility
read(iin,1) str
n = nrdfp(str(IT:),tmp,2)
if( n .lt. 1 ) go to 100
thxmvs = tmp(1)
thymvs = tmp(n)
write(istat,3)'Smear compressibility scale of fluctuation,
> X and Y directions (m)= ',thxmvs,thymvs

c          27 Consolidation time
read(iin,1) str
if( nrdfp(str(IT:),ctime,1) .lt. 1 ) go to 100
write(istat,3)'Consolidation time (day)= ',ctime

c          28 Target degree of consolidation
read(iin,1) str
if( nrdfp(str(IT:),uravg,1) .lt. 1 ) go to 100
write(istat,3)'Target degree of consolidation for
> radial drainage= ',uravg

c          get some defaults first
varfnc      = 'dlavx2'
c          close the input file
50 close(iin)
return
c          error reading data file

100 write(istat,1)'Error reading data file. Last line read was:'
write(istat,1) str
write(6,1)'Error reading data file. Last line read was:'
write(6,1) str
write(istat,1)'Execution stopped while reading data.'
write(6,1)'Execution stopped while reading data.'
stop
end

c-----
c          subroutine statcons
c-----
c  Wrtitten by Md. Wasiul Bari
c  PURPOSE: Compute statistics of  $U^*$  function and probability of
c          achieving a target degree of consolidation at a given time.
c-----
subroutine statcons(iin,istat,job,ldetrm,lstoch,re,lkhsv,
>    lsmok,rw,lsck,lwellr,lkhmv,lsckmv,rs,dl,qw,kmn,mvmn,
>    ksmn,mvsmn,ksd,mvsd,kssd,mvssd,thxku,thyku,thxks,
>    thyks,thxmvu,thymvu,thxmvs,thymvs,ctime,uravg,varfnc)

real*8 dvar, dpb, dthx, dthy, dthz, ddx, ddy, oned
real thxku,thyku,thxks,thyks,thxmvu,thymvu,thxmvs,thymvs
real*8 dlavx2
real*8 dmin1, dble, zed, zed1, zed2
real kmn, kmne, ksd, ksde, kcov, mvmn, ksmn, mvsmn, mvsd
real kssd,mvssd
real mustar, pkcov,mvcov,kscov, mvscov
logical lsck, lwellr
logical ldetrm, lstoch, lkhmv
logical lsckmv, lkhsv, lsmok
character*(150) job, sub1, sub2
character*(6) varfnc

```

```

external dlavx2
save pkmn, pksd, kcov, chmn, pchmn, nn
c      export parameters to variance function
common/dparam/ dvar, dpb, dthx, dthy, dthz
data ifirst/1/
data zero/0.0/, half/0.5/, one/1.0/, two/2.0/, oned/1.d0/
data pi/3.14159/,gamw/9.81/

1  format(a,a)
2  format(a,i4,a,i4,a)
3  format(a,e12.5)
4  format()
5  format(//a//)
6  format(a//)
7  format(/a,i4/)
8  format(a)
9  format(//a)
10 format(//a,e12.5)
123 format(e12.4)
-----
c      Deterministic Analysis

      write(istat,5)'Start of deterministic Analysis'

      write(istat,6)'Calculation of deterministic time for
> achieving target degree of consolidation
> (due to radial drainage only) '

      chmn = kmn/(mvmn*gamw)
      dsr = re/rw

      write(istat,3)'Drain sapacing ratio= ',dsr
      write(istat,3)'Coeff. of volume compressibility= ',mvmn
      write(istat,3)'Mean of horizontal coeff. of
> consolidation= ',chmn

      if( .not. lsmok) then

      write(istat,5)'No smear effects is considered '

      fn = alog(dsr)-0.75
      fs = 0.0
      if (.not.lwellr) then
      fr = 0.0
      write(istat,5)'Well-resistance effect is not considered '
      elseif (lwellr) then
      fr = (two*pi*d1*d1*kmn)/(3.0*qw)
      write(istat,5)'Well-resistance effect is considered '
      endif

      geop = fn+fs+fr
      dtime =(alog (one/(one-uravg))*(re*re*geop))/(two*chmn)
      duavg = one-exp(-((two*ctime*chmn)/(re*re*geop)))
      pduavg = duavg*100.0

      write(istat,3)'Drain spacing factor= ',fn
      write(istat,3)'Smear factor= ',fs
      write(istat,3)'Well-resistance factor= ',fr
      write(istat,3)'Parameter representing the drain spacing,
> smear and well-resistance effect = ',geop

```

```

        write(istat,10)'Deterministic time for achieving target
> degree of consolidation (day)= ',dtime
        write(istat,10)'Deterministic degree of consolidation
> at specified time (%)= ',pduavg

        elseif (lsmok .and. lkhsv) then

            write(istat,5)'Smear effect is considered but only
> permeability is assumed to be changed in the smear zone
> and compressibility remains unchanged in both undisturbed
> and smear zone '

            srat = rs/rw
            fn = alog(dsr)-0.75
            fs = ((kmn/ksmn)-one)*alog(srat)

            if (.not.lwellr) then
                fr = 0.0
            write(istat,5)'Well-resistance effect is not considered '
            elseif (lwellr) then
                fr = (two*pi*dl*dl*kmn)/(3.0*qw)
            write(istat,5)'Well-resistance effect is considered '
            endif

            geop = fn+fs+fr
            dtime = (alog (one/(one-uravg)))*(re*re*geop)/(two*chmn)
            duavg = one-exp(-((two*ctime*chmn)/(re*re*geop)))
            pduavg = duavg*100.0

            write(istat,3)'Drain spacing factor= ',fn
            write(istat,3)'Smear factor= ',fs
            write(istat,3)'Well-resistance factor= ',fr
            write(istat,3)'Parameter representing the drain spacing,
> smear and well-resistance effect = ',geop
            write(istat,10)'Deterministic time for achieving target
> degree of consolidation (day)= ',dtime
            write(istat,3)'Deterministic degree of consolidation
> at specified time (%)= ',pduavg

        endif

        if (lsmok .and. lkhmv) then

            write(istat,5)'Smear effect is considered and both
> permeability and compressibility are assumed to be changed
> in the smear zone '
            write(istat,6)'N.B.: The modified geomerty/smear zone
> parameter(alpha-star) proposed by Walker (2006) is used to
> take into account increased compressibility
> in the smear zone '

            srat = rs/rw
            fn = alog(dsr)-0.75
            fs = ((kmn/ksmn)-one)*alog(srat)

            rmv = (mvsmn/mvmn)
            gpar = (dsr*dsr-srat*srat)/(dsr*dsr-1.0)
            hpar = (srat*srat-1.0)/(dsr*dsr-1.0)

```

```

        if (.not.lwellr) then
            fr = 0.0
            write(istat,5)'Well-resistance effect is not considered '
        elseif (lwellr) then
            fr = (two*pi*d1*d1*kmn)/(3.0*qw)
            write(istat,5)'Well-resistance effect is considered '
        endif

        geop = fn+fs+fr
        geomv = gpar+hpar*rmv

        write(istat,3)'Drain spacing factor= ',fn
        write(istat,3)'Smear factor= ',fs
        write(istat,3)'Well-resistance factor= ',fr
        write(istat,3)'Parameter representing the drain spacing,
> smear and well-resistance effect = ',geop
        write(istat,3)'Smear zone compressibility
> parameter, = ',geomv

        dtime=(alog(one/(one-ravg)))*(re*re*geop*geomv))/(two*chmn)
        duavg = one-exp(-((two*ctime*chmn)/(re*re*geop*geomv)))
        pduavg = duavg*100.0

        write(istat,10)'Deterministic time for achieving target
> degree of consolidation (day)= ',dtime
        write(istat,3)'Deterministic degree of consolidation
> at specified time (%)= ',pduavg

        endif

        write(istat,5)'End of deterministic analysis'

c          Stochastic design of prefabricated vertical drain
c          Calculation of horizontal degree of consolidation

        if(lstoch .and. lkhsv ) then
            write(istat,5)'Start of stochastic analysis and only
> permeability is spatially random'
            write(istat,6)'Calculation of probability of achieving a
> target degree of consolidation within a specific time frame'

            mustar=alog(one/(one-uravg))
            dsr = re/rw

            write(istat,3)'Drain sapacing ratio= ',dsr
            write(istat,3)'Targer mean of lognormally distributed U*
> function= ',mustar

            if(.not. lsmok) then
                write(istat,5)'Start of analysis considering no
> smear effect '

                fn = alog(dsr)-0.75
                fs = 0.0

                if (.not.lwellr) then
                    fr = 0.0
                    write(istat,5)'Well-resistance effect is
> not considered '
                elseif (lwellr) then
                    fr = (two*pi*d1*d1*kmn)/(3.0*qw)

```

```

write(istat,5)'Well-resistance effect is considered '
endif

geop = fn+fs+fr
cpara1 = (two*dtime)/((re*re)*geop*mvmn*gamw)
cpara2 = (two*ctime)/((re*re)*geop*mvmn*gamw)

write(istat,3)'Parameter representing the drain spacing,
> smear and well resistance effect = ',geop

write(istat,5)'Calculation of statistical parameters of
> the U* function'

kcov = ksd/kmn
pkcov = kcov*100.0

pkvr = alog(one + (ksd*ksd)/(kmn*kmn))
pkmn = alog(kmn) - half*pkvr
pkstd = sqrt(pkvr)

write(istat,3)'Coeff. of variation of permeability
> (%)=',pkcov
write(istat,3)'Mean of the logarithm of undisturbed zone
> permeability (normally distributed)= ',pkmn
write(istat,3)'Standard deviation of the logarithm of
> permeability(normally distributed)= ',pkstd

c      Calculation of variance reduction factor

wiz = re-rw

dvar = oned
dthx = thxku
dthy = thyku

dx      = wiz
dy      = dl

ddx = dble(dx)
ddy = dble(dy)
dvar = -dvar
vf = dlavx2(ddx,ddy)
write(istat,3)'Variance reduction factor= ',vf
dvar = -dvar

pumn1= alog(cpara1)+alog(kmn)-half*alog(one+(kcov*kcov))
pumn2= alog(cpara2)+alog(kmn)-half*alog(one+(kcov*kcov))
pusd = sqrt(vf*alog(one+(kcov*kcov)))
zed1 = (alog(mustar)-pumn1)/pusd
zed2 = (alog(mustar)-pumn2)/pusd

pono1 = dphi(zed1)
pono2 = dphi(zed2)
prob1 = (one-pono1)*100.0
prob2 = (one-pono2)*100.0

write(istat,10)'Mean of normally distributed U*
> function at deterministic time= ',pumn1
write(istat,3)'Mean of normally distributed U*
> function at given time= ',pumn2
write(istat,3)'Standard dev. of normally distributed

```

```

> U* function= ',pusd
      write(istat,3)'Standard normal function= ',zed1
      write(istat,9)'Probability of acieveing
> target degree of '
      write(istat,3)'consolidation at deterministic time to
> achieve target degree of consolidation (%)= ',prob1
      write(istat,10)'Probability of acieveing target degree
> of consolidation at specified time (%)= ',prob2

      write(istat,5)'End of stochastic analysis considering no
> smear effect '

      endif

      if(lsmok .and. lsck) then

          write(istat,5)'Start of analysis considering spatially
> variable permeability (special case with smear) '
          write(istat,6)'N.B.: No x-correlation between
> undisturbed zone permeability and smear
> permeability is considered '

          srat = rs/rw
          fn = alog(dsr)-0.75

          if (.not.lwellr) then
              fr = 0.0
              write(istat,5)'Well-resistance effect is
> not considered '
          elseif (lwellr) then
              fr = (two*pi*dl*dl*kmn)/(3.0*qw)
              write(istat,5)'Well-resistance effect is considered '
          endif

          write(istat,5)'Calculation of statistical parameters of
> the U* function'

          kcov = ksd/kmn
          pkcov = kcov*100.0

          pkvr = alog(one + (ksd*ksd)/(kmn*kmn))
          pkmn = alog(kmn) - half*pkvr
          pksd = sqrt(pkvr)

          kscov = kssd/ksmn
          pkscov = kscov*100.0

          pksvr = alog(one + (kssd*kssd)/(ksmn*ksmn))
          pksmn = alog(ksmn) - half*pksvr
          pkssd = sqrt(pksvr)

          write(istat,3)'Coeff. of variation of undisturbed zone
> permeability (%)=' ,pkcov
          write(istat,3)'Mean of the logarithm of undisturbed zone
> permeability (normally distributed)= ',pkmn
          write(istat,3)'Standard deviation of the logarithm of
> undisturbed zone permeability(normally distributed)= ',pkdsd

```

```

c          Check especial case or not

          if (kcov. eq. kscov .and. thxku . eq. thxks .and.
>          thyku .eq. thyks) then
          write(istat,5)'This is a special smear case
> with only random permeability.'
          else
          write(istat,5)'This is not a special smear case with
> permeability. Please check input parameters'
          stop
          endif

c          Variance reduction function for smear zone

          wiz = re-rw

          dvar = oned
          dthx = thxks
          dthy = thyks

          dx      = wiz
          dy      = dl

          ddx = dble(dx)
          ddy = dble(dy)
          dvar = -dvar
          vfs = dlavx2 (ddx,ddy)
          write(istat,3)'Variance reduction factor = ',vfs
          dvar = -dvar

          pakvr = pkvr*vfs
          paksvr = pksvr*vfs

          akmn = exp(pkmn+(0.5*pakvr))
          aksmn = exp(pksmn+(0.5*paksvr))
          akvr= akmn*akmn*(exp(pakvr)-1)
          aksd= sqrt(akvr)
          aksvr= aksmn*aksmn*(exp(paksvr)-1)
          akssd= sqrt(aksvr)

          rkhks = (akmn/aksmn)
          fs = ((akmn/aksmn)-one)*alog(srata)

          fnmn = fn+fs+fr
          cpara1 = (two*dtime)/((re*re)*mvmn*gamw*fnmn)
          cpara2 = (two*ctime)/((re*re)*mvmn*gamw*fnmn)

          write(istat,3)'Effective mean of undisturbed zone
> permeability (m/day)= ',akmn
          write(istat,3)'Effective parameter representing the
> drain spacing, smear and well resistance effect = ',fnmn

          pumn1 = alog(cpara1)+pkmn
          pumn2 = alog(cpara2)+pkmn
          pusd = sqrt(pakvr)
          zed1 = (alog(mustar)-pumn1)/pusd
          zed2 = (alog(mustar)-pumn2)/pusd

          pono1 = dphi(zed1)
          pono2 = dphi(zed2)
          prob1 = (one-pono1)*100.0

```

```

        prob2 = (one-pono2)*100.0

        write(istat,10)'Mean of normally distributed U*
> function at deterministic time= ',pumn1
        write(istat,3)'Mean of normally distributed U*
> function at given time= ',pumn2
        write(istat,3)'Standard dev. of normally distributed
> U* function= ',pusd
        write(istat,3)'Standard normal function= ',zed1
        write(istat,9)'Probability of acieveing
> target degree of '
        write(istat,3)'consolidation at deterministic time to
> achieve target degree of consolidation (%)= ',probl
        write(istat,10)'Probability of acieveing target degree
> of consolidation at specified time (%)= ',prob2

        write(istat,5)'End of analysis considering spatially
> variable permeability (special case with smear) '

        elseif(lsmok .and. .not. lsck) then

        write(istat,5)'Start of analysis considering spatially
> variable permeability (general case with smear) '
        write(istat,6)'N.B.: No x-correlation between
> undisturbed zone permeability and smear
> permeability is considered '

        srat = rs/rw
        fn = alog(dsr)-0.75
        fns = alog(dsr/srat)-0.75

        if (.not.lwellr) then
        fr = 0.0
        write(istat,5)'Well-resistance effect is
> not considered '
        elseif (lwellr) then
        fr = (two*pi*dl*dl*kmn)/(3.0*qw)
        write(istat,5)'Well-resistance effect is considered '
        endif

        write(istat,5)'Calculation of statistical parameters of
> the U* function'

        kcov = ksd/kmn
        pkcov = kcov*100.0

        pkvr = alog(one + (ksd*ksd)/(kmn*kmn))
        pkmn = alog(kmn) - half*pkvr
        pksd = sqrt(pkvr)

        kscov = kssd/ksmn
        pkscov = kscov*100.0

        pksvr = alog(one + (kssd*kssd)/(ksmn*ksmn))
        pksmn = alog(ksmn) - half*pksvr
        pkssd = sqrt(pksvr)

        write(istat,3)'Coeff. of variation of undisturbed zone
> permeability (%)=',pkcov
        write(istat,3)'Mean of the logarithm of undisturbed zone

```

```

> permeability (normally distributed)= ',pkmn
    write(istat,3)'Standard deviation of the logarithm of
> undisturbed zone permeability(normally distributed)= ',pkspd
    write(istat,3)'Coeff. of variation of smear zone
> permeability (%)=' ,pkscov
    write(istat,3)'Mean of normally distributed smear zone
> permeability= ',pksmn
    write(istat,3)'Standard deviation of the logarithm of
> smear zone permeability(normally distributed)= ',pkssd

c      Check especial case or not

        if (kcov. eq. kscov .and. thxku . eq. thxks .and.
>         thyku .eq. thyks) then
        write(istat,5)'This problem also can be solved
> by considering as a special smear case with permeability.'
        else
        write(istat,5)'This is a general smear case with
> only random permeability'
        endif

c      Variance reduction function for smear zone

wiz = re-rw
dvar = oned
dthx = thxks
dthy = thyks

dx    = wiz
dy    = dl

ddx  = dble(dx)
ddy  = dble(dy)
dvar = -dvar
vfs  = dlavx2(ddx,ddy)
write(istat,3)'Variance reduction factor for smear
> parameter= ',vfs
dvar = -dvar

c      Variance reduction function for undisturbed zone

wiz = re-rw
dvar = oned
dthx = thxku
dthy = thyku

dx    = wiz
dy    = dl

ddx  = dble(dx)
ddy  = dble(dy)
dvar = -dvar
vfud = dlavx2(ddx,ddy)
write(istat,3)'Variance reduction factor undisturbed
> parameter= ',vfud
dvar = -dvar

pakvr = pkvr*vfud
paksvr = pksvr*vfs
akmn = exp(pkmn+(0.5*pakvr))
aksmn = exp(pksmn+(0.5*paksvr))

```

```

akvr= akmn*akmn*(exp(pakvr)-1)
aksd= sqrt(akvr)
aksvr= aksmn*aksmn*(exp(paksvr)-1)
akssd= sqrt(aksvr)

rkhks = (akmn/aksmn)
bpar = alog (srat)
apar = fns+fr

pwmn = pkmn-pksmn
pwvr = (pakvr + paksvr)/2.0
wmn = exp(pwmn+0.5*pwvr)
anuk = sqrt(akvr)/akmn
anuks = sqrt(aksvr)/aksmn
alpmn = apar+ (bpar*(exp(pwmn+0.5*pwvr)))
alpvr = ((2.0*anuks)/(anuk+anuks))*bpar*bpar*wmn*wmn
>      *(exp(pwvr)-1.0)
palpvr = alog(1.0+(alpvr/(alpmn*alpmn)))
palpmn = alog(alpmn)-0.5*palpvr
cpara1 = (two*dtime)/((re*re)*mvmn*gamw)
cpara2 = (two*ctime)/((re*re)*mvmn*gamw)

write(istat,3)'Mean of the logarithm of alpha
> parameter= ',palpmn
write(istat,3)'Variance of the logarithm of alpha
> parameter= ',palpvr
write(istat,3)'Effective mean of the ratio of
> undisturbed and smear permeability = ',wmn
write(istat,3)'Variance of logarithm of the ratio of
> undisturbed and smear permeability = ',pwvr

pumn1 = alog(cpara1)+pkmn-palpmn
pumn2 = alog(cpara2)+pkmn-palpmn
pusd = sqrt(palpvr)
zed1 = (alog(mustar)-pumn1)/pusd
zed2 = (alog(mustar)-pumn2)/pusd
pono1 = dphi(zed1)
pono2 = dphi(zed2)
prob1 = (one-pono1)*100.0
prob2 = (one-pono2)*100.0

write(istat,10)'Mean of normally distributed U*
> function at deterministic time= ',pumn1
write(istat,3)'Mean of normally distributed U*
> function at given time= ',pumn2
write(istat,3)'Standard dev. of normally distributed
> U* function= ',pusd
write(istat,3)'Standard normal function= ',zed1
write(istat,9)'Probability of acieveing target degree of
,

write(istat,3)'consolidation at deterministic time to
> achieve target degree of consolidation (%)= ',prob1
write(istat,10)'Probability of acieveing target degree
> of consolidation at specified time (%)= ',prob2

write(istat,5)'End of analysis considering spatially
> variable permeability (general case with smear) '

endif

endif

```

```

if(lstoch .and. lkhmv ) then

    write(istat,9)'Start of stochastic analysis considering
> both permeability and '
    write(istat,8)'coeff. of volume compress. is spatially
> random '
    write(istat,6)'N.B.: No x-correlation between permeability
> and compressibility is considered '
    write(istat,6)'Calculation of probability of achieving a
> target degree of consolidation within a specified time frame'

    mustar=log(one/(one-uravg))
    dsr = re/rw

    write(istat,3)'Drain spacing ratio= ',dsr
    write(istat,3)'Target mean of lognormally distributed U*
>function= ',mustar

    if(.not. lsmok) then

        write(istat,9)'Start of analysis without considering
> smear effect. '

        fn = alog(dsr)-0.75
        fs = 0.0

        if (.not.lwellr) then
            fr = 0.0
            write(istat,5)'Well-resistance effect is
> not considered '
        elseif (lwellr) then
            fr = (two*pi*dl*dl*kmn)/(3.0*qw)
            write(istat,5)'Well-resistance effect is considered '
        endif

        geop = fn+fs+fr
        cpara1 = (two*dtime)/((re*re)*geop*gamw)
        cpara2 = (two*ctime)/((re*re)*geop*gamw)
        write(istat,3)'Parameter representing the drain spacing,
> smear and well resistance effect = ',geop

        write(istat,5)'Calculation of statistical parameters of
> the U* function'

        kcov = ksd/kmn
        pkcov = kcov*100.0

        pkvr = alog(one + (ksd*ksd)/(kmn*kmn))
        pkmn = alog(kmn) - half*pkvr
        pksd = sqrt(pkvr)

        mvcov = mvsd/mvmn
        pmvcov = mvcov*100.0

        pmvvr = alog(one + (mvsd*mvsd)/(mvmn*mvmn))
        pmvnm = alog(mvnm) - half*pmvvr
        pmvds = sqrt(pmvvr)

        write(istat,3)'Coeff. of variation of
> permeability (%)=',pkcov

```

```

        write(istat,3)'Mean of normally distributed
> permeability= ',pkmn
        write(istat,3)'Standard deviation of the logarithm of
> permeability(normally distributed)= ',pkstd
        write(istat,3)'Coeff. of variation of coeff. of
> volume compressibility (%)=' ,pmvcov
        write(istat,3)'Mean of normally distributed coeff. of
> volume compressibility =' ,pmvmn
        write(istat,3)'Standard dev. of the logarithm of coeff.
> of volume compressibility (normally distributed)= ',pmvstd

```

c Variance reduction function for compressibility

```

wiz = re-rw

dvar = oned
dthx = thxmvu
dthy = thymvu

dx     = wiz
dy     = dl

ddx   = dble(dx)
ddy   = dble(dy)
dvar  = -dvar
vfmvu = dlavx2(ddx,ddy)
write(istat,3)'Variance reduction factor for
> compressibility= ',vfmvu
dvar  = -dvar

```

c Variance reduction function for permeability

```

wiz = re-rw

dvar = oned
dthx = thxku
dthy = thyku

dx     = wiz
dy     = dl

ddx   = dble(dx)
ddy   = dble(dy)
dvar  = -dvar
vfud  = dlavx2(ddx,ddy)
write(istat,3)'Variance reduction factor for
> permeability= ',vfud
dvar  = -dvar

pumn1 = alog(cpara1)+pkmn-pmvmn
pumn2 = alog(cpara2)+pkmn-pmvmn
puvr  = (vfud*pkvr)+(vfmvu*pmvvr)
pusd  = sqrt(puvr)
zed1  = (alog(mustar)-pumn1)/pusd
zed2  = (alog(mustar)-pumn2)/pusd

pono1 = dphi(zed1)
pono2 = dphi(zed2)
prob1 = (one-pono1)*100.0
prob2 = (one-pono2)*100.0

```

```

        write(istat,10)'Mean of normally distributed U*
> function at deterministic time= ',pumn1
        write(istat,3)'Mean of normally distributed U*
> function at given time= ',pumn2
        write(istat,3)'Standard dev. of normally distributed
> U* function= ',pusd
        write(istat,3)'Standard normal function= ',zed1
        write(istat,9)'Probability of acieveing
> target degree of '
        write(istat,3)'consolidation at deterministic time to
> achieve target degree of consolidation (%)= ',probl
        write(istat,10)'Probability of acieveing target degree
> of consolidation at specified time (%)= ',prob2

        write(istat,9)'End of stochastic analysis
> considering both permeability and compressibility as random '
        write(istat,6)'but no smear effect.'

endif

if(lsmok .and. lsckmv) then

        write(istat,5)'Start of analysis considering both
> permeability and compressibility as random variable
> (special case with smear) '

        srat = rs/rw
        fn = alog(dsr)-0.75

        if (.not.lwellr) then
                fr = 0.0
                write(istat,5)'Well-resistance effect is
> not considered '
                elseif (lwellr) then
                        fr = (two*pi*dl*dl*kmn)/(3.0*qw)
                        write(istat,5)'Well-resistance effect is considered '
                endif

        write(istat,5)'Calculation of statistical parameters of
> the U* function'

        kcov = ksd/kmn
        pkcov = kcov*100.0

        pkvr = alog(one + (ksd*ksd)/(kmn*kmn))
        pkmn = alog(kmn) - half*pkvr
        pksd = sqrt(pkvr)

        kscov = kssd/ksmn
        pkscov = kscov*100.0

        pksvr = alog(one + (kssd*kssd)/(ksmn*ksmn))
        pksmn = alog(ksmn) - half*pksvr
        pkssd = sqrt(pksvr)

        mvcov = mvsd/mvmn
        pmvcov = mvcov*100.0

        pmvvr = alog(one + (mvsd*mvsd)/(mvmn*mvmn))
        pmvmn = alog(mvmn) - half*pmvvr
        pmvsd = sqrt(pmvvr)

```

```

        mvscov = mvssd/mvsmn
        pmvscov = mvscov*100.0

        pmvsvr = alog(one + (mvssd*mvssd)/(mvsmn*mvsmn))
        pmvsmn = alog(mvsmn) - half*pmvsvr
        pmvssd = sqrt(pmvsvr)

        write(istat,3)'Coeff. of variation of undisturbed zone
> permeability (%)=',pkcov
        write(istat,3)'Mean of the logarithm of undisturbed zone
> permeability (normally distributed)= ',pkmn
        write(istat,3)'Standard deviation of the logarithm of
> undisturbed zone permeability (normally distributed)= ',pkstd
        write(istat,3)'Coeff. of variation of smear zone
> permeability (%)=',pkscov
        write(istat,3)'Mean of normally distributed smear zone
> permeability= ',pksmn
        write(istat,3)'Standard deviation of the logarithm of
> smear zone permeability (normally distributed)= ',pkssd
        write(istat,3)'Coeff. of variation of undisturbed zone
> compressibility (%)=',pmvcov
        write(istat,3)'Mean of the logarithm of undisturbed zone
> compressibility (normally distributed)= ',pmvmn
        write(istat,3)'Standard deviation of the logarithm of
> undisturbed zone compressibility
> (normally distributed)= ',pmvstd
        write(istat,3)'Coeff. of variation of smear zone
> compressibility (%)=',pmvscov
        write(istat,3)'Mean of normally distributed smear zone
> compressibility= ',pmvsmn
        write(istat,3)'Standard deviation of the logarithm of
> smear zone compressibility (normally distributed)= ',pmvssd

c          Check especial case or not

        if (kcov. eq. kscov .and. thxku . eq. thxks .and.
>          thyku .eq. thyks) then
        if (mvcov. eq. mvscov .and. thxmvu . eq. thxmvsv
>          .and. thymvu .eq. thymvsv) then
            cec = 1.0
        else
            cec = 0.0
        endif

        else
            cec = 0.0
        endif

        if (cec == 1.0) then
            write(istat,5)'This is a special smear case
> with randon permeability and compressibility.'
        elseif (cec == 0.0) then
            write(istat,5)'This is not a special smear case with
> permeability and compressibility. Please check input
> parameters'
            stop
        endif

c          Variance reduction function for permeability

        wiz = re-rw

```

```

dvar = oned
dthx = thxks
dthy = thyks

dx      = wiz
dy      = dl

ddx = dble(dx)
ddy = dble(dy)
dvar = -dvar
vfk = dlavx2(ddx,ddy)
write(istat,3)'Variance reduction factor for
> permeability = ',vfk
dvar = -dvar

c      Variance reduction function for compressibility

wiz = re-rw

dvar = oned
dthx = thxmvs
dthy = thymvs

dx      = wiz
dy      = dl

ddx = dble(dx)
ddy = dble(dy)
dvar = -dvar
vfmv = dlavx2(ddx,ddy)
write(istat,3)'Variance reduction factor for
> permeability = ',vfmv
dvar = -dvar

pakvr = pkvr*vfk
paksvr = pksvr*vfk

akmn = exp(pkmn+(0.5*pakvr))
aksmn = exp(pksmn+(0.5*paksvr))
akvr= akmn*akmn*(exp(pakvr)-1)
aksd= sqrt(akvr)
aksvr= aksmn*aksmn*(exp(paksvr)-1)
akssd= sqrt(aksvr)

rkhks = (akmn/aksmn)
fs = ((akmn/aksmn)-one)*alog(srat)

alphp = fn+fs+fr

pamvvr = pmvvr*vfmv
pamvsvr = pmvsvr*vfmv

amvmn = exp(pmvmn+(0.5*pamvvr))
amvsmn = exp(pmvsmn+(0.5*pamvsvr))
amvvr= amvmn*amvmn*(exp(pamvvr)-1)
amvsvr= amvsmn*amvsmn*(exp(pamvsvr)-1)
amvssd= sqrt(amvsvr)

rmvmvs = (amvsmn/amvmn)

```

```

gpar = (dsr*dsr-srat*srat)/(dsr*dsr-1.0)
hpar = (srat*srat-1.0)/(dsr*dsr-1.0)
alphmvp = gpar+hpar*rmvmvs

cpara1 = (two*dtime)/((re*re)*gamw*alphp*alphmvp)
cpara2 = (two*ctime)/((re*re)*gamw*alphp*alphmvp)

pumn1 = alog(cpara1)+pkmn-pmvmn
pumn2 = alog(cpara2)+pkmn-pmvmn
puvr = (vfk*pkvr)+(vfmv*pmvvr)
pusd = sqrt(puvr)
zed1 = (alog(mustar)-pumn1)/pusd
zed2 = (alog(mustar)-pumn2)/pusd

pono1 = dphi(zed1)
pono2 = dphi(zed2)
prob1 = (one-pono1)*100.0
prob2 = (one-pono2)*100.0

write(istat,10)'Mean of normally distributed U*
> function at deterministic time= ',pumn1
write(istat,3)'Mean of normally distributed U*
> function at given time= ',pumn2
write(istat,3)'Standard dev. of normally distributed
> U* function= ',pusd
write(istat,3)'Standard normal function= ',zed1
write(istat,9)'Probability of acieveing
> target degree of '
write(istat,3)'consolidation at deterministic time to
> achieve target degree of consolidation (%)= ',prob1
write(istat,10)'Probability of acieveing target degree
> of consolidation at specified time (%)= ',prob2

write(istat,5)'End of analysis considering random
> permeability and compressibility (special case with smear) '

elseif(lsmok .and. .not. lsckmv) then

write(istat,5)'Start of analysis considering both
> permeability and compressibility as random variable
> (general case with smear) '

srat = rs/rw
fn = alog(dsr)-0.75
fns = alog(dsr/srat)-0.75

if (.not.lwellr) then
fr = 0.0
write(istat,5)'Well-resistance effect is
> not considered '
elseif (lwellr) then
fr = (two*pi*dl*dl*kmn)/(3.0*qw)
write(istat,5)'Well-resistance effect is considered '
endif

write(istat,5)'Calculation of statistical parameters of
> the U* function'

kcov = ksd/kmn
pkcov = kcov*100.0

```

```

pkvr = alog(one + (ksd*ksd)/(kmn*kmn))
pkmn = alog(kmn) - half*pkvr
pkzd = sqrt(pkvr)

kscov = kssd/ksmn
pkscov = kscov*100.0

pksvr = alog(one + (kssd*kssd)/(ksmn*ksmn))
pksmn = alog(ksmn) - half*pksvr
pkzsd = sqrt(pksvr)

mvcov = mvzd/mvmn
pmvcov = mvcov*100.0

pmvvr = alog(one + (mvzd*mvzd)/(mvmn*mvmn))
pmvmn = alog(mvmn) - half*pmvvr
pmvzd = sqrt(pmvvr)

mvscov = mvssd/mvsmn
pmvscov = mvscov*100.0

pmvsvr = alog(one + (mvssd*mvssd)/(mvsmn*mvsmn))
pmvsmn = alog(mvsmn) - half*pmvsvr
pmvssd = sqrt(pmvsvr)

write(istat,3)'Coeff. of variation of undisturbed zone
> permeability (%)=' ,pkcov
write(istat,3)'Mean of the logarithm of undisturbed zone
> permeability (normally distributed)= ' ,pkmn
write(istat,3)'Standard deviation of the logarithm of
> undisturbed zone permeability (normally distributed)= ' ,pkzd
write(istat,3)'Coeff. of variation of smear zone
> permeability (%)=' ,pkscov
write(istat,3)'Mean of normally distributed smear zone
> permeability= ' ,pksmn
write(istat,3)'Standard deviation of the logarithm of
> smear zone permeability (normally distributed)= ' ,pkzsd
write(istat,3)'Coeff. of variation of undisturbed zone
> compressibility (%)=' ,pmvcov
write(istat,3)'Mean of the logarithm of undisturbed zone
> compressibility (normally distributed)= ' ,pmvmn
write(istat,3)'Standard deviation of the logarithm of
> undisturbed zone compressibility
> (normally distributed)= ' ,pmvzd
write(istat,3)'Coeff. of variation of smear zone
> compressibility (%)=' ,pmvscov
write(istat,3)'Mean of normally distributed smear zone
> compressibility= ' ,pmvsmn
write(istat,3)'Standard deviation of the logarithm of
> smear zone compressibility (normally distributed)= ' ,pmvssd

c          Check especial case or not

if (kcov. eq. kscov .and. thxku . eq. thxks .and.
>      thyku .eq. thyks) then
if (mvcov. eq. mvscov .and. thxmvu . eq. thxmvz
>      .and. thymvu .eq. thymvz) then
cec = 1.0
else
cec = 0.0

```

```

        endif
    else
        cec = 0.0
    endif

    if (cec == 1.0) then
        write(istat,5)'This problem also can be solved
> by considering as a special smear case with permeability
> and compressibility.'
    elseif (cec == 0.0) then
        write(istat,5)'This is a general smear case with
> random permeability and compressibility'
    endif

c      Variance reduction function for undisturbed permeability

        wiz = re-rw

        dvar = oned
        dthx = thxku
        dthy = thyku

        dx      = wiz
        dy      = dl

        ddx = dble(dx)
        ddy = dble(dy)
        dvar = -dvar
        vfku = dlavx2(ddx,ddy)
        write(istat,3)'Variance reduction factor for
> undisturbed permeability = ',vfku
        dvar = -dvar

c      Variance reduction function for smear permeability

        wiz = re-rw

        dvar = oned
        dthx = thxks
        dthy = thyks

        dx      = wiz
        dy      = dl

        ddx = dble(dx)
        ddy = dble(dy)
        dvar = -dvar
        vfks = dlavx2(ddx,ddy)
        write(istat,3)'Variance reduction factor for
> smear permeability = ',vfks
        dvar = -dvar

c      Variance reduction function for undisturbed compressibility

        wiz = re-rw

        dvar = oned
        dthx = thxmvu
        dthy = thymvu

        dx      = wiz

```

```

dy      = dl

ddx = dble(dx)
ddy = dble(dy)
dvar = -dvar
vfmvu = dlavx2(ddx,ddy)
write(istat,3)'Variance reduction factor for
> undisturbed compressibility = ',vfmvu
dvar = -dvar

c      Variance reduction function for smear compressibility

wiz = re-rw

dvar = oned
dthx = thxmvs
dthy = thymvs

dx      = wiz
dy      = dl

ddx = dble(dx)
ddy = dble(dy)
dvar = -dvar
vfmvs = dlavx2(ddx,ddy)
write(istat,3)'Variance reduction factor for
> smear permeability = ',vfmvs
dvar = -dvar

pakvr = pkvr*vfku
paksvr = pksvr*vfks

akmn = exp(pkmn+(0.5*pakvr))
aksmn = exp(pksmn+(0.5*paksvr))
akvr= akmn*akmn*(exp(pakvr)-1)
aksd= sqrt(akvr)
aksvr= aksmn*aksmn*(exp(paksvr)-1)
akssd= sqrt(aksvr)

rkhks = (akmn/aksmn)
bpar = alog (srat)
apar = fns+fr

pwmn = pkmn-pksmn
pwvr = (pakvr + paksvr)/2.0
wmn = exp(pwmn+0.5*pwvr)
anuk = sqrt(akvr)/akmn
anuks = sqrt(aksvr)/aksmn
alpmn = apar+ (bpar*(exp(pwmn+0.5*pwvr)))
alpvr = ((2.0*anuks)/(anuk+anuks))*bpar*bpar*wmn*wmn
>      *(exp(pwvr)-1.0)
palpvr = alog(1.0+(alpvr/(alpmn*alpmn)))
palpmn = alog(alpmn)-0.5*palpvr

pamvvr = pmvvr*vfmvu
pamvsvr = pmvsvr*vfmvs

amvmn = exp(pmvmn+(0.5*pamvvr))
amvsmn = exp(pmvsmn+(0.5*pamvsvr))
amvvr= amvmn*amvmn*(exp(pamvvr)-1)
amvsd= sqrt(amvvr)

```

```

amvsvr= amvsmn*amvsmn*(exp(pamvsvr)-1)
amvssd= sqrt(amvsvr)

rmvmvs = (amvsmn/amvmn)
gpar = (dsr*dsr-srat*srat)/(dsr*dsr-1.0)
hpar = (srat*srat-1.0)/(dsr*dsr-1.0)

pvmn = pmvsmn-pmvmn
pvvr = (pamvvr + pamvsvr)/2.0
vmn = exp(pvmn+0.5*pvvr)
anumv = sqrt(amvvr)/amvmn
anumvs = sqrt(amvsvr)/amvsmn
alpmvmn = gpar+ (hpar*(exp(pvmn+0.5*pvvr)))
alpmvvr= ((2.0*anumvs)/(anumv+anumvs))*hpar*hpar*vmn*vmn
> * (exp(pvvr)-1.0)
palpmvr = alog(1.0+(alpmvvr/(alpmvmn*alpmvmn)))
palpmmn = alog(alpmvmn)-0.5*palpmvr

cpara1 = (two*dtime)/((re*re)*gamw)
cpara2 = (two*ctime)/((re*re)*gamw)

write(istat,3)'Mean of the logarithm of alpha
> parameter= ',palpmn
write(istat,3)'Variance of the logarithm of alpha
> parameter= ',palpvr
write(istat,3)'Effective mean of the ratio of
> undisturbed and smear permeability = ',wmn
write(istat,3)'Variance of logarithm of the ratio of
> undisturbed and smear permeability = ',pvvr
write(istat,3)'Mean of the logarithm of alphamv
> parameter= ',palpmmn
write(istat,3)'Variance of the logarithm of alphamv
> parameter= ',palpmvr
write(istat,3)'Effective mean of the ratio of
> undisturbed and smear compressibility = ',vmn
write(istat,3)'Variance of logarithm of the ratio of
> undisturbed and smear compressibility = ',pvvr

pumn1 = alog(cpara1)+pkmn-pmvmn-palpmn-palpmmn
pumn2 = alog(cpara2)+pkmn-pmvmn-palpmn-palpmmn
puvr = palpvr+palpmvr
pusd = sqrt(puvr)
zed1 = (alog(mustar)-pumn1)/pusd
zed2 = (alog(mustar)-pumn2)/pusd

pono1 = dphi(zed1)
pono2 = dphi(zed2)
prob1 = (one-pono1)*100.0
prob2 = (one-pono2)*100.0

write(istat,10)'Mean of normally distributed U*
> function at deterministic time= ',pumn1
write(istat,3)'Mean of normally distributed U*
> function at given time= ',pumn2
write(istat,3)'Standard dev. of normally distributed
> U* function= ',pusd
write(istat,3)'Standard normal function= ',zed1
write(istat,9)'Probability of acieveing

```

```

> target degree of '
      write(istat,3)'consolidation at deterministic time to
> achieve target degree of consolidation (%)= ',prob1
      write(istat,10)'Probability of acieveing target degree
> of consolidation at specified time (%)= ',prob2

      write(istat,5)'End of analysis considering random
> permeability and compressibility (general case with smear) '

      endif

      endif

999 return
      end

```

```

c-----
c                               subroutine openin
c-----
c  PURPOSE  to open a data file given by an argument on the command
c           line
c  Courtesy: http://www.engmath.dal.ca/rfem/
c-----
      subroutine openin( iin, base, ib )
      parameter (karg = 0)
      character*(*) base
      logical found

1     format(a,a)
2     format(a,$)
c     get the data file name
      narg = iargc()
      if( narg .lt. (karg+1) ) then
        write(6,2)'Please enter the data file name: '
        read(5,1) base
      else
        call getarg( (karg+1), base )
      endif

      inquire( file=base, exist=found)
      if( .not. found ) then
        il = lnblnk(base)
        write(6,1)'Data file not found: ',base(1:il)
        write(6,1)'Please create or check spelling.'
        stop
      endif
c     open the data file
      open( iin, file = base, status = 'OLD' )
c     find basename
      il = lnblnk( base )
      do 10 id = il, 1, -1
        if( base(id:id) .eq. '.' ) then
          ib = id - 1
          if( ib .le. 0 ) then
            base = 'mrflow'
            ib = 6
          endif
          return
        endif
      do 10
      endif

```

```

10 continue
   ib = il

   return
end

```

```

-----
c
c                               Function dlavx2
c-----
c  PURPOSE  returns the covariance between two points in a 2-D
c            Markovian random field.
c  Courtesy: http://www.engmath.dal.ca/rfem/
c-----

real*8 function dlavx2( X, Y )
parameter (NG = 20)
implicit real*8 (a-h,o-z)
dimension w(NG/2), z(NG/2)
common/dparam/ var, dpb, dthx, dthy, dthz
data zero/0.d0/, one/1.d0/, two/2.d0/, three/3.d0/
data quart/0.25d0/, half/0.5d0/

data w/0.017614007139152118312d0, 0.040601429800386941331d0,
> 0.062672048334109063570d0, 0.083276741576704748725d0,
> 0.101930119817240435037d0, 0.118194531961518417312d0,
> 0.131688638449176626898d0, 0.142096109318382051329d0,
> 0.149172986472603746788d0, 0.152753387130725850698d0/
data z/0.993128599185094924786d0, 0.963971927277913791268d0,
> 0.912234428251325905868d0, 0.839116971822218823395d0,
> 0.746331906460150792614d0, 0.636053680726515025453d0,
> 0.510867001950827098004d0, 0.373706088715419560673d0,
> 0.227785851141645078080d0, 0.076526521133497333755d0/

exp(zz) = dexp(zz)
abs(zz) = dabs(zz)
sqrt(zz) = dsqrt(zz)

aY = abs(Y)
aX = abs(X)
if( var .lt. zero ) then ! return variance function
  if( (dthx .eq. zero) .and. (dthy .eq. zero) ) then
    if( (X .eq. zero) .and. (Y .eq. zero) ) then
      dlavx2 = -var
    else
      dlavx2 = zero
    endif
  elseif( dthx .eq. zero ) then
    if( X .eq. zero ) then
      r2 = half*aY
      ty = two/dthy
      d1 = zero
      do 10 j = 1, NG
        if( j .le. 10 ) then
          yj = r2*(one - z(j))
          tz = w(j)*(one + z(j))
        else
          yj = r2*(one + z(21-j))
          tz = w(21-j)*(one - z(21-j))
        endif
        a2 = ty*yj
        d1 = d1 + tz*exp(-a2)
      enddo
    endif
  endif
endif

```

```

10         continue
           dlavx2 = -half*var*d1
         else
           dlavx2 = zero
         endif
elseif( dthy .eq. zero ) then
  if( Y .eq. zero ) then
    r1 = half*aX
    tx = two/dthx
    d1 = zero
    do 20 i = 1, NG
      if( i .le. 10 ) then
        xi = r1*(one - z(i))
        qz = w(i)*(one + z(i))
      else
        xi = r1*(one + z(21-i))
        qz = w(21-i)*(one - z(21-i))
      endif
      a1 = tx*xi
      d1 = d1 + qz*exp(-a1)
20      continue
           dlavx2 = -half*var*d1
         else
           dlavx2 = zero
         endif
else
  r1 = half*aX
  r2 = half*aY
  tx = two/dthx
  ty = two/dthy
  d1 = zero
  do 40 i = 1, NG
    if( i .le. 10 ) then
      xi = r1*(one - z(i))
      qz = w(i)*(one + z(i))
    else
      xi = r1*(one + z(21-i))
      qz = w(21-i)*(one - z(21-i))
    endif
    a1 = tx*xi
    d2 = zero
    do 30 j = 1, NG
      if( j .le. 10 ) then
        yj = r2*(one - z(j))
        tz = w(j)*(one + z(j))
      else
        yj = r2*(one + z(21-j))
        tz = w(21-j)*(one - z(21-j))
      endif
      a2 = ty*yj
      T = sqrt(a1*a1 + a2*a2)
      d2 = d2 + tz*exp(-T)
30      continue
           d1 = d1 + qz*d2
40      continue
           dlavx2 = -quart*var*d1
         endif
else
           ! var > 0, return covariance
  if( (dthx .eq. zero) .and. (dthy .eq. zero) ) then
    if( (X .eq. zero) .and. (Y .eq. zero) ) then

```

```

        dlavx2 = var
    else
        dlavx2 = zero
    endif
elseif( dthx .eq. zero ) then
    if( X .eq. zero ) then
        dlavx2 = var*exp(-two*aY/dthy)
    else
        dlavx2 = zero
    endif
elseif( dthy .eq. zero ) then
    if( Y .eq. zero ) then
        dlavx2 = var*exp(-two*aX/dthx)
    else
        dlavx2 = zero
    endif
else
    a1 = two*aX/dthx
    a2 = two*aY/dthy
    T = sqrt(a1*a1 + a2*a2)
    dlavx2 = var*exp( -T )
endif
endif

return
end

```

```

c-----
c                               Integer Function Lnblnk
c-----
c  PURPOSE  returns the index of the last non-blank character in a
c            string.
c  Courtesy: http://www.engmath.dal.ca/rfem/
c-----

integer function lnblnk( str )
character*(*) str
character*1 space, tab, null, char
data space/' '/, tab/' '/

null = char(0)
i = len( str )
do 10 j = i, 1, -1
    if(      str(j:j) .ne. space
>      .and. str(j:j) .ne. null
>      .and. str(j:j) .ne. tab ) then
        lnblnk = j
        return
    endif
10 continue
lnblnk = 0

return
end

```

```

c-----
c
c                                     Function dphi
c-----
c Double Precision Version 1.1
c PURPOSE:  to return the standard normal probability distribution
c           function
c Courtesy: http://www.engmath.dal.ca/rfem/
c-----

      real*8 function dphi(z)
      implicit real*8 (a-h,o-z)
      parameter (NPROBS = 768)
      dimension p(NPROBS)
      real*8 nine
c
c       real*8 constants
      data zero, pt01,  pt025,  sixth/
>      0.d0, 0.01d0, 0.025d0, 0.166666666666666667d0/
      data half, one, two, three, four, five, six, eight,nine/
>      0.5d0, 1.d0, 2.d0, 3.d0, 4.d0, 5.d0, 6.d0, 8.d0, 9.d0/
      data ten, fifteen, twnty4, one00, one20, one29, sevn20/
>      10.d0,15.d0, 24.d0, 100.d0, 120.d0, 129.d0, 720.d0/
      data rt2pi/2.5066282746310005024d0/, eund/-300.d0/
c
c       probability tables
      data (p(i),i=1,15)/
>4.960106436853684d-01,4.920216862830980d-01,4.880335265858873d-01,
>4.840465631471693d-01,4.800611941616275d-01,4.760778173458932d-01,
>4.720968298194789d-01,4.681186279860126d-01,4.641436074148279d-01,
>4.601721627229710d-01,4.562046874576832d-01,4.522415739794162d-01,
>4.482832133454389d-01,4.443299951940936d-01,4.403823076297575d-01/
      data (p(i),i=16,30)/
>4.364405371085672d-01,4.325050683249616d-01,4.285762840990993d-01,
>4.246545652652046d-01,4.207402905608970d-01,4.168338365175577d-01,
>4.129355773517854d-01,4.090458848579941d-01,4.051651283022042d-01,
>4.012936743170763d-01,3.974318867982395d-01,3.935801268019605d-01,
>3.897387524442028d-01,3.859081188011227d-01,3.820885778110474d-01/
      data (p(i),i=31,45)/
>3.782804781779807d-01,3.744841652766800d-01,3.706999810593465d-01,
>3.669282639639719d-01,3.631693488243809d-01,3.594235667820088d-01,
>3.556912451994533d-01,3.519727075758372d-01,3.482682734640177d-01,
>3.445782583896759d-01,3.409029737723226d-01,3.372427268482495d-01,
>3.335978205954577d-01,3.299685536605936d-01,3.263552202879201d-01/
      data (p(i),i=46,60)/
>3.227581102503477d-01,3.191775087825558d-01,3.156136965162226d-01,
>3.120669494173905d-01,3.085375387259869d-01,3.050257308975195d-01,
>3.015317875469662d-01,2.980559653948764d-01,2.945985162156980d-01,
>2.911596867883464d-01,2.877397188490270d-01,2.843388490463242d-01,
>2.809573088985644d-01,2.775953247534649d-01,2.742531177500736d-01/
      data (p(i),i=61,75)/
>2.709309037830058d-01,2.676288934689831d-01,2.643472921156776d-01,
>2.610862996928617d-01,2.578461108058648d-01,2.546269146713361d-01,
>2.514288950953101d-01,2.482522304535706d-01,2.450970936743094d-01,
>2.419636522230730d-01,2.388520680899867d-01,2.35762497792512d-01,
>2.326950923008975d-01,2.296499971647906d-01,2.266273523768682d-01/
      data (p(i),i=76,90)/
>2.236272924375995d-01,2.206499463426497d-01,2.176954375857332d-01,
>2.147638841636371d-01,2.118553985833966d-01,2.089700878716017d-01,
>2.061080535858131d-01,2.032693918280685d-01,2.004541932604497d-01,
>1.976625431226924d-01,1.948945212518084d-01,1.921502021036962d-01,
>1.894296547767121d-01,1.867329430371727d-01,1.840601253467595d-01/
      data (p(i),i=91,105)/
>1.814112548917973d-01,1.787863796143717d-01,1.761855422452580d-01,
>1.736087803386246d-01,1.710561263084818d-01,1.685276074668378d-01,
>1.660232460635296d-01,1.635430593276923d-01,1.610870595108309d-01,
>1.586552539314571d-01,1.562476450212546d-01,1.538642303727349d-01,
>1.515050027883437d-01,1.491699503309815d-01,1.468590563758959d-01/
      data (p(i),i=106,120)/
>1.445722996639096d-01,1.423096543559392d-01,1.400710900887691d-01,

```

```

>1.378565720320355d-01,1.356660609463827d-01,1.334995132427472d-01,
>1.313568810427307d-01,1.292381122400178d-01,1.271431505627982d-01,
>1.250719356371502d-01,1.230244030513434d-01,1.210004844210182d-01,
>1.190001074552007d-01,1.170231960231087d-01,1.150696702217083d-01/
data (p(i),i=121,135)/
>1.131394464439773d-01,1.112324374478346d-01,1.093485524256919d-01,
>1.074876970745869d-01,1.056497736668553d-01,1.038346811213005d-01,
>1.020423150748192d-01,1.002725679544421d-01,9.852532904974787d-02,
>9.680048458561030d-02,9.509791779523907d-02,9.341750899347179d-02,
>9.175913565028082d-02,9.012267246445249d-02,8.850799143740207d-02/
data (p(i),i=136,150)/
>8.691496194708503d-02,8.534345082196698d-02,8.379332241501425d-02,
>8.226443867766897d-02,8.075665923377101d-02,7.926984145339244d-02,
>7.780384052654643d-02,7.635850953673912d-02,7.493369953432705d-02,
>7.352925960964835d-02,7.214503696589381d-02,7.078087699168556d-02,
>6.94366233333178d-02,6.811211796672545d-02,6.680720126885809d-02/
data (p(i),i=151,165)/
>6.552171208891650d-02,6.425548781893586d-02,6.300836446397839d-02,
>6.178017671181191d-02,6.057075800205902d-02,5.937994059479307d-02,
>5.820755563855307d-02,5.705343323775425d-02,5.591740251946942d-02,
>5.479929169955799d-02,5.369892814811972d-02,5.261613845425206d-02,
>5.155074849008934d-02,5.050258347410369d-02,4.947146803364810d-02/
data (p(i),i=166,180)/
>4.845722626672283d-02,4.745968180294735d-02,4.647865786372007d-02,
>4.551397732154983d-02,4.456546275854306d-02,4.363293652403194d-02,
>4.271622079132897d-02,4.181513761359495d-02,4.092950897880737d-02,
>4.005915686381706d-02,3.920390328748263d-02,3.836357036287125d-02,
>3.753798034851680d-02,3.672695569872630d-02,3.593031911292582d-02/
data (p(i),i=181,195)/
>3.514789358403880d-02,3.437950244589000d-02,3.362496941962834d-02,
>3.288411865916385d-02,3.215677479561369d-02,3.144276298075271d-02,
>3.074190892946599d-02,3.005403896119979d-02,2.937898004040940d-02,
>2.871655981600180d-02,2.806660665977251d-02,2.742894970383680d-02,
>2.680341887705495d-02,2.618984494045268d-02,2.558805952163862d-02/
data (p(i),i=196,210)/
>2.499789514822043d-02,2.441918528022258d-02,2.385176434150854d-02,
>2.329546775021185d-02,2.275013194817921d-02,2.221559442943144d-02,
>2.169169376764679d-02,2.117826964267228d-02,2.067516286607007d-02,
>2.018221540570442d-02,1.969927040937691d-02,1.922617222751732d-02,
>1.876276643493774d-02,1.830889985165896d-02,1.786442056281656d-02/
data (p(i),i=211,225)/
>1.742917793765708d-02,1.700302264763282d-02,1.658580668360504d-02,
>1.617738337216612d-02,1.577760739109052d-02,1.538633478392548d-02,
>1.500342297373219d-02,1.462873077598925d-02,1.426211841066888d-02,
>1.390344751349859d-02,1.355258114642000d-02,1.320938380725628d-02,
>1.287372143860205d-02,1.254546143594659d-02,1.222447265504473d-02/
data (p(i),i=226,240)/
>1.191062541854704d-02,1.160379152190355d-02,1.130384423855280d-02,
>1.101065832441139d-02,1.072411002167578d-02,1.044407706195111d-02,
>1.017043866871969d-02,9.903075559164254d-03,9.641869945358317d-03,
>9.386705534838558d-03,9.137467530572652d-03,8.894042630336774d-03,
>8.656319025516557d-03,8.424186399345668d-03,8.197535924596155d-03/
data (p(i),i=241,255)/
>7.976260260733725d-03,7.760253550553653d-03,7.549411416309215d-03,
>7.343630955348346d-03,7.142810735271399d-03,6.946850788624337d-03,
>6.755652607140672d-03,6.569119135546753d-03,6.387154764943170d-03,
>6.209665325776159d-03,6.036558080412646d-03,5.867741715332553d-03,
>5.703126332950670d-03,5.542623443082595d-03,5.386145954066668d-03/
data (p(i),i=256,270)/
>5.233608163555781d-03,5.084925748991054d-03,4.940015757770644d-03,
>4.798796597126176d-03,4.661188023718732d-03,4.527111132967332d-03,
>4.396488348121286d-03,4.269243409089352d-03,4.145301361036025d-03,
>4.024588542758334d-03,3.907032574852809d-03,3.792562347685491d-03,
>3.681108009174983d-03,3.572600952399752d-03,3.466973803040674d-03/
data (p(i),i=271,285)/
>3.364160406669203d-03,3.264095815891321d-03,3.166716277357817d-03,
>3.071959218650500d-03,2.979763235054556d-03,2.890068076226160d-03,
>2.802814632765049d-03,2.717944922701276d-03,2.635402077904969d-03,

```

```
>2.555130330427924d-03,2.477074998785855d-03,2.401182474189245d-03,
>2.327400206731556d-03,2.255676691542308d-03,2.185961454913232d-03/
data (p(i),i=286,300)/
>2.118205040404608d-03,2.052358994939774d-03,1.988375854894309d-03,
>1.926209132187884d-03,1.865813300384045d-03,1.807143780806431d-03,
>1.750156928676083d-03,1.694810019277238d-03,1.641061234157026d-03,
>1.588869647364877d-03,1.538195211738036d-03,1.488998745237446d-03,
>1.441241917340019d-03,1.394887235492248d-03,1.349898031630096d-03/
data (p(i),i=301,315)/
>1.306238448769467d-03,1.263873427672299d-03,1.222768693592260d-03,
>1.182890743104407d-03,1.144206831022698d-03,1.106684957409247d-03,
>1.070293854678923d-03,1.035002974802841d-03,1.000782476614011d-03,
>9.676032132183563d-04,9.354367195140999d-04,9.042551998223409d-04,
>8.740315156315670d-04,8.447391734586284d-04,8.163523128285638d-04/
data (p(i),i=316,330)/
>7.888456943755737d-04,7.621946880672361d-04,7.363752615539311d-04,
>7.113639686453650d-04,6.871379379158485d-04,6.636748614399681d-04,
>6.409529836600560d-04,6.189510903868352d-04,5.976484979344154d-04,
>5.770250423907672d-04,5.570610690246212d-04,5.377374218296949d-04,
>5.190354332069722d-04,5.009369137857219d-04,4.834241423837776d-04/
data (p(i),i=331,345)/
>4.664798561075492d-04,4.500872405921174d-04,4.342299203816563d-04,
>4.188919494503698d-04,4.040578018640217d-04,3.897123625820324d-04,
>3.758409184000837d-04,3.624291490330445d-04,3.494631183379715d-04,
>3.369292656768813d-04,3.248143974188780d-04,3.131056785812003d-04,
>3.017906246086373d-04,2.908570932907434d-04,2.802932768161773d-04/
data (p(i),i=346,360)/
>2.700876939634748d-04,2.602291824274666d-04,2.507068912805378d-04,
>2.415102735678360d-04,2.326290790355250d-04,2.240533469910931d-04,
>2.157733992947175d-04,2.077798334806213d-04,2.000635160073205d-04,
>1.926155756356333d-04,1.854273969332782d-04,1.784906139048473d-04,
>1.717971037459309d-04,1.653389807201100d-04,1.591085901575340d-04/
data (p(i),i=361,375)/
>1.530985025737555d-04,1.473015079074726d-04,1.417106098758194d-04,
>1.363190204458020d-04,1.311201544204847d-04,1.261076241384867d-04,
>1.212752342853580d-04,1.166169768153681d-04,1.121270259822471d-04,
>1.077997334773883d-04,1.036296236740311d-04,9.961138897591672d-05,
>9.573988526891469d-05,9.201012747410561d-05,8.841728520080404d-05/
data (p(i),i=376,390)/
>8.495667849799789d-05,8.162377370268624d-05,7.841417938358505d-05,
>7.532364237868341d-05,7.234804392511995d-05,6.948339587986524d-05,
>6.672583702968470d-05,6.407162948887459d-05,6.151715518325534d-05,
>5.905891241892255d-05,5.669351253425669d-05,5.441767663369976d-05,
>5.22823240182019d-05,5.012211099618837d-05,4.809634401760274d-05/
data (p(i),i=391,405)/
>4.614806055620888d-05,4.427448431207072d-05,4.247293078876124d-05,
>4.074080455855082d-05,3.907559659778755d-05,3.747488169107352d-05,
>3.593631590285383d-05,3.445763411505314d-05,3.303664762940245d-05,
>3.167124183311996d-05,3.035937392661827d-05,2.909907071193095d-05,
>2.788842644056393d-05,2.672560071949210d-05,2.560881647404153d-05/
data (p(i),i=406,420)/
>2.453635796640967d-05,2.350656886859557d-05,2.251785038852544d-05,
>2.156865944818060d-05,2.065750691254679d-05,1.978295586822407d-05,
>1.894361995055329d-05,1.813816171813091d-05,1.736529107360408d-05,
>1.662376372965224d-05,1.591237971908220d-05,1.522998194797792d-05,
>1.457545479086707d-05,1.394772272688124d-05,1.334574901590634d-05/
data (p(i),i=421,435)/
>1.276853441373497d-05,1.221511592525306d-05,1.168456559470741d-05,
>1.117598933212056d-05,1.068852577493443d-05,1.022134518398408d-05,
>9.773648372917573d-06,9.344665670196364d-06,8.933655912827005d-06,
>8.539905470991814d-06,8.162727302763068d-06,7.801460038101355d-06,
>7.455467091355145d-06,7.124135801495341d-06,6.806876599334045d-06/
data (p(i),i=436,450)/
>6.503122200992801d-06,6.212326826901514d-06,5.933965445624679d-06,
>5.667533041826751d-06,5.412543907703856d-06,5.168530957224142d-06,
>4.935045062533278d-06,4.711654411897247d-06,4.497943888567909d-06,
>4.293514469971870d-06,4.097982646636362d-06,3.910979860280711d-06,
>3.732151960514484d-06,3.561158679597556d-06,3.397673124730062d-06/
```

```

data (p(i),i=451,465)/
>3.241381287353394d-06,3.091981568956177d-06,2.949184322891521d-06,
>2.812711411724217d-06,2.682295779638856d-06,2.557681039451524d-06,
>2.438621073779427d-06,2.324879649934414d-06,2.216230048117548d-06,
>2.112454702502847d-06,2.013344854809340d-06,1.918700219970900d-06,
>1.828328663524165d-06,1.742045890344663d-06,1.659675144371463d-06/
data (p(i),i=466,480)/
>1.581046918970512d-06,1.505998677596157d-06,1.434374584420136d-06,
>1.366025244606141d-06,1.300807453917281d-06,1.238583957352471d-06,
>1.179223216516399d-06,1.122599185436174d-06,1.068591094545936d-06,
>1.017083242568706d-06,9.679647960327358d-07,9.211295961671412d-07,
>8.764759729292055d-07,8.339065659229126d-07,7.933281519755972d-07/
data (p(i),i=481,495)/
>7.546514791463692d-07,7.177911069469003d-07,6.826652525616647d-07,
>6.491956428613364d-07,6.173073720091949d-07,5.869287644666382d-07,
>5.579912432097829d-07,5.304292029750950d-07,5.041798883575367d-07,
>4.791832765903206d-07,4.553819648407320d-07,4.327210618617021d-07,
>4.111480838439311d-07,3.906128543183266d-07,3.710674079633336d-07/
data (p(i),i=496,510)/
>3.524658981764252d-07,3.347645082736184d-07,3.179213661852820d-07,
>3.018964625208491d-07,2.866515718791945d-07,2.721501772855827d-07,
>2.583573976399725d-07,2.452399180653704d-07,2.327659230486003d-07,
>2.209050322695440d-07,2.096282390183694d-07,1.989078511037129d-07,
>1.887174341580604d-07,1.790317572498343d-07,1.698267407147598d-07/
data (p(i),i=511,525)/
>1.610794061221380d-07,1.527678282945667d-07,1.448710893025085d-07,
>1.373692343578420d-07,1.302432295332016d-07,1.234749212365168d-07,
>1.170469973726320d-07,1.109429501263468d-07,1.051470403035407d-07,
>9.964426316933494d-08,9.442031572442990d-08,8.946156536290779d-08,
>8.475501985682844d-08,8.028829861495895d-08,7.604960516488729d-08/
data (p(i),i=526,540)/
>7.202770080965977d-08,6.821187941186212d-08,6.459194325982505d-08,
>6.115817997230602d-08,5.790134039964602d-08,5.481261748095645d-08,
>5.188362601842435d-08,4.910638333128551d-08,4.647329075344129d-08,
>4.397711594005889d-08,4.161097594981976d-08,3.936832107075916d-08,
>3.724291935887129d-08,3.522884185984314d-08,3.332044848542857d-08/
data (p(i),i=541,555)/
>3.151237451708229d-08,2.979951771053636d-08,2.817702597603999d-08,
>2.664028560996721d-08,2.518491005446115d-08,2.380672916270041d-08,
>2.250177894826861d-08,2.126629179795917d-08,2.009668712817647d-08,
>1.898956246588774d-08,1.794168493584716d-08,1.694998313655083d-08,
>1.601153938809098d-08,1.512358233576103d-08,1.428347989392278d-08/
data (p(i),i=556,570)/
>1.348873251527842d-08,1.273696677129993d-08,1.202592923015495d-08,
>1.135348061903221d-08,1.071759025831089d-08,1.011633075554139d-08,
>9.547872947704290d-09,9.010481080699081d-09,8.502508215475082d-09,
>8.022391850663509d-09,7.568649751997725d-09,7.139875979218420d-09,
>6.734737101557546d-09,6.351968593271951d-09,5.990371401063532d-09/
data (p(i),i=571,585)/
>5.648808675570940d-09,5.326202659455512d-09,5.021531724924521d-09,
>4.733827553845581d-09,4.462172453901613d-09,4.205696804522029d-09,
>3.963576626597628d-09,3.735031270249742d-09,3.519321215174624d-09,
>3.315745978326164d-09,3.123642123930022d-09,2.942381371044379d-09,
>2.771368794094646d-09,2.610041112012914d-09,2.457865061808032d-09/
data (p(i),i=586,600)/
>2.314335852578571d-09,2.178975696160569d-09,2.051332410772609d-09,
>1.930978094185322d-09,1.817507863099436d-09,1.710538655567010d-09,
>1.609708093434255d-09,1.514673401922662d-09,1.425110383596567d-09,
>1.340712444091877d-09,1.261189667101099d-09,1.186267936225734d-09,
>1.115688101417170d-09,1.049205187833157d-09,9.865876450377014d-10/
data (p(i),i=601,615)/
>9.276166345691163d-10,8.720853539929702d-10,8.197983956451329d-10,
>7.705711383542473d-10,7.242291705137658d-10,6.806077429504144d-10,
>6.395512501096636d-10,6.009127381488439d-10,5.645534385958076d-10,
>5.303423262948813d-10,4.981557004231254d-10,4.678767874181614d-10,
>4.393953647146701d-10,4.126074042396769d-10,3.874147346675664d-10/
data (p(i),i=616,630)/
>3.637247214840693d-10,3.414499639547374d-10,3.205080081373417d-10,

```

```

>3.008210751196840d-10,2.823158037043269d-10,2.649230067999402d-10,
>2.485774408153008d-10,2.332175873867525d-10,2.187854468029041d-10,
>2.052263425218952d-10,1.924887362065496d-10,1.805240527313422d-10,
>1.692865146423052d-10,1.587329855769880d-10,1.488228221762322d-10/
  data (p(i),i=631,645)/
>1.395177340430679d-10,1.307816513264241d-10,1.225805995286331d-10,
>1.148825811560307d-10,1.076574638512162d-10,1.008768746639295d-10,
>9.451410013495054d-11,8.854399188407803d-11,8.294287740902139d-11,
>7.768847581709834d-11,7.275981822590379d-11,6.813717258273434d-11,
>6.380197266544754d-11,5.973675103973090d-11,5.592507575942690d-11/
  data (p(i),i=646,660)/
>5.235149060764004d-11,4.900145868690975d-11,4.586130917672491d-11,
>4.291818708617980d-11,4.016000583859125d-11,3.757540253348849d-11,
>3.515369573951724d-11,3.288484567954244d-11,3.075941667656468d-11,
>2.876854173604333d-11,2.690388914682007d-11,2.515763098911859d-11,
>2.352241344404167d-11,2.199132880464250d-11,2.055788909399524d-11/
  data (p(i),i=661,675)/
>1.921600120077499d-11,1.795994344767311d-11,1.678434351254311d-11,
>1.568415762649946d-11,1.465465097730285d-11,1.369137925025025d-11,
>1.279017124247953d-11,1.194711249009093d-11,1.115852985079933d-11,
>1.042097698796524d-11,9.731220704826869d-12,9.086228080565395d-12,
>8.483154362502072d-12,7.919331571248458d-12,7.392257778017862d-12/
  data (p(i),i=676,690)/
>6.899587015569721d-12,6.439119786395897d-12,6.008794133785011d-12,
>5.606677243315662d-12,5.230957544144618d-12,4.879937281169313d-12,
>4.552025530768030d-12,4.245731634354438d-12,3.959659025435898d-12,
>3.692499427235594d-12,3.443027399236997d-12,3.210095212234586d-12,
>2.992628032635060d-12,2.789619397847642d-12,2.600126965638169d-12/
  data (p(i),i=691,705)/
>2.423268521298989d-12,2.258218227411716d-12,2.104203101851851d-12,
>1.960499710509255d-12,1.826431061976962d-12,1.701363692195681d-12,
>1.584704927736075d-12,1.475900317055532d-12,1.374431219685123d-12,
>1.279812543885835d-12,1.191590623864497d-12,1.109341228159143d-12,
>1.032667691294276d-12,9.611991612689379d-13,8.945889558769916d-13/
  data (p(i),i=706,720)/
>8.325130212702670d-13,7.746684865636528d-13,7.207723086467529d-13,
>6.705600017118691d-13,6.237844463331584d-13,5.802147732383270d-13,
>5.396353172029230d-13,5.018446367696487d-13,4.666545957513176d-13,
>4.338895027178080d-13,4.033853048947575d-13,3.749888331162318d-13,
>3.485570946752429d-13,3.239566111061341d-13,3.010627981117446d-13/
  data (p(i),i=721,735)/
>2.797593850166439d-13,2.599378712863654d-13,2.414970178016698d-13,
>2.243423707173588d-13,2.083858158672078d-13,1.935451618009657d-13,
>1.797437496562159d-13,1.669100881779288d-13,1.549775123019207d-13,
>1.438838638157592d-13,1.335711927020462d-13,1.239854778550311d-13,
>1.150763659422917d-13,1.067969272592302d-13,9.910342749547497d-14/
  data (p(i),i=736,750)/
>9.195511439940067d-14,8.531401838998034d-14,7.914476622443238d-14,
>7.341440688571708d-14,6.809224890620008d-14,6.314970839286098d-14,
>5.856016706548484d-14,5.429883966255224d-14,5.034265011012925d-14,
>4.667011588719071d-14,4.326124005658145d-14,4.009741046439491d-14,
>3.716130564205506d-14,3.443680697493761d-14,3.190891672910920d-14/
  data (p(i),i=751,765)/
>2.956368155375915d-14,2.738812110130123d-14,2.537016142999860d-14,
>2.349857287541125d-14,2.176291209708596d-14,2.015346802575318d-14,
>1.866121145397440d-14,1.727774802974088d-14,1.599527442805322d-14,
>1.480653749004804d-14,1.370479613286938d-14,1.268378584624278d-14,
>1.173768560367169d-14,1.086108702736900d-14,1.004896565652634d-14/
  data (p(i),i=766,768)/
>9.296654178339954d-15,8.599817490408714d-15,7.954429471721532d-15/

```

c conversion statement functions

```

abs(x)     = dabs(x)
exp(x)     = dexp(x)
float(i)   = dble(i)
int(x)     = idint(x)

```

```

c-----start executable statements -----
c          convert z to an index into p
c          by multiplying by 1/0.01
      r = abs(z)
      i = int(half + one00*r)
c          |z| < 0.01 ?
      if( i .lt. 1 ) then
          zz = r*r
          dphi = half - r*(one + zz*(-sixth + pt025*zz))/rt2pi
      else if( i .gt. NPROBS ) then
c          |z| > 7.68, use asymptotic
          z0 = r*r
          hz0 = -half*z0
          if( hz0 .lt. eund ) then
              dphi = zero
          else
              z1 = z0 + two
              z2 = z1*(z0 + four)
              z3 = z2*(z0 + six)
              z4 = z3*(z0 + eight)
              z5 = z4*(z0 + ten)
              dphi=one-(one/z1)+(one/z2)-(five/z3)+(nine/z4)-one29/z5)
              dphi = exp(hz0)*dphi/(rt2pi*r)
          endif
      else
c          interpolate using table values
          zo = float(i)*pt01
          zo2 = zo*zo
          zo3 = zo*zo2
          zo4 = zo2*zo2
          zo5 = zo*zo4
          r = r - zo
          a1 = -half*zo
          a2 = (zo2-one)*sixth
          a3 = (three*zo - zo3)/twnty4
          a4 = (three - six*zo2 + zo4)/one20
          a5 = (-fifteen*zo + ten*zo3 - zo5)/sevn20
          f = r*exp(-half*zo2)/rt2pi
          dphi=p(i)-f*(one+r*a1+r*(a2+r*(a3+r*a4+a5*r))))
      endif

      if( z .gt. zero ) dphi = one - dphi

      return
      end

```

```

c-----
c          integer function nrdfp
c-----
c  PURPOSE   read a sequence of real variables from an internal
c            character string using free format with provision for
c            sequences
c  Courtesy: http://www.engmath.dal.ca/rfem/
c-----
      integer function nrdfp(str,v,MX)
      real v(*)
      real f(3)
      character*(*) str
      character*1 c, tab, spc
      logical lseq, linc

```

```
nrdfp = 0
tab = char(9)
spc = char(32)

ls = lnblnk(str)
i = 1
j = 1
k = 1
s = 1.
me = 1
f(1) = 0.
f(2) = 0.
f(3) = 0.
f3 = 1.
lseq = .false.
linc = .false.
i2 = 0
i3 = 0
jt = 1

10 if( i .gt. ls ) return
   c = str(i:i)
   if( (c .eq. spc) .or. (c .eq. tab) ) then
     i = i + 1
     go to 10
   endif
   if( c .eq. '-' ) then
     s = -1.
     i = i + 1
     c = str(i:i)
   endif

20 if( c .eq. '0' ) then
     f(k) = 10.*f(k)
elseif( c .eq. '1' ) then
     f(k) = 10.*f(k) + 1.
elseif( c .eq. '2' ) then
     f(k) = 10.*f(k) + 2.
elseif( c .eq. '3' ) then
     f(k) = 10.*f(k) + 3.
elseif( c .eq. '4' ) then
     f(k) = 10.*f(k) + 4.
elseif( c .eq. '5' ) then
     f(k) = 10.*f(k) + 5.
elseif( c .eq. '6' ) then
     f(k) = 10.*f(k) + 6.
elseif( c .eq. '7' ) then
     f(k) = 10.*f(k) + 7.
elseif( c .eq. '8' ) then
     f(k) = 10.*f(k) + 8.
elseif( c .eq. '9' ) then
     f(k) = 10.*f(k) + 9.
elseif( c .eq. 'e' .or. c .eq. 'E'
> .or. c .eq. 'd' .or. c .eq. 'D' ) then
     if( k .eq. 3 ) go to 999
     if( k .eq. 2 ) i3 = i
     k = 3
     i = i + 1
     c = str(i:i)
     if( c .eq. '+' .or. c .eq. '-' ) then
       if( c .eq. '-' ) me = -1
```

```

        i = i + 1
        c = str(i:i)
    endif
    go to 20
elseif( c .eq. '.' ) then
    if( k .eq. 2 .or. k .eq. 3 ) go to 999
    k = 2
    i2 = i+1
elseif( c .eq. '-' ) then
    lseq = .true.
    if( f(3) .ne. 0. ) then
        s = s*10.**(float(me)*f(3))
    endif
    if( k .eq. 2 ) i3 = i
    fr = f(2)/(10.**(i3-i2))
    f1 = s*(f(1) + fr)
    i = i + 1
    s = 1.
    me = 1
    f(1) = 0.
    f(2) = 0.
    f(3) = 0.
    k = 1
    i2 = 0
    i3 = 0
    go to 10
elseif( c .eq. ',' ) then
    if( .not. lseq ) go to 999
    linc = .true.
    if( f(3) .ne. 0. ) then
        s = s*10.**(float(me)*f(3))
    endif
    if( k .eq. 2 ) i3 = i
    fr = f(2)/(10.**(i3-i2))
    f2 = s*(f(1) + fr)
    i = i + 1
    s = 1.
    me = 1
    f(1) = 0.
    f(2) = 0.
    f(3) = 0.
    k = 1
    i2 = 0
    i3 = 0
    go to 10
elseif( (c .eq. spc) .or. (c .eq. tab) .or. (i .ge. ls) ) then
    if( lseq ) then
        if( f(3) .ne. 0. ) then
            s = s*10.**(float(me)*f(3))
        endif
        if( k .eq. 2 ) i3 = i
        fr = f(2)/(10.**(i3-i2))
        if( linc ) then
            f3 = s*(f(1) + fr)
        else
            f2 = s*(f(1) + fr)
        endif
        if( f3 .eq. 0. ) go to 999
        n = int( 1.000001*(f2 - f1)/f3 )
        if( n .lt. 0 ) go to 999
        do 30 L = 0, n

```

```

        if( j .le. MX ) v(j) = f1 + float(L)*f3
        j = j + 1
30      continue
        nrdfp = j - 1
        lseq = .false.
        linc = .false.
        f3    = 1.0
    else
        if( j .le. MX ) then
            if( f(3) .ne. 0 ) then
                s = s*10.**(float(me)*f(3))
            endif
            if( k .eq. 2 ) i3 = i
            fr = f(2)/(10.**(i3-i2))
            v(j) = s*(f(1) + fr)
        endif
        nrdfp = j
        j      = j + 1
    endif
    jt      = jt + 1
    i       = i + 1
    s       = 1.
    me      = 1
    f(1)    = 0.
    f(2)    = 0.
    f(3)    = 0.
    k       = 1
    i2      = 0
    i3      = 0
    go to 10
else
    go to 999
endif
i = i + 1
if( i .gt. ls ) then
    c = spc
else
    c = str(i:i)
endif
go to 20
c      read error
999   if( j .gt. MX ) return
      nrdfp = -jt
      return
      end

```

```

c-----
c                                     integer function nrdint
c-----
c  PURPOSE   read a sequence of integer variables from an internal
c            character string using free format with special
c            provision for sequences
c  Courtesy: http://www.engmath.dal.ca/rfem/
c-----
      integer function nrdint(str,nv,MX)
      integer nv(*)
      character*(*) str
      character*1 c, tab, spc
      logical lseq, linc

```

```
nrdint = 0
tab = char(9)
spc = char(32)

ls = lnblnk(str)
i = 1
j = 1
jt = 1
k = 0
m = 1
i3 = 1
lseq = .false.
linc = .false.

10 if( i .gt. ls ) return
   c = str(i:i)
   if( (c .eq. spc) .or. (c .eq. tab) ) then
     i = i + 1
     go to 10
   endif
   if( c .eq. '-' ) then
     m = -1
     i = i + 1
     c = str(i:i)
   endif
20 if( c .eq. '0' ) then
     k = 10*k
elseif( c .eq. '1' ) then
     k = 10*k + 1
elseif( c .eq. '2' ) then
     k = 10*k + 2
elseif( c .eq. '3' ) then
     k = 10*k + 3
elseif( c .eq. '4' ) then
     k = 10*k + 4
elseif( c .eq. '5' ) then
     k = 10*k + 5
elseif( c .eq. '6' ) then
     k = 10*k + 6
elseif( c .eq. '7' ) then
     k = 10*k + 7
elseif( c .eq. '8' ) then
     k = 10*k + 8
elseif( c .eq. '9' ) then
     k = 10*k + 9
elseif( c .eq. '-' ) then
     lseq = .true.
     i1 = m*k
     i = i + 1
     k = 0
     m = 1
     go to 10
elseif( c .eq. ',' ) then
     linc = .true.
     i2 = m*k
     i = i + 1
     k = 0
     m = 1
     go to 10
elseif( (c .eq. spc) .or. (c .eq. tab) .or. (i .ge. ls) ) then
     if( lseq ) then
```

```

        if( linc ) then
            i3 = m*k
        else
            i2 = m*k
        endif
        if( i3 .eq. 0 ) go to 999
        n = (i2 - i1)/i3
        if( n .lt. 0 ) go to 999
        do 30 L = 0, n
            if( j .le. MX ) nv(j) = i1 + L*i3
            j = j + 1
30      continue
        nrdint = j - 1
        lseq = .false.
        linc = .false.
        i3 = 1
        elseif( linc ) then
            i3 = m*k
            do 40 L = 1, i3
                if( j .le. MX ) nv(j) = i2
                j = j + 1
40      continue
        nrdint = j - 1
        linc = .false.
        i3 = 1
        else
            if( j .le. MX ) nv(j) = m*k
            nrdint = j
            j = j + 1
        endif
        jt = jt + 1
        i = i + 1
        k = 0
        m = 1
        go to 10
    else
        go to 999
    endif
    i = i + 1
    if( i .gt. ls ) then
        c = spc
    else
        c = str(i:i)
    endif
    go to 20
c      read error
999  if( j .gt. MX ) return
      nrdint = -jt
      return
      end

```

```

c-----
c                                     integer function nrdlog
c-----
c  PURPOSE   read a sequence of logical variables from an internal
c            character string using free format
c  Courtesy: http://www.engmath.dal.ca/rfem/
c-----
      integer function nrdlog(str,lv,MX)
      logical lv(*), lf, lc

```

```
character*(*) str
character*1 c, tab, spc

tab = char(9)
spc = char(32)

ls = lnblnk(str)
nrdlog = 0
i = 1
j = 1
10 if( i .gt. ls ) return
   c = str(i:i)
   if( (c .eq. spc) .or. (c .eq. tab)
>.or.(c .eq. ',') .or. (c .eq. '.') ) then
       i = i + 1
       go to 10
   endif
   lf = ((c .eq. 't') .or. (c .eq. 'T'))
   if( lf .or. c .eq. 'f' .or. c .eq. 'F' ) then
       if( j .le. MX ) lv(j) = lf
       nrdlog = j
       j = j + 1
20   i = i + 1
       c = str(i:i)
       lc = ( (c .ne. spc) .and. (c .ne. tab) .and. (c .ne. ',') )
       if( lc .and. i .lt. ls ) go to 20
   else
       if( j .gt. MX ) return
       nrdlog = -j
       return
   endif
   go to 10

end
```